The molecular characterisation of MET addiction in lung cancer

Thesis submitted by

Niamh Coleman

for the degree of Doctor of Philosophy

Institute of Cancer Research

Royal Marsden Hospital

University of London

February 2020

Declaration of originality

The work described in this thesis was carried out in the Molecular Addictions Group, Cancer Therapeutics Division, Institute of Cancer Research. Unless otherwise stated, the author performed the experiments described. This thesis is submitted in support of the author's application for the degree of Doctor of Philosophy. It has been composed by the author and has not been submitted in any previous application for any degree.

I, hereby, confirm that this thesis is an original work, representing my own academic effort and that all sources have been fully acknowledged.

Niamh Coleman

Abstract

The traditional classification of lung cancer has been radically altered with increased understanding of the molecular alterations and genomic biomarkers that drive the development of the disease. Whilst molecularly targeted therapies, and immunotherapy agents, have transformed NSCLC treatment in recent years, only a subset of patients respond to these treatments, and there remains a pressing need for treatment alternatives in the majority of patients.

The large-scale profiling of lung cancer genomes has allowed for the identification of a number of novel therapeutic targets, and, MET, the tyrosine kinase hepatocyte growth factor (HGF) receptor, has emerged as an attractive candidate. Clinical studies on MET-targeting cancer therapies, however, have produced mixed results, and MET-relevant predictive biomarkers remain elusive. This has led to some pessimism about the role of MET in the pathogenesis of NSCLC and the validity of MET as a targetable oncogenic driver. The identification of MET exon 14 (METex14) splicing alterations in recent years, however, and the subsequent clinical successes treating NSCLC patients with these alterations, has led to renewed enthusiasm.

In this thesis, potential causes for the failure of MET TKIs in the clinic to date are explored, and the potential of MET as a primary oncogenic driver in lung cancer is discussed. An over-looked resistance mechanism to MET TKIs in MET-amplified NSCLC patients is investigated, and the possible molecular basis behind this resistance is discussed. We demonstrate a number of strategies developed to overcome HGF-induced resistance to MET TKIs in MET-amplified NSCLC, and also present data involving a novel target in MET-driven cancer. Finally, we look to the future, and discuss clinical trial design in MET-driven lung cancer. Our ultimate aim: to treat molecularly selected NSCLC patients with true MET-positive disease, using the appropriate MET targeting drug or drug combination in an appropriately designed clinical trial.

Acknowledgements

Firstly, I would like to express my deep and sincere gratitude to my research supervisor Igor Vivanco. Thank you for your guidance, for your vision, and for giving me the opportunity to undertake a PhD in your laboratory. It is an experience I will always be grateful for. To my clinical supervisor, Sanjay Popat, thank you for your clinical insight in this project, for your wisdom, and for always making my bench work seem relevant (and worth it!). I am grateful to the rest of the Lung Unit in the Royal Marsden Chelsea, especially Nadia Yousaf, Sophie, Jo and Louise: thank you for making me feel part of your team, and for always making me feel like I was part of something bigger.

To everyone in the Molecular Addictions Lab, past and present, I am so grateful to all of you for showing me the science way. From the first days of pipetting, to the late, long hours of western blotting and failed phosphoproteomics. I know that I have made life-long friendships, and thank each and every one of you for your patience, kindness and support. You have all made me a better scientist, and a better doctor. A personal thank you to Alice, for your early guidance in the lab, for the endless cups of tea, and a friendship I truly value. Too much to say! Thank you, Sara, for your never-ending enthusiasm, positivity and support. I already miss our Team MET days. Lefteris and Glori, thank you for always being there for questions, calculations and images! Thank you, Irene, for always helping me to focus on the bigger picture, and Aasia for all the welcome distractions and baked goods!

To my family: my parents and siblings, thank you for your love and continual support. To my mother: thank you for your endless sacrifices, and for always encouraging me to follow my true passions.

Finally, to my long-suffering wife, Sarah. Thank you for your patience. Thank you for letting me do this! I am sorry for the long nights spent in the lab, the weekends spent in

the lab, and all of the long hours obsessing about the lab and this research project. I know that I could not have done this without you and your support, and know that everything I do is for you and our girls, Nora and Maeve. You have made this possible.

Finally, I am thankful to the Cancer Research United Kingdom and the Institute of Cancer Research for creating this Ph.D. opportunity and generously funding this studentship.

TABLE OF CONTENTS

TABLE OF SUPPLEMENTARY FIGURES

Index of Tables

1 Background

1.1 General Introduction

Lung cancer remains one of the leading causes of cancer death worldwide[1]. The traditional classification of lung cancer into small-cell lung cancer (SCLC) and non-small cell lung cancer (NSCLC), the latter of which accounts for nearly 90% of all cases, has been radically transformed with the increased understanding of the molecular alterations that drive the development of the disease (Figure 1). Indeed, for certain patients with NSCLC, molecularly targeted therapies have transformed treatment and markedly improved patient outcomes.

For instance, in patients with activating epidermal growth factor receptor (*EGFR*) mutations, anaplastic lymphoma kinase (*ALK*), and *ROS1* rearrangements, targeted therapies represent the standard of care, with superior efficacy and improved tolerability, as compared with cytotoxic chemotherapy[2–7]. More recently, immune checkpoint inhibitors have been added to the arsenal of available therapeutic options[8–12]. However, despite evidence of long-term therapeutic benefit, only a fraction of lung cancer patients responds to these agents, and relapsed disease is inevitable. Thus, there remains a pressing need for alternatives to toxic systemic therapies in the majority of lung cancer patients.

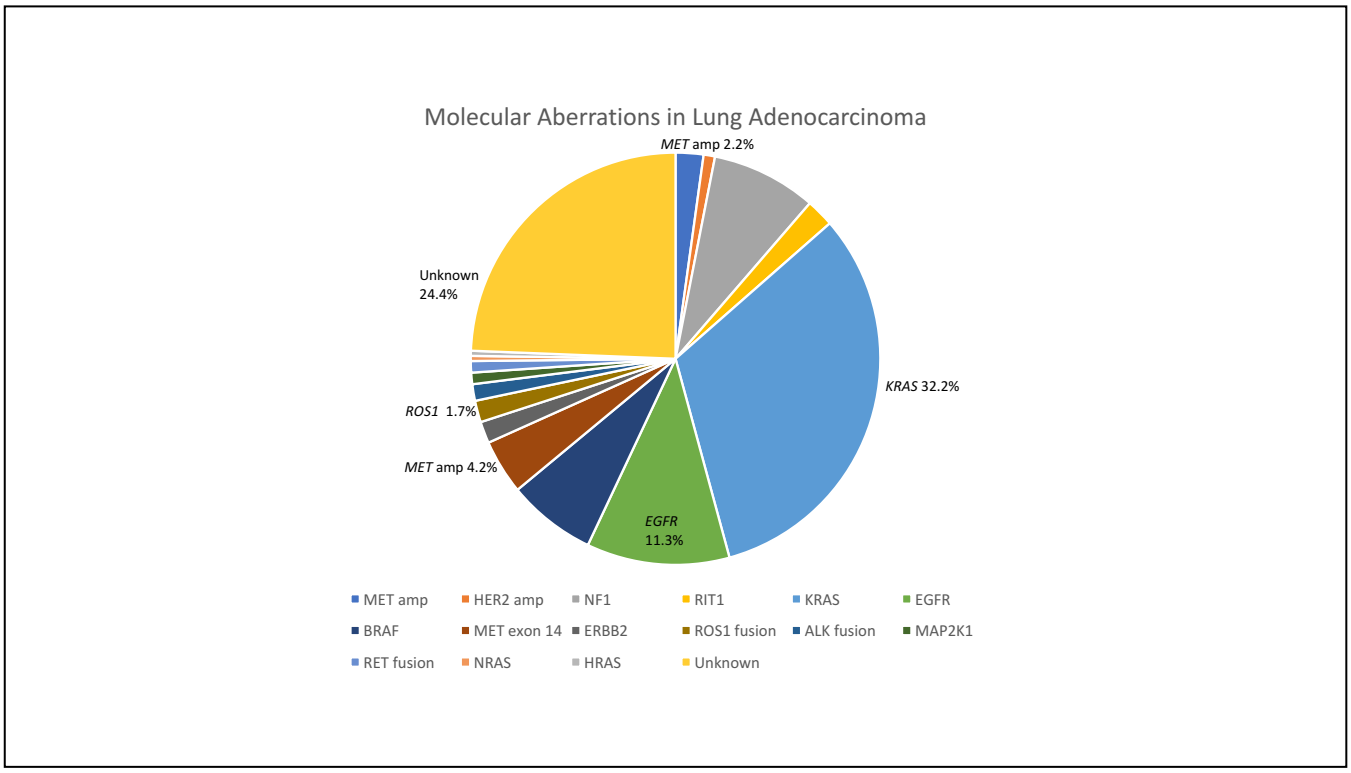

Figure 1. Genomic Aberrations in lung adenocarcinoma. The results shown here are based upon data generated by the TCGA Research Network[13,14].

In recent years, the large scale profiling of lung cancer genomes has provided a framework for the identification of additional therapeutic targets [15–17]. These extensive profiling efforts have identified molecular drivers that are found in smaller subsets of NSCLC, often in just 1 or 2% of patients. Although the incidence of these alterations is low, these low frequency mutations are currently driving clinical trial design.

The National UK Lung Matrix Trial (NLMT)[18], a genomic-driven UK-wide phase II trial, is an example of one such trial in lung cancer, which explores the activity of rationally selected biomarker-specific compounds. National Cancer Institute-Molecular Analysis

for Therapy Choice[19] (NCI-MATCH) is a similar US-based genomic-driven trial, which includes 39 arms. Targeting these smaller pieces of the "oncogenomic pie"

could have significant impact, owing to the high prevalence of lung cancer and the potential for dramatic improvements in outcome.

MET, the mesenchymal epithelial transition factor tyrosine kinase hepatocyte growth factor (HGF) receptor, has emerged as an attractive therapeutic candidate. A number of different types of recurrent lesions have been shown to cause aberrant MET signalling, including MET gene amplification and/or mutation as well as gene amplification and/or mutation of its cognate ligand, HGF, reported in approximately 8-20% of SCLC and NSCLC tumours[13,14] (Figure 2). MET, along with its cognate ligand HGF, plays a key role in cell proliferation, apoptosis, and motility/invasion [20,21], and dysregulation of MET signalling has been implicated in a number of malignancies[22–24].

Indeed, high levels of MET overexpression have been reported in a number of tumour streams, with varying frequencies noted. For example, Ma et al reported MET overexpression in 16% of breast cancer tissues, 30% of ovarian cancer and 70% of renal cancer samples[25]. MET overexpression has also been noted in 10% of primary and 18% of metastatic colorectal carcinoma[26]. Furthermore, high expression of MET has also been shown to be associated with advanced stage and poor prognosis in lung, breast, bladder, colorectal , gastric, and kidney cancers [27–30].

MET aberrant activation can also result from an overexpression of its ligand HGF, which has notably been observed in breast, gastric, colon, and lung cancers, and has been associated with a poor prognosis[31]. In fact, HGF can be supplied by either the tumour itself or the tumour microenvironment[32], secreted by cells such as fibroblasts[33]. Previous studies have highlighted the key role for HGF secreted from the tumour microenvironment in the development of drug resistance[32,34,35]. However, the

mechanistic basis of how the presence of excess HGF alters the response to MET TKIs is still unknown.

Despite the abundant number of agents developed to target the MET receptor, initial studies undertaken with small molecule MET tyrosine kinase inhibitors (TKIs) and MET-targeting agents were disappointing[36–38]. However, the recent emergence of splicing alterations of *MET* proto-oncogene receptor tyrosine kinase gene MET exon 14 (MET ex14) in NSCLC as a primary driver, has reinvigorated interest in the development of MET inhibitors in lung cancer[39,40].

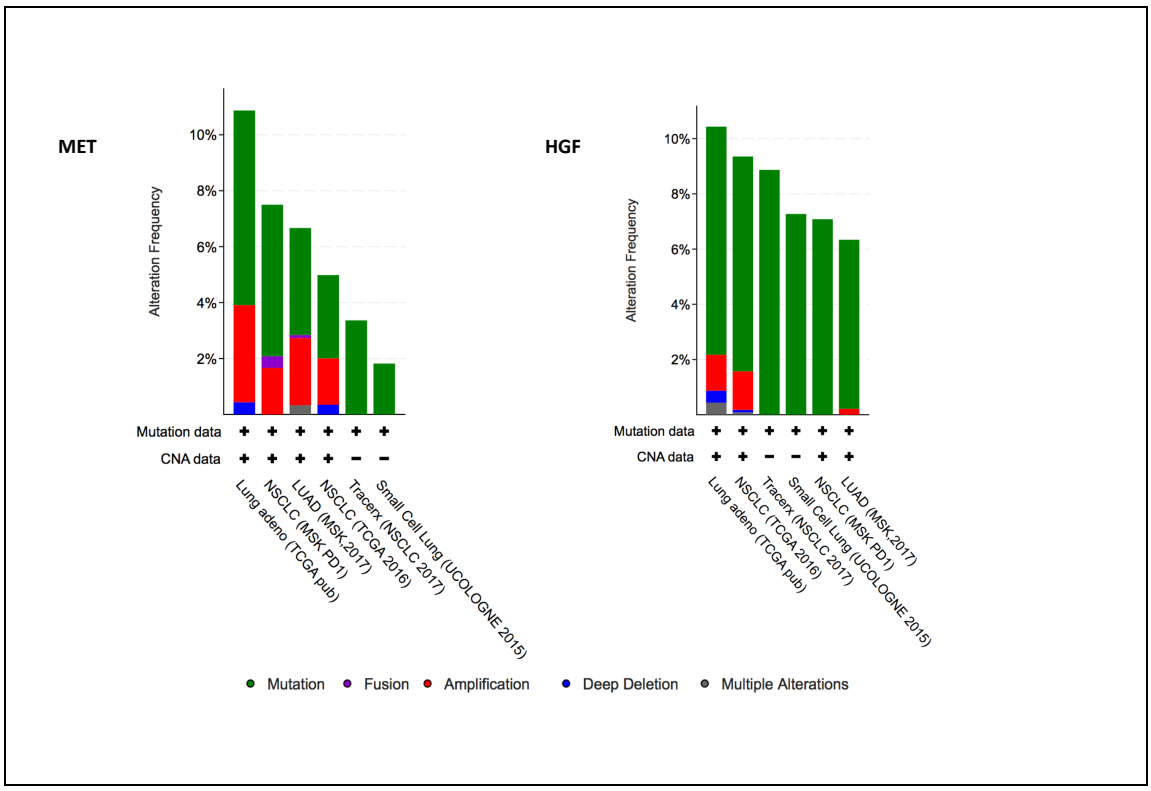

Figure 2. The MET and HGF genes are frequently altered in lung cancer. Data shown were compiled from the indicated studies[13,14].

1.1.1 HGF-MET Biology

The MET proto-oncogene, and HGF, its high-affinity physiological ligand, were both originally discovered thirty years ago. MET was initially characterized as a transforming MET fusion protein, translocated promoter region (TPR)–MET partner, and first identified in a chemically transformed osteosarcoma-derived cell line[41]. The proto-oncogene was later discovered to encode the receptor tyrosine kinase (RTK) MET, an RTK activated by an endogenous ligand, scatter factor, or HGF[42–45]. Indeed, HGF, a liver mitogen[46–48] and a fibroblast-derived epithelial motility factor (or scatter factor (SF))[49,50] were actually independently characterized and then found to be the same protein, denoted as HGF or SF[51,52]. The human gene MET is located on chromosome 7q31.2, is approximately 125 kilobases long, with 21 exons; the gene encoding its ligand protein, HGF is located on chromosome 7q21.1[53,54].

In general, RTKs such as MET, contain an N-terminal extracellular binding domain, a single transmembrane α helix, and a cytosolic C-terminal domain with tyrosine kinase activity[55]. MET is a disulfide linked heterodimeric RTK consisting of an extracellular α chain, a β chain that encompasses the remainder of extracellular domain, the juxtamembrane and the kinase domains (Figure 3). The extracellular component groups several domains, including a large N-terminal semaphorin (Sema) domain (exon 2), a plexin-semaphorin-integrin (PSI) domain, and a stalk structure consisting of four immunoglobulin-plexin- transcription factor (IPT) domains. The intracellular component contains a juxtamembrane region responsible for signal downregulation and receptor degradation, a catalytic region with the enzyme activity, and a C-terminal region acting as a docking site for adaptor proteins such as GRB2 and GAB-1, which leads to downstream signalling via PI3K, STAT and MAPK[56–58].

HGF, the only natural ligand of MET, is a large, disulfide, multidomain protein that is related to the blood proteinase precursor plasminogen[59]. HGF consists of six domains including an N-terminal domain, four kringle domains and a C-terminal domain which is a serine proteinase homology (SPH) domain[45,60] (Figure 3). HGF is secreted from

mesenchymal cells as an inactive, single chain precursor and is converted to an active two-chain heterodimer by one of three serine proteinases: the soluble HGF activator, and the type II transmembrane enzymes matriptase and hepsin[61,62]. In addition to transcriptional regulation, a key post-translational step in the regulation of HGF-MET signalling, is the proteolytic activation of pro-HGF to the active ligand[59]. Activation of HGF is finely tuned by the expression of at least two inhibitors, which are known as HGF activator inhibitor 1 (HAI1; also known as SPINT1) and HAI2 (also known as SPINT2)[63,64]. Increased expression of matriptase and/or hepsin induces cancer cell invasion and metastasis, as does decreased expression of HAI1 and/or HAI2[65].

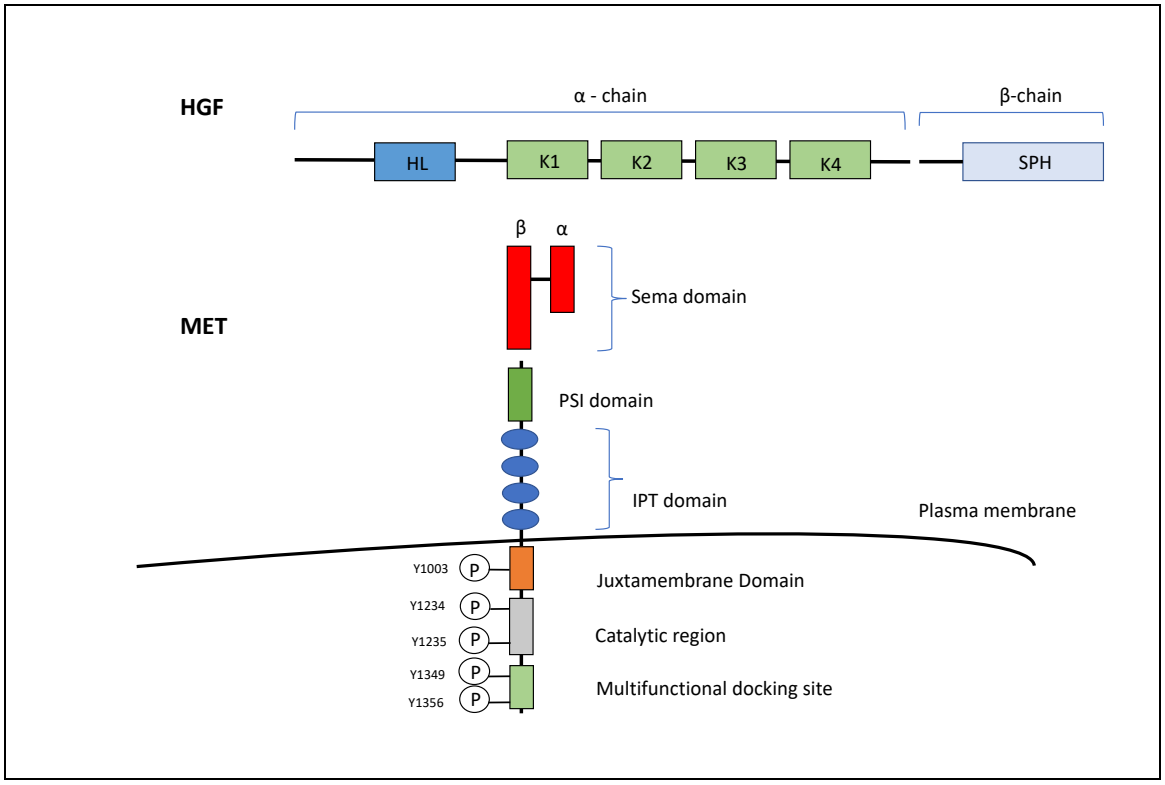

Figure 3. The structure of HGF and MET. HGF consists of six domains including an N-terminal domain, four kringle domains and a C-terminal domain which is a serine proteinase homology (SPH) domain. MET is a disulfide linked heterodimeric RTK consisting of an extracellular α chain, a β chain that encompasses the remainder of extracellular domain, the juxtamembrane and the kinase domains. MET is synthesized as a single chain

precursor and cleaved by furin during transit through the endoplasmic reticulum, which accounts for the smaller, amino-terminal α-chain and a larger β-chain. The extracellular component groups several domains including a large N-terminal semaphorin (Sema) domain, a plexin-semaphorin-integrin (PSI) domain, and a stalk structure consisting of four immunoglobulin-plexin-transcription factor (IPT) domains. The intracellular component contains a juxtamembrane region, a catalytic region with the enzyme activity, and a C-terminal region which acts as a docking site for adaptor proteins.

1.1.2 HGF and MET Signalling.

Structurally, it is the SPH domain of HGF that binds the large, amino-terminal domain of MET (the SEMA domain)[66]. Binding of HGF to MET leads to receptor dimerization and phosphorylation of tyrosine residues (Tyr1230, Tyr1234, and Tyr1235) in the kinase domain[67–69]. This leads to autophosphorylation of the carboxy-terminal bidentate substrate-binding site (Tyr1349 and Tyr1356) of MET[67–69], and the resulting phospho-tyrosines function as docking sites for other proteins involved in RTK-mediated signal transduction[67–69].

For instance, various cytoplasmic effector proteins, including GAB1, GRB2, phospholipase C (PLC) and SRC are directly recruited to this site, and bind to activate distinct downstream signaling pathways[42,44,70]. Phosphorylated GAB1, attached to MET at the cell membrane can attract further docking molecules and enzymes, such as PI3K, CRK-like protein (CRKL), SRC homology 2 domain-containing phosphatase 2 (SHP2) and others, that altogether activate various downstream signalling cascades[56–58].

These activated signaling pathways include phosphoinositide 3-kinase (PI3K)/AKT (protein kinase B), mitogen-activated protein kinase (MAPK), signal transducer and activator of transcription proteins, and nuclear factor-kB[71–73](Figure 4).

The variety of cellular responses that follow activation of MET is a remarkable feature of the HGF–MET signaling system. More recently, several types of signal co-operation and crosstalk are thought to occur between MET and other receptor pathways, such as epidermal growth factor receptor (EGFR), vascular endothelial growth factor receptor (VEGFR) and MET–WNT pathways, and there is evidence that cooperative signaling between MET and the epidermal growth factor receptor (EGFR) occurs during kidney development[74]. This signalling network may obviously have serious implications for targeted therapies.

Overall, depending on the cellular context, the physiologic function of the MET pathway can involve cell proliferation, cell motility, morphogenesis, angiogenesis, organ regeneration and the epithelial to mesenchymal transition[75,76]. In normal physiology, activation of the MET signalling pathway leads to activation of cytoplasmic and nuclear processes, resulting in a variety of cellular functions, including proliferation and protection from apoptosis[71–73]. The MET pathway also facilitates functions such as hepatic regeneration, and wound healing, and has key role in normal liver development[22], embryonic placental development, and the development of neurons and muscle[77,78].

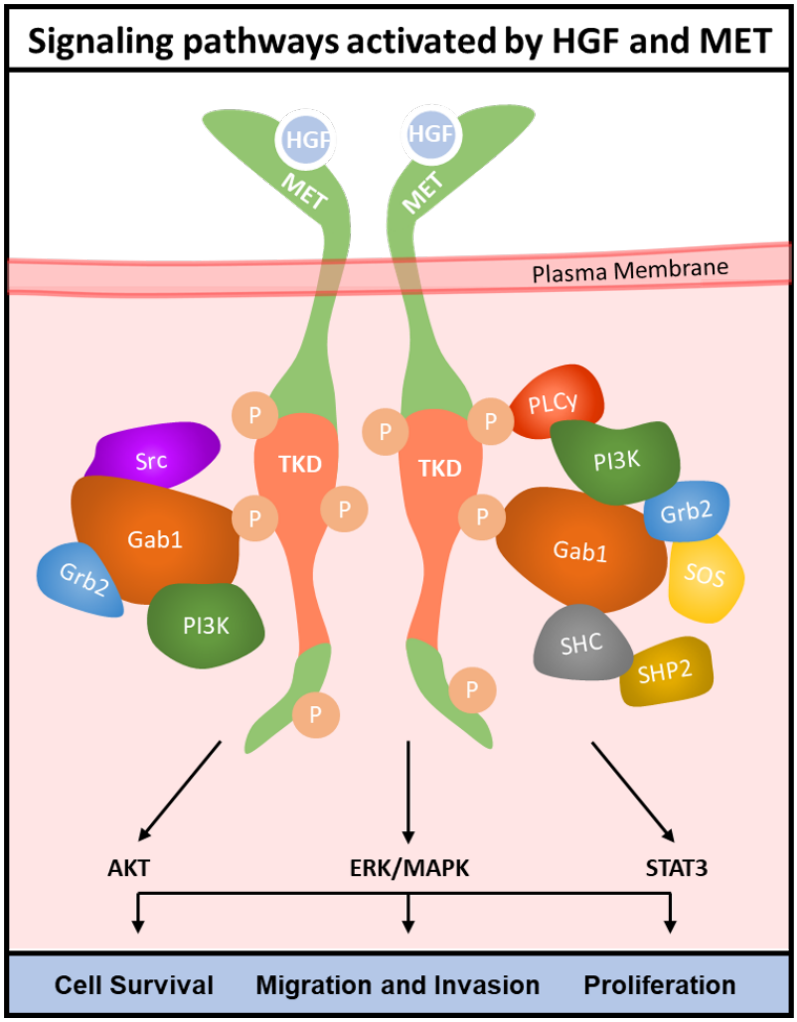

Figure 4. Signalling pathways activated by HGF and MET.

1.1.2.1 MET ubiquitylation, endocytosis and shedding.

Similar to other RTKs, on ligand binding MET is internalized through endocytosis, and the internalized receptor is subsequently either degraded or recycled to the plasma membrane. Consequently, aberrant receptor trafficking, degradation, and deranged recycling, can all cause sustained signaling which can contribute to cell transformation, tumorigenesis and metastasis[78].

Casitas B-lineage lymphoma (CBL), a ubiquitin E3 ligase, contains a phosphotyrosine-binding module that recognizes the phosphorylated tyrosine residue 1003 (Y1003) residue in the juxtamembrane region of MET and induces degradation[79]. Y1003, which serves as the binding site of CBL, is located in the juxtamembrane region of MET and is encoded by exon 14 (METex14)[80]. CBL thus mediates the ubiquitylation of MET, and ubiquitylated MET is then degraded in a late endosomal or lysosomal compartment in a proteasome-dependent manner[81,82]. Mutation or deletion of this CBL-binding site converts MET into a transforming protein, and has recently been a cause of much interest in the MET field[79]. Such receptor variants are still internalized on ligand activation, but because of a change in endosomal sorting, they escape degradation, and lead to increased MET signalling[79].

1.1.3 MET and HGF in lung cancer

Gain of function alterations in MET in lung cancer are varied, and include gene copy-number amplification, protein overexpression, and point mutations in the juxtamembrane and Sema domains[83] (Figure 5). Pathologic activation of MET via gene amplification is a well-characterized driver of oncogenesis, that occurs in many different cancers[40]. In lung cancer, amplification of MET occurs in approximately 4% of lung adenocarcinomas and 1% of squamous cell lung cancers[15,16]. The overall incidence of MET mutations in lung cancer varies, occurring in 3% of squamous cell lung cancers[15] and 8% of lung adenocarcinomas[16]. Somatic mutations affecting splice sites of exon 14 of the MET gene (METex14) alone have been shown to occur in approximately 3% of lung adenocarcinoma cases [84–89]. (METex14 mutations have also been observed in neuroblastoma, and gastric cancer cell lines[90,91]).

Overexpression of MET is associated with poor prognosis in NSLC, and high MET gene copy number linked with reduced overall survival, and an increased risk of death after surgical resection[85,92].

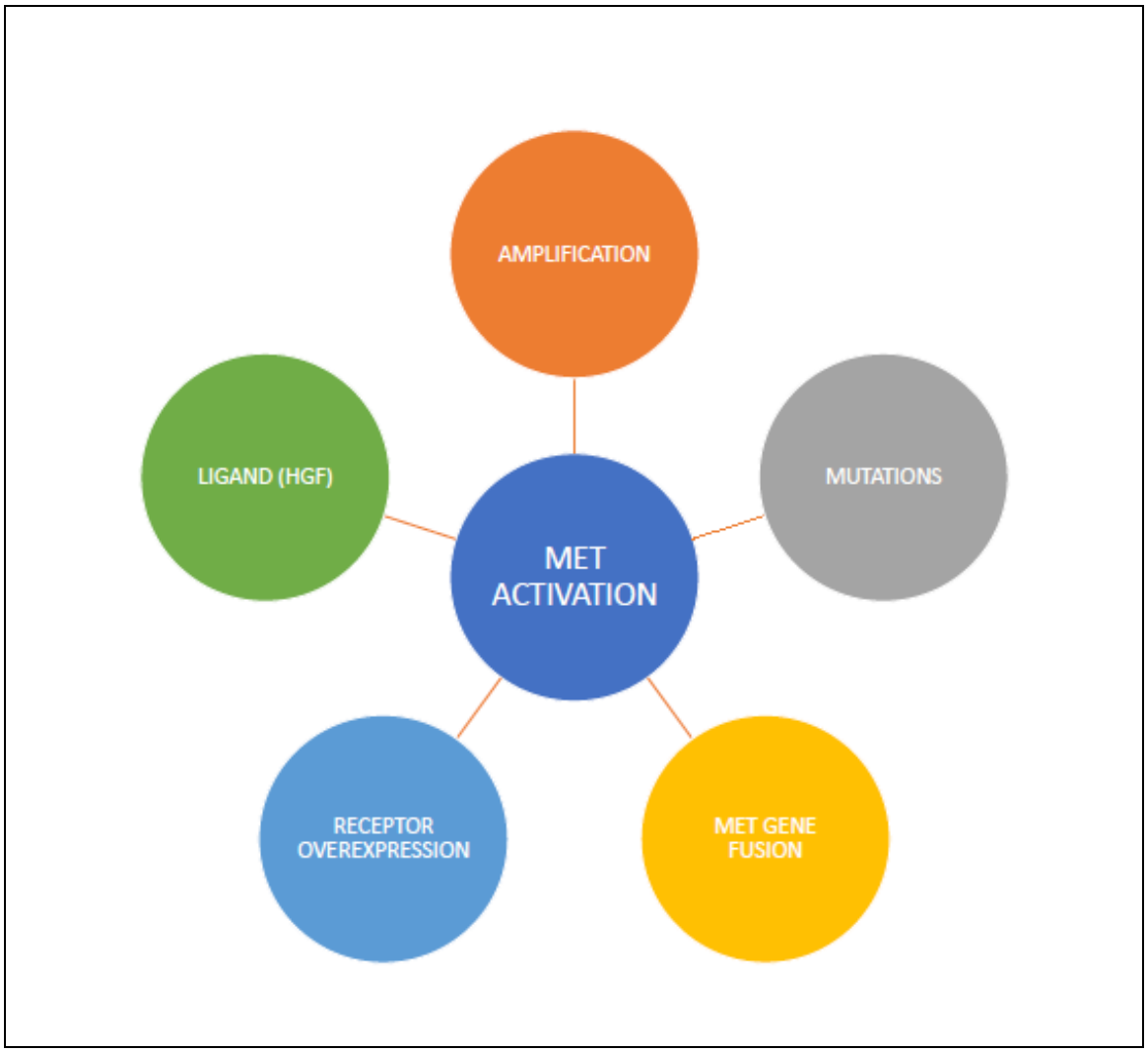

Figure 5. Schematic diagram illustrating well-documented mechanisms of activation of MET receptor in human cancers. Multiple reported mechanisms of activation of the MET receptor and its oncogenic signalling pathways are identified, including genomic amplification, receptor protein overexpression, mutations (which can be germline, somatic; exon 14 juxtamembrane skipping mutations cause alternative splicing variant, (METex14), and MET gene chromosomal fusion.

Mutations are also seen in HGF, and the overall incidence of HGF mutations varies, occurring in 5% of squamous cell lung cancers[15] and 8% of lung adenocarcinomas[16].

Interestingly, the frequency of HGF mutations in NSCLC (adenocarcinoma and squamous combined) is approximately 3 times higher than epidermal growth factor protein (EGF) in the same datasets, despite the protein being smaller[15,16] (Figure 6). Moreover, whether these mutations can cause constitutive MET activation or render cells MET dependent has not yet been explored. Furthermore, with the exception of METex14, whether different types of MET activating lesions are associated with either specific responses to different classes of MET targeting agents, and/or distinct signal transduction signatures, has not been investigated.

Recent successes in targeting these smaller pieces of the "oncogenomic pie" (Figure 1), such as ROS1 in lung cancer[4,7] (a lesion which accounts for roughly 1% of all lung adenocarcinomas) should serve as a reminder: select the correct patient (with a molecularly selected target) and treat with the appropriate drug and clinical success can follow. Recent achievements in the management of NSCLC have been driven by such approaches[7,93,94].

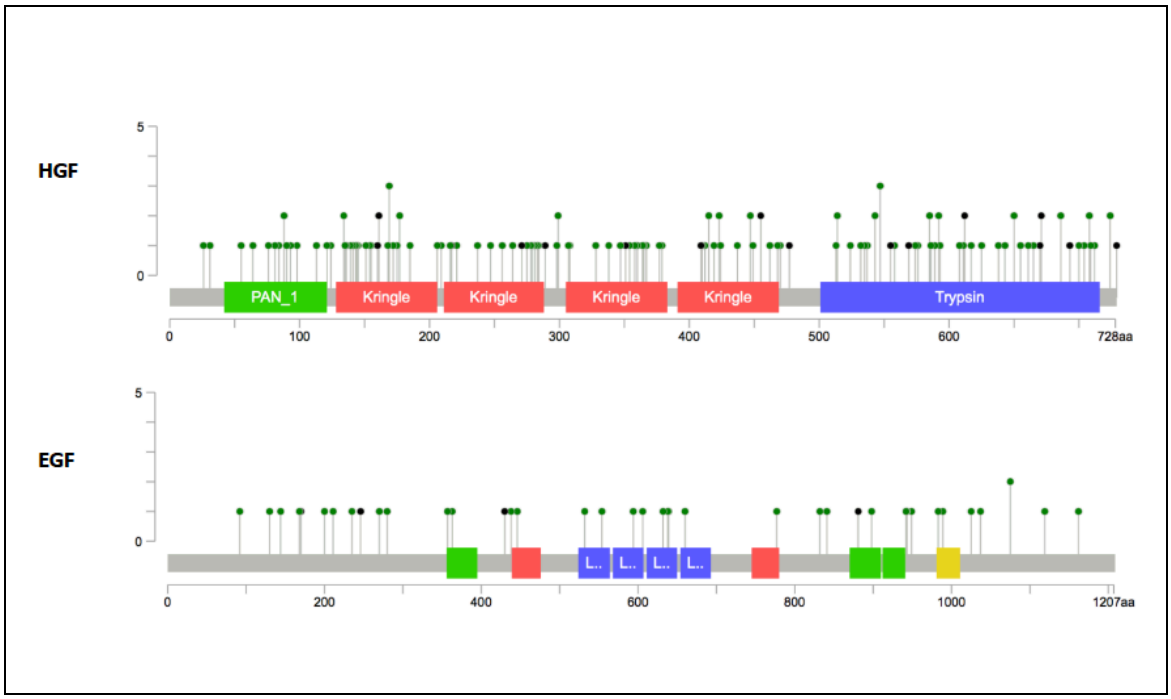

Figure 6. The frequency of mutations in HGF compared with epidermal growth factor (EGF) is vastly different using the same datasets[13,14]. Note the difference in size.

1.1.3.1 METex14 alterations.

Peschard et al initially reported that mutations of Y1003 in the binding domain of c-CBL, abolished c-CBL binding to MET, disrupting c-CBL-mediated degradation and leading to MET oncogenic activity[79]. Mutations in the METex14 splice sites were reported by Ma et al in small cell lung cancer and NSCLC[84,95]. Ubiquitination tags the MET receptor for degradation. As discussed previously, METex14 encodes part of the JMD containing Y1003, the c-Cbl E3 ubiquitin ligase binding site[86], and JMD mutations that disrupt splice sites flanking METex14 cause aberrant splicing.

Thus, Exon 14 mutations result in MET ex14 skipping, creating a truncated MET receptor that lacks the Y1003 c-Cbl binding site. Losing this binding site leads to decreased ubiquitination and degradation of the MET protein, sustained MET activation, and oncogenesis[96] (Figure 7). MET mutations affecting exon 14 splicing elements occur in up to 5% of lung adenocarcinoma[97], and result in a juxtamembrane-domain-lacking MET protein with extended half-life after HGF stimulation that has been considered an oncogenic driver event. They are also more likely to occur with concurrent MET genomic amplification (concurrent MET amplification have been reported in 15–21% of METex14+ NSCLC) [97–99].

Decreased degradation of the MET receptor caused by METex14 was thought to potentially cause MET overexpression in some tumours detectable by IHC[100], however recent published data suggests otherwise.

The French Thoracic Co-operative Intergroup investigated advanced NSCLC patients, aiming to determine whether NSCLC with high MET overexpression could define a subset of patients with a high rate of METex14 mutations[101]. Investigating 108 NSCLC samples with high MET overexpression (defined by an immunochemistry score 3+) they found that the rate of METex14 mutations in NSCLC with high MET overexpression was actually similar to the rate found in unselected NSCLC samples, i.e. high MET overexpression did not predict for the presence of METex14 splice mutations[101].

These data were replicated in an American data set, where, data was collected from a tri-institutional cohort from Lung Cancer Mutation Consortium (LCMC)[102]. Guo et al confirmed MET IHC as a poor screen for METex14 mutations in lung adenocarcinomas, however, in addition, they also noted that the same was true for MET amplification: high MET overexpression did not predict for the presence of MET amplification[102].

In reality, there is high diversity of METex14 alterations, as an extremely diverse set of mutations (point mutations, insertions/deletions (indels) or large deletions) can all result in similar biology which relies on increased MET activity. This presents an ongoing challenge for diagnostic testing: it makes these alterations hard to detect by DNA sequencing in clinical practice.

For example, base substitutions (or indels) can disrupt several gene positions which are important for splicing out introns flanking METex14, including the branch point, polypyrimidine tract, 3' splice site of intron 13, and the 5' splice site of intron 14[100]. Furthermore, point mutations or deletions within METex14 can affect the Y1003 residue, which results in c-Cbl binding site loss-of-function, without even causing METex14 skipping[99,103,104]. DNA-based broad, hybrid-capture next generation sequencing (NGS) is now used tool in clinical practice[105], however, in reality, this is a platform and not a standardised test: detection of a specific genomic alterations will always depend on the primers designed and used in the NGS panel. Given the diversity of METex14 alterations, it certainly cannot be assumed that these METex14 variants will be equally detected.

While many cases of METex14 alterations are found in lung adenocarcinomas (up to 5%[97]), these events have a much higher reported incidence in pulmonary sarcomatoid carcinomas, where approximately 20–30% of these tumours have been shown to harbour METex14 alterations[97,106]. Pulmonary sarcomatoid carcinomas also have a higher reported incidence rate of MET amplification[93], suggesting that consideration

should be given to enrichment for this subgroup of patients in the design of future MET-targeted studies.

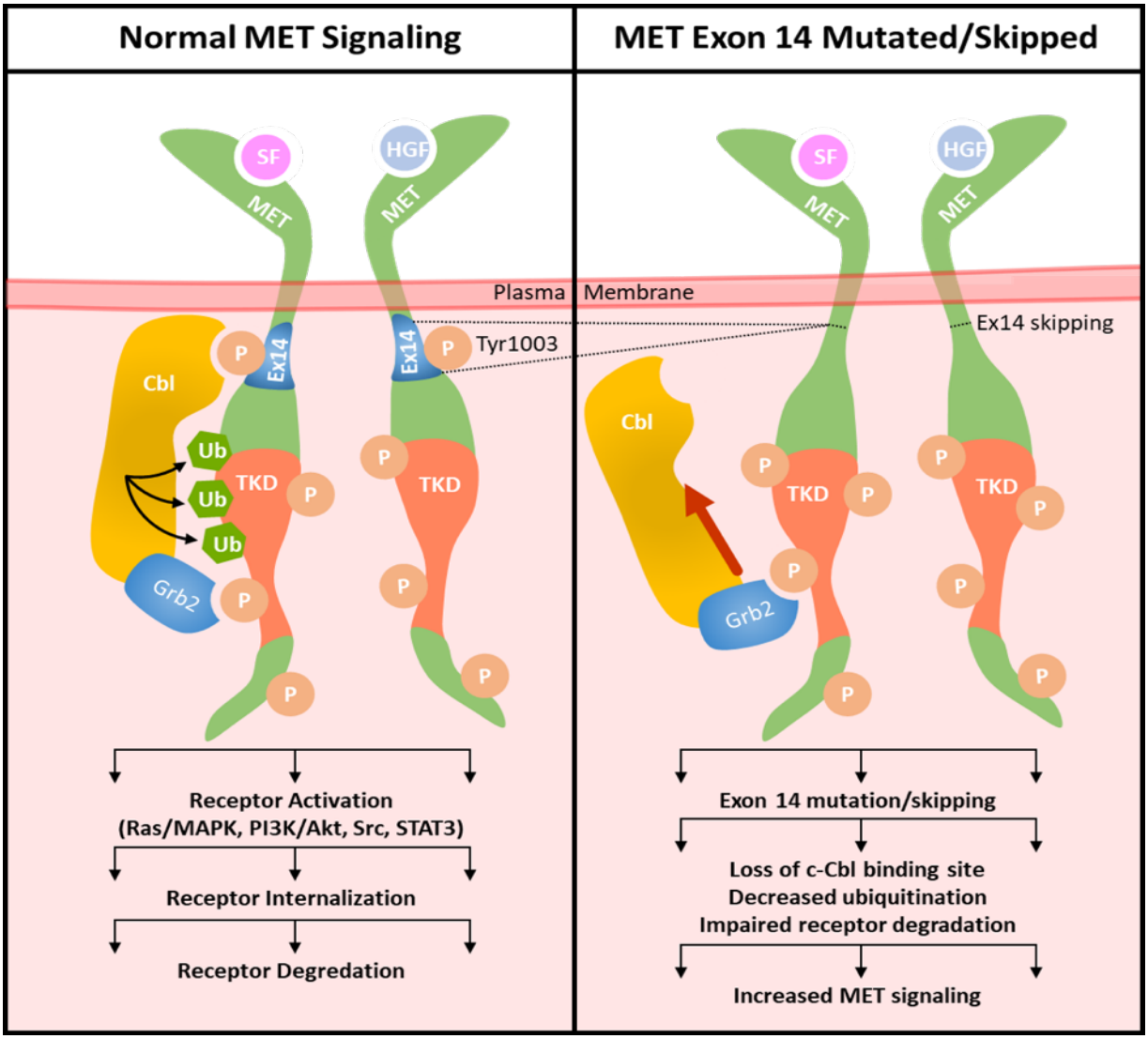

Figure 7. MET Exon 14 mutation leads to loss of c-CBL binding site and increased MET signalling.

1.1.3.2 Learning from past failures.

MET has been the focus of therapeutic studies in lung cancer for a number of years. Pre-clinical[20,107] and recent clinical evidence suggests that targeting the MET receptor can

elicit meaningful therapeutic responses in carefully selected patients[39,108]. In reality however, clinical studies on MET-targeting cancer therapies have produced mixed results. Phase III randomized control trials, for instance, undertaken with MET inhibitors have ultimately proved disappointing[36,109]. However, the recent emergence of splicing alterations of MET ex14 in NSCLC as a primary driver, and subsequent clinical success of TKI crizotinib in patients with this genomic aberration, has certainly reinvigorated interest in the development of MET inhibitors in NSCLC[39,40,108].

Typically, clinical trials of MET-targeted therapies have taken two approaches: monoclonal antibody therapy, directed against the MET receptor or HGF ligand, and tyrosine kinase inhibition (Figure 8).

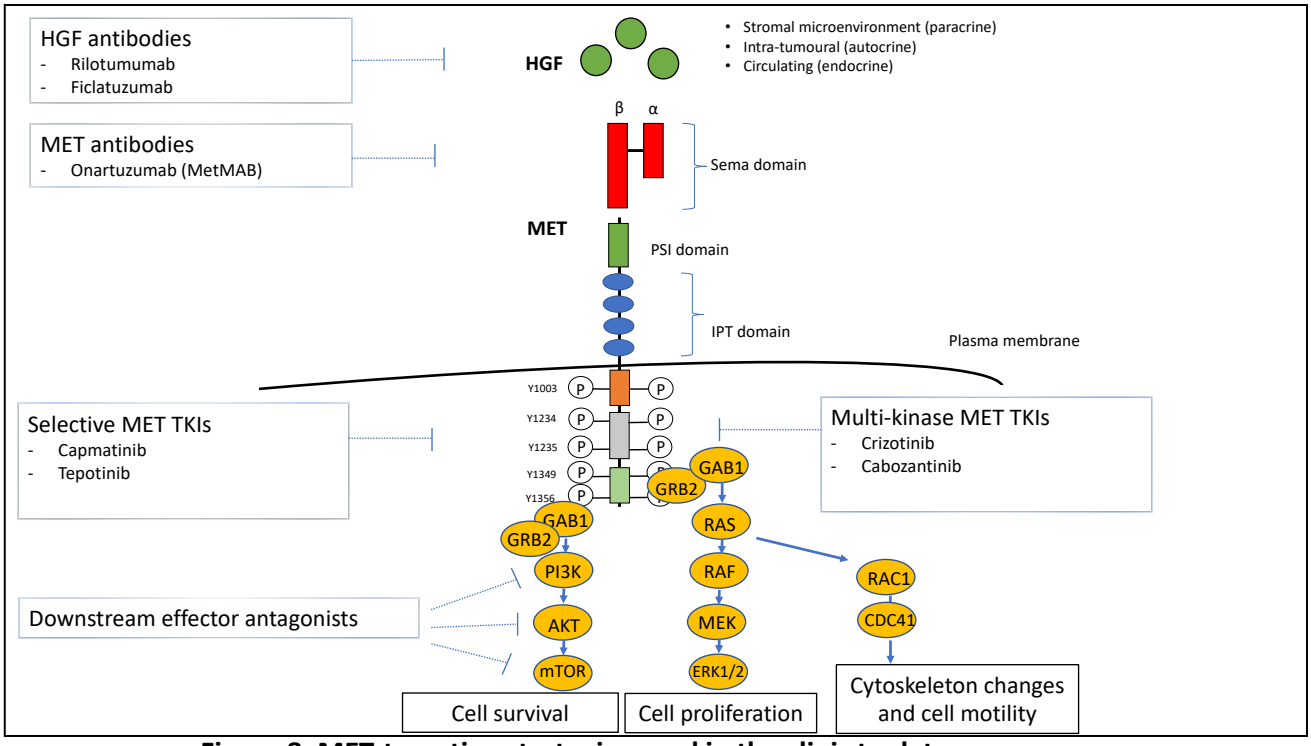

Figure 8. MET-targeting strategies used in the clinic to date.

The failure of MET-targeted therapy in the phase III setting is multifactorial. Poor drug choice, coupled with inadequate patient selection and variable assay use are all reasonable critiques. Two studies highlight this expertly.

In the METLung trial, Spigel et al[109] investigated second-line onartuzumab (a monoclonal antibody that binds the extracellular domain of MET) +/- erlotinib (the epidermal growth factor receptor (EGFR)-targeted drug) in tumours demonstrating high MET protein expression by centrally-confirmed immunohistochemistry (IHC). Of note, EGFR mutation status was not used as an inclusion criterion.

The phase II results[110] suggested that MET-IHC status could predict clinical benefit from the onartuzumab/erlotinib combination, thus the METLung phase III trial was designed to include patients with MET-IHC 2+/3+ in ≥50% tumour cells. The METLung phase III study, however, was terminated early due to a lack of clinically meaningful efficacy; ultimately, it failed to demonstrate improved clinical outcomes, with shorter overall survival (OS) in the onartuzumab arm, compared with erlotinib in patients with MET-positive NSCLC[111].

In this trial, patients were deemed 'MET-positive' using central IHC testing: roughly 80% of each arm was MET IHC2+, and 20% MET IHC3+, thus suggesting that this assay is ineffective. In addition to this, the use of a TKI which targets EGFR, in combination with a MET-targeting antibody, in a population where 11% of each arm were EGFR mutation positive is perplexing. If the hypothesis was that MET was the primary oncogenic driver, then there was no clear justification for combining onartuzumab with erlotinib.

This study perfectly highlights the futility of using targeted therapies in an unselected NSCLC patient population.

In the phase III MARQUEE study, Scagliotti et al[112] investigated the combination of tivantinib and erlotinib in advanced non-squamous NSCLC. Tivantinib (or ARQ 197) is an orally available selective small molecule MET TKI[113,114], and this was combined with

erlotinib and compared 1:1 with erlotinib +/- placebo in an unselected cohort of patients with advanced non-squamous NSCLC.

Of note, MET expression status/ MET FISH status was unknown in 55-60% of patients in each arm all patients. In addition to this, collectively, 35% of patients on each arm were documented mutant EGFR (10%) or mutant KRAS (25%). The MARQUEE study was discontinued for futility at the interim analysis, and ultimately did not meets its primary endpoint, as OS did not improve, although final analysis showed some improvement in progression-free survival (PFS) and overall response rates (ORR) were improved. Additionally, the tivantinib treatment group did show significant OS improvement in the subgroup with MET-high expression, essentially recapitulating the phase II MetMab study results. This study failure highlights the importance of evaluating drugs in the appropriately selected patient cohort.

Another phase III trial of tivantinib plus erlotinib compared with tivantinib plus placebo in previously treated Asian patients with non-squamous NSCLC was discontinued early due to toxicity concerns (due to the incidence of interstitial lung disease), underscoring the important of selecting the appropriate compound(s) in clinical trial design[38].

In addition to these critiques, the role of HGF as a cause of resistance to MET-TKIs, was also not taken into consideration in any of these clinical studies. In reality, there has been a paucity in studies to understand the mechanistic basis of these clinical trial failures.

1.1.3.3 Defining 'MET-positive' disease.

Another challenge which is staggering progress in MET-driven cancer research, is that in the literature, to date, there is no consensus on the definition of 'MET positive' cancer. Indeed, the most appropriate method and criteria for defining 'MET positivity' are uncertain. MET IHC was initially investigated as a biomarker for MET activity, however the disappointing experience with onartuzumab and erlotinib in MET-overexpressing

NSCLCs emphasises the point that, in isolation, MET overexpression is not an optimal predictive biomarker of response to MET-directed therapy[111].

In reality, overexpression of MET occurs with a high frequency (35%–72%) in NSCLC tumours. For example, in one recent study which included 222 NSCLC samples, 37% were scored as IHC2+ for MET expression[115]. The group found that neither MET expression nor the gene amplification status selected patients for MET targeting therapies, as no correlation with MET activation status was observed[115]. Another study found that expression of c-Met was found in all 23 of the NSCLC tumours examined, and most of the cell lines (89% of n=9). Furthermore, sixty-one percent of tumour tissues strongly expressed total c-Met, which was confirmed as particularly common in adenocarcinoma (67%)[84].

There is also no consensus regarding the definition of 'MET-positive' NSCLC by gene copy number. In theory, increases in MET copy number are postulated to cause excessive amounts of MET protein, and subsequent auto-aggregation, ligand-independent MET signalling and subsequent oncogenic addiction to the MET pathway[100]. The challenge is that changes in MET copy number represent a continuous variable, and this variable has been assessed in different ways, defined as either the ratio of MET relative to another region of chromosome 7, such as CEP7 (to show true amplification), or as the absolute number of MET copies (which can also be increased by polysomy)[100].

Thus, an ongoing difficulty with MET copy number studies has been to define a threshold for any given methodology above which a MET-directed therapy will likely be active. It is a persistent challenge with any defined cut-off criteria: a less stringent criteria could include more patients but then dilute the clinical benefit; conversely, a more stringent criteria could identify fewer patients, but include those patients who may derive the greatest clinical benefit. The risk is always the potential of excluding patients who may still derive some benefit.

The cut point for high MET gene copy number in the literature ranges between 3 and 5; some studies use in-situ hybridization, and others RT PCR. Tong et al[97] recently identified four distinct patterns of MET copy number alterations in a sample set of six hundred eighty-seven NSCLCs:

1. High-level amplification, defined as clustered MET signals or *MET*/CEP7 ratio≥ 5,
2. Polysomy: MET signal ≥ 5, without gene amplification
3. Low-level amplification/ high gene copy number: 2 < *MET*/CEP7 < 5, MET signal ≥ 5
4. Low-level amplification/low gene copy number: 2 < *MET*/CEP7 < 5, MET signal < 5.

Given its lack of overlap with other oncogenic drivers, high levels of amplification (MET/CEP7 ratio ≥5 by FISH) are thought to potentially represent a driver state of its own[97].

A recent small series further emphasised the significance of choosing patients with high copy number, as demonstrated ORR to crizotinib differed dramatically between cases with different MET/CEP7 ratios (for a ratio of ≥1.8 to < 2.2, ORR 1⁄4 0%; for a ratio of >2.2 to <5, ORR 1⁄4 17%; and for a ratio of ≥ 5, ORR 1⁄4 67%).[116]

Noonan et al used oncogene overlap analysis to further define FISH MET/ CEP7 ratio of 5 or higher as a "MET-positive" group with no oncogenic overlap, as this criteria was associated with the highest response rate to MET inhibition, the group concluding that this represents the clearest definition of a MET copy number gain–addicted state[117].

One potential drawback of using the MET/CEP7 gene ratio is that this technique may not identify all amplified patients due to the unique pathophysiology of NSCLC, and in some cases, amplicons occur that may include the centromere control protein and the MET gene or the centromere protein but not the MET gene; in the latter case, the ratio may be falsely lowered[118].

Regardless, identifying the appropriate patients, with true high-level focally-amplified *MET*, and treating them with the appropriate MET-targeting strategy, will likely be the key to designing an informative biomarker-driven clinical trial in *MET*-driven NSCLC.

1.1.3.4 MET with success

The recent clinical successes in MET-targeting are largely related to targeting METex14 alterations. Initial clinical reports documented the impressive responses to the MET inhibitors crizotinib and cabozantinib in patients with lung adenocarcinoma and METex14 alterations[98,99,119–125]. Consequently, a number of clinical trials testing the activity of MET inhibitors in patients harbouring METex14 and MET amplification are now under way.

Drilon et al[126] have recently published the METex14 data from the innovative PROFILE-1001 study, reporting on the activity and safety of crizotinib (a multi-kinase inhibitor with potent activity against MET[127]) in 69 patients with advanced NSCLCs harbouring MET exon 14 alterations[126]. The early reports of this study documented encouraging responses[98], however, the success reported in the subsequent *Nature* paper publication is more muted: ORR was 32% (95% CI, 21–45) among 65 response-evaluable patients treatment-naive or chemotherapy-refractory MET ex14-aberrant NSCLC[126].

This is the first prospective study to characterize the activity of a MET inhibitor in a dedicated cohort of patients with MET exon 14-altered NSCLC and local primarily DNA- or RNA-based NGS was used[126]. In addition to a 32% ORR, median duration of response of 9.1 months, and median PFS of 7.3 months was reported.

These outcomes are comparable with first-line platinum platinum-doublet chemotherapy (ORR, 31–35%; median time to progression, 4.8–6.2 months)[128,129], but exceed responses observed with second-line chemotherapy (ORR, 7–23%; median PFS, 2.4–4.5 months)[130,131]. However, they are noticeably inferior to reported outcomes observed with first-line chemo-immunotherapy combinations in unselected NSCLC[132],

and overwhelmingly inferior to the ORR 60–80% achieved with targeted therapy for other NSCLC drivers such as ALK, EGFR, and ROS1[93,94,133].

MET exon-14-alterations are diverse, and accordingly, MET14 alteration NSCLCs are a heterogeneous group. The possibility of sub-populations perhaps driving down the response rate was explored, however, in an exploratory analysis of this series: the group found, however, that mutation type and splice-site region did not affect outcomes, and that MET copy number was not a major differentiating factor[126].

The updated data presented on patients with MET amplified NSCLC treated with crizotinib in PROFILE 1001 were similarly disappointing[134]. Rapid and durable responses were observed, however, ultimately reported ORR was 40% in patients classified as high-level amplification, defined as MET/CEP7 ratio$\geq$ 5.

Altogether, these ORRs of 30-40% in selected cohorts suggest there are elements of trial design that require further modification: perhaps there are elements of resistance that are currently not being considered in the design of MET-driven clinical trials.

1.1.3.5 Increasing specificity, increasing clinical efficacy.

It is certainly true that the type of MET inhibitor used to treat MET-exon-14-altered lung cancers may affect clinical outcomes. Recently, more potent and selective MET-targeting agents are yielding impressive clinical results – two highly specific, potent and selective MET inhibitors, in particular, have recently demonstrated promising clinical efficacy: capmatinib[135] and tepotinib[136]. Indeed, both of these compounds have been granted Breakthrough Therapy designation from the FDA based on the preliminary findings of their respective phase II trials presented at the American Society of Clnical Oncology (ASCO) Annual Meeting 2019[137,138].

The phase II GEOMETRY trial is examining capmatinib across several cohorts, with cohort 4 and 5b selected for presentation at ASCO. Cohort 4 contained pretreated patients with METex14 alterations in the second or third-line setting (n = 69) while cohort 5b included

treatment-naive patients (n = 28). Encouragingly, capmatinib showed an ORR of 67.9% (95% CI, 47.6%-84.1%) in treatment-naive patients with METex14-altered NSCLC. Furthermore, responses were seen in patients with intra-cranial disease as 54% the patients with brain metastases at baseline experienced an intracranial response with capmatinib (7 of 13; 54%); the intracranial disease control rate (DCR) was 92.3% (12 of 13). In pre-treated patients with METex14 alterations, the ORR was 40.6% (95% CI, 28.9%-53.1%), the disease control rate (DCR; ORR plus stable disease) was 78.3% (95% CI, 66.7%-87.3%).

Tepotinib is another highly specific potent MET-selective agent generating robust and durable clinical response in patients with METex14 alterations in the VISION trial. The phase II VISION trial, also presented at the ASCO annual meeting, consisted of 2 cohorts: cohort A enrolled patients with METex14 skipping mutations, and cohort B included those with METamplification[138]. The first cohort included a total of 87 patients with alterations that had been identified by either liquid biopsy (n = 57) or tumor tissue biopsy (n = 58), 33 patients were treatment-naïve and 54 were previously treated[138]. Across all lines of treatment, the ORR in liquid biopsy-identified METex14-positive tumors was 50%, the median DOR was 12.4 months and the DCR was 66.7%. For those identified by tissue biopsy, the ORR was 45.1% and the median DOR was 15.7 months with a DCR of 72.5%. In the second-line and beyond, the ORR was 45.2%. For those with tissue biopsy assessed tumors, the ORR was 44.4% and 50%, in the first- and second-line, respectively. In the second-line or greater, the ORR by IR was 45.5%.

These data highlight some important points to be considered when treating a select cohort of MET-targeted patients: clinical efficacy appears to greatest when

- using more-specific and more potent MET-targeting agents, and
- when these potent drugs are deployed earlier in treatment i.e. when these MET-specific drugs are given in the first-line setting, patients gain the most benefit.

While the recently published METex14 crizotinib results from PROFILE 1001[126] have been somewhat disappointing, the trial data of tepotinib and capmatinib are clear: MET-positive NSCLC patients should be genomically-selected upfront, and treated with the appropriate MET-specific agent to yield the greatest benefit in the clinical setting.

1.1.4 Resistance to MET TKIs

1.1.4.1 HGF causes upfront resistance to MET inhibitors.

We, and others, have demonstrated that overexpression of MET's ligand HGF, causes resistance to MET inhibitors in MET-addicted NSCLC cell lines[34,139]. Methods suggested to overcome this resistance have included using a small molecule inhibitor of pro-HGF activation[139] or using HGF-antibody ficlatuzumab[34], neither of which are current clinically feasible solutions. While recent studies that have suggested AKT/PI3K re-activation as a possible driver of HGF-induced drug resistance, the molecular basis for this resistance has not yet been determined. Furthermore, whether HGF binding is shifting the conformation of the MET receptor, and thus affecting how MET-targeted TKIs bind to the receptor has not been considered.

There are clinical data suggesting the HGF can be detected in a significant proportion of lung tumours. For instance, one group demonstrated that seventy percent of resected lung tumours showed strong HGF expression[140]. Additionally, there are pre-clinical data showing that HGF produced in lung fibroblasts enhances NSCLC cell survival and promotes tumour progression[141].

In spite of this, the significance of the role of HGF excess has not been explored in lung cancer research, and indeed the presence of HGF remains largely ignored in the design, to date, of MET-driven clinical trials.

Given that HGF can be supplied by either the tumour itself or the tumour microenvironment[32], secreted by cells such as fibroblasts[33], HGF-mediated resistance to MET TKIs could be a critical unidentified cause for the primary failure of MET-TKIs in the clinic.

1.1.4.2 Acquired resistance to MET TKIs

A key challenge of the precision medicine era is understanding and addressing the inevitable development of drug resistance that occurs with molecularly targeted agents. The landscape of MET-specific targeting agents remains underdeveloped, and consequently current knowledge of mechanisms of resistance to MET TKIs is limited.

Recent data has revealed, broadly, two distinct classes of resistance mechanism: on-target resistance, and off-target bypass tract activation.

Table 1 summarises reported clinical knowledge to date. Documented on-target alterations include mutations in MET (including D1246, Y1248H, H1094Y, G1163R, L1195F, L1195V, D1228N, Y1230H, and Y1230S), METex14 amplification, and HGF amplification[142–147]. Off-target bypass mechanisms of resistance include amplification of KRAS, BRAF, EGFR, KRAS mutations, MDM2 amplification, and EGFR amplification[142–144,148].

It is clear, that we are only starting to understand the complexity of these resistance mechanisms, yet they do bear a striking resemblance to the known resistance mechanisms of other oncogenic addicted lung cancers, such as EGFR-driven NSCLC[149].

Perhaps, an important approach to consider will be using combination of small molecule MET TKIs with neutralising antibodies that inhibit the MET receptor, or its ligand, HGF[34], thus allowing for total blockade of the MET axis. Nonetheless, it is clear that oovercoming these multiple complex mechanisms of acquired MET TKI resistance in METex14 and MET amplified NSCLC with novel therapeutic strategies will clearly be a challenge moving forward.

	Resistance alteration	MET inhibitor	Refs	
MET EXON 14	HGF amplification	Crizotinib	140	On-target
	D1228N	Crizotinib Gleasatinib	140, 144, 141	
	D1246N	Crizotinib	142	
	Y1230H, Y1230S	Crizotinib	141, 145	
	MET G1163R	Crizotinib Gleasatinib	141	
	L1195V	Gleasatinib	141	
	H1049Y	Gleasatinib	141	
	MET exon 14 amplification	Geasatinib	141	
	EGFR amplification	Crizotinib	140	BYPASS
	KRAS amplification	Crizotinib	143	
	KRAS G12S/ G13V	Crizotinib	140	
	RASA1 S724	Crizotinib	140	
MET amplification	MET D1228V	Savlotinib	143	On-target
	KRAS mutation	Crizotinib	142	BYPASS
	HER2 amplification	Crizotinib	142	
MET Fusion	Y1248H	Crizotinib	142	

Table 1. Summary of current known mechanisms of resistance to MET TKIs in Met exon 14 and MET amplified NSCLC.

1.2 Conclusion

NSCLC is no longer a single-disease entity. It is instead, being divided into a collection of molecularly-defined tumours, each with different clinical characteristics and treatment options. The clinical failure of MET–targeted agents underscores the importance of appropriate predictive biomarkers for patient stratification in the new era of personalized medicine. Shaw et al[4] have previously demonstrated that it is possible to conduct trials in small subgroups of patients with NSCLC and demonstrate practice-changing results. We intended to further understand and interrogate MET oncogene addiction in lung cancer, with the final aim of designing a biomarker-driven trial in an appropriately selected cohort of NSCLC patients.

1.3 PhD Objectives

The primary objective of my PhD was to confirm HGF as a mechanism of resistance to MET TKIs in *in vitro* models of MET-dependence, to explore the potential of MET as a primary oncogenic driver in lung cancer and to develop strategies to overcome HGF-induced primary MET TKI resistance in lung cancer.

In summary, I aimed:

- To identify *in vitro* models of MET-dependence
- To assess the impact of MET activation mechanism on response to various MET targeting agents
- To understand the role of HGF overexpression in resistance to MET inhibitors
- To characterise the subcellular distribution of MET as a function of activation mechanism
- To characterise the phosphoproteomic signatures of MET activation
- To develop a clinically feasible strategy to overcome *de novo* HGF-mediated resistance to MET TKIs.

2 Characterising *in-vitro* models of MET dependence

2.1 Introduction

Assessing the impact of MET activation mechanism on response to various MET targeting agents.

Vivanco et al have previously shown[150] that in the case of EGFR-dependent cancers (including NSCLC), the nature of the activating *EGFR* lesion defines distinct shifts in the conformational equilibrium of the receptor that determines whether conformation selective compounds (e.g. type I vs type II kinase inhibitors) can bind and inhibit *EGFR* effectively. Thus, we hypothesized that perhaps using different types of conformational selective compounds could produce different results in MET-driven lung cancer cells.

To address the question of whether MET is inhibited better with a type I inhibitor or a type II inhibitor in MET-dependant NSCLC, we compared the activity of various type I and type II MET TKIs in MET-addicted cells (Table 2). Type I TKIs (such as JNJ-38877605 and crizotinib) are ATP-competitive small-molecule TKIs that bind at the ATP binding site while in the active kinase conformation, while type II inhibitors (such as cabozantinib and SGX-523) bind at and/or near the ATP binding site in the inactive kinase conformation (Figure 9).

Both crizotinib and cabozantinib were initially developed as MET inhibitors, and are now used for other clinical indications. For instance, crizotinib is a potent oral small-molecule tyrosine kinase inhibitor of MET, ALK and ROS1 kinases[151], currently FDA-licenced for ALK, ROS1 and METex14 positive NSCLC. Cabozantinib is a multi-kinase inhibitor with potent activity toward MET and VEGF receptor 2, as well as RET, KIT, AXL, and FLT3[152], approved for the treatment of advanced renal cell carcinoma, and hepatocellular carcinoma. JNJ-38877605[153] and SGX-523[154], in comparison to these clinically approved compounds, are exquisitely selective MET ATP competitive tyrosine kinase inhibitors,

that were associated with renal toxicities which precluded their further clinical development.

Finding a clinically relevant strategy, thus, often dictated choice of compound used in different experimental models.

MET TKI	**Kinase binding**
Crizotinib	Type I (active conformation)
JNJ-38877605	Type I (active conformation)
Capmatinib	Type I (active conformation)
Cabozantinib	Type II (inactive conformation)
SGX-523	Type II (inactive conformation)

Table 2. Classification of reversible ATP-competitive MET kinase inhibitors based on crystal structures.

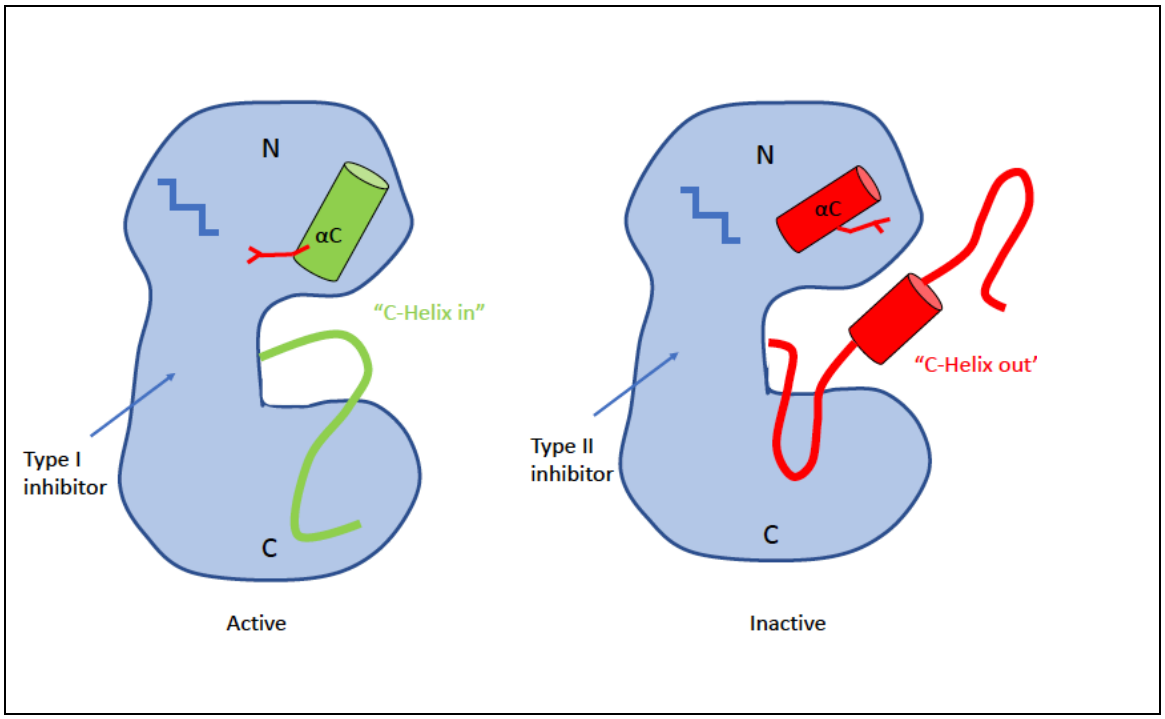

Figure 9. Illustration of the active and inactive conformations of MET tyrosine kinase domain. In the inactive state (right), the key αC helix is displaced, which breaks an important salt bridge between a glutamate in αC (red sticks) and a lysine in the ATP-binding site (blue sticks). In the active conformation (left), αC is moved in towards the centre of the N-lobe, so that this salt bridge forms to stabilise ATP binding. Type I inhibitors such as crizotonib and JNJ-38877605 bind to the active conformation (left), whereas type II inhibitors, such as cabozantinib bind only to the inactive conformation.

2.2 Results

2.2.1 MET amplified cell lines are sensitive to type I and type II MET tyrosine kinase inhibition.

Sensitivity to various MET tyrosine kinase inhibitors was assessed in MET-amplified cancer cell lines. MET-amplified NSCLC cell line EBC-1 was sensitive to both type I and type II MET tyrosine kinase inhibition, demonstrable from doses as low as 25nM (Figure 10). With regards to cell death and MET phosphorylation, no significant difference was noted between type I and type II MET tyrosine kinase inhibition. Indeed, maximum amount of cell death was achieved with as little as 25nM of either SGX-523 and JNJ-38877605, and remained at this level with doses as high as 200nM. However, downstream signalling revealed interesting variations, as it appeared type I inhibitor JNJ-38877605 was more potent at suppressing phosphorylation of the adaptor protein GAB-1 and of the mitogen-activated protein kinase (MAPK) pathway (as judged by pERK1/2 levels) (Figure 10).

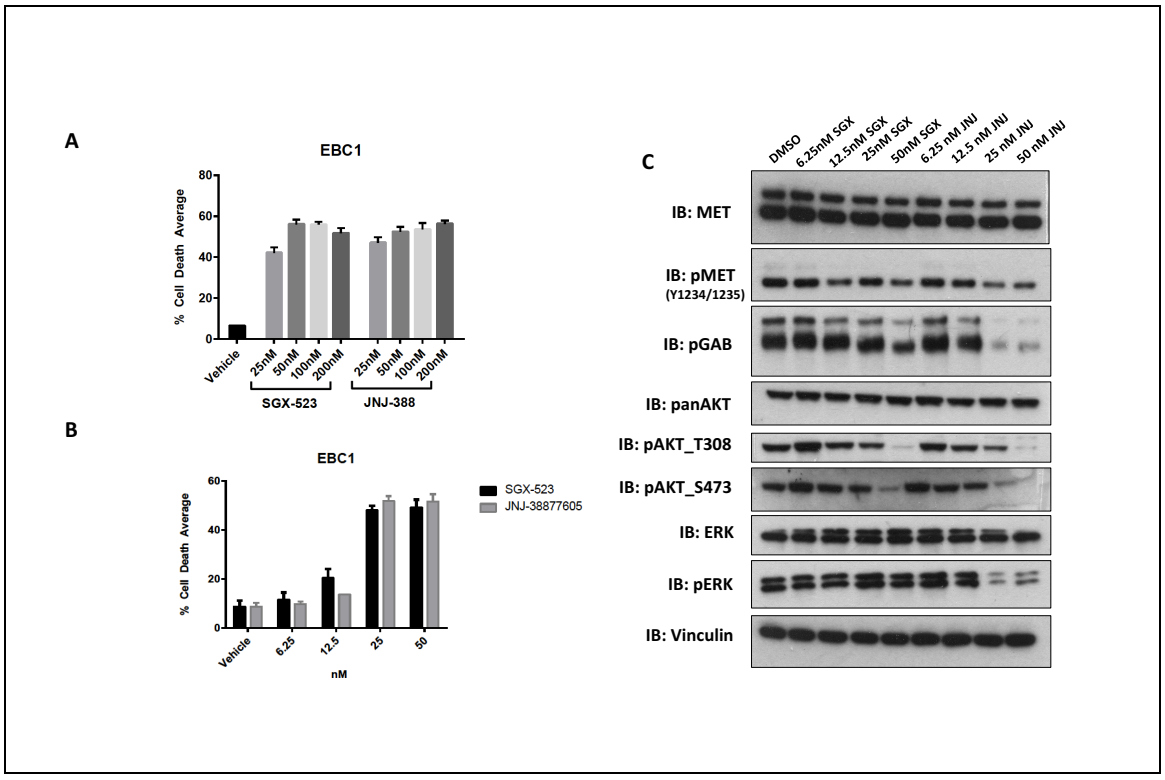

Figure 10. MET amplified cells are sensitive to type I and type II MET tyrosine kinase inhibition. (A and B) Analysis of the responses of MET amplified cell line, EBC-1, to 72h treatment with MET inhibitors, JNJ-38877605 and SGX-523. Cell death percentages (mean ± SEM) in A and B were assessed via automated trypan blue method (ViCell), and is expressed as the fraction of stain-positive cells. (C) Western blot analysis of the responses of MET amplified (EBC1) cell lines to 8h treatment with MET inhibitors, type I inhibitor JNJ-38877605 and type II inhibitor SGX-523 respectively.

This experiment was repeated in EBC1 cells with an alternative type II tyrosine kinase inhibitor, cabozantinib. Again, comparable levels of robust cell death were observed using both type I and type II MET TKIs (Figure 11A). However, there were clear differences in phosphorylation of MET, as on western blotting cabozantinib appeared to be more potent than JNJ-38877605 in inhibiting MET phosphorylation (Figure 11B), despite inducing comparable cell death at the same dose.

Sensitivity to MET tyrosine kinase inhibition was subsequently confirmed in MET-amplified NSCLC line H1993 and MET-amplified gastric cancer cell line GTL16 (Figure 11).

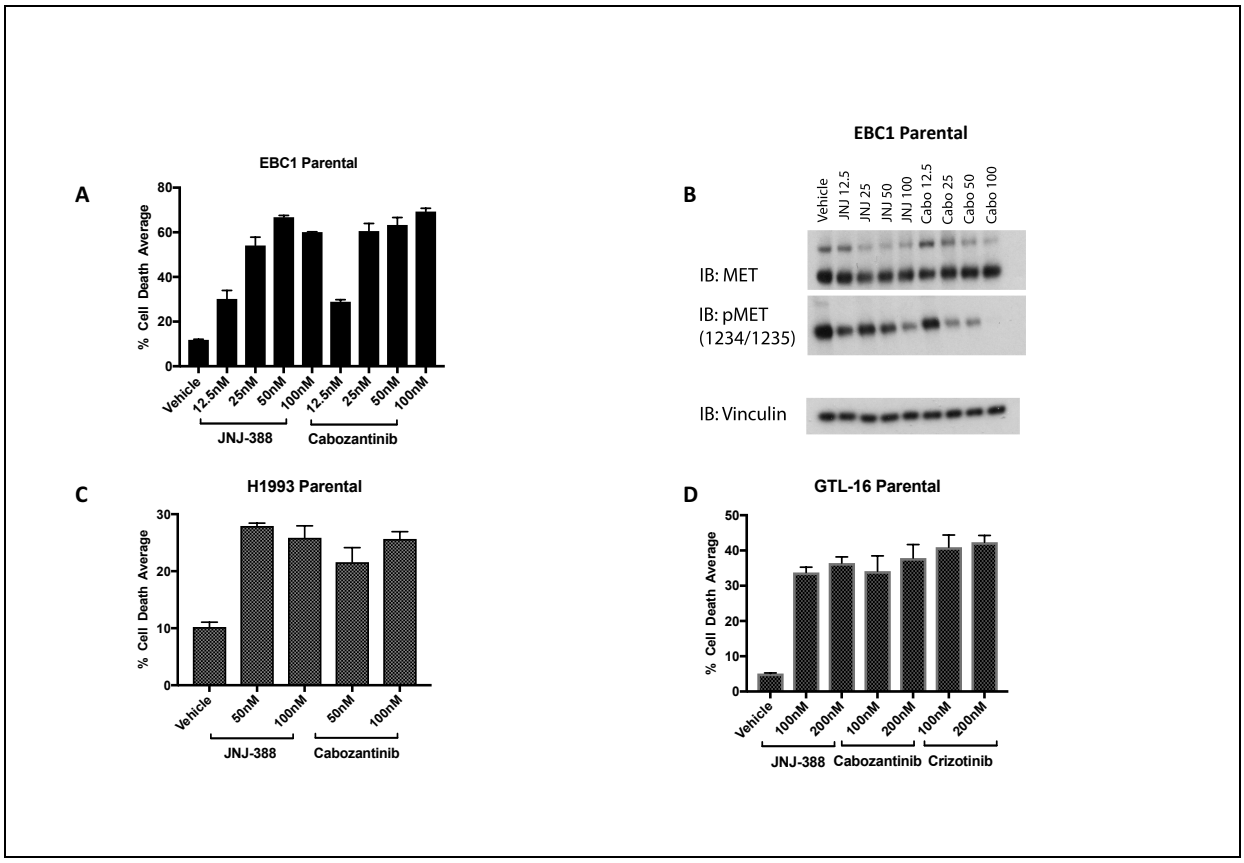

Figure 11. MET amplified cells are sensitive to type I and type II MET tyrosine kinase inhibition. (A, C, D) Analysis of the responses of MET amplified cell lines (EBC1, H1993, GTL-16 respectively) to 72h treatment with type I MET inhibitors JNJ-38877605 or Crizotinib, and type II inhibitor Cabozantinib. Cell death percentages (mean ± SEM) were assessed via automated trypan blue method (ViCell). (B) Western blot analysis of the responses of MET amplified (EBC1) cell lines to 6h treatment with MET inhibitors, JNJ-38877605 and Cabozantinib respectively. In this instance, Cabozantinib appears more potent than JNJ-38877605 in inhibiting MET phosphorylation.

Clinically relevant MET compounds crizotinib and capmatinib (a highly selective and potent MET inhibitor), were then tested in MET amplified cell line EBC-1 and GTL-16, with comparable levels of cell death again observed from low doses (Figure 12).

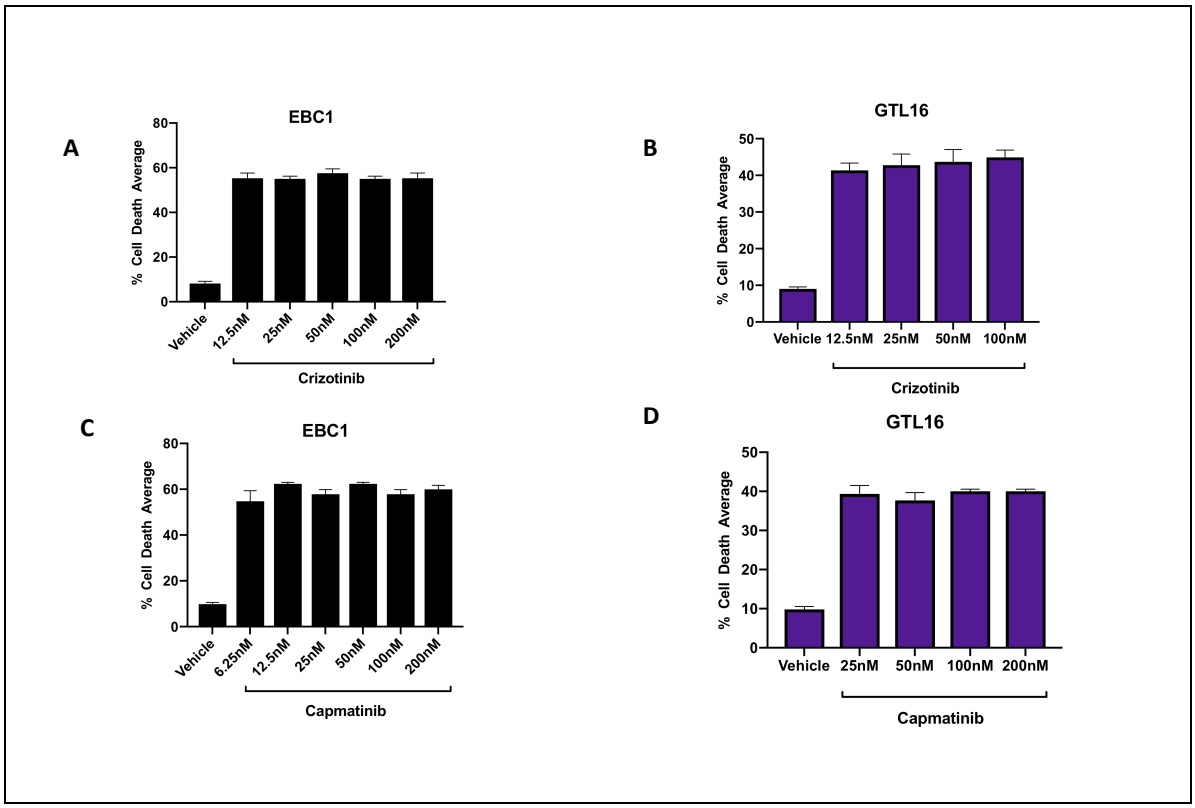

Figure 12. MET amplified cells are sensitive to type Ia and type Ib MET tyrosine kinase inhibition. (A - D) Analysis of the responses of MET amplified cell lines EBC1 and GTL-16 respectively) to 72h treatment with MET inhibitors, type Ia inhibitor, crizotinib and type Ib inhibitor, capmatinib. Cell death percentages (mean ± SEM) were assessed via automated trypan blue method (ViCell).

2.2.2 Exon 14 splicing mutation cells insensitive to MET-TKI inhibition

Sensitivity to various MET tyrosine kinase inhibitors was assessed in METex14 skipping cancer cell lines H596 and Hs746t. Hs746t, a gastric cancer METex14 skipping cell line and H596, a NSCLC METex14 skipping cell line were both, respectively, insensitive to high dose single agent MET-TKI inhibition, at various doses (Figure 13).

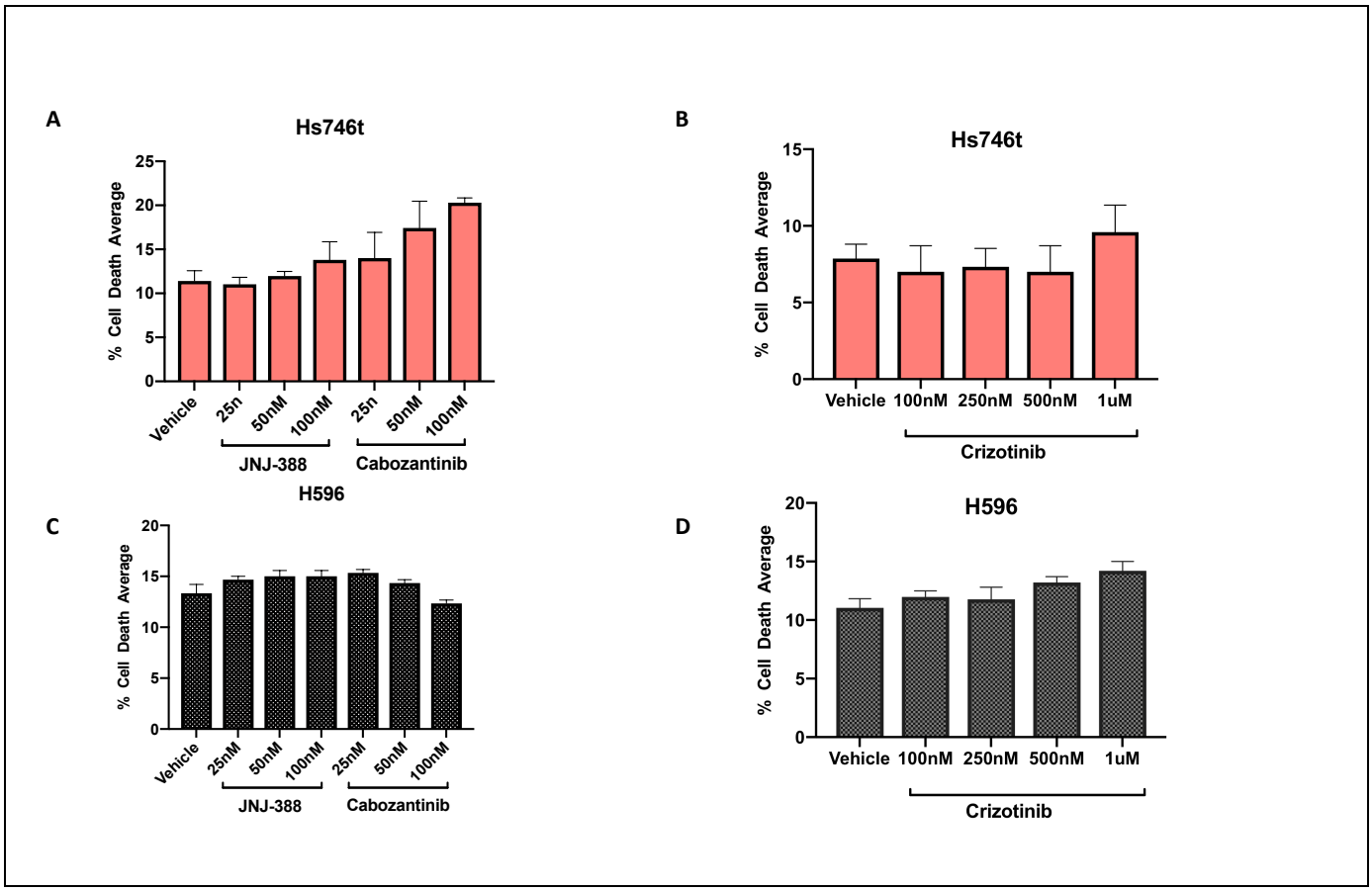

Figure 13. MET exon 14 skipping mutation cells are insensitive to type I and type II MET tyrosine kinase inhibition. (A, B, C, D) Analysis of the responses of MET exon 14 splicing cell lines (Hs746t (gastric) and H596 (NSCLC) respectively) to 7 days treatment with MET inhibitors, type I inhibitors JNJ-38877605, Crizotinib and type II inhibitor Cabozantinib. Cell death percentages (mean ± SEM) were assessed via automated trypan blue method (ViCell).

2.3 Discussion

2.3.1 MET amplified cell lines are sensitive to type I and type II MET tyrosine kinase inhibition.

We aimed to address the question of whether MET (when highly over-expressed through high level gene amplification) is inhibited differently if using different conformation-selective MET TKIs. To do this, we treated a panel of MET-amplified cancer cell lines with type I inhibitor or type II MET kinase inhibitors. As previously mentioned, type I TKIs (such as JNJ-38877605 and Crizotinib) are ATP-competitive small-molecule TKIs that bind at the ATP binding site while in the **active** kinase conformation, while type II inhibitors (such as Cabozantinib and SGX-523) bind at and/or near the ATP binding site in the **inactive** kinase conformation.

Vivanco et al[150] have previously shown, that in the case of EGFR-driven cancers (including NSCLC), the nature of the driving oncogene matters. Using lung cancer and GBM models, Vivanco et al demonstrated that the nature of the driving EGFR lesion can lead to distinct shifts in the conformational equilibrium of the receptor, and this determines whether conformation specific compounds (i.e. type I or type II kinase inhibitors) can bind and inhibit EGFR effectively[150]. More specifically, the group noted that EGFR mutations in lung cancer target the intracellular kinase domain (KD)[150]. EGFR mutations in GBM, on the other hand, tend to cluster in the extracellular (EC) domain, and tellingly, in contrast to KD mutants found in lung cancer, glioma-specific EGFR EC mutants are poorly inhibited by EGFR inhibitors that target the active kinase conformation (drugs such as erlotinib)[150]. Inhibitors which bind to the inactive EGFR conformation, on the other hand, potently inhibit EGFR EC mutants and induce cell death in EGFR mutant GBM cells[150].

We sought to assess if MET-driven NSCLC cancer cells demonstrated any similar specificities regarding ATP-site competitive MET kinase inhibitors. Consequently, we initially began experiments using the highly selective type I and II inhibitors JNJ-

38877605[153] and SGX-523[154], which are exquisitely selective MET targeting-compounds compared to the clinically approved compounds, crizotinib and cabozantinib. We then extended our drug panel to include these clinically relevant compounds, including capmatinib, which became commercially available at the end of the project.

We have demonstrated that in the setting of MET-amplified cells, both types of MET TKIs appear to cause comparable cell death in MET-amplified cell lines, which confirms that these cells are addicted to MET signalling (Figure 10-12). Furthermore, once robust cell death is achieved (for example with JNJ-38877605 at 25nM in Figure 10), increasing the dose of MET TKI does not appear to significantly alter the extent of cell death in these MET-addicted cells, a phenomenon that was repeated with all MET TKIs trialled in these cells (in a 3-day or 5-day assay).

Looking at the biochemical effect of these MET TKIs, we noticed some inconsistencies in pMET changes in response to MET TKI treatment. pMET was not a robust PD marker of MET TKI activity in the models used, particularly at low doses that were already biologically active. For instance, on initial testing, no significant difference was noted between type I and type II MET tyrosine kinase inhibition (SGX-523 and JNJ-38877605 in Figure 10); here no significant drop is seen in pMET, even at doses of drug at which we see robust cell death. Intriguingly, Initially, it appeared the changes alone were in downstream signalling, as type I inhibitor JNJ-38877605 was more potent than SGX-523 at suppressing the mitogen-activated protein kinase (MAPK) pathway, as evidenced by reduced phosphorylation of pGAB-1 and p-Erk1/2 (Figure 10).

We tested another type II inhibitor, cabozantinib, in the same MET-addicted NSCLC cell line, and in this case, cabozantinib appeared more potent than JNJ-38877605 in inhibiting MET phosphorylation (Figure 11). Yet, there is still a lagging effect, with the reduced signal in pMET seen fully with cabozantinib at 100nM, yet we know that comparatively at cabozantinib 25nM there is robust and similar levels of cell death (Figure 11). This suggests that perhaps pMET is not a robust pharmacodynamic marker

for MET activity. Cabozantinib also proved more potent at reducing phosphorylation of pGAB1 and pERK (Figure 14, Figure 15), suggesting that cabozantinib is better at supressing this arm of the pathway. Perhaps the specific conformation that cabozantinib targets is more active towards GAB-1. pGAB-1 / pMAPK does not seem to be associated with cell survival. Altogether, this suggests that GAB1/MAPK may be dispensable for MET-dependent survival.

The lack of specificity of MET phosphorylation as a marker for MET activity is apparent on reviewing the MET literature: the lack of correlation between pMET as an indicator of target engagement is seen time[155] and time again[34]. And yet, using phosphorylated MET has, of course, been suggested as a marker for MET pathway activation, especially as it represents a practical and feasible approach to demonstrate MET activity in *in vitro* studies using cell/tissue lysates.

There are some data suggesting its potential as a biomarker in lung cancer[156], or more specifically, certain forms of pMET. In one particular study of the expression and prognostic role of MET, p-MET, and HGF in patients with NSCLC and SCLC cancer[156] (including 129 patients), high expression of two specific forms of p-MET, cytoplasmic expression of Y1003 and nuclear expression of Y1365, was associated with significantly worse overall survival [OS; P= . 0.016; hazard ratio (HR), 1.86; 95% confidence interval: 1.12–3.07; and P=0.034; HR: 1.70; 95% confidence interval: 1.04-2.78, respectively). Yet, somewhat predictably, large-scale studies convincingly demonstrating pMET scoring in lung cancer tissue and correlating with MET pathway activity and/or with efficacy of MET-targeted therapies are absent[157].

2.3.2 Exon 14 splicing mutation cells insensitive to MET-TKI inhibition

Given the recent clinical interest in MET exon 14 splicing, I interrogated METex14 skipping cells H596 (lung cancer) and Hs746t (gastric cancer) using MET TKIs, and both cell lines demonstrated little sensitivity to type I and type II MET-TKIs. Here (Figure 13), we replicate published data[155], which suggests that MET-TKIs may have little clinical

efficacy in patients with lung cancer with MET mutations. Tanizaki et al[155] interrogated METex14 skipping lung cancer cells H1437 and H596 cells, and H2122, a cell line which harbours the N375S mutation of MET using crizotinib. Our data are consistent with their observation that, although crizotinib exerted a marked antitumor action in lung cancer cells with MET amplification, those without this genetic change, including in those with a MET mutation, crizotinib had no substantial antitumor effect on lung cancer cells with an exon 14 deletion either *in vitro,* or indeed, *in vivo*[155].

Clinically, response to MET inhibitors has been observed in lung cancer patients whose tumours contained mutations leading to MET exon 14 skipping[39,98,99,108]. Thus, the paucity of preclinical evidence demonstrating the effectiveness of crizotinib and other MET TKIs in METex14 skipping cells, is confounding, especially given that crizotinib and capmatinib have received Breakthrough Therapy designation from the FDA for patients with metastatic NSCLC with MET exon 14 based on these clinical responses[108], and that crizotinib has been used as the MET-targeting agent of choice in the METex14 arms of both US and UK genomic driven cancer studies[158,159]. The relative clinical success of crizotinib in METex14 could, perhaps, be related to the observation that approximately 15-21% of tumours harbouring MET exon14 skipping also have concurrent MET amplification[160].

Patient derived xenograft (PDX) models are useful preclinical models for cancer research for the development of anti-cancer drugs[161]. There are few PDX models of METex14 commercially available, however these are not without significant cost, and can only be used at the will of certain commercial companies, which of course limits the capability of independent laboratory work.

The lack of valid pre-clinical METex14 models highlights an obvious challenge in interrogating MET-driven disease – the rarity of these lesions can limit the number of valid models available, and this can, of course, limit the possibility of generating accurate reproducible data.

3 HGF and resistance to MET-TKIs

3.1 Introduction

As mentioned previously, HGF can be supplied by either the tumour itself or by the tumour microenvironment[32], secreted by cells in the microenvironment such as fibroblasts[33]. Indeed, HGF is a major component of the fibroblast secretome, and cancer associated fibroblasts (CAFs) have been shown to promote epithelial-mesenchymal transition, cell scattering, and cancer cell survival by providing tumour-promoting chemokines, growth factors, cytokines and extracellular matrix proteins[162].

Previous studies have highlighted the key role for HGF secreted from the tumour microenvironment in the development of drug resistance[32,34,35], however the mechanistic basis of how the presence of excess HGF alters the response to MET TKIs remains unknown. Additionally, there are pre-clinical data showing that HGF produced in lung fibroblasts enhances NSCLC cell survival and promotes tumour progression[141]. In spite of this, the significance of the role of HGF excess has not been thoroughly explored in lung cancer, and indeed the presence of HGF remains largely ignored in the design, to date, of MET-driven clinical trials. We propose HGF-mediated resistance as another potentially critical unidentified cause for the large-scale failure of MET-directed lung cancer trials to date.

3.2 Results

3.2.1 HGF overexpression causes resistance to MET tyrosine kinase inhibition in MET-addicted cells

To further understand the role of excessive HGF exposure, HGF was ectopically over-expressed in various MET-amplified cancer cell lines (Table 3). Overexpression was confirmed with western blotting and HGF-ELISA (Figure 16). SBC-5, a small cell lung

(SCLC) cancer cell line with HGF and MET co-expression was also used as an endogenous model of HGF expression.

Parental Cells	Cell Lines Generated
BEAS2B	BEAS2B-HGF
	BEAS2B-MET
	BEAS2B-MET/HGF
	BEAS2B-HGF_C211S
	BEAS2B-HGF_R220Q
	BEAS2B-HGF_ C232Y
EBC-1	EBC1-HGF
H1993	H1993-HGF
GTL-16	GTL-16-HGF
Hs746t	Hs746t-HGF
H596	H596-HGF

Table 3. Cell lines generated to explore the significance of HGF expression.

HGF-overexpression rescued MET-amplified lung cancer cells from MET tyrosine kinase inhibition-induced cell death, using both type I and type II MET TKIs (Figure 14 and 15).

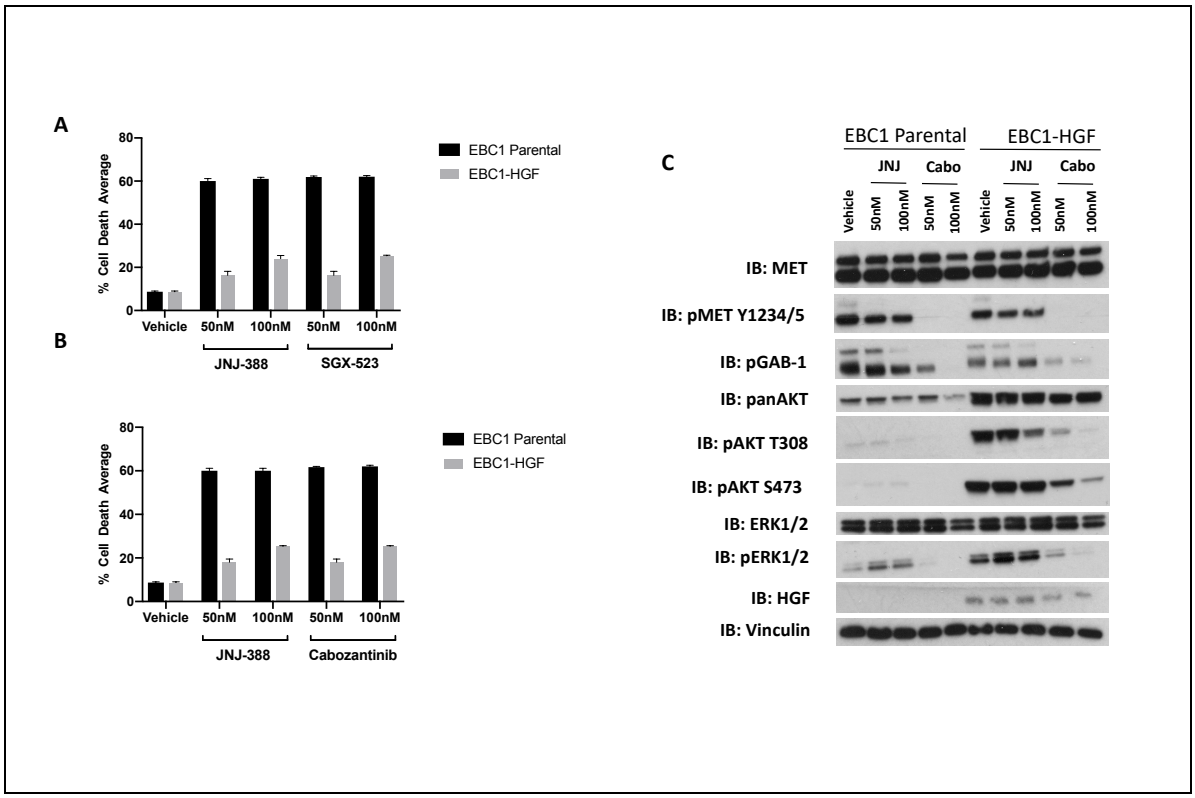

Figure 14. HGF overexpression causes resistance to MET tyrosine kinase inhibition in MET-addicted cells. (A, B) Analysis of the responses of MET amplified cell line, EBC-1, to 72h treatment with MET inhibitors, type I inhibitor JNJ-38877605 and type II inhibitors cabozantinib and SGX-523, respectively. Cell death percentages (mean ± SEM) were assessed via automated trypan blue method (ViCell), and expressed as the fraction of stain-positive cells. (C) Western blot analysis of the responses of MET amplified (EBC1) cell line and EBC1-HGF to 6h treatment with MET inhibitors, JNJ-38877605 and Cabozantinib respectively. In this instance, cabozantinib appears more potent than JNJ-38877605 in inhibiting MET phosphorylation.

Of note, I did not observe any correlation between the biochemical effects of these drugs on MET phosphorylation and biological response (Figure 14, C). Both cabozantinib and JNJ-3887760 induced robust cell death. However, in this instance, cabozantinib

appeared more potent than JNJ-38877605 in inhibiting MET phosphorylation. In addition, both of these drugs showed similar induction of cell death at 25nM in EBC1 parental cells (Figure 15). However, crizotinib appeared more potent than cabozantinib in inhibiting MET phosphorylation in these experiments. Therefore, pMET does not appear to be a robust readout of target engagement. Similarly, in HGF-overexpressing EBC1 cells, we see that despite robust inhibition of MET phosphorylation by cabozantinib (Figure 15, B), cells were significantly resistant to treatment (Figure 15, A). This is additional evidence that pMET is not a robust PD marker of MET inhibitor efficacy. Even canonical downstream effectors such as GAB1 or MAPK, may not be good PD biomarkers based on the observed lack of correlation between response and the extent of canonical pathway inhibition (Figure 14, Figure 15).

Interestingly, HGF-overexpressing EBC1 cells demonstrated a significant increase in the levels of panAKT, pAKT s473 and pAKT T308, compared to parental controls (Figure 14, Figure 15).

To further validate our model of MET TKI resistance, I generated further HGF-overexpressing cell lines. I overexpressed HGF in the MET-amplified gastric cancer cell line GTL16. Similar to EBC1, HGF-overexpression rescued MET-amplified gastric cancer cells from MET tyrosine kinase inhibition-induced cell death, using both type I and type II MET TKIs (Figure 15).

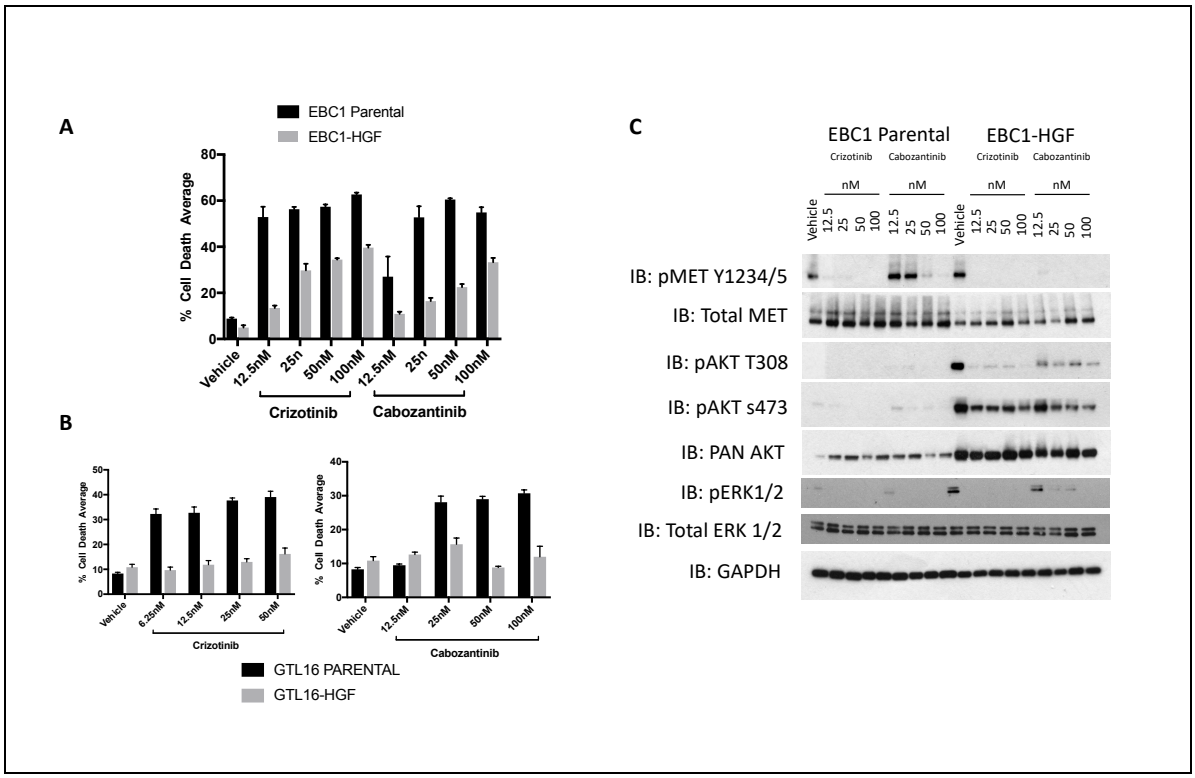

Figure 15. HGF overexpression causes resistance to MET tyrosine kinase inhibition in MET-addicted cells. (A,B) Analysis of the responses of MET amplified cell line, EBC1 and GTL16, to 72h treatment with MET inhibitors, type I inhibitor crizotinib and type II inhibitor cabozantinib. Cell death percentages (mean ± SEM) were assessed via automated trypan blue method (ViCell), and expressed as the fraction of stain-positive cells. (C) Western blot analysis of the responses of MET amplified EBC1 cell line and EBC1-HGF to 6h treatment with MET inhibitors, crizotinib and cabozantinib respectively. In this instance, crizotinib appears more potent than cabozantinib in inhibiting MET phosphorylation.

3.2.2 A model of endogenous HGF and MET overexpression shows resistance MET TKIs.

SBC-5 cells were used as a naturally-occurring model of HGF-mediated resistance to MET TKIs. SBC-5 is a SCLC cell line with documented gene amplification and co-expression of

HGF and MET[13,14] (Figure 16), and was interrogated with comparable doses of multiple type I and type II MET TKIs. However, no significant increase in cell death was noted as they remained insensitive to single agent MET TKIs.

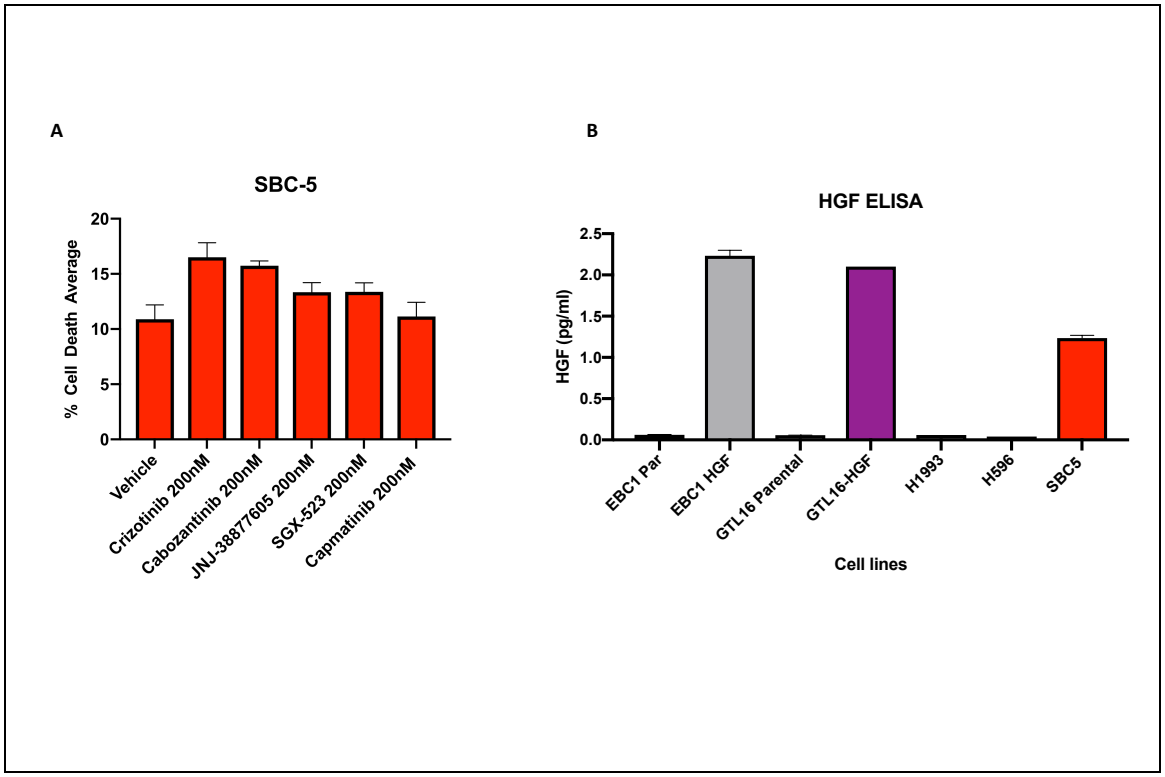

Figure 16. SBC-5 cells appear insensitive to type I and type II MET tyrosine kinase inhibition. (A) Analysis of response of SBC-5, SCLC model with high levels of HGF and MET co-expression, to 72h treatment with MET inhibitors, type I inhibitor crizotinib, JNJ38877605, capmatinib and type II inhibitors cabozantinib, SGX-523. Cell death percentages (mean ± SEM) were assessed via automated trypan blue method (ViCell), and expressed as the fraction of stain-positive cells. Note the inactivity of these compounds in these cells. (B) HGF ELISA confirming elevated HGF levels in generated cell lines EBC1-HGF, GTL16-HGF and SBC-5, a cell line with established endogenous elevated levels of HGF.

3.2.3 HGF secreted in the tumour microenvironment.

A growing body of evidence suggests that components of the tumour microenvironment, including cancer-associated fibroblasts (CAFs), may modulate the treatment sensitivity of tumour cells. Indeed, recent evidence has shown that the tumour microenvironment[163] and more specifically HGF produced in lung fibroblasts[141] may play a significant role in NSCLC progression.

To study the relevance of HGF secreted by the microenvironment in MET inhibitor response, we interrogated lung CAFs. Primary lung CAFs (obtained through a commercial source) were first immortalised through ectopic expression of hTERT. Then, HGF ELISA confirmed that lung CAFs produce HGF, and significantly higher levels of HGF compared with the MET-addicted EBC1 parental cell line (Figure 17), where the EBC1 cell line had essentially undetectable HGF levels compared with lung CAFs. Lung CAFs also produced higher levels of HGF compared with the non-cancerous bronchial epithelial cell line BEAS2B (Figure 18). MET-amplified EBC1 parental cells, HGF-overexpressing models, CAF-HGF, and EBC1-HGF, were all confirmed to secrete high levels of HGF as judged by ELISA (Figure 17).

Given that cisplatin, and platinum-doublet chemotherapy, remains the mainstay of treatment for patients with advanced NSCLC[164], and because this patient population is the most likely to be recruited into MET inhibitor trials, we wanted to investigate the effect of cisplatin on HGF expression. We found that HGF levels reduced by up to approximately 50% in lung CAFs with increasing dose of cisplatin (Figure 18 and Figure 17). This was in contrast to both lung cancer EBC1 cells (Figure 17) or immortalized bronchial epithelial cells (BEAS2B cells) (Figure 18), which showed no significant change. In these cells, when compared separately with lung CAFs, cisplatin treatment had no demonstrable effect on HGF produced, likely due to the fact that HGF levels in these cells were negligible on ELISA assay testing.

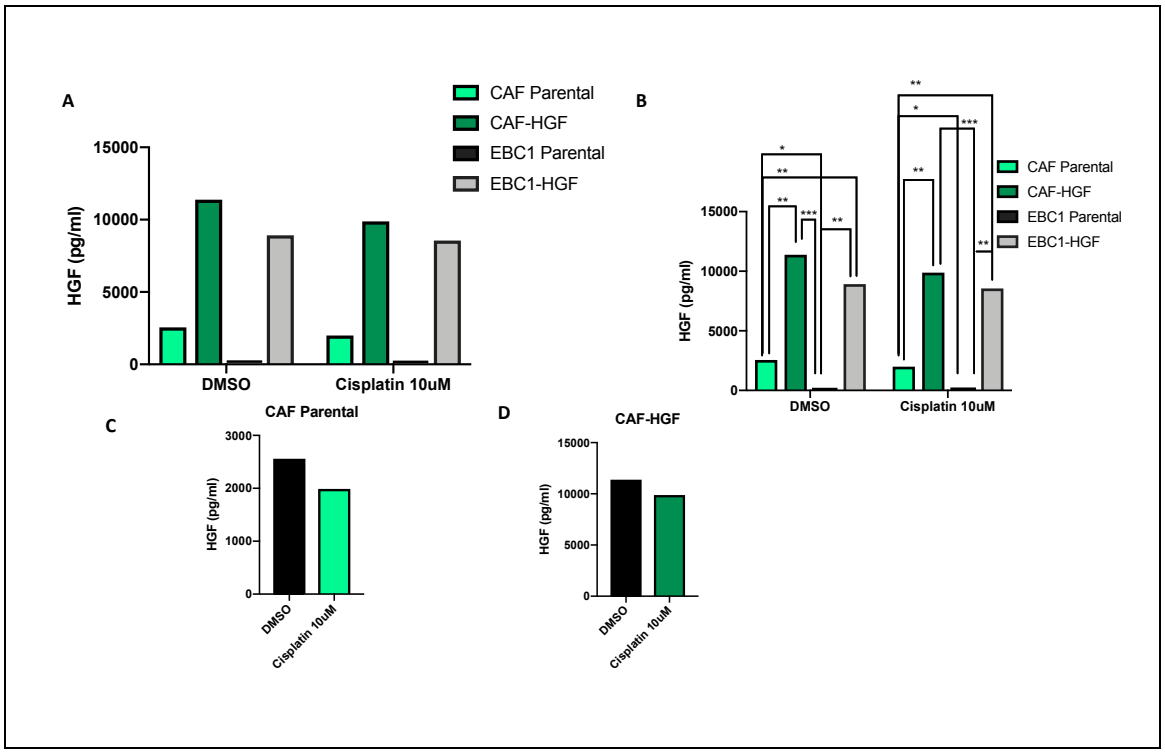

Figure 17. Lung CAFs produce elevated levels of HGF compared to EBC1 lung cancer cells and treatment with cisplatin reduce levels of HGF. ELISA HGF is used to assess HGF levels (A-C). Cells were treated with cisplatin 10uM or DMSO where indicated for 24hours. In Lung CAFs, HGF levels show a downward trend with cisplatin treatment.

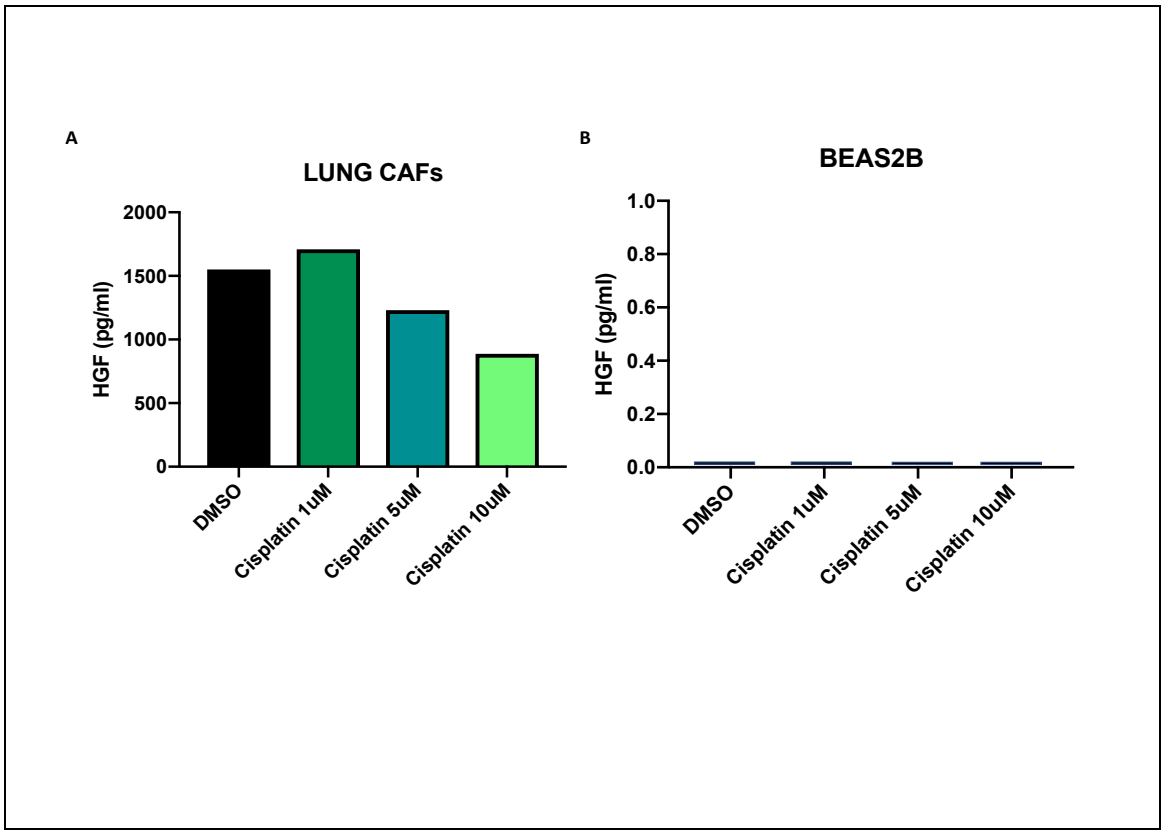

Figure 18. HGF levels reduce with cisplatin treatment in CAFs, but not in non-cancerous bronchial epithelial cells. (A,B) Cells were treated with increasing doses of chemotherapy agent cisplatin (1um, 5uM, 10uM), for 18hours. Results of ELISA assay in lung CAFs (A) and immortalised bronchial epithelial cell line BEAS2B (B) are shown respectively. CAFs treated with cisplatin, at increasing doses, showed a reduction in HGF levels in these cells (A). HGF levels in BEAS2B cells remained undetectable on ELISA assay testing, with or without cisplatin treatment.

Interleukin-6 (IL-6) is a pro-inflammatory cytokine produced by macrophages that plays important roles in the acute phase reaction, inflammation, erythropoiesis, bone remodelling, inflammatory diseases and inflammatory cancers [165–169].

IL-6 is also thought to regulate HGF expression[170], and so we wanted to assess whether cisplatin could affect HGF expression through an IL-6 dependant mechanism, by assessing levels of IL-6 using a Human IL-6 Immunoassay.

Lung CAFs had higher levels of IL-6 on baseline testing compared with EBC1 parental cells (Figure 19). Lung CAFs, EBC-1 and EBC1-HGF cells were treated with increasing doses of platinum agent cisplatin (5µM – 10µM and IL-6 levels were then assessed using ELISA. In the lung CAFs, ELISA assay testing revealed reduced levels of IL-6 with cisplatin treatment, and a strikingly similar trend was observed with the HGF-overexpressed EBC-1 cell line. (Figure 19). EBC1-HGF showed a similar pattern of a reduction in IL-6 levels using all doses of cisplatin, suggesting that when you provide excess HGF, these lung cancer cell lines behave similar to the CAF cells (Figure 19). Of note, in lung CAFs, IL-6 levels followed the similar trend of reducing HGF levels on treatment with cisplatin (Figure 19).

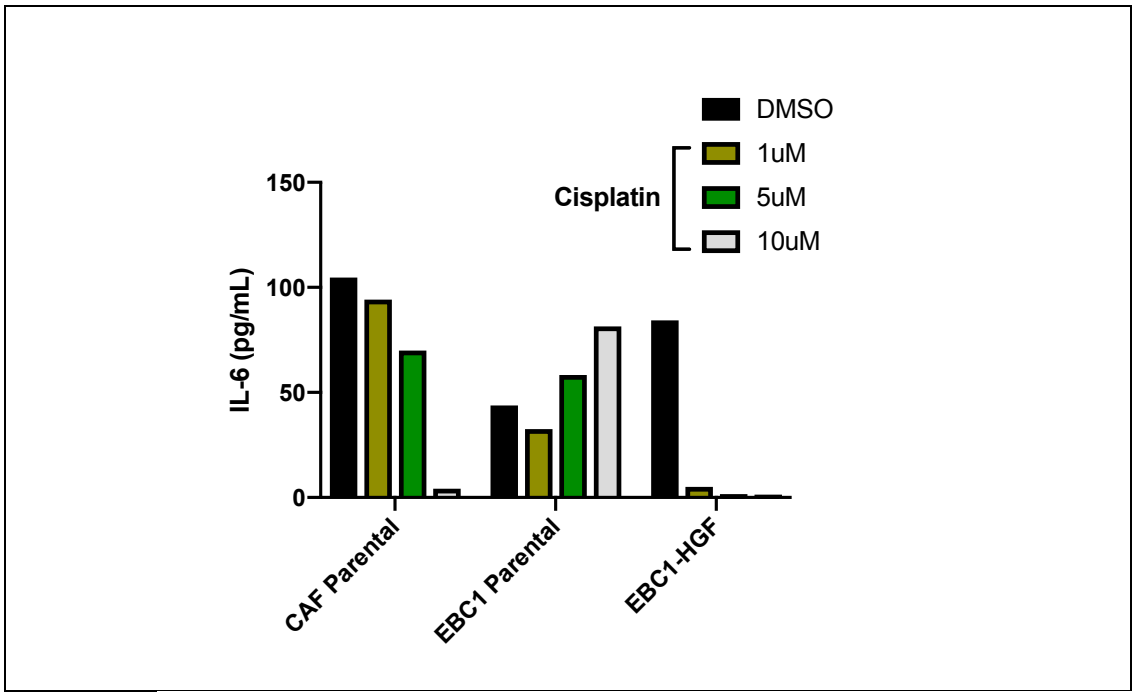

Figure 19. IL-6 produced by CAF and EBC1-HGF cells reduce with cisplatin treatment. (A) Cells were treated with cisplatin for 18hours. Lysates were measured for IL-6 using ELISA

assay. Note the downward trend for HGF-expressing cells, when platinum agent cisplatin is added to cells.

3.2.4 HGF scoring in lung cancer tumours: HGF exposure matters.

Previously, Tsao et al[171] reported that seventy percent of the 166 lung tumours showed strong HGF expression with higher frequency noted in adenocarcinoma (84%) as compared with squamous cell carcinoma (57%) or large cell carcinoma (57%). Through a collaboration with colleagues in Trinity College Dublin (TCD), we aimed to characterise levels of HGF in a current patient cohort, to further clarify the fraction of patients with detectable levels of HGF.

Semiquantitative immunohistochemistry (IHC), using the Allred scoring system, is a near-universal method of determining tumour hormone receptor (estrogen receptor,ER and progesterone receptor, PR) in breast cancer[172]. Pathology laboratories have adopted ≥1% positive staining for tumour cells as the definition of 'ER-positive' clinically, and a 1% cut-off has now been clinically validated in a number of studies[173]. This 1% cut-off corresponds to Allred score greater than or equal to 2[174]. A modified Allred scoring system has also been suggested[175], where positive score is 3 or above: high scores were defined as Allred 6-8, and low scores as Allred 3–5[175].

Dr Stephen Finn and colleagues in TCD noted that, HGF staining was found mainly in the cytoplasm of cancer cells (Figure 20), and that Allred score HGF scoring 268/286 of evaluable lung cancer readings had detectable levels of HGF, i.e. 94% of cases demonstrated detectable HGF scoring levels. Using a modified Allred scoring, this corresponded to 249/286 (87%) of evaluable lung samples defined as Allred positive, 138/259 53% as high 111/249 45% low Allred score.

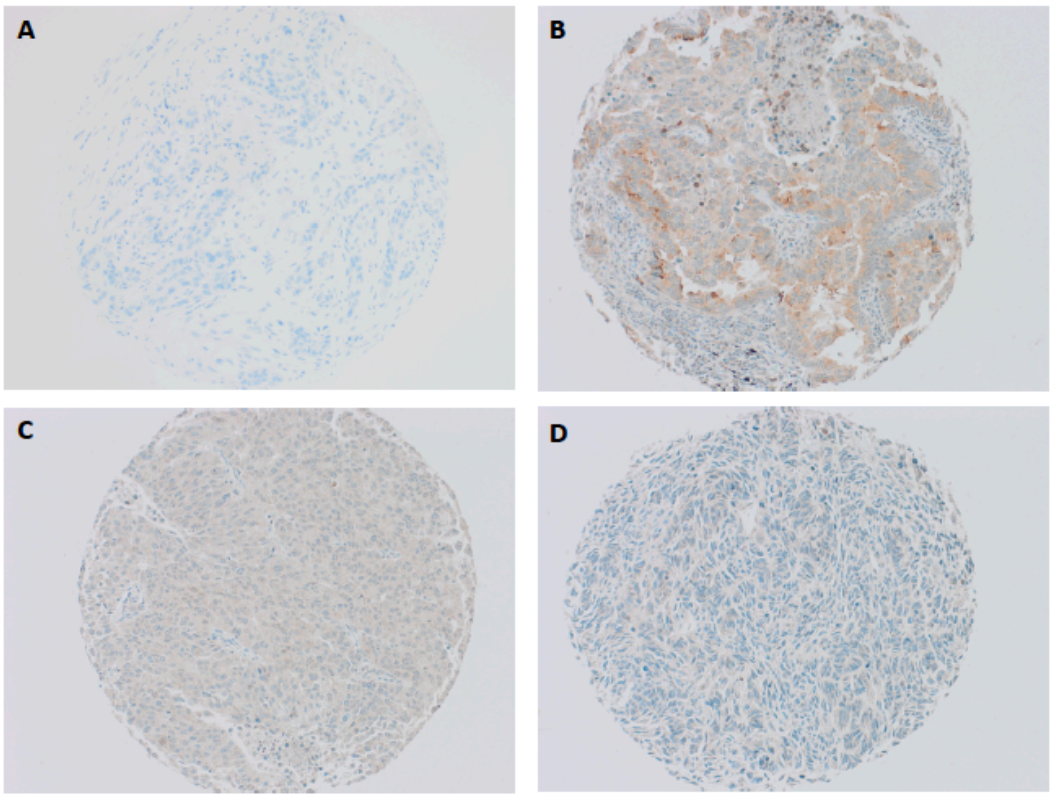

Figure 20. Representative IHC staining of lung samples using HGF-specific antibody. Positive expression HGF is shown (in images B to D), A is the negative control (original magnification 10X). Allred Scoring System are as follows: (A) Proportion Score: 0, Intensity Score: 0, Allred Score: 0; (B) Proportion Score: 5, Intensity Score: 2, Allred Score: 7; (C) Proportion Score: 5, Intensity Score: 1, Allred Score: 6; (D) Proportion Score: 4, Intensity Score: 1, Allred Score: 5.

3.2.5 Known resistance model in *MET*exon14 - KRAS mutations

We have described HGF as a mechanism of de novo resistance to type I and type II MET TKIs in MET-addicted cancer cells. In the clinic, thus far, it appears that secondary mutations in *MET*[146,176] and *KRAS*[143,148] pathway activation are emerging as mechanisms of acquired resistance to MET TKIs in MET exon 14 mutant patients. Specifically, Suzawa et al[148] show that *KRAS G12* mutations result in constitutive activation of RAS/ERK signalling and resistance to MET inhibition, acting as mediators of primary and secondary resistance. To assess how our resistance model measures up against a model of a clinically validated mechanism of MET TKI resistance, *KRAS* mutants *G12C* and *G12V* were both ectopically expressed in EBC1 parental cells. Response to type I and type II MET inhibitors was assessed. *KRAS* mutants *G12C* and *G12V*, in addition to HGF-overexpression in EBC-1 cells, rescued NSCLC MET-amplified lung cancer cells from MET tyrosine kinase inhibition-induced cell death to a similar extent, using both type I and type II MET TKIs (Figure 21).

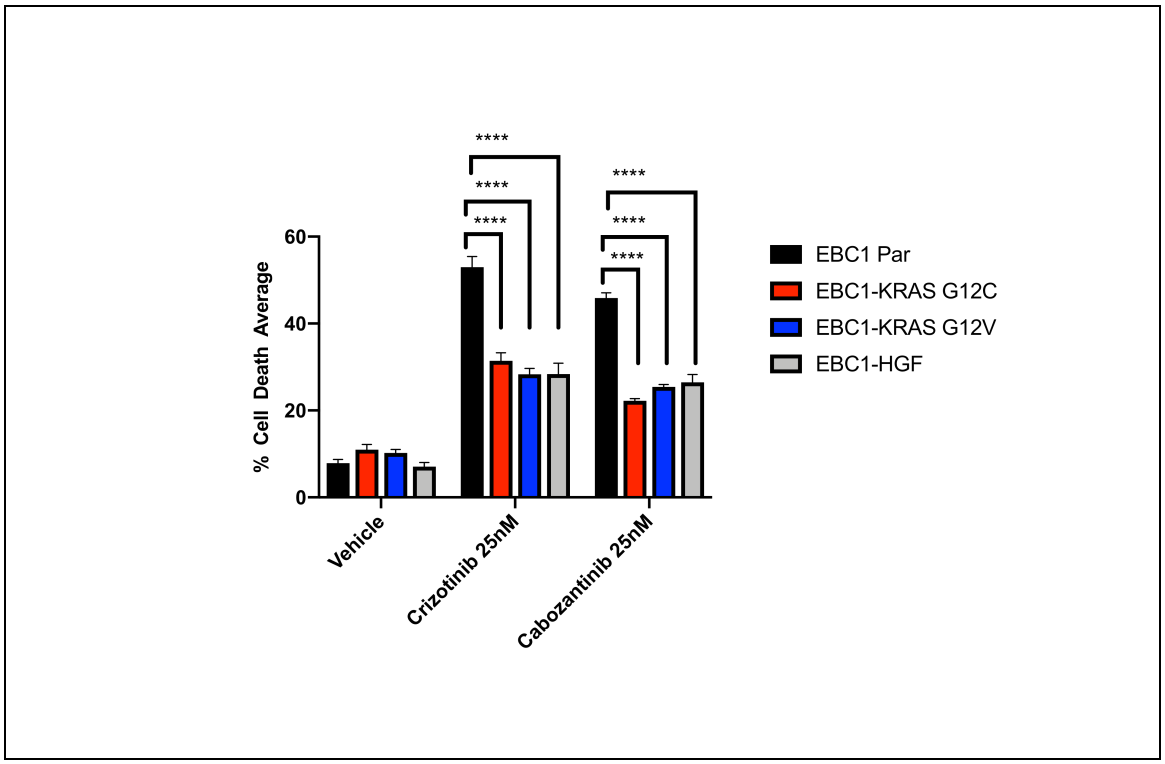

Figure 21. HGF-excess, as a model of resistance, is comparable when compared with documented mechanisms of resistance in METex14 NSCLC, KRAS mutants *G12C* and *G12V*. Analysis of the responses of MET amplified cell line, EBC1 and to 72h treatment with MET inhibitors, type I inhibitor crizotinib and type II inhibitor cabozantinib. Cell death percentages (mean ± SEM) were assessed via automated trypan blue method (ViCell), and expressed as the fraction of stain-positive cells. 2-way anova performed. Adjusted P-value is <0.0001.

3.3 Discussion

3.3.1 HGF overexpression causes resistance to MET tyrosine kinase inhibition in MET-addicted cells.

A consistent and challenging aspect of treating NSCLC patients with targeted therapies in the era of precision medicine, is that complete clinical responses are rare due to both primary and acquired mechanisms of treatment resistance. My data suggest that HGF-excess is one such form of de novo resistance to MET TKIs.

To confirm that excess HGF causes resistance to MET TKIs, we over-expressed HGF in MET addicted models, and demonstrated significant protection from the cytotoxic effects of both type 1 and type 2 MET TKIs (Figure 14, Figure 15). Importantly, these HGF-overexpressing cells have been generated multiple times over the course of this PhD project, with consistent results throughout. These data have also been replicated using different HGF expression constructs, further supporting the reproducibility of these data. We also show that SBC-5 cells, the endogenous model of HGF-excess, are resistant to single agent MET TKIs, further highlighting the significance of this resistance model.

These results are consistent with a strong phenotype, reported previously[34,139], in which HGF rescues MET-amplified lung cancer cells from MET tyrosine kinase inhibition overexpression in MET-addicted cells confers resistance to both MET tyrosine kinase inhibitors, indicating that MET activation mechanism can indeed influence MET inhibitor response. The resistance of SBC-5, the endogenous model of resistance provides rationale to avoid using MET TKIs alone in the case of co-amplification, where high levels of HGF are also present, and suggests that alternative methods of targeting are certainly required.

While previous studies have commented on the effect of HGF in causing resistance to MET tyrosine kinase inhibition, the mechanistic basis behind this resistance mechanism

remains undetermined. In an effort to further understand the mechanism, a phosphoproteomic profiling experiment was performed, discussed in further detail in Chapter 4.

One potential hypothesis is that chronic HGF exposure shifts the conformation of the MET receptor making it less accessible to MET TKIs (Figure 22). HGF, of course, is the cognate ligand of MET, an RTK. RTKs comprise an extracellular domain containing a ligand-binding site, a single hydrophobic transmembrane α helix, and a cytosolic domain, which includes a region with protein-tyrosine kinase activity[177]. Binding of the ligand causes most RTKs to dimerize, and autophosphorylation occurs: the protein kinase of each receptor monomer phosphorylates a distinct set of tyrosine residues in the cytosolic domain of its dimer partner[177] (Figure 22).

During autophosphorylation, tyrosine residues in the phosphorylation lip residing near the catalytic site are phosphorylated and this leads to a conformational change that facilitates binding of ATP in some receptors (for example, the insulin receptor) and binding of protein substrates in other receptors. For MET, ligand-induced MET dimerization activates the tyrosine kinase by phosphorylation of tyrosine residues (Tyr1230, Tyr1234, and Tyr1235) in the kinase domain, which leads to autophosphorylation of the carboxy-terminal bidentate substrate-binding site (Tyr1349 and Tyr1356) of MET[67–69]. Receptor kinase activity then phosphorylates other sites in the cytosolic domain and the resulting phospho-tyrosines function as docking sites for other proteins involved in RTK-mediated signal transduction[67–69].

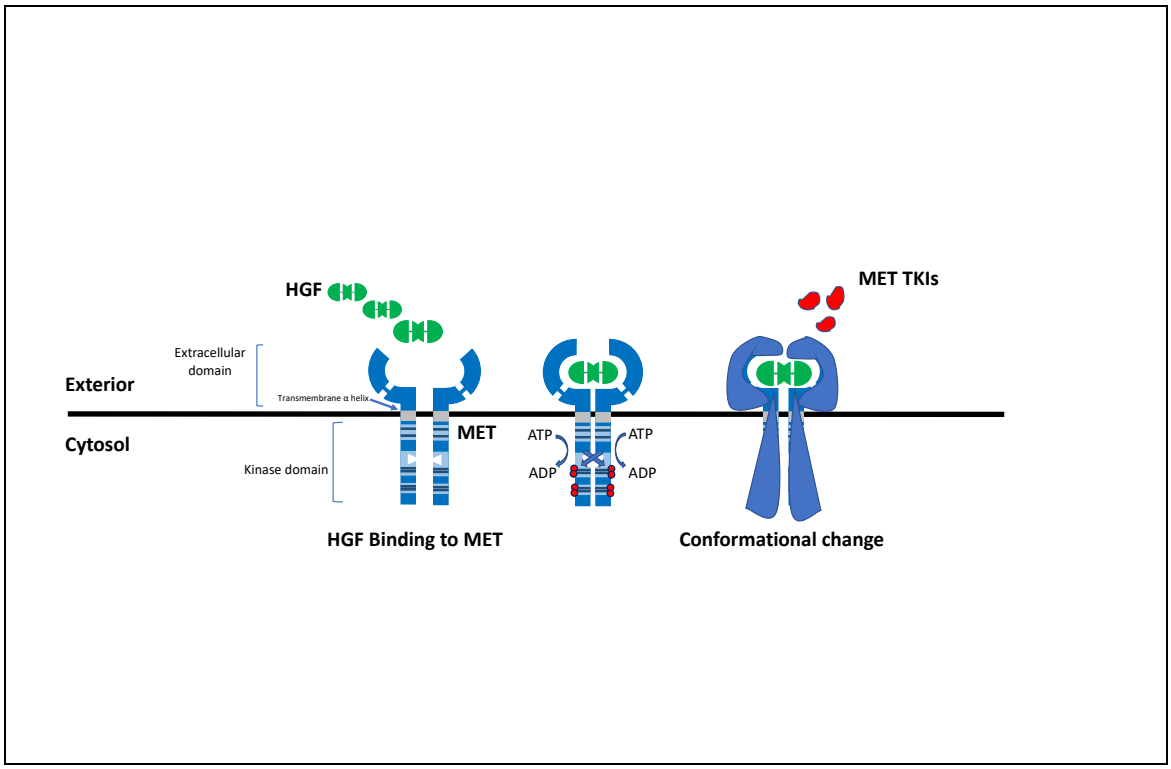

Figure 22. MET receptor on binding of its ligand, HGF, causes conformational change, making receptor inaccessible to MET TKIs. Schema representing potential induction of resistance to MET TKIs.

Kinase conformational plasticity describes the capability of kinases to reversibly switch between distinct conformations observed in many crystal structures of kinases[178]. Structural plasticity appears to be essential for kinase regulation and enzymatic activity, as different conformations reflect distinct functional states. Substrate binding, catalysis, and product release, for example, all require conformational changes and intrinsic dynamic properties in the kinase domain[179]. Although catalytic domains of different kinases appear to have strikingly similar structures in the active state, crystal structures of inactive kinases have shown remarkable plasticity in the kinase domain that allows binding of regulatory domains or proteins to promote distinct conformational chages[178].

My working hypothesis is that chronic HGF exposure, perhaps through receptor desensitization, to the MET receptor shifts the conformation of the receptor to a transitional state, between 'active' and 'inactive', which makes it difficult for both type I

and type II MET TKIs to bind to the kinase domain (Figure 22). The observed rescue of MET TKI-induced toxicity by HGF overexpression, suggests that for patients whose tumours have co-amplification of MET and HGF, (or MET amplification with elevated HGF levels), single agent MET TKIs might not to be sufficient to elicit a measurable clinical response. Thus, interfering with HGF binding and its ability to induce any conformational changes on MET could re-sensitise the receptor to both type I and type II TKIs.

Potential strategies to do this could involve using antibodies that either 1) sequester HGF away from MET, or 2) block the HGF binding site on the receptor. Given that currently there are no HGF antibodies in clinical development, MET-directed antibodies may be a clinically feasible option. Interestingly, there has been some success in overcoming resistance to EGFR TKIs with this dual inhibition strategy in the pre-clinical setting[180]. Clinically, however while afatinib and cetuximab demonstrated robust clinical activity in a heavily treated cohort of NSCLC patients[181], the combination resulted in considerable toxicities. Some of these toxicities appear to be on-target[181]. Therefore, it is conceivable that this strategy may be tolerated when targeting MET.

3.3.2 pMET is a poor surrogate marker for MET activity.

We demonstrate again in Figure 14 and Figure 15, that on examining the biochemical effect of MET TKIs, at the molecular level, MET phosphorylation is inconsistent and as such, remains a poor surrogate marker for MET activity. Again, both JNJ-38877605 and cabozantinib show similar induction of cell death in EBC1 parental cells, yet if pMET were to be used as an indicator of target engagement, it would not be predictive (Figure 14), and the same is true again for pERK1/2 and other downstream effectors. Similarly, in the HGF-overexpressing EBC1 cells (Figure 15), it appears that cabozantinib is potent at suppressing MET phosphorylation. However, these EBC1-HGF cells are resistant to MET TKIs. Together with previous data, this is now additional evidence that pMET is not a good predictor of response to targeted agents, and even canonical downstream effectors do not appear to be reliable pharmacodynamic biomarkers because there does

not appear to be a correlation between response and the extent of canonical pathway inhibition. Better biomarkers for MET activity are clearly needed.

3.3.3 Significance of HGF in the tumour microenvironment.

It is becoming increasingly clear that one cannot think of lung tumours as simply an accumulation of malignant cells. Rather, the true picture is that of a highly complex tissue, composed of neoplastic and stromal cells. Stromal cells comprise a variety of cell types: mesenchymal cells, particularly fibroblasts, myofibroblasts, endothelial cells, pericytes and inflammatory cells associated with the immune system, extracellular matrix (ECM), and the vascular network[182,183]. Accumulating evidence has confirmed that tumour cells must recruit and essentially reprogram the surrounding normal cells to serve as contributors to tumour progression, such that tumour cells and the supporting normal cells form an organ-like structure and make concerted efforts for rapid proliferation, local invasion and metastases[182,183](Figure 23). Hence, the tumour microenvironment plays an active, rather than a passive role, in tumour progression and metastasis. Indeed, we now know that the tumour microenvironment plays a key role in tumour initiation, progression, metastasis and even therapeutic resistance[35,184].

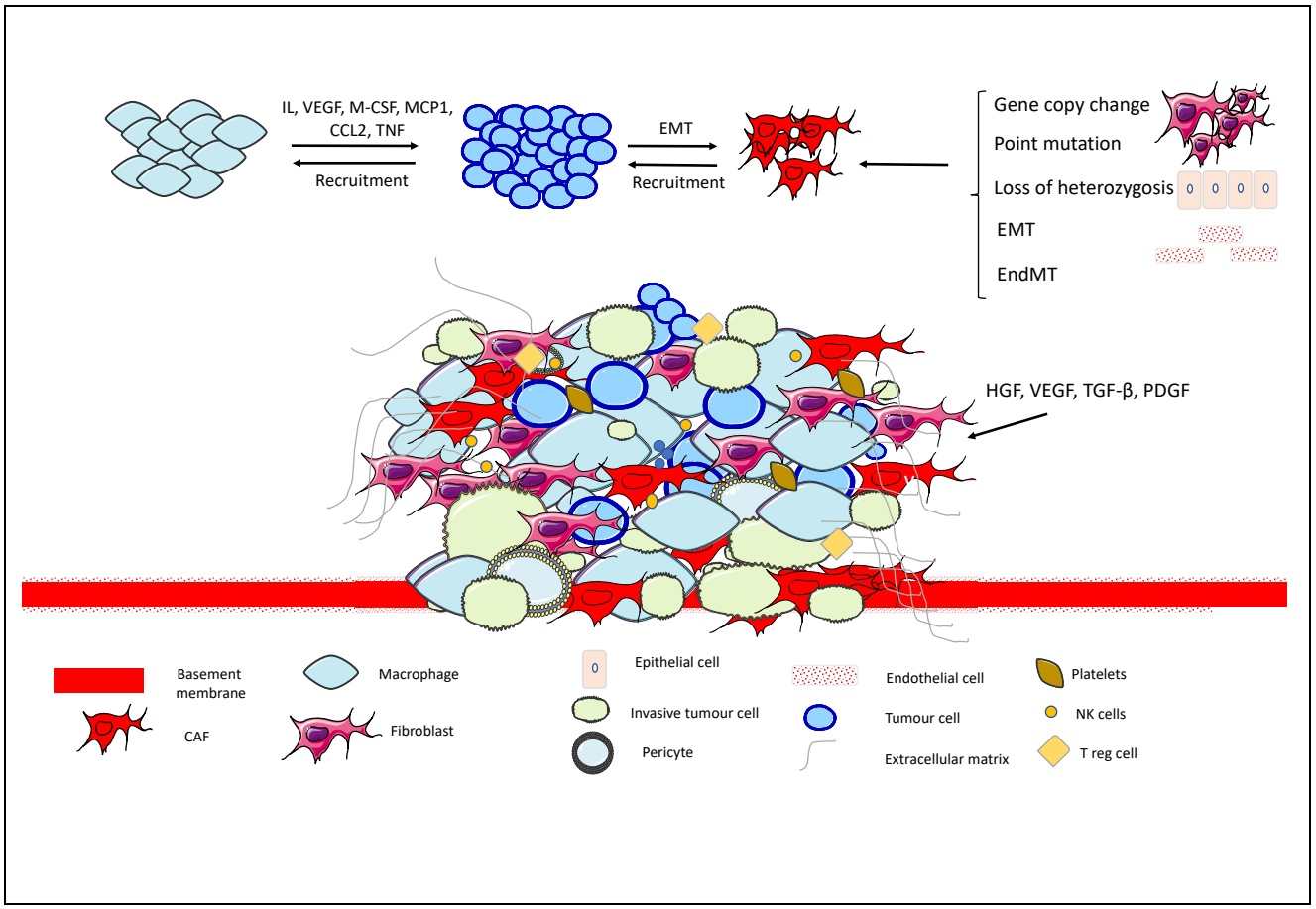

Figure 23. Formation of the tumour microenvironment. Figure representing the construction of the tumour microenvironment, including the detailed processes involved in the recruitment of various cell types are shown. The tumour cells recruit CAFs, epithelial cells, fibroblasts, pericytes, macrophages and endothelial cells to the primary tumour site. Important components of the tumour microenvironment also include the extracellular matrix and the vascular network, which is composed of blood vessels, and lymphatic vessels. VEGF, vascular endothelial growth factor; CCL2, chemokine chemokine (C-C motif) ligand 2; TNF, tumour necrosis factor; M-CSF, macrophage-colony stimulating factor; MCP-1, monocyte chemotactic protein 1; TGF-β, transforming growth factor β; PDGF, platelet-derived growth factor; HGF, hepatocyte growth factor; EMT, epithelial-to-mesenchymal transition; EndMT, endothelial-to-mesenchymal transition.

Fibroblasts and myofibroblasts comprise a significant proportion of the cells in the tumour stroma, and while these cells secrete several tumour-promoting chemokines, growth factors, cytokines and extracellular matrix proteins, HGF is a major component of the fibroblast secretome[162]. Consequently, HGF is abundant in the tumour microenvironment, but it can also be supplied by the tumour itself[185]. CAFs have been shown to promote epithelial-mesenchymal transition, cell scattering, tumour-promoting chemokines, growth factors, cytokines and extracellular matrix proteins[162]. Recent evidence has shown that the tumour microenvironment[163] and more specifically HGF produced in lung fibroblasts[141], may play a significant role in NSCLC progression. Most notably, there are data that HGF can elicit resistance to targeted therapies[32,34,139,184,186].

Interestingly, one study noted that stromal cells secreted HGF resulting in activation of MET, and resistance to RAF inhibition in *BRAF*-mutant melanoma cell lines treated with BRAF inhibitor[32]. They also demonstrated that patients confirmed to have stromal HGF had a significantly poorer response to treatment compared to those lacking expression[32]. In addition to this, they showed that HGF led to sustained activation of both AKT and ERK, and suggested reactivation of AKT and the mitogen-activated protein kinase (MAPK) signalling pathways as a possible mechanism of this HGF-induced resistance[32].

Remarkably, when MET activation acts as a mechanism of acquired resistance to EGFR kinase inhibitors, it can occur in the absence of c-MET amplification via HGF-induced activation of the AKT pathway[187,188]. Another study, has demonstrated that PI3K/AKT signaling is sustained by recruitment of the GAB1 adaptor protein[189]. Consistent with this role of HGF in mediating secondary resistance to EGFR inhibitors, acquired resistance to gefitinib and erlotinib in patients with lung cancer has also been shown to be associated with high HGF levels in the tumor microenvironment[187,190] and even when measured in patients plasma samples[191].

My work has focused on primary MET-driven disease, where HGF could be acting as a mechanism of primary resistance to MET TKIs. It is, therefore, clear that HGF levels in the tumour microenvironment could influence drug response. My data, showing that lung CAFs secrete significantly higher levels of HGF compared to both MET-addicted lung cancer cells, and non-cancerous immortalized bronchial epithelial cells (Figure 17 and 18), strongly suggest that the tumour microenvironment could be an important source of excess HGF for tumour cells.

There are no published data investigating the effect of chemotherapy on HGF expression, and our data suggest that cisplatin does indeed have an effect on HGF expression, particularly in CAFs. We demonstrate that HGF levels reduce by up to approximately 50% in lung CAFs with increasing dose of cisplatin (Figure 17, 18), in contrast to MET amplified EBC1 cells (Figure 17) or immortalized bronchial epithelial cells (BEAS2B cells) (Figure 18), which showed no significant change. We also show that treating MET-amplified HGF overexpressing lung cancer cells and lung CAFs (both with documented elevated levels of HGF) with cisplatin causes a decrease (albeit not statistically significant) in HGF production (Figure 17, 18).

We also demonstrate reduced levels of IL-6 in lung CAFs and EBC1-HGF cells when treated with cisplatin (Figure 19), and that both CAFs and EBC1-HGF expressed higher basal levels of IL-6 compared to parental EBC1 cells. HGF has been shown to activate IL-6/JAK2/STAT3/twist1 pathway by up-regulating IL-6 receptor (IL-6R) expression[192]. These data suggest that perhaps cisplatin can affect HGF expression through an IL-6-dependant mechanism, at least in the case of CAFs and EBC1-HGF cells.

Finally, given that CAFs, through production of HGF, could modulate the treatment sensitivity of MET-driven lung cancer cells, it would be interesting to see the effect of HGF produced by lung CAFs on the response to MET TKIs in EBC1 cells using a co-culture system, and ultimately *in vivo*. These experiments will help to validate the relevance of non-tumour-cell-derived HGF on the response to MET TKIs, and provide rationale for the

clinical assessment of MET-targeting approaches involving combinations of HGF neutralising antibodies and MET kinase inhibitors.

3.3.4 Significance of HGF levels in NSCLC tumours.

It has been reported that lung cancer samples show high levels of HGF expression when scored on immunohistochemistry. Indeed, Tsao et al[171] reported in their cohort that seventy percent of 166 tumors showed strong HGF expression with higher frequency noted in adenocarcinoma (84%) as compared with squamous cell carcinoma (57%) or large cell carcinoma(57%)[171]. This is consistent with older data published on 42 patients with primary NSCLC[185], not previously subjected to chemo- or radiotherapy, who were analysed, with each cancer sample compared with adjacent normal lung tissue; here, HGF was found to be 10 to 100-fold overexpressed in carcinoma samples ($P<0.0001$)[185], showing that HGF/SF is overexpressed and consistently activated in non-small-cell lung carcinomas and may contribute to the invasive growth of lung cancer[185].

Our results (Figure 20) confirm that a significant proportion of lung cancer samples demonstrate detectable levels of HGF, and as such, its presence should not be ignored. Of course, what is deemed 'HGF-High' is debatable, and similar to the definition of 'MET positive' NSCLC, has not been agreed in the literature.

Given the potential for high-levels of HGF exposure to interfere with MET targeting drugs, such as MET TKIs, we argue for the inclusion of HGF-level testing in routine clinical practice for MET+ NSCLC. To date, and to the best of our knowledge, HGF levels are not routinely considered or tested for, in MET-driven clinical trial design. This is a clear weakness, but the development of reliable quantitative assays for the assessment of HGF in NSCLC tumours is warranted.

3.3.5 Activation of mutant KRAS Mediates Resistance to MET TKIs in MET Ex14 NSCLC.

Determining mechanisms of resistance of METex14 altered, or MET-amplified, lung cancers to MET therapy is a relatively new area of study, with very few validated mechanisms of resistance. Secondary mutations in *MET,* specifically D1228N/V and Y1230C[146,176] and *KRAS* pathway activation[143,148] are emerging as mechanisms of resistance in MET exon 14 mutant patients. Suzawa et al[148], for example, have demonstrated that *KRAS G12* mutations result in constitutive activation of RAS/ERK signaling and resistance to MET TKIs, acting as mediators of both primary and secondary resistance to crizotinib. Of note, in this study lung cancer models with METex14 skipping or MET amplification were both used, and expression of oncogenic KRAS mediated resistance to MET TKI. Importantly, the group also noted that dual inhibition of MET and MEK, using a combination of trametinib and crizotinib, was more effective at reducing tumour growth than either agent alone *in vitro* and *in vivo*[148], suggesting that combination therapy in these cases might represent a more effective therapeutic strategy compared to single-agent TKI use.

Based on the data from Suzawa et al[148], we overexpressed *KRAS* mutants *G12C* and *G12V* in EBC1 parental cells and showed that, similar to our model of HGF-mediated resistance, these cells are rescued from MET tyrosine kinase inhibition-induced cell death, using both type I and type II MET TKIs (Figure 21). While Suzawa et al used a different mutant KRAS (*KRAS* G12D) and a different MET-amplified model (H1993), we reproduce their finding in EBC1, another model of NSCLC MET-amplification, and add to current data suggesting that KRAS activation is a mechanism of clinical significance in MET-amplified NSCLC. Our data further implies that HGF-mediated de novo resistance to MET TKIs is another under-estimated and under-reported mechanism of resistance, worthy of further investigation.

4 Characterising the phosphoproteomic signature of HGF-mediated resistance.

4.1 Introduction

Cellular signalling, mediated commonly by phosphorylation through protein kinases, is found to be deregulated in most cancer types[193]. For example, a single constitutively active kinase originating from the fusion of the BCR and ABL genes, can give rise to and sustain chronic myeloid leukemia (CML)[194]. Accordingly, the small molecule inhibitor of the BCR-ABL kinase, imatinib, was developed. After demonstrating extraordinary therapeutic effectiveness in CML patients[195], imatinib has become the poster-child for targeted therapy, heralding the modern era of precision medicine. Consequently, protein kinases have become subject to intense investigations in cancer research, to understand their role in oncogenesis and to discover new therapeutic targets.

Often, phosphorylation is used as a surrogate for monitoring kinase activity in cells. Quantitative phosphoproteomic analysis by mass spectrometry (MS) therefore provides a wide-scale view of cellular phosphorylation networks, and is a valuable tool that allows researchers to characterise signalling pathways, investigate aberrantly activated signalling pathways, and identify therapeutic targets in cancers.

HGF is a multifunctional growth factor that can induce a number of diverse biological events. The MET receptor, as previously mentioned, is the only known receptor for HGF and, as such, mediates all HGF-induced biological activities. Upon HGF binding, MET is tyrosine-phosphorylated, which is followed by the recruitment of a group of signalling molecules and/or adaptor proteins to its cytoplasmic domain and its multiple docking sites. This action leads to the activation of several different signalling cascades that form a complete network of intra and extracellular responses, as previously described.

In order to understand the systems-level perturbations mediated by HGF-excess in MET-driven NSLC, we carried out mass spectrometry (MS) -based phosphoproteomic analysis of MET-amplified NSCLC cell line EBC-1, and the EBC1 cells with ectopic HGF-expression.

Although type I and type II MET TKIs had differential effects on canonical MET-dependent signalling, we reasoned that because HGF could confer resistance to all MET TKIs tested, excess HGF might confer biochemical resistance to a MET-dependent pathway, and that this resistance would be common across TKIs.

Thus, EBC1 and EBC1-HGF cells were treated with a single dose of type I MET TKI crizotinib and type II MET TKI cabozantinib (Table 4), and their effects were profiled on the phosphoproteome using mass spectrometry. This was undertaken through a collaboration with Dr Pedro Cutillas and his team in Barts Cancer Institute. Drug concentrations were chosen based on the ability of HGF to rescue the growth inhibitory and cell killing effects of the MET TKIs at this concentration, and five biological replicates were performed.

Cells	Treatments		
EBC1 Parental	Vehicle	Crizotinib 25nM	Cabozantinib 25nM
EBC1-HGF	Vehicle	Crizotinib 25nM	Cabozantinib 25nM

Table 4. Cells and conditions used in phosphoproteomic profiling experiment.

MS-based phosphoproteomics enables the identification of *thousands* of phosphorylated peptides in a single experiment, and since every phosphorylation event results from the activity of a protein kinase, high-coverage phosphoproteomics data indirectly contains comprehensive information about the activity of protein kinases. To help extract this type of information, we used kinase substrate enrichment analysis (KSEA), a computational method for the estimation of kinase activities based on

phosphoproteomics data and using prior-knowledge about kinase-substrate relationships[196]. KSEA activity scores describe the activity of a kinase in one condition relative to another[196,197], and was used to identify effector kinases whose function might be selectively altered by MET TKI inhibition.

Recently, two studies using a large panel of oncogene-addicted human cancer cells investigated the effect of growth factors on the response to targeted anticancer agents and identified HGF as the most relevant microenvironment-borne source of resistance[32,198]. Intriguingly, both of these works recognised a recurrent theme in this HGF-mediated resistance, that PI3K re-activation, compensated for the survival signal transduced by the targeted kinase. Interestingly, PI3K also represents a key mediator of survival in MET-addicted tumour cells, in the setting of EGFR resistance[199,200]. It therefore remains rather surprising, that the role of HGF in innate or acquired resistance to MET-targeted agents has not been properly investigated.

4.2 Results

4.2.1 AKT, specifically isoform AKT2, is implicated in HGF-driven resistance.

During the course of our experiments, we noticed on western blotting, that HGF overexpression caused increased AKT signalling, with increased levels of total AKT protein as well as pAKT S473 and pAKT T308 (Figure 24). Both of these phosphorylation sites are necessary for the maximal activation of AKT kinase[201].

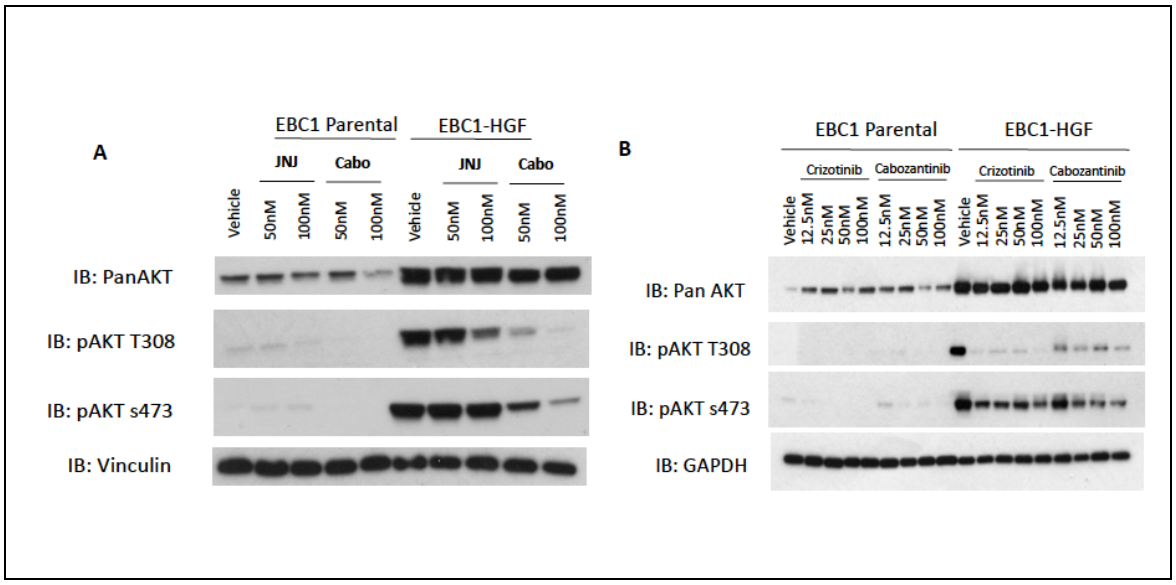

Figure 24. Increased AKT signalling in HGF-overexpressed EBC1 cells. (A,B) Western blot analysis of the responses of MET amplified (EBC1) cell line and EBC1-HGF to 6h treatment with MET inhibitors, JNJ-38877605, crizotinib and cabozantinib respectively. Note that in EBC1-HGF cells, in both experiments, there is increased signalling in panAKT and pAKT sites.

In order to assess on a broader scale what the potential signalling mediators associated with HGF-induced resistance could be, MS-based phosphoproteomic profiling was used as a tool.

To look for potential MET substrates, we were, initially, interested in identifying any tyrosine-phosphorylated peptides with higher abundance in the HGF-overexpressing cell line (vehicle treated) compared to the parental cells (also vehicle treated), and whose abundance decreases after drug treatment in either parental cells only, or in both cell lines, to try and identify which pathways become resistant to MET inhibitors with HGF overexpression.

Phosphoproteomic data demonstrated that tyrosine phosphorylation of AKT2 was significantly affected by HGF expression in MET amplified NSCLC cells. Looking specifically at tyrosine-phosphorylated peptides with higher abundance in the HGF-overexpressing cell line (vehicle treated) compared to the parental cells (also vehicle treated), and whose abundance changes after drug treatment, AKT2 phosphotyrosine sites were significantly altered (Figure 25, Supplementary Figure 1).

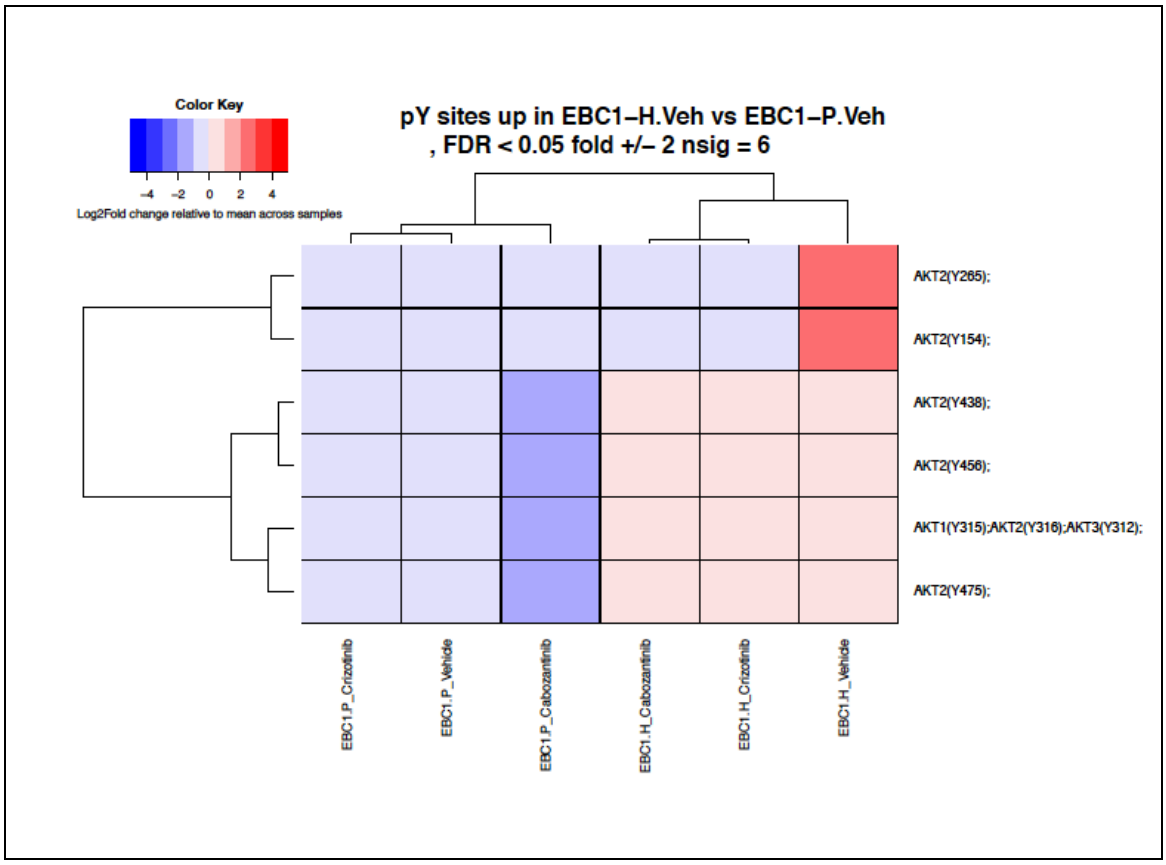

Figure 25. AKT2 is a potential mediator of resistance in HGF-expressed MET-addicted lung cancer. (A) Clustered heatmap of KSEA analysis showing AKT2 phosphosites with increased signal, and (B) Volcano plot of phosphoproteomic data, comparing vehicles in EBC1 Parental and EBC1-HGF, with regards to tyrosine-phosphorylated peptides. The colour intensities correspond to the values of the scores of each signalling pathway indicating upregulated sites (red, upregulated; blue, downregulated). AKT2-specific tyrosine phosphosites are upregulated.

Further analysis of all phosphopeptides sites showed an upregulation of multiple AKT2-specific phospho-sites, predominantly serine/threonine phosphopeptides (Figure 26).

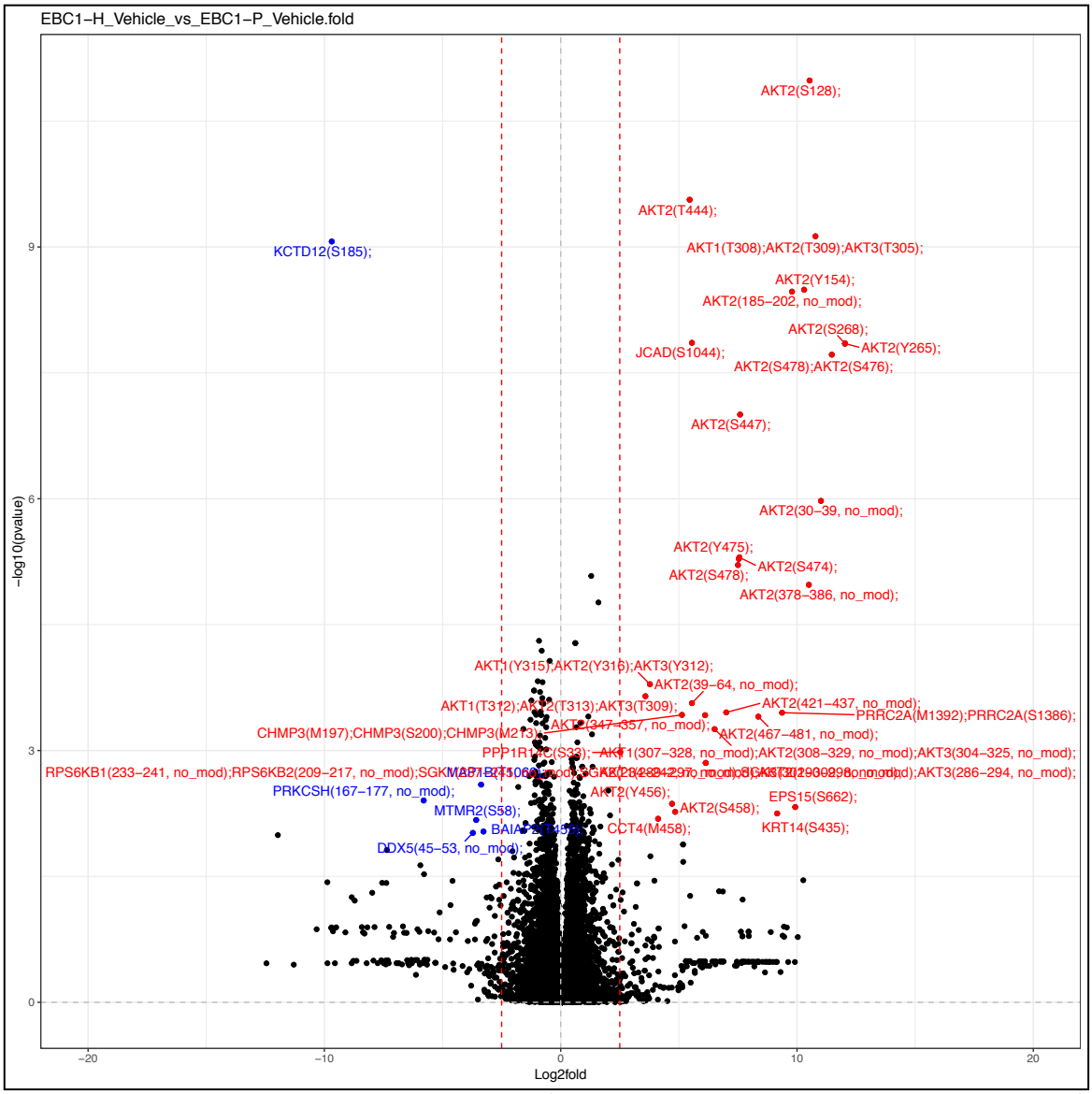

Figure 26. AKT2 is upregulated in analysis of all phosphopeptide sites. Volcano plot of phosphoproteomics data. Red circles, and red text show phosphosites which have significant increases. Blue circles and corresponding blue text show phosphosites which have significant decreases. Log-transformed *P* values (*t* test) associated with individual

peptides and phosphopeptides plotted against EBC1-HGF. Multiple AKT2 phosphosites, highlighted by red text and circles, are identified as significantly upregulated.

We undertook a separate analysis with phospho-serine and phospho-threonine (pSer/pThr) peptides, again to identify which pathways become resistant to MET inhibitors with HGF overexpression. On analysis of pSer/pThr sites, upregulation of AKT2 phosphosites was noted (Figure 27-28, Supplementary Figures 1-3). Consistent with our western blotting results, these data showed a significant basal increase in AKT activation which was resistant to MET TKI treatment in HGF-overexpressing cells compared to parental controls, suggesting that increased cellular AKT activation is primarily driven by activation of the AKT2 isoform.

On further analysis of the phosphoproteomic profiling data, except for the upregulation of AKT2, there were no other findings of significance in all comparisons.

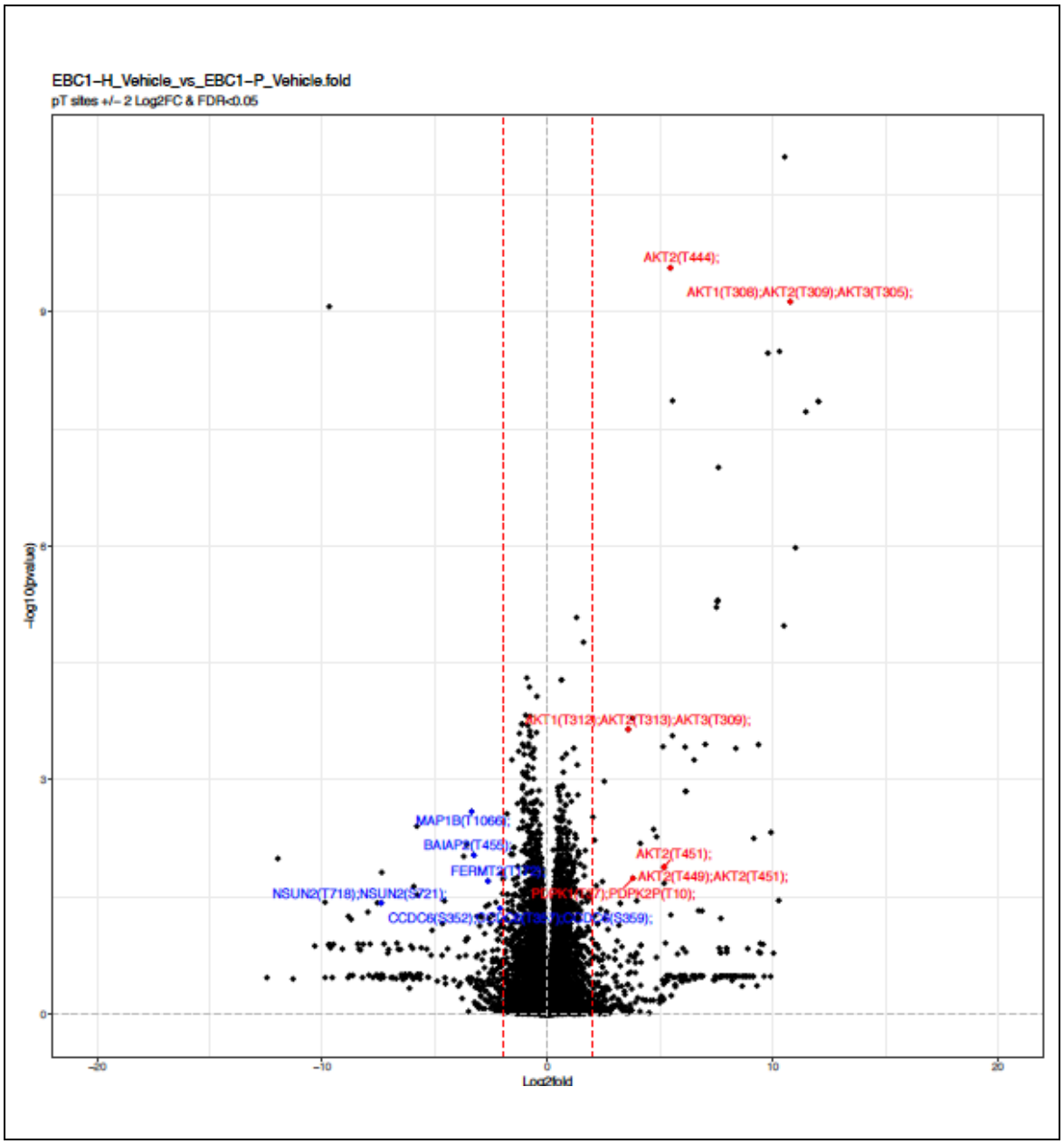

Figure 27. AKT2 is a potential mediator of resistance in HGF-expressed MET-addicted lung cancer. Volcano plot showing AKT phosphosites with increased signal, comparing vehicles in EBC1 Parental and EBC1-HGF, with regards to threonine-phosphorylated peptides threonine-phosphorylated peptides. The colour intensities correspond to the values of the scores of each signalling pathway indicating upregulated sites (red, upregulated; blue, downregulated). AKT2-specific threonine phosphosites are upregulated.

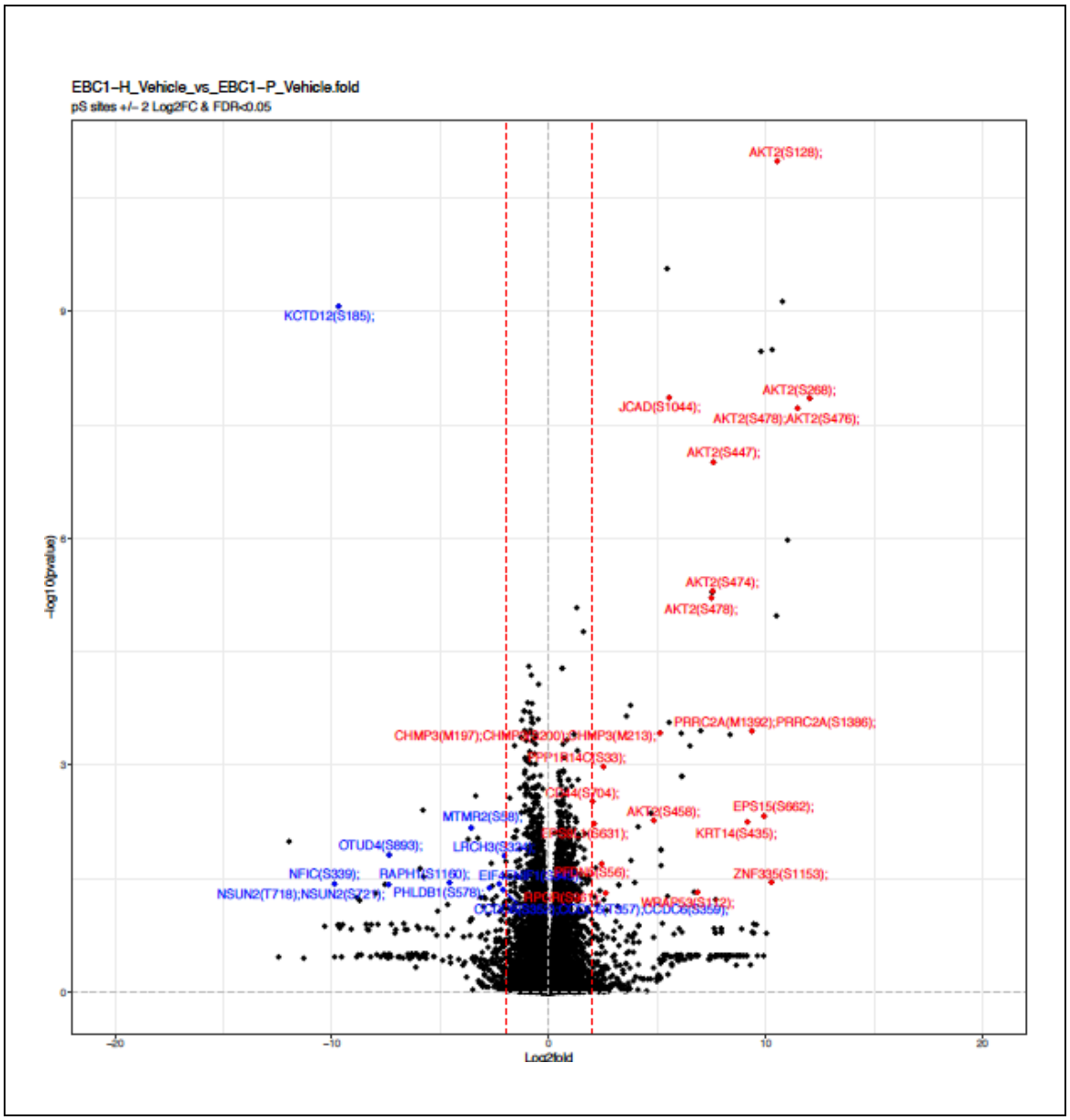

Figure 28. AKT2 is a potential mediator of resistance in HGF-expressed MET-addicted lung cancer. Volcano plot of phosphoproteomic data demonstrating AKT2 phosphosites with increased signal, comparing vehicles in EBC1 Parental and EBC1-HGF, with regards to serine-phosphorylated peptides. The colour intensities correspond to the values of the scores of each signalling pathway indicating upregulated sites (red, upregulated; blue, downregulated). AKT2-specific serine phosphosites are upregulated.

4.2.2 Validation of phosphoproteomic profiling results.

We then validated this increase in AKT2 specific signalling seen in phosphoproteomic profiling using western blotting, probing with AKT2-specific antibodies (Figure 29). Again, in MET-addicted NSCLC EBC1 cells with HGF overexpression, there were significant differences in AKT signalling compared with parental EBC1 cells, with increased levels of panAKT and pAKT T308. Guided by our MS data, we also wanted to confirm the isoform-specific upregulation of AKT in HGF-overexpressing cells. Indeed, we observed striking differences between AKT1 and AKT2, as noticeably, there was a selective increase in the levels of total AKT2 and phosphorylated AKT2 (as shown by the pAKT2 s474-specific antibody), in comparison to the signal seen in total AKT1 and pAKT1 (with the specific antibody for pAKT1 s473). Thus, increased activation of AKT2 in HGF-expressed EBC1 cells is demonstrated using two independent techniques.

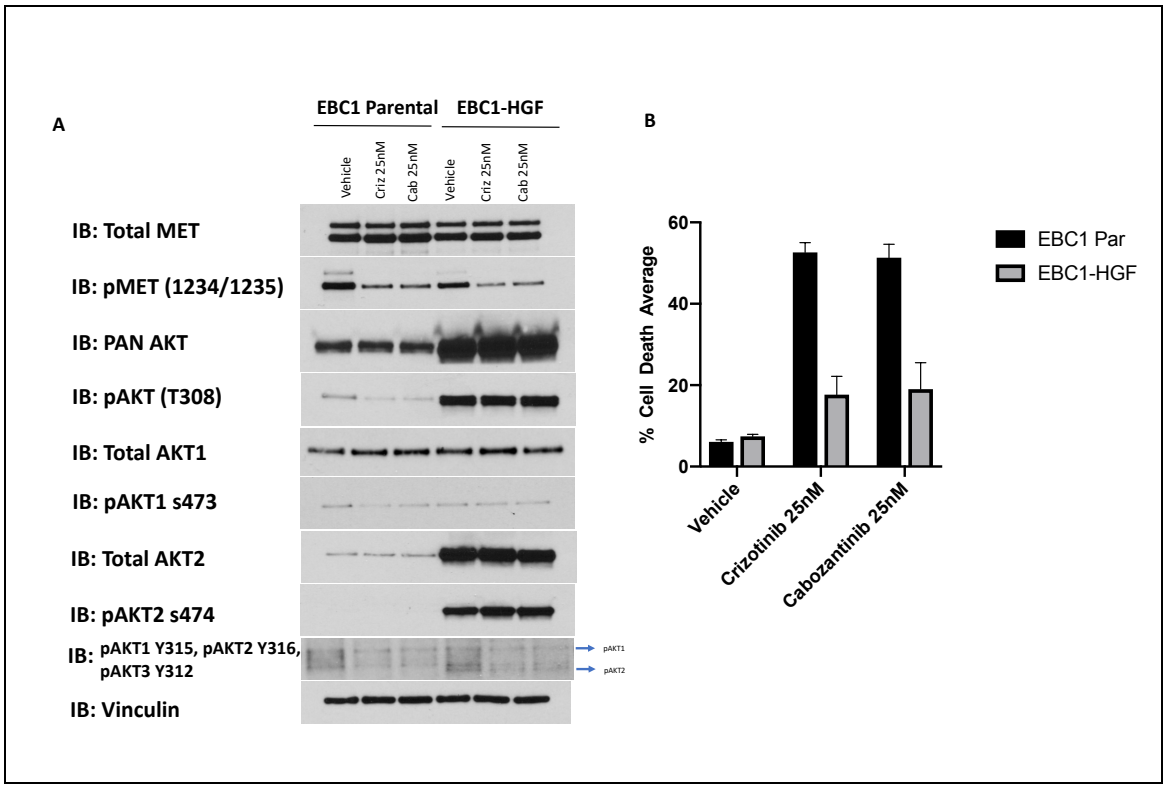

Figure 29. AKT2 specifically is a potential mediator of HGF-induced resistance to MET TKIs in MET-addicted lung cancer. (A) Western blot analysis of the responses of EBC1 and EBC1-HGF to 6h treatment with MET inhibitors, crizotinib and cabozantinib respectively. (B) Analysis of the responses of EBC1 and EBC1-HGF to 72h treatment with 25nM crizotinib and cabozantinib. Cell death percentages (mean ± SEM) were assessed via automated trypan blue method (ViCell). In this instance, crizotinib and cabozantinib induce robust cell death (B), yet pMET is poorly inhibited. AKT2 specific antibodies are increased in HGF-expressed cells (A), s474 and total AKT2, in contrast to AKT1 specific antibodies s473 and total AKT1.

4.2.3 AKT2 as a mediator of resistance

We then sought to further characterise how AKT2 might be driving HGF-mediated resistance by using immunoprecipitation experiments to seek out an interaction between MET and AKT2.

Co-immunoprecipitations (Co-IP) are routinely used to detect protein-protein interactions in cells. The tight binding between biotin and avidin (or streptavidin) makes biotin-labelling a useful tool for many applications such as detection, immobilization, and purification[202]. The applications of this system have been furthered greatly by the discovery of BirA, an *Escherichia coli* biotin ligase[203,204]. BirA can catalyse the covalent attachment of biotin to the lysine side chain, within a 15-amino acid peptide termed the Avi-tag[203,204]. Using this system, co-expression of an Avi-tagged protein of interest with BirA leads to specific biotinylation[205].

Initially, a co-IP was performed in HEK 293T cells to first assess a potential interaction between MET and AKT2 using an overexpressed epitope-tagged AKT2 (avi-tagged) and over-expressed MET (Figure 30, A). Using this system, we found no evidence of interaction between AKT2 and MET. We then examined this endogenously in EBC1 and EBC1-HGF cells. However, once again immunoprecipitated MET in these cells did not show any interactions with AKT2 (Figure 30, B).

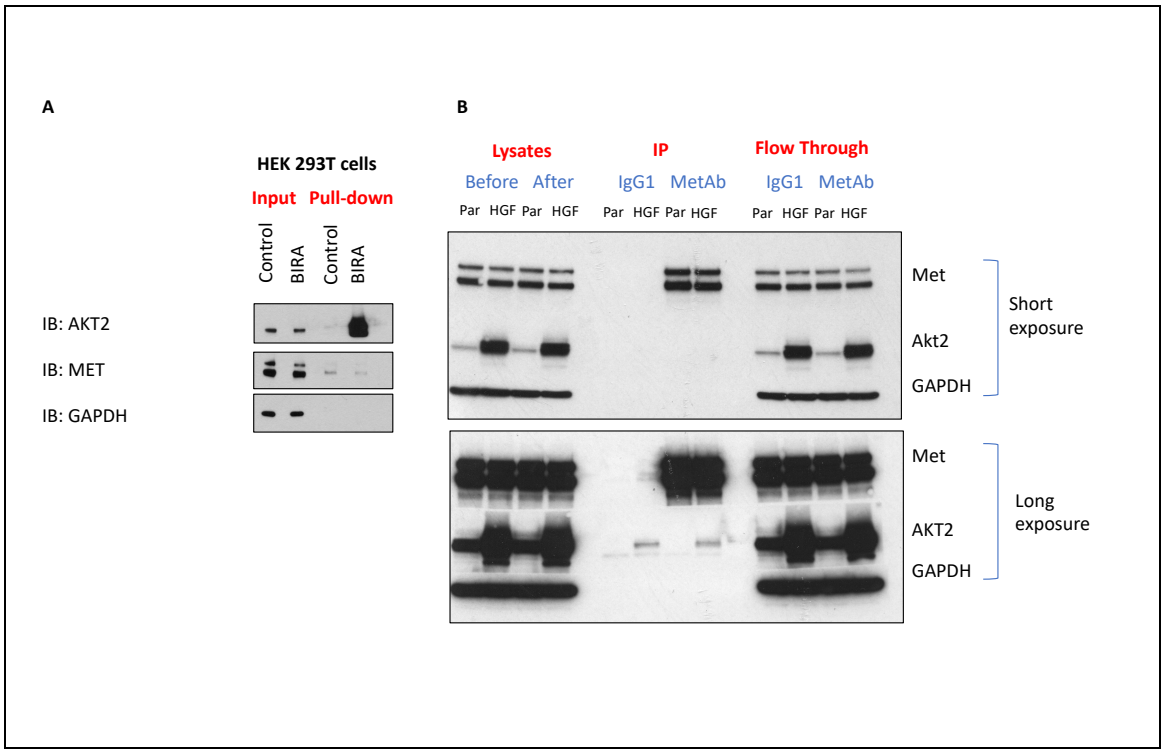

Figure 30. Immunoprecipitation experiments investigating if AKT2 be mediating MET TKI resistance. In both A and B, there was no evidence of a direct interaction between AKT2 and HGF. Cell lysates were immunoprecipitated using anti-MET antibodies and analysed by western blotting with antibodies directed against AKT2 and MET.

In order to assess whether the increased levels of AKT in HGF-overexpressing cells had any impact on its subcellular distribution, we stained EBC1 and EBC1-HGF cells with antibodies against AKT.

The localization of AKT was assessed by immunofluorescence. HGF excess was associated with increased cytoplasmic and nuclear AKT staining, with only weak cytosolic staining evident in the EBC1 parental cell line (

Figure 31).

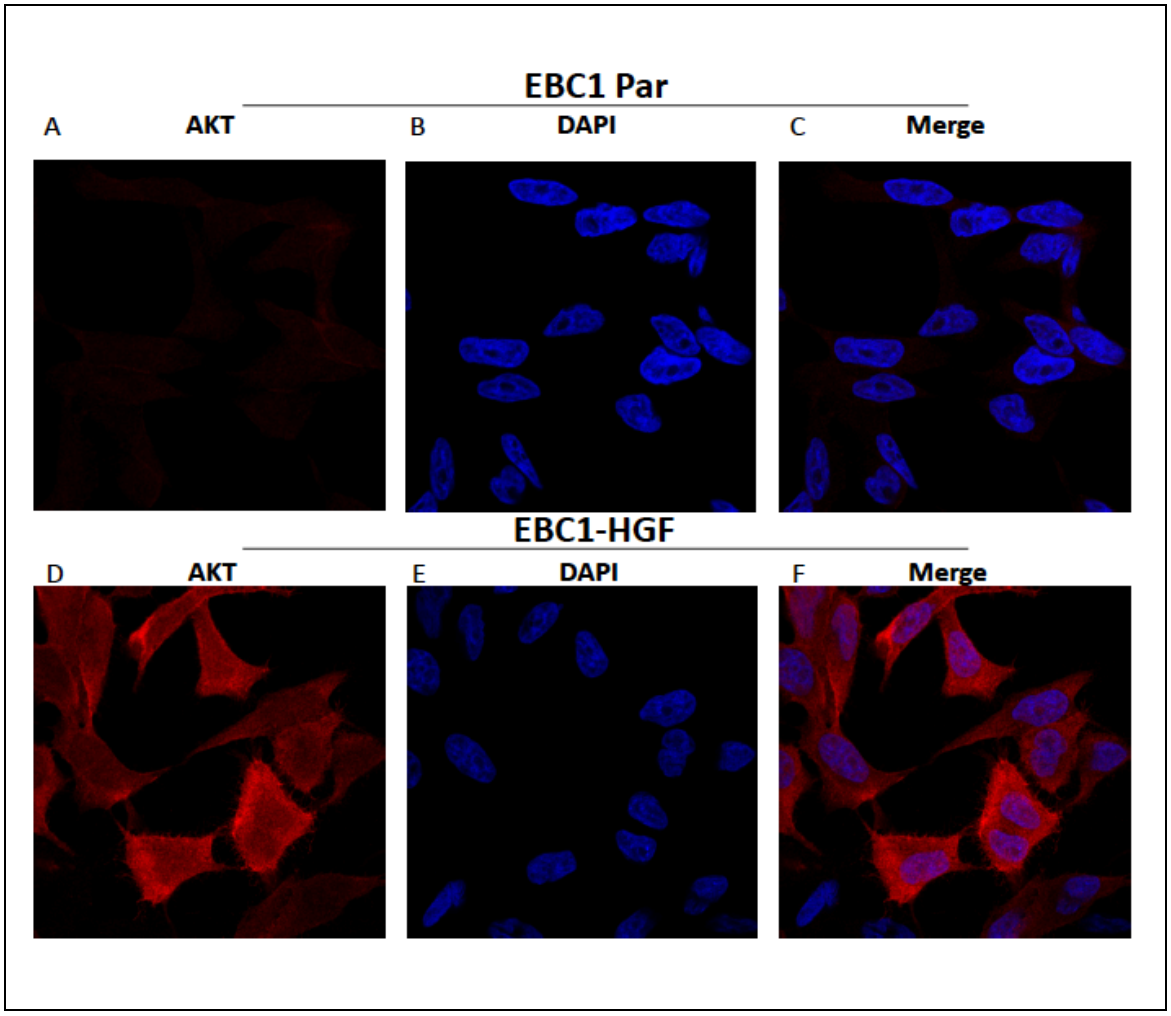

Figure 31. Expression and localisation of AKT differs in HGF excess in EBC1 cells. The localization of AKT was assessed in EBC1 parental cells (A-C) and EBC1-HGF cells (D-F) by immunofluorescence. We demonstrate that AKT localisation differs in EBC1 parental those cells exposed to HGF excess. Note, both cytoplasmic and nuclear evidence of AKT signalling in EBC1-HGF.

4.3 Discussion

4.3.1 AKT2 is implicated in HGF-induced resistance to MET TKIs in MET-addicted lung cancer.

There are a number of recent studies that have implicated AKT re-activation as a possible driver of HGF-induced drug resistance. Firstly, two recent studies using a large panel of oncogene-addicted human cancer cells investigated the effect of growth factors in general, on the response to targeted anticancer agents and while they identified HGF as the most relevant microenvironment-borne source of resistance[32,198]. Interestingly, both studies noted that PI3K re-activation, compensated for the survival signal transduced by the targeted kinase[32,198]. More specifically, in the setting of NSCLC and primary HGF-induced resistance, Owusu et al[139], demonstrated that while HGF drives resistance to anti-MET therapy in MET-amplified lung cancer cells, MET-amplified NSCLC cells become addicted to HGF upon MET inhibition, and HGF reactivates and restores AKT and ERK signaling[139]. Pennachietti et al[34] noted that HGF restored PI3K signaling through recruitment of the physiologic GAB1 adaptor protein and postulated that this signaling adaptor shift may be explained by the different mechanisms of MET activation involved. For example, HGF stimulation conceivably causes the stabilization of MET homodimers, perhaps explaining why HGF-induced MET activation is qualitatively different from overexpression-sustained MET activation, and the two signals behave in effect, as two distinct redundant pathways in terms of cell survival[34].

Intriguingly, in the setting of MET-mediated resistance to EGFR inhibitors in lung cancer, resistance has been found to occur even in the absence of MET amplification via HGF-induced activation of the AKT pathway[187,188].

Our data demonstrate, through multiple approaches - western blotting, phosphoproteomic profiling and immunofluorescent studies - that HGF excess in MET

amplified NSCLC causes increased AKT activation, suggesting that perhaps sustained activation of the AKT pathway is driving innate HGF-induced resistance in MET-amplified NSCLC.

To the best of our knowledge, the results of our phosphoproteomic profiling, and subsequent western blotting implicating AKT2 specifically as the major AKT isoform associated with HGF-mediated MET TKI-resistance, is entirely novel. Our data strongly suggest that the activation of pro-survival AKT signalling pathways in tumour cells in the presence of excess HGF in MET amplified NSCLC plays a major role in *de novo* MET TKI resistance.

A common feature of many human cancers, including lung cancer[206,207], is the unregulated activation of the AKT pathway. The protein kinase AKT is a critical signal transducer of the phosphatidylinositol 3-kinase (PI3K) pathway, and plays a pivotal role in the maintenance of many cellular processes including cell growth, proliferation, survival and metabolism. Indeed, the PI3K/AKT pathway is arguably the most commonly disrupted signalling pathway in human cancers[208], with pathway aberrations having been identified in up to 40% of all tumour types (PTEN loss by immunohistochemistry occurring most frequently (30%), followed by mutations in PIK3CA (13%), PTEN (6%) and AKT (1%))[208].

There are three AKT isoforms, transcribed from separate genes, which share three highly conserved domains (and more than 80% sequence homology): a central catalytic domain and two regulatory domains: a lipid-binding N-terminal pleckstrin homology (PH) domain, and a C-terminal hydrophobic motif[209]. AKT1 and AKT2 are ubiquitously expressed in all tissues, whereas AKT3 has a more restricted expression pattern[210]. Because of their similar tissue distribution and activation pattern, it had previously been assumed that the AKT1 and AKT2 isoforms had overlapping functions[211,212], and that due to the shared 80% sequence homology, all AKT isoforms had been considered to possess similar substrate specificity[211,212].

In vivo studies, however, using knockout mouse models have provided evidence for isotype-specific functions of AKT: for example, AKT2 knockout mice show diabetes-like symptoms due to an impaired insulin response[213,214] and AKT3 knockout mice show reduced brain size[215]. Phosphoproteomic screens have demonstrated unique and common substrates for each of the AKT isoforms, and functional studies have recently started to highlight their physiological relevance, for example during RNA processing in lung cancer[216]. Altogether, these data suggest that AKT isoforms have both distinct and overlapping functions under physiological conditions.

Why AKT2, specifically, is so active in the presence of excess HGF in MET-amplified NSCLC cells above other isoforms is uncertain, and these data are driving current research efforts in our lab. Of critical importance is to determine whether AKT2 activation is sufficient to confer MET TKI resistance. To do this, we are currently generating MET TKI-sensitive cell lines ectopically expressing constitutively active alleles of AKT1 or AKT2. We are also generating cell line models where individual AKT isoforms are selectively depleted using CRISPR/Cas9 gene editing to test whether this restricts the ability of HGF overexpression to confer MET TKI resistance.

Our western blotting data using AKT isoform-specific antibodies (Figure 29), clearly demonstrate increased AKT2 signal in EBC1 HGF-expressed cells, compared to AKT1. Our IP experiments (Figure 30) failed to show a direct association between AKT2 and MET molecules in EBC1 cells, and in HEK293T cells, suggesting that the effects of AKT2 on MET function might influence MET-dependent signalling rather than MET itself.

However, it is also possible that AKT2, through its effects on signal transduction, could impact MET receptor conformation and/or localization. Further experiments are ongoing (described in Chapter 5) to try to determine the fate of cell-surface MET when chronically exposed to excess HGF.

It is possible that a desensitised MET receptor (as a consequence of chronic HGF exposure) might have distinct steady-state signalling properties (such as increased AKT2 activation).

From a clinical point of view, this provides the rationale for another reasonable strategy to overcome innate HGF-induced resistance to MET TKIs in MET amplified NSCLC – combining MET TKIs with clinically available AKT inhibitors.

5 Overcoming HGF-mediated MET TKI resistance in NSCLC.

5.1 Introduction

The development of molecularly targeted agents has undoubtedly led to multiple successes in cancer medicine, and the clinical success of small molecule EGFR tyrosine kinase inhibitors in the treatment of EGFR-mutant NSCLC exemplifies this[217,218]. However, not all patients will respond to these targeted treatments, and drug resistance is inevitable with resulting disease progression in most if not all patients. Thus, targeted therapies are often inadequate when used as single agents, and rational combinatorial strategies are generally necessary to overcome compensatory escape mechanisms[219].

We have demonstrated in our *in-vitro* models of MET-addiction sensitivity to type I and type II MET TKIs (Figure 10-12), and subsequently shown clear rescue to these inhibitors when HGF is overexpressed in these models (Figure 14, Figure 15). As previously mentioned, quantification of tumour HGF given its potential role in MET TKI resistance, has been largely ignored as part of clinical trial design for lung cancer. Based on our data supporting excess HGF as a mechanism of primary resistance to MET TKIs, we explored potential therapeutic strategies to overcome this resistance. Clinical experience tells us that sometimes one option is not enough, we therefore wanted to design multiple strategies to overcome resistance.

5.2 Results

5.2.1 Strategy 1: Overcoming resistance with increasing dose MET TKI.

We reasoned that this mechanism of resistance is MET-dependent because it relies on overexpression of its physiological ligand, HGF, which is selective for MET. Thus, our initial strategies were focused on alternative MET-targeting approaches. Firstly, using increasing doses of MET TKIs HGF-induced MET TKI-resistance could be overcome, in our MET-addicted models with HGF-overexpression. Yet, perhaps unsurprisingly, the dose at

which this was achieved varied depending on the compound (Figure 32). Similarly, relatively high doses of crizotinib (1uM) were required to induce robust cell death in SBC5, the SCLC cell line with endogenous over-expression of HGF and MET.

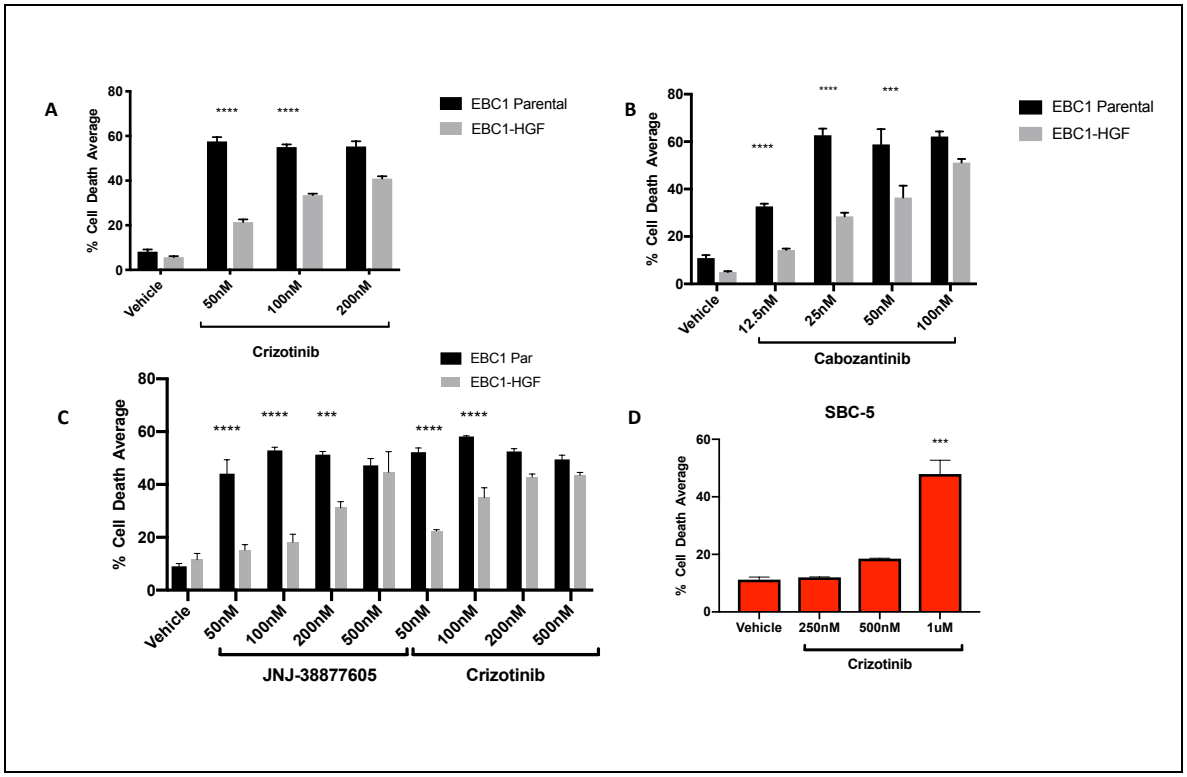

Figure 32. Increasing dose MET TKI can overcome HGF-induced resistance in MET-amplified NSCLC. (A-C) Analysis of the responses of MET amplified cell line, EBC1 and EBC1-HGF to 72h treatment with MET inhibitors, type I inhibitor JNJ-38877605, crizotinib and type II inhibitor cabozantinib. 2-way Anova performed where indicated. Adjusted P-value is <0.0001 when specified as **. (D) Analysis of SBC5 cell line, SCLC cell line with high level HGF and MET co-expression. Cell death percentages (mean ± SEM) were assessed via automated trypan blue method (ViCell), and expressed as the fraction of stain-positive cells. One sample t and Wilcoxon test of Data performed, p value <0.0009.**

These data suggest that increasing the dose of MET TKI could overcome HGF-mediated resistance. However, increasing drug concentrations in the clinic remains a challenge, and achieving prolonged exposure of tumours to high drug concentrations may not be feasible. Therefore, we decided to investigate whether duration of exposure of MET+ NSCLC cells to MET TKIs affects the biological response.

I carried out washout experiments (initially using a fixed dose of crizotinib and cabozantinib (50nM)) to define the shortest time of exposure needed to elicit a meaningful biological response (Figure 33). In these experiments, cells are treated with compound for a fixed amount of time, after which the drug is "washed out" and the cells are allowed to grow in drug-free media. Intriguingly, in EBC1 parental cells (Figure 33, B), between 30mins and 2 hours of continuous exposure with crizotinib at 50nM, was sufficient to induced robust cell death (almost to full effect). For cabozantinib, much longer exposure time was required, as it took 96 hours of continuous exposure to induce cell death. Furthermore, resistance in HGF-overexpressing EBC1 cells was maintained throughout this experiment.

Subsequently, I performed another experiment with crizotinib at a higher dose and with additional time points, and asked whether it was possible to achieve a biological response earlier in parental cells, and also to assess whether the EBC1-HGF cells maintained their resistance (Figure 33, C). Here, only 15mins exposure to 200nM crizotinib was required to cause cell death in EBC1 parental cells, however resistance was maintained throughout in the HGF-overexpressing subline. Furthermore, even at increasing doses of crizotinib (up to 200nM) it took three full days of drug exposure to fully overcome resistance.

These data suggest that both the dose, and the duration of drug exposure, influence the response to treatment. Therefore, my data suggest that to improve future clinical trial design alternative dosing schedules (including pulsatile high dose crizotinib) should be considered.

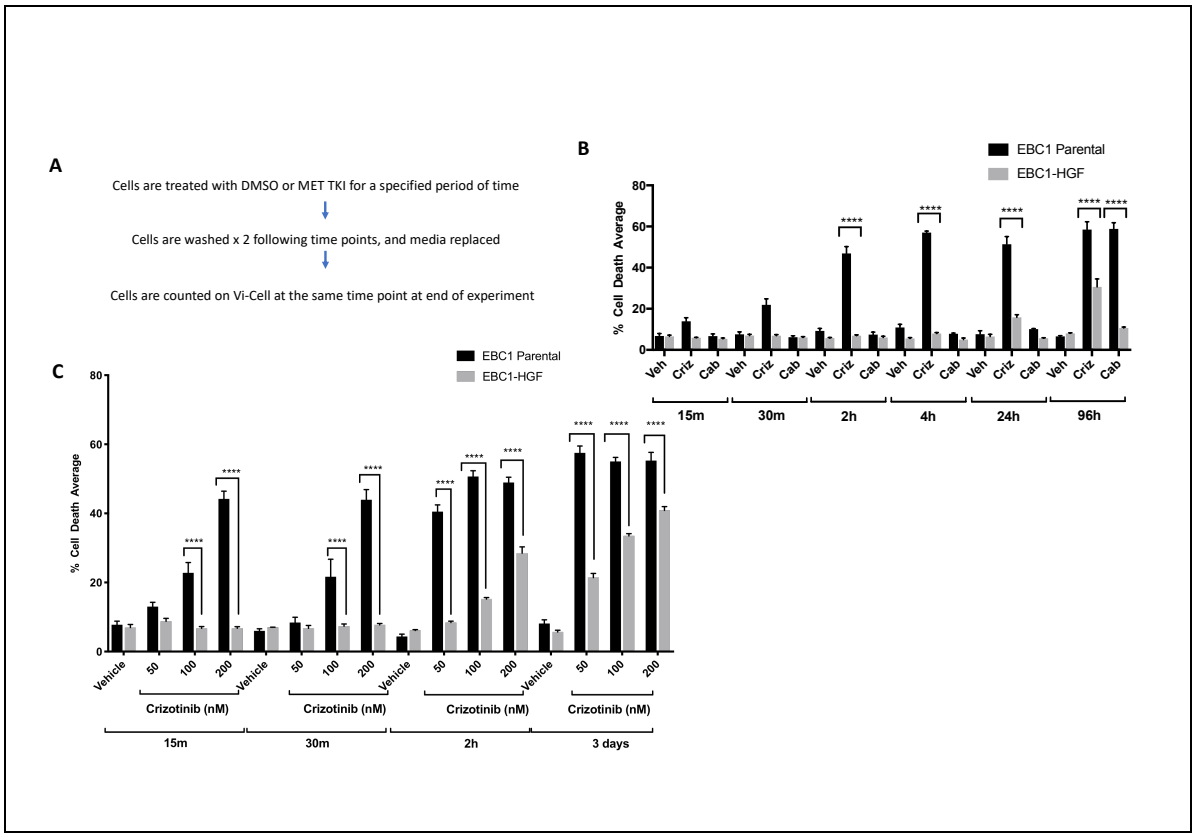

Figure 33. Washout experiments indicating that duration of drug exposure counts. (A) Depicts the design of the washout experiments. (B) Analysis of the responses of MET amplified cell line, EBC1 and EBC1-HGF to 50nM of treatment with MET inhibitors, type I inhibitor crizotinib and type II inhibitor cabozantinib. (C) Analysis of the responses of MET amplified cell line, EBC1 and EBC1-HGF to 15minutes, 30 minutes, 2 hours, 3 days drug treatment with crizotinib. Cell death percentages (mean ± SEM) were assessed via automated trypan blue method (ViCell), and expressed as the fraction of stain-positive cells.

5.2.2 Strategy 2: HGF-mediated MET TKI resistance can be overcome by multi-modality MET targeting.

Given that our mechanism of resistance is MET-dependent, relying solely on the overexpression of MET's physiological ligand HGF, we sought further MET-based strategies to overcome this resistance. Firstly, we evaluated the MET-specific monovalent antibody MetMAB (or onartuzumab). While this compound demonstrated weak single agent activity, when used in combination with type I and type II MET TKIs in MET-addicted NSCLC cell line EBC1 and the HGF-expressed cells, this combination induced robust cell death (Figure 34). This strategy of combining MET targeting antibody MetMAB with MET TKI also proved successful in overcoming HGF-induced resistance in our MET-amplified gastric carcinoma model GTL16.

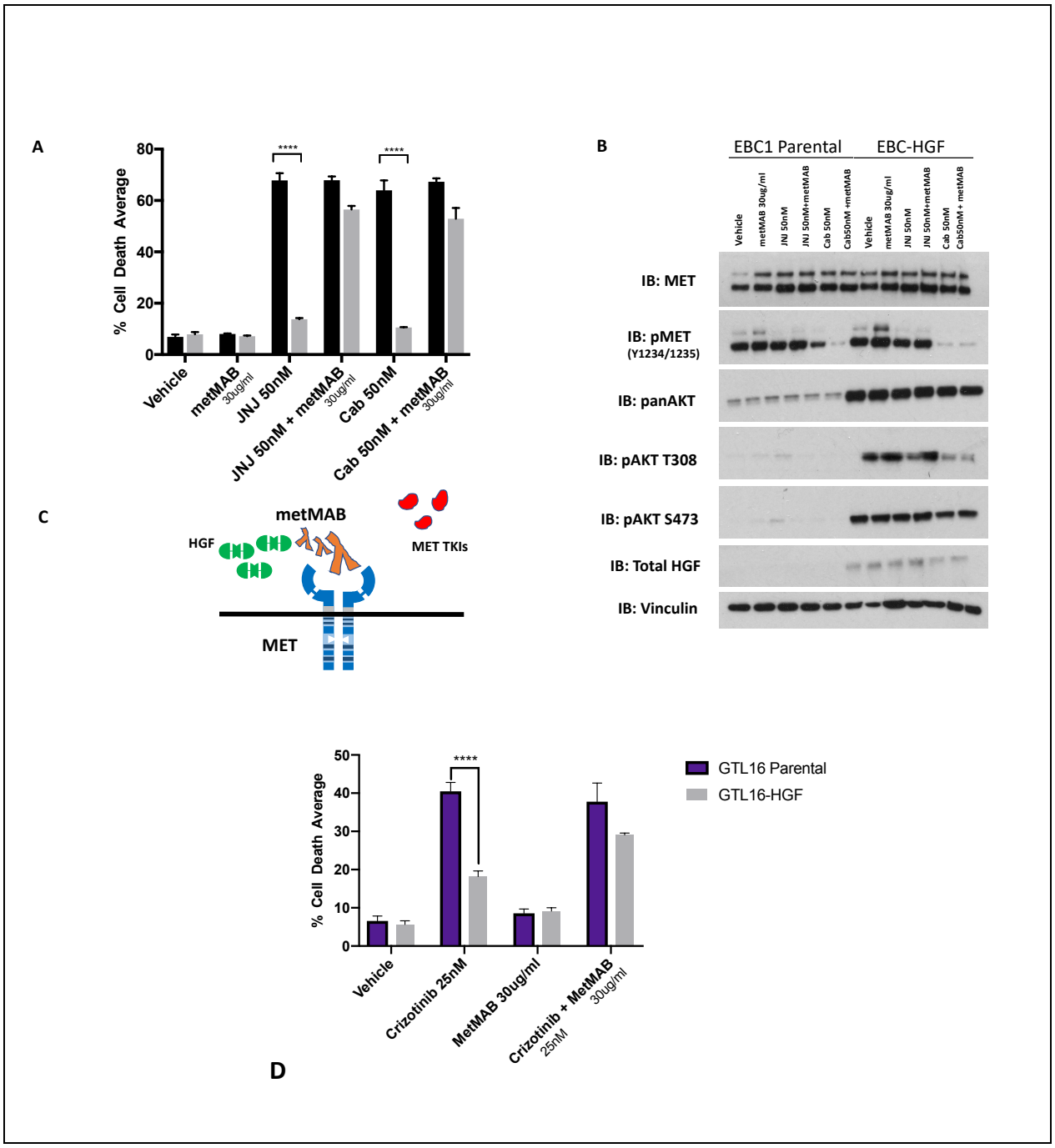

Figure 34. MET-targeted antibody in combination with MET TKI overcomes HGF-induced resistance. (A) Analysis of the responses of MET amplified cell line, EBC1 and EBC1-HGF to 96h treatment with MET inhibitors, type I inhibitor JNJ-38877605, and type II inhibitor cabozantinib alone and combined with MET-targeting antibody metMAB. 2-way anova performed where indicated. Adjusted P-value is <0.0001 when specified as **. (B)**

Biochemical effects of combination therapy. Note, here that again, pMET does not correlate with response and there is again evidence of increased AKT signalling in EBC1-HGF. (C) Schema representing the potential action of MetMAB blocking HGF access to binding site on MET receptor, allowing TKIs to bind efficiently and induce cell death. (D) Analysis of response of MET amplified gastric cancer cell line, GTL16 and HGF-over expressed GTL16, to 72h treatment with MET inhibitor, crizotinib and MET-targeting antibody MetMAB. Cell death percentages (mean ± SEM) were assessed via automated trypan blue method (ViCell), and expressed as the fraction of stain-positive cells. Combination therapy with crizotinib and metMAB is synergistic, causing increased cell death in GTL16-HGF cells. Adjusted P-value is <0.0001 when specified as **.**

5.2.3 Strategy 3: mTOR kinase inhibitors overcome HGF-mediated MET TKI resistance

We have demonstrated in MET-addicted NSCLC EBC1 cells, that AKT levels are significantly increased following ectopic HGF overexpression. Interestingly, I noticed that there were differences in terms of the response of specific AKT phosphorylation sites to MET TKI treatment (Figure 24). Phosphorylation of the PDK1 site in the activation loop (Thr308) was much more sensitive to MET TKI treatment, compared to the mTORC2 site in the hydrophobic motif (Ser473), particularly with the more selective inhibitor JNJ-38877605 (Figure 24).

Given that the mTORC2 phosphorylation site on AKT appeared to be refractory to MET TKI-induced dephosphorylation in HGF-overexpressing cells, we suspected that mTORC2 activity was unaffected by MET TKI treatment. We therefore hypothesised that mTORC2 inhibition might overcome HGF-mediated MET TKI resistance.

Importantly, AZD2014 (or Vistusertib) a mTORC1/2 kinase inhibitor, was being tested in the phase II genomic-driven National Lung Matrix Trial (NLMT)[18] in NSCLC at the Royal Marsden Hospital. Thus, we evaluated this compound in combination with MET TKIs in our NSCLC MET-driven model. Combination of mTORC1/2 inhibitor AZD2014 with either type I or type II MET TKI overcame HGF-mediated resistance in MET-addicted NSCLC cells (Figure 35).

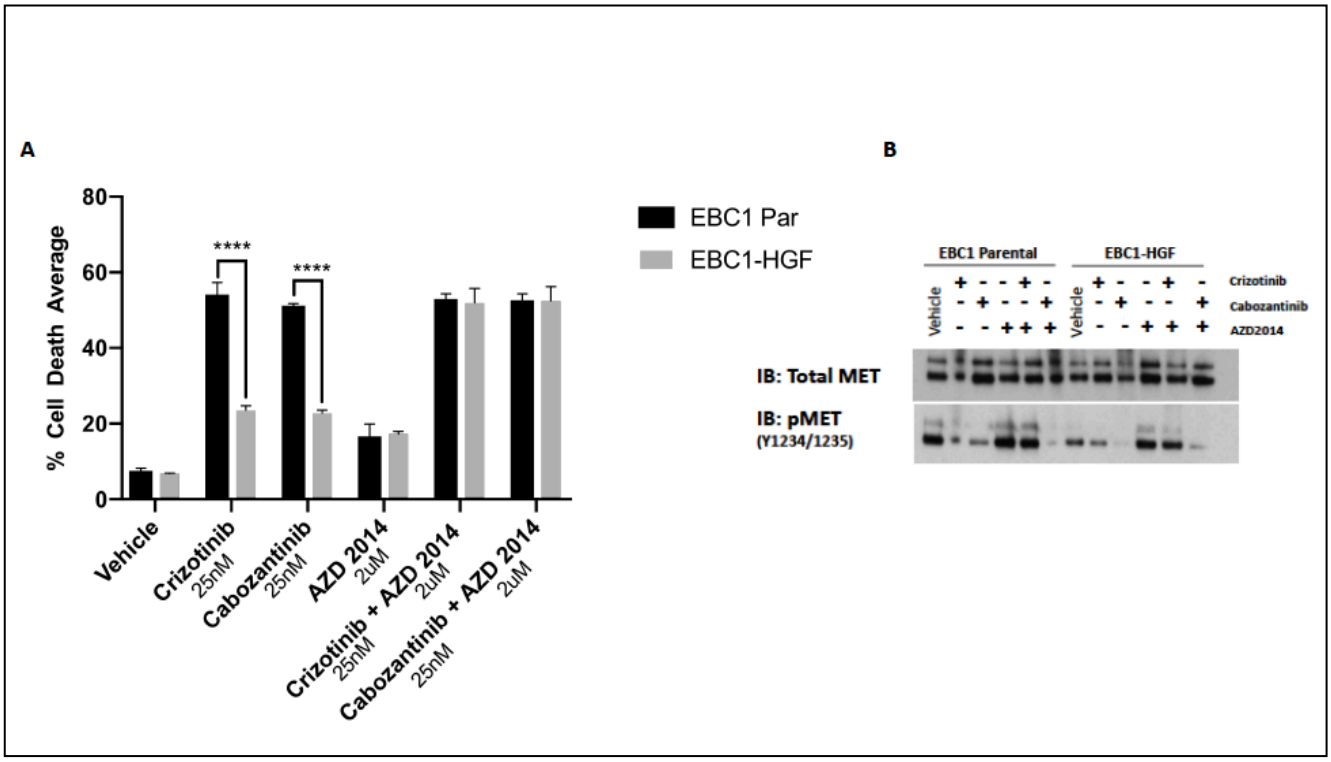

Figure 35. MET TKI combined with mTORC1/2 inhibitor AZD2014 overcomes HGF-induced resistance in EBC1 cells. Analysis of the responses of MET amplified cell line, EBC1 and EBC1-HGF to 72h treatment with MET inhibitors, type I inhibitor crizotinib, and type II inhibitor cabozantinib alone and combined with mTORC1/2 inhibitor AZD2014. 2-way anova performed. Adjusted P-value is <0.0001 when specified as **.**

Unfortunately, updated clinical data from the NLMT indicated that this compound was not clinically active in NSCLC[220], and subsequently this led to re-focusing efforts on more clinically relevant NSCLC strategies. Additionally, this inhibitor combination did not overcome resistance in our second model (Figure 36), the gastric MET-amplified cell line GTL16, suggesting that it may not be broadly applicable.

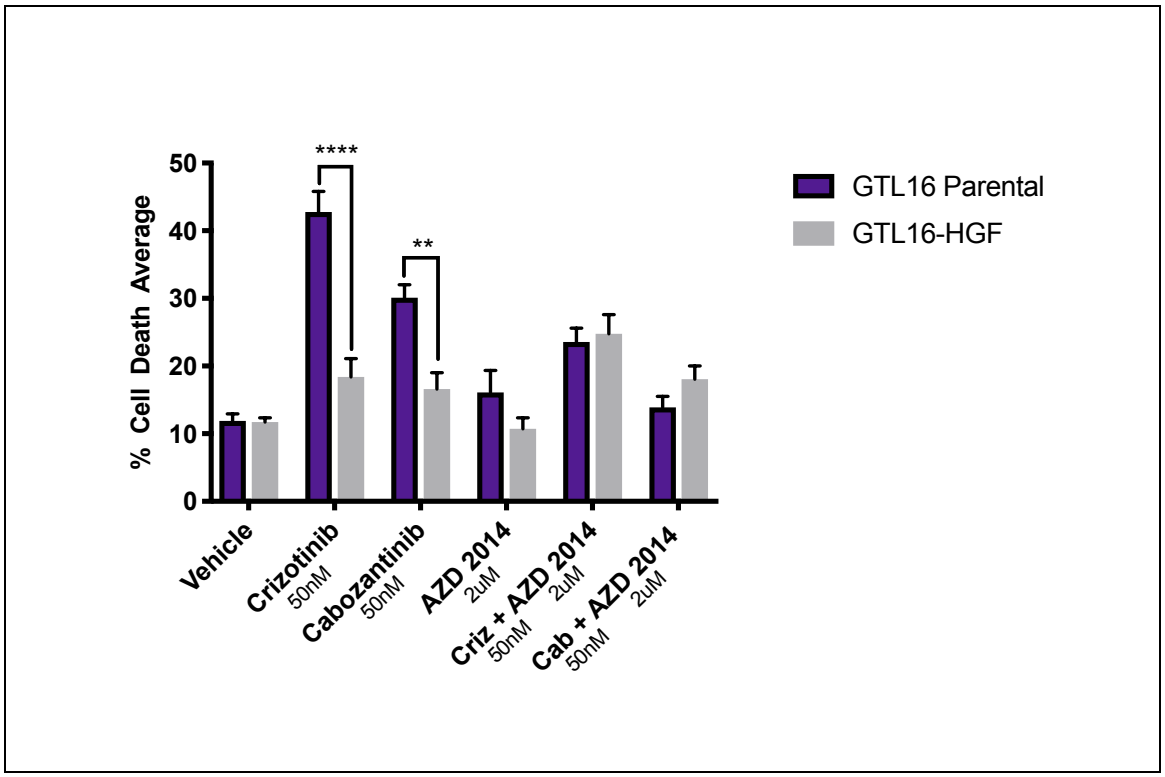

Figure 36. AZD 2014 inactive in combination with MET TKIs in MET-addicted gastric cancer models. Analysis of the responses of MET amplified gastric cell line, GTL16 and GTL16-HGF to 72h treatment with MET inhibitors, type I crizotinib, and type II inhibitor cabozantinib alone and combined with mTORC1/2 inhibitor AZD2014.

5.2.4 Strategy 4: Overcoming TKI resistance with combination MET TKI + allosteric AKT inhibitor, ARQ092.

The results from our phosphoproteomic profiling experiments, together with the western blot analyses showing that HGF-overexpressing EBC1 cells demonstrated increased AKT signalling, suggested that combining MET TKIs with an AKT inhibitor could be another reasonable approach to overcome HGF-mediated MET TKI resistance. Furthermore, finding a clinically relevant strategy was paramount. Recent encouraging data from biomarker-driven basket studies of ATP-competitive AKT inhibitor AZD5363 (or capvisertib) [221,222] have re-boosted enthusiasm for the utility of AKT-targeting compounds. And, while the allosteric AKT inhibitor MK2206 has failed to show single agent activity in a number of clinical trials[209], another potent and selective allosteric AKT inhibitor called ARQ092 (or miransertib) has shown promising results in early phase studies[223] and is currently undergoing phase I testing in solid tumours. ATP-competitive inhibitors and allosteric inhibitors are the two distinct classes of AKT inhibitors that are currently in clinical trial development. Allosteric inhibitors, such as ARQ092, bind to AKT through interactions with the PH-domain/kinase-domain interface[224], a key feature of the inactive kinase (Figure 37). ATP-competitive inhibitors, such as AZD5363, bind to the active conformation in which the PH domain has swung away from the kinase domain and expose the ATP-binding pocket (Figure 37).

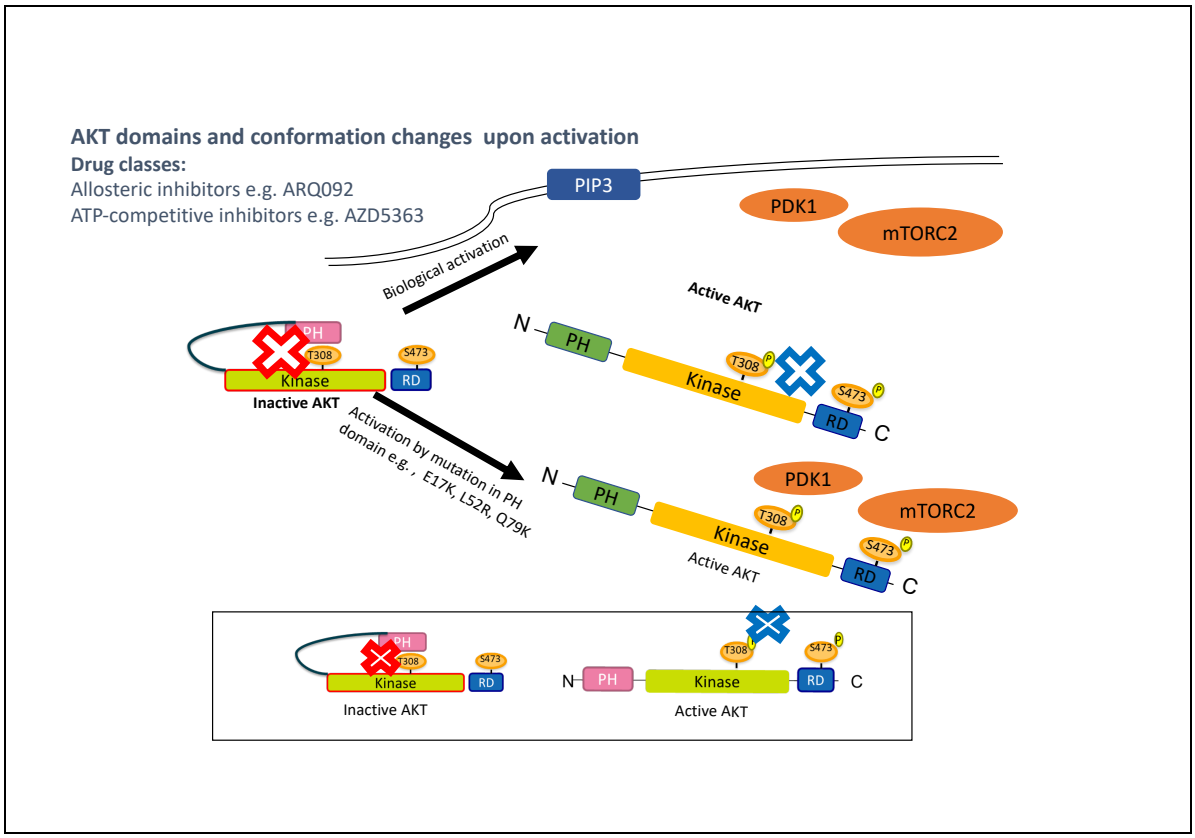

Figure 37. AKT has 3 isoforms and have similar domain structures. The interaction between PH domain and kinase domain keeps AKT inactive and upon activation and the PH domain dislodges from this conformation enabling the phosphorylation of threonine T308 and S473. AKT however can also be activated by mutation in the PH domain, locking the kinase in a constitutively active state, independent of a growth factor signal. Deregulation of the PI3K/AKT is common in cancer and there are various drugs that target it. The differential AKT conformation states that these drug classes target.

Treatment with type I or type II MET TKIs in combination with ARQ 092 (miransertib) induced robust cell death in MET-addicted EBC1 parental and EBC1-HGF cells. In contrast, ATP-competitive AKT inhibitors AZD5363 and GDC0068 (Figure 38) failed to synergise with MET TKIs. These encouraging combination data involving ARQ092 plus

MET TKI were reproduced many times (>10) using different models of EBC1-HGF resistance generated at different time points.

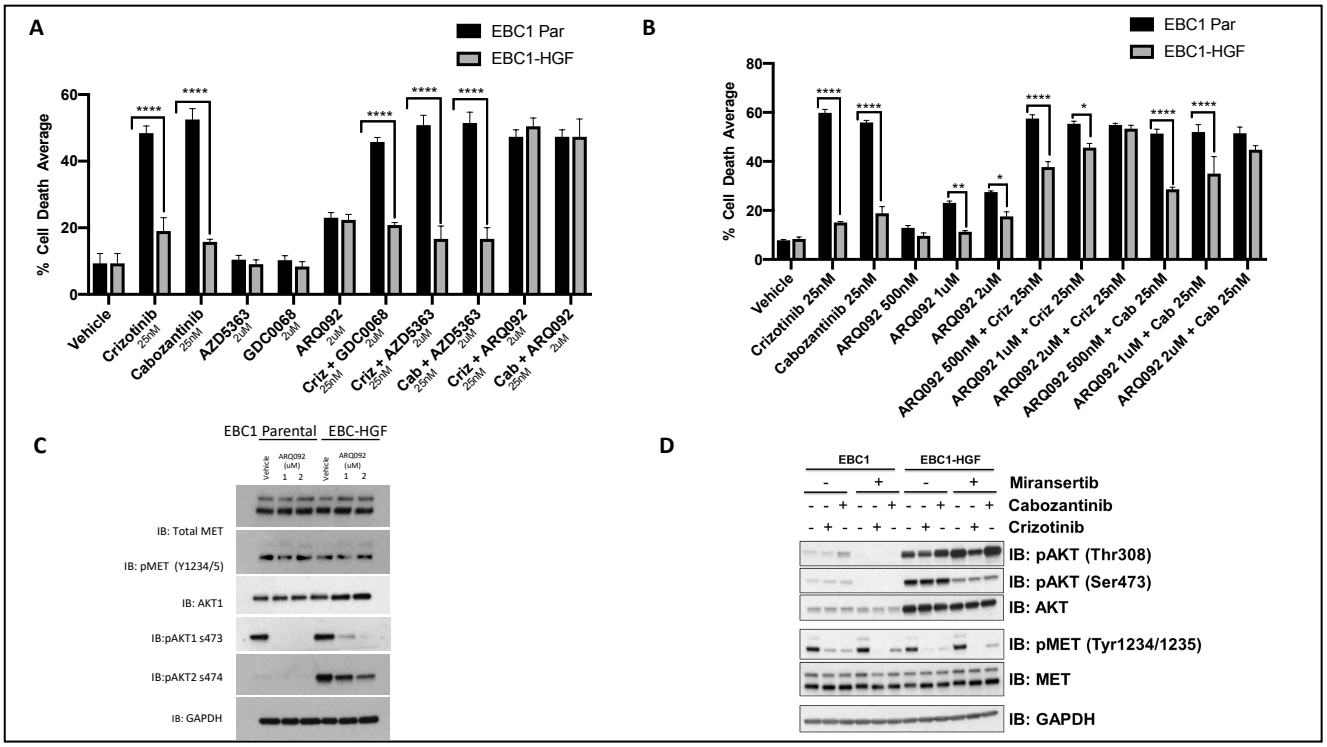

Figure 38. ARQ092 in combination with MET TKI overcomes HGF-induced resistance. (A, B) Analysis of the responses of MET amplified cell line, EBC1 and EBC1-HGF to 72h treatment with MET inhibitors, crizotinib and cabozantinib alone and combined with allosteric AKT inhibitor ARQ092. 2-way anova performed where indicated. (C) Biochemical effects of ARQ092 in EBC1 Parental and EBC1-HGF. Note, here that maximal inhibition of AKT occurs at 2uM. (D) Biochemical effects of ARQ092 (2uM) used in combination with crizotinib (25nM) or cabozantinib (25nM). Note the differences in phosphorylation of pAKT sites, s473 and T308.

Dose titration experiments and western blotting were used to confirm that 2uM of ARQ092 was required in combination with MET TKIs to sufficiently overcome HGF-resistance, as when increased to 2uM, the maximum biochemical and biological effect was achieved (Figure 38).

Intriguingly, when looking at the biological effect of the ARQ092 combination, there appeared to be a difference in the pattern of AKT phosphorylation in the HGF-overexpressing cell line. In the western blot depicted in Figure 38D, as demonstrated previously, there was increased levels of AKT protein in the HGF-overexpressing cell line. However, there were subtle changes in AKT phosphorylation on Ser473 and Thr308. In the parental EBC1 cells, ARQ092 inhibits AKT phosphorylation at both sites, as expected. In the HGF overexpressing cell line, however, ARQ092 appeared to lead to a decrease in S473 phosphorylation but not in T308 phosphorylation. Indeed, it appears that ARQ092 (alone and in combination) caused an increase in AKT-T308 phosphorylation (Figure 38). One possibility is that HGF overexpression affects the sub-cellular localisation of AKT which may restrict access of site-specific phosphatases (PP2A in the case of Thr308 and PHLPP in the case of Ser473).

The combination of ARQ092 and MET TKI also proved effective at inducing cell death in our MET-amplified SCLC model with endogenous high levels of HGF, SBC-5. In Figure 39 robust cell death is induced in SBC-5 using combination therapy crizotinib and ARQ092.

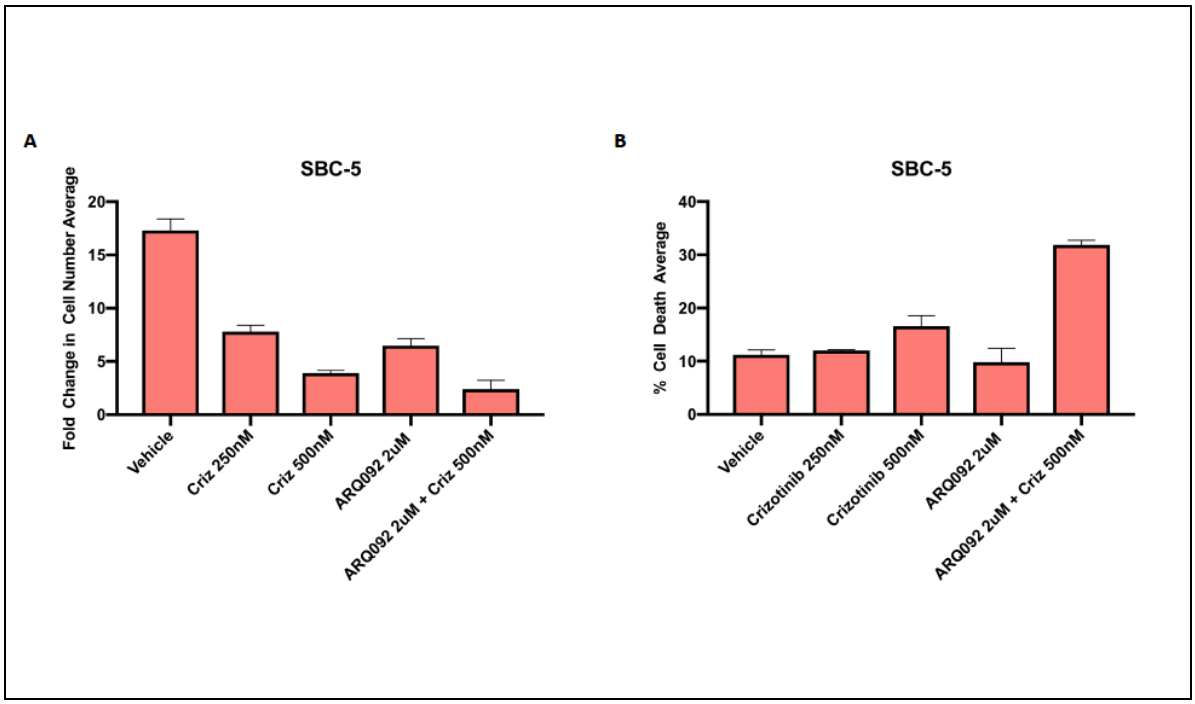

Figure 39. AKT inhibitor ARQ092, in combination with MET TKI, overcomes HGF-mediated MET TKI resistance in MET-amplified SCLC model with HGF co-expression. Analysis of the responses of SBC5, to 72h treatment with MET inhibitor, crizotinib, and allosteric AKT inhibitor ARQ092, alone and in combination. Synergy is seen with the combination treatment.

ADC8830 and ADC11368 are allosteric AKT inhibitors currently in development. Compared to these allosteric AKT inhibitors, ARQ092 was confirmed most efficient at inducing robust cell death in combination with MET TKI, overcoming HGF-induced resistance most effectively (Figure 40). Compared to these compounds, ARQ092 also appeared more potent at inhibiting AKT on western blotting, and was notably more effective at inhibiting AKT1 compared with AKT2 (Figure 40).

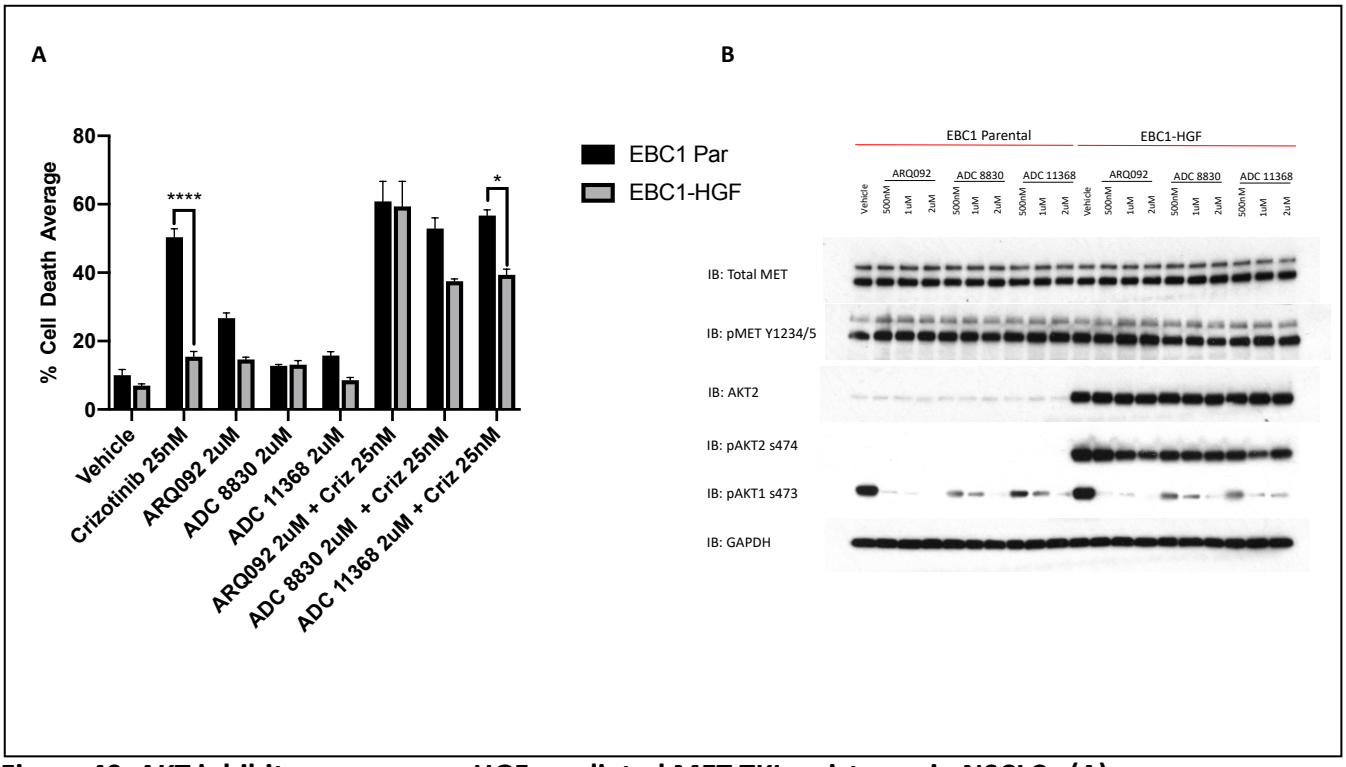

Figure 40. AKT inhibitors overcome HGF-mediated MET TKI resistance in NSCLC. (A) Analysis of the responses of MET amplified cell line, EBC1 and EBC1-HGF to 72h treatment with MET inhibitor, crizotinib and allosteric AKT inhibitors ARQ092, ADC8830 and ADC 11368. 2-way anova performed where indicated. (B) Western blot comparing efficacy of allosteric AKT inhibitors using doses 500nM, 1 ARQ092 is undoubtedly the most efficient allosteric AKT inhibitor tested.

To confirm the potent inhibition of AKT by these compounds, AKT1 and AKT2 were both ectopically re-expressed in AKT-null HCT116 cells (DKO in Figure 41). These cell lines were a kind gift from Bert Vogelstein's laboratory at Johns Hopkins University, and have been previously described[225]. The ability of these allosteric AKT drugs to inhibit AKT was assessed. Again, these drugs were confirmed to be potent inhibitors of the AKT1 phosphorylation site (Figure 41).

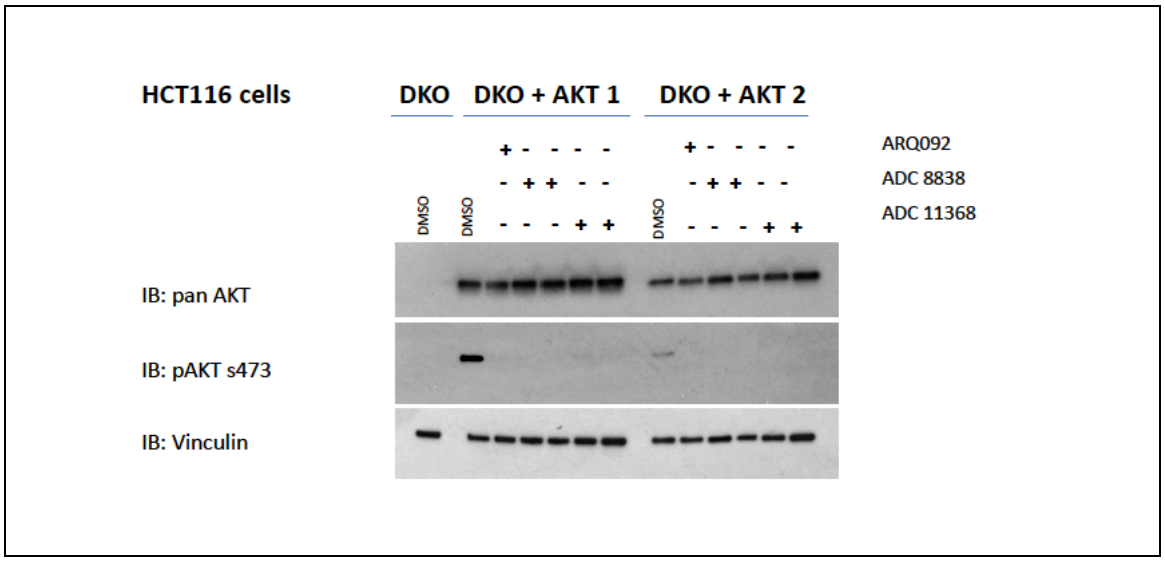

Figure 41. HCT116 knockout cells used to demonstrate allosteric AKT inhibitors potent inhibition of AKT1. (Doses used: ARQ1uM, ADC 8838 1uM and 2uM; ADC 11368 1uM and 2uM).

Strikingly, in the gastric MET-addicted model GTL16, ARQ 092 in combination with MET TKIs did not overcome HGF-mediated resistance to MET TKIs (Figure 42). Of note, in contrast to EBC1 cells, western blotting in this cell line showed no increase in AKT levels when HGF was overexpressed (Figure 42, B+C), suggesting that perhaps the tissue of origin might play a permissive role in HGF-induced AKT overexpression.

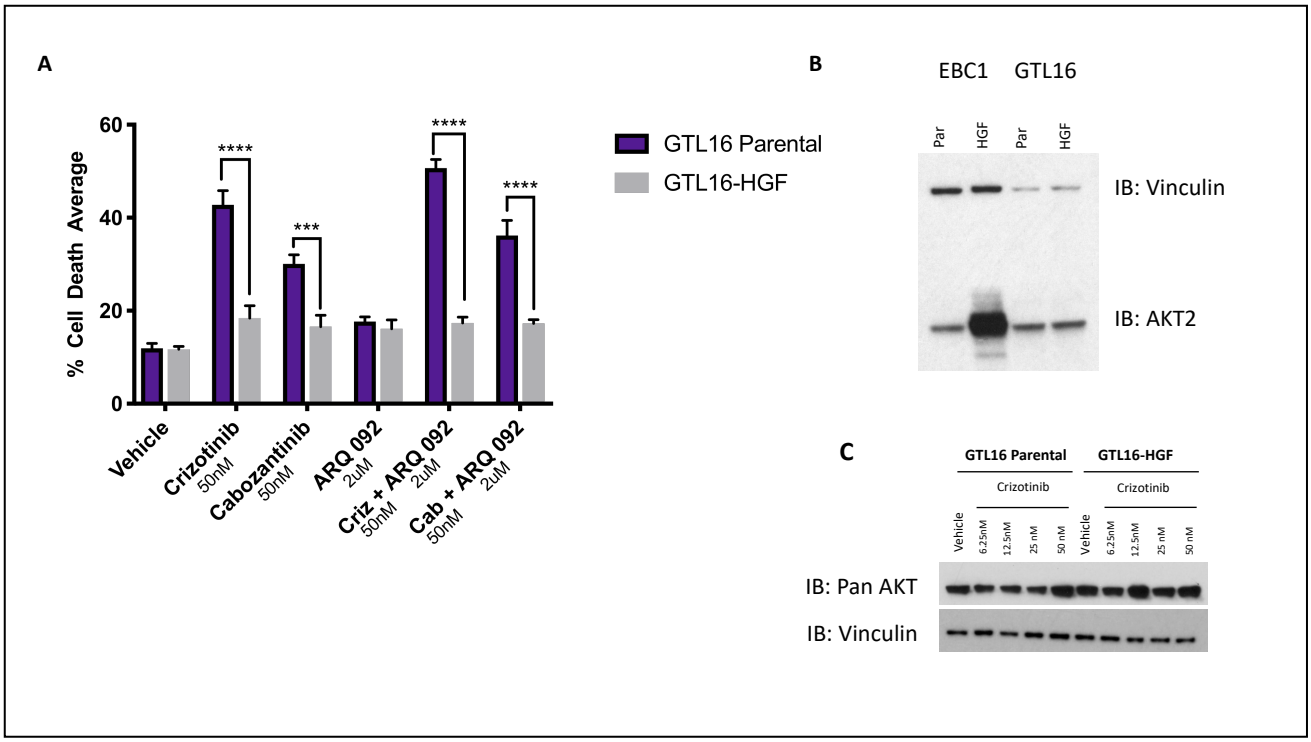

Figure 42. AKT inhibitor ARQ092 unable to overcomes HGF-mediated MET TKI resistance in gastric MET-amplified model. (B, C) Western blotting showing, in contrast to MET-addicted NSCLC EBC1, when HGF is overexpressed in these cells there is no increased AKT signalling, specifically there is no increased AKT2 signalling.

5.2.5 Understanding the relationship between AKT, HGF excess and MET

5.2.5.1 shRNA knockout experiments

In an effort to interrogate the role that AKT, and more specifically the role that AKT2, plays in mediating the HGF-induced resistance to MET TKIs, we knocked down AKT2 in EBC1 and EBC1-HGF cells using doxycycline-inducible short hairpins (shAKT2). Western blotting confirmed doxycycline-inducible knockdown of AKT2 in these cells (Figure 43B). However, the residual protein level of AKT2 following induction of the shRNA remained significantly higher compared to untreated parental EBC1 cells, and these EBC1-HGF cells with shAKT2-mediated knockdown remained resistant to MET TKIs (Figure 43A+C).

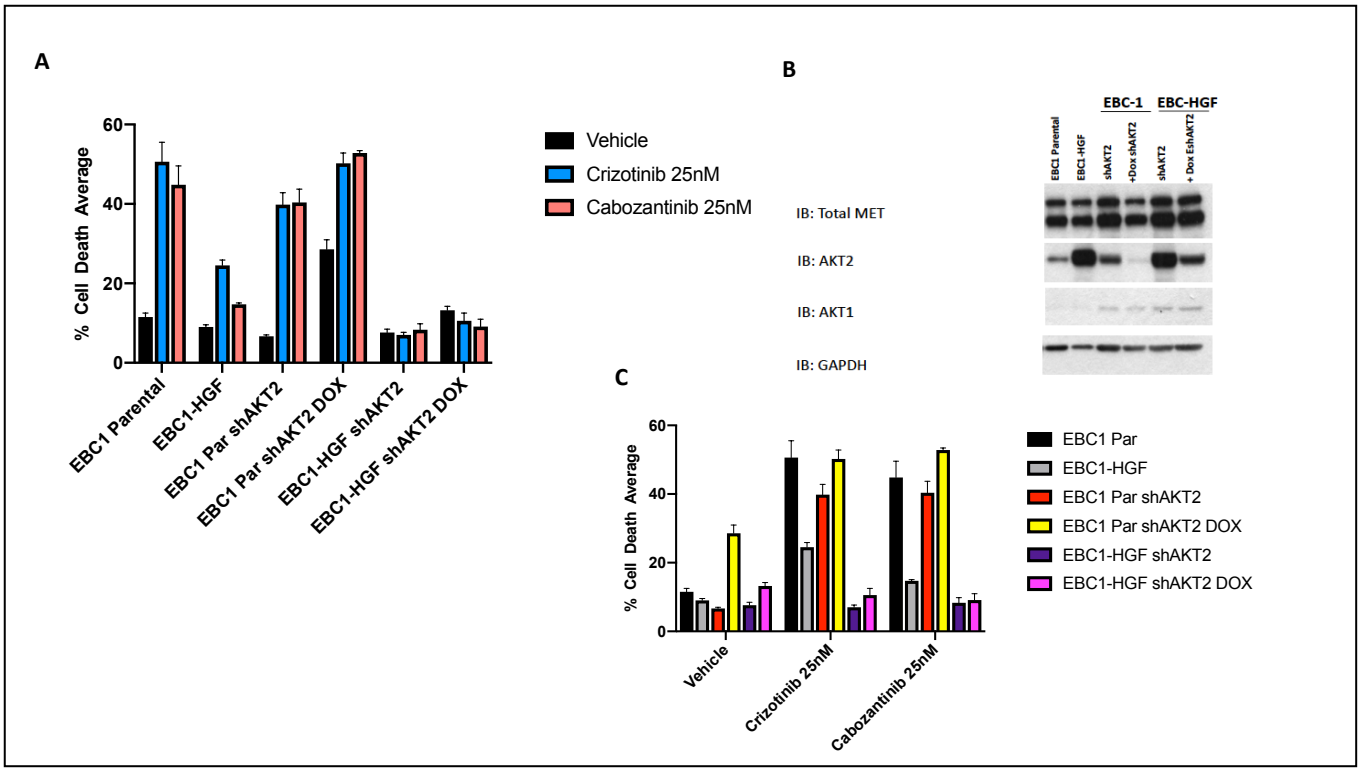

Figure 43. AKT2 knockdown using doxycycline-inducible short hairpins (shAKT2) resulted in no significant change to HGF-induced resistance to MET TKIs in EBC1-HGF, (A)+(C). In (B), note, the residual protein level of AKT2 following induction of the shRNA remained significantly higher compared to untreated parental EBC1 cells.

The same doxycycline-inducible shRNA-mediated knockdown approach was used to knockdown HGF in SBC-5, the SCLC cell line with endogenous HGF and MET co-expression. The cells were generated and selected, however, knockdown was incomplete, and residual protein of HGF following induction of shRNA remained higher compared with untreated parental SBC5 cells. No difference was observed in cell death in the doxycycline inducible HGF-knockdowns following multiple growth assays and experimental procedure optimizations (Figure 44. HGF knockdown using doxycycline-inducible short hairpins (shHGF) resulted in no significant change to HGF-induced resistance to MET TKIs in SBC5 cells.

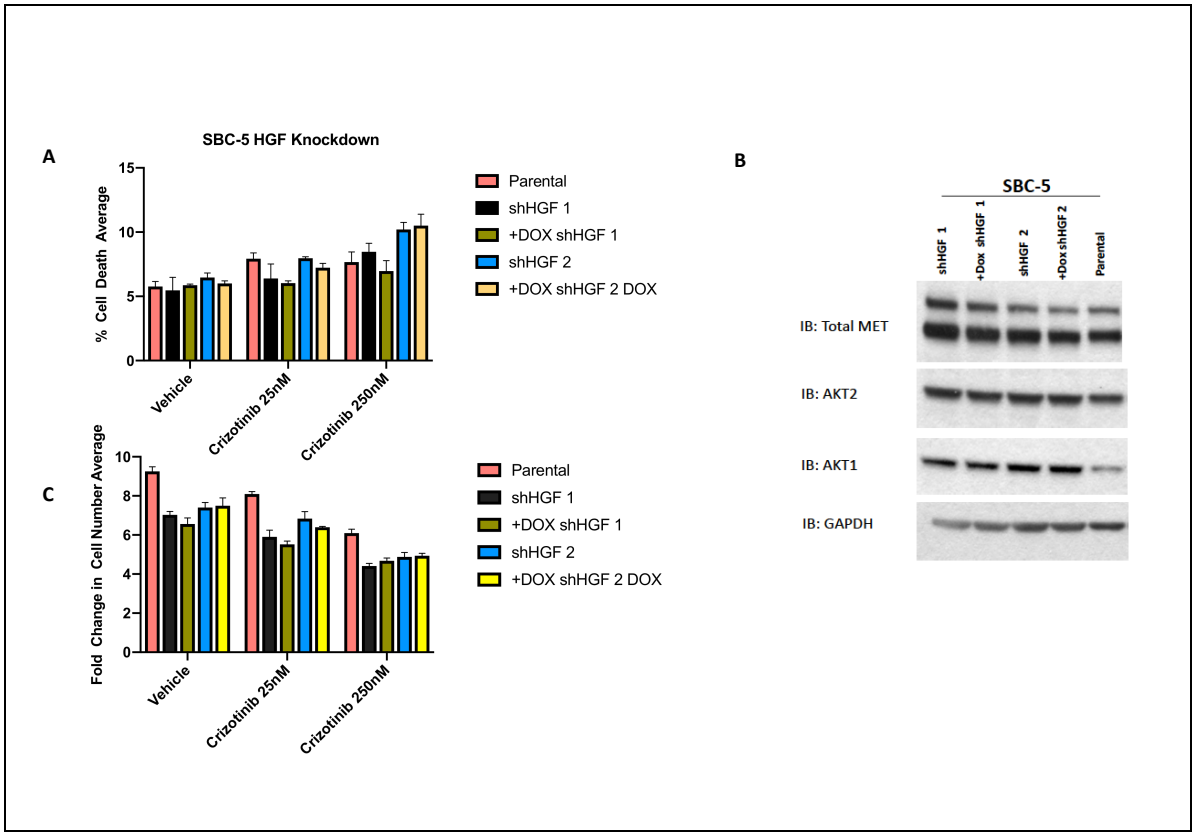

Figure 44. HGF knockdown using doxycycline-inducible short hairpins (shHGF) resulted in no significant change to HGF-induced resistance to MET TKIs in SBC5 cells.

5.2.5.2 Does HGF change availability of MET at the cell surface.

In an effort to assess whether chronic exposure to excess HGF changes the localisation of the MET receptor, we undertook a number of experiments to measure the levels of receptor at the cell surface. From a therapeutic point of view, this question is of particular relevance for antibody drug conjugates (ADC)[226,227] (which are currently being developed as another strategy to target MET in cancer) because the efficacy of these drugs relies on high expression levels of the target at the cell surface.

For example, ABBV-399 is an ADC currently in development, which is comprised of the ABT-700 monoclonal anti-MET antibody conjugated to the clinically validated cytotoxic

microtubule inhibitor monomethylauristatin E (MMAE) via a cleavable valine–citrulline linker[228,229]. We wanted to see whether having excess HGF could impact the levels of cell surface MET which could, at least in theory, affect the efficacy of ADCs such as ABBV-399.

First, using flow cytometry, and a MET-specific antibody that recognises an extracellular epitope, we asked whether HGF affects the availability of the epitope to be recognised by the antibody. We hypothesised that if chronic HGF exposure promotes a conformational change in MET, it could affect the accessibility of the epitope to an antibody, and therefore change its binding efficiency. We found that, in both lung MET-addicted cell line EBC1, and gastric MET-addicted cell line, GTL16, HGF overexpression reduced binding of the MET antibody in intact cells (represented by the blue shift in Figure 45).

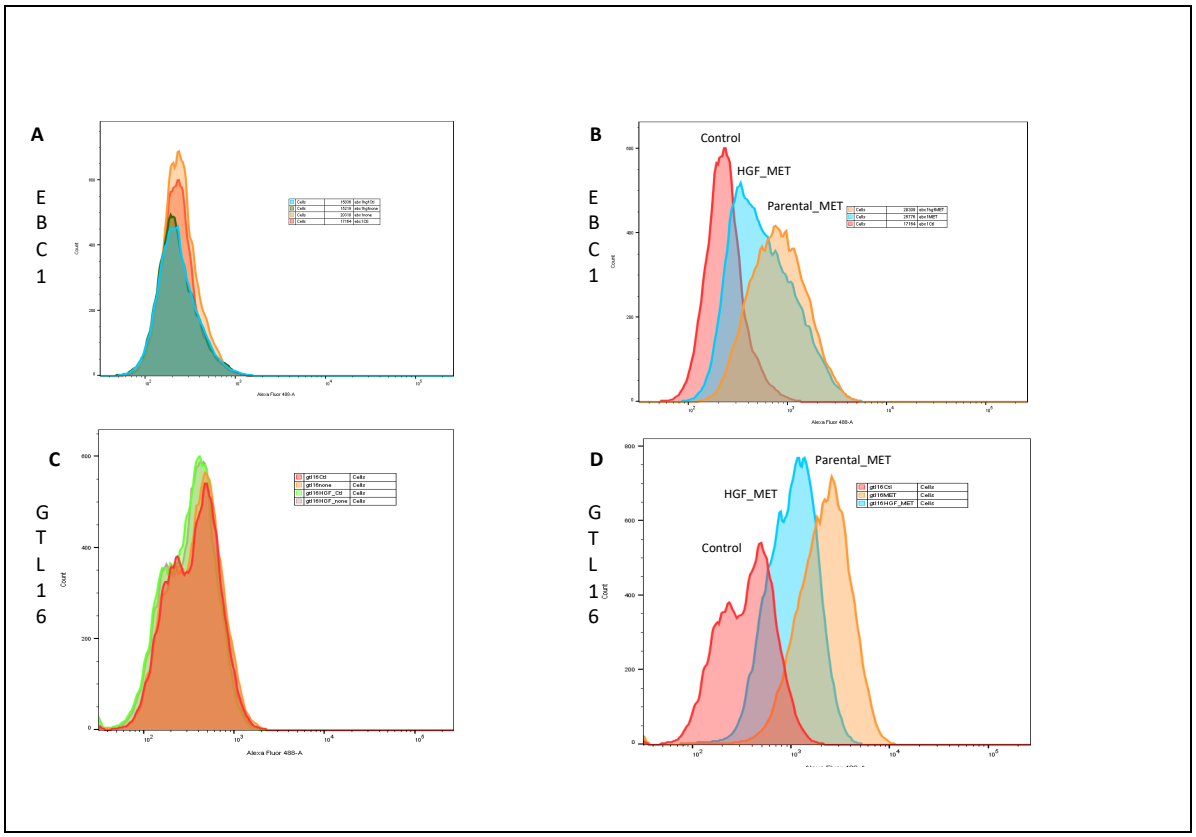

Figure 45. Flow cytometry analysis of EBC1 parental, EBC1-HGF (A+B), GTL16 parental and GTL16-HGF cells (C+D) respectively quantifying surface expression of c-Met using a MET specific antibody. Histograms A and C show relative fluorescence intensities of isotype controls and cell samples. In Histograms B and D, the red represents the control, the orange represents the Parental cell line binding with MET specific antibody, and the blue represents the HGF-expressed cell line binding with MET specific antibody. Note, the HGF-expressed cells, both EBC1-HGF and GTL16-HGF both cause a binding shift represented by a blue shift in B+D.

This difference (demonstrated by the blue shift in Figure 45, images B + D) could be interpreted in two ways: firstly, it could be a change in the conformation of MET receptor that hides the epitope recognised by the specific MET antibody causing a loss of signal. Secondly, perhaps HGF overexpression increases the basal rate of receptor

internalisation, and there is simply less protein at the cell surface. Regardless, these experiments provide proof-of-principle evidence that binding of antibodies directed against the extracellular domain of MET can be affected by excess HGF. Furthermore, it suggests that binding of a MET-targeted ADC could be affected by excess HGF, thereby reducing its efficacy. This raises the possibility that adding an HGF antibody, as a way to reverse the effects of HGF on MET conformation, could help to overcome this resistance.

To assess the possibility that excess HGF is causing increased MET receptor internalisation, cell surface biotinylation experiments were performed. These experiments involve the labelling of cell surface MET protein using a biotinylating probe. Through this approach, all lysines on the extracellular surface are labelled. Therefore, any regional changes in conformation should have minimal effects on overall receptor biotinylation, subsequent pulldown, and quantification. We found that in both EBC1 and GTL16, in the presence of HGF, there was no loss of signal in biotinylated MET (Figure 46). In these two MET-addicted cell lines, there was no observable difference in cell surface biotinylated MET (Figure 46A,B) indicating that in the presence of excess HGF there is no significant change on cell surface MET levels.

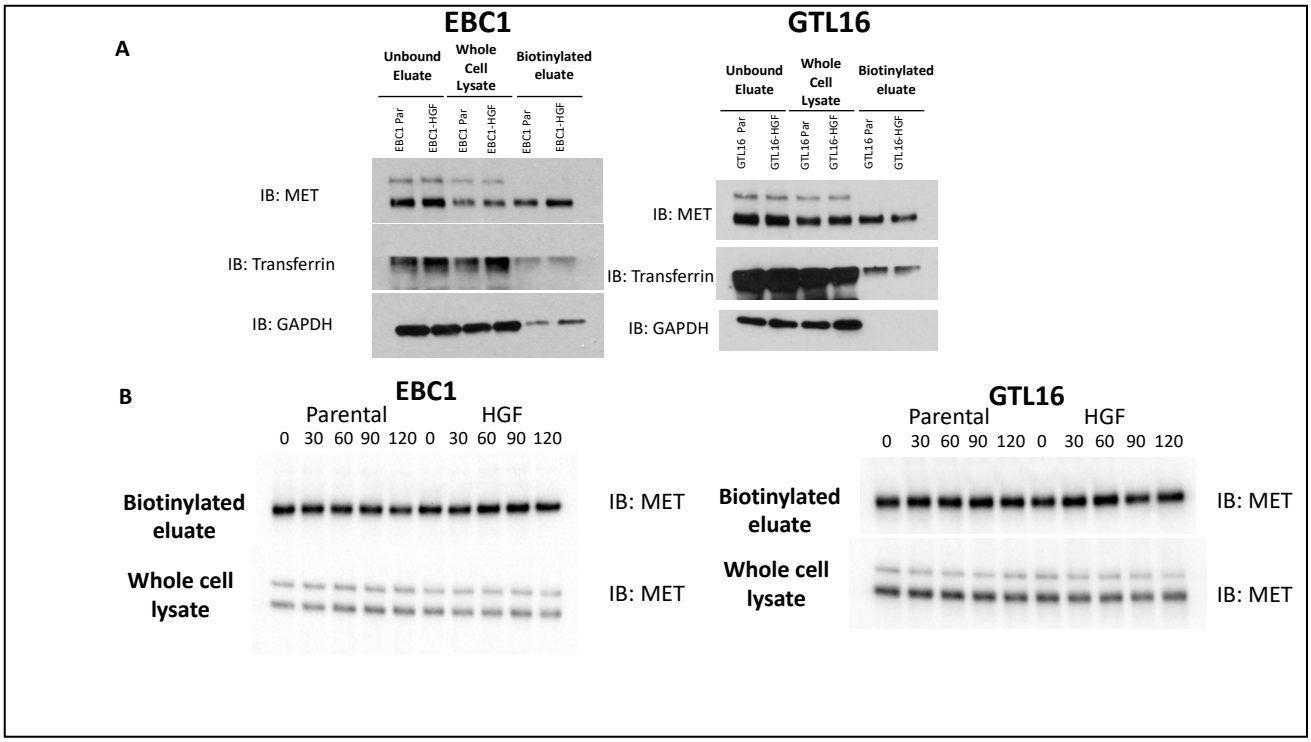

Figure 46. HGF excess does not alter biotinylated MET at the cell surface. In (A) a simplified cell surface biotinylation technique is used, with EBC1, EBC1-HGF, GTL16, GTL16-HGF cells respectively were cell surface biotinylated for 30mins at 4degrees. In (B), same cell types were cell surface biotinylated for the expanded time points indicated. Note, for the biotinylated samples for MET, for each cell line, a distinct lack of significant change in signalling, indicating that HGF excess does not alter MET at the cell surface.

5.2.5.3 HGF excess does not affect localisation of MET.

In order to assess whether excess HGF had any impact on the subcellular distribution of MET in MET-amplified NSCLC, we stained EBC1 parental and EBC1-HGF cells with antibodies against pMET (1234/5) and total MET. The localization of MET and pMET was then assessed using immunofluorescence. There was no significant change in MET/ pMET expression or localisation in EBC1 parental compared with EBC1-HGF. HGF excess

was not associated with any significant change in cytoplasmic and/or nuclear MET/pMET (Figure 47).

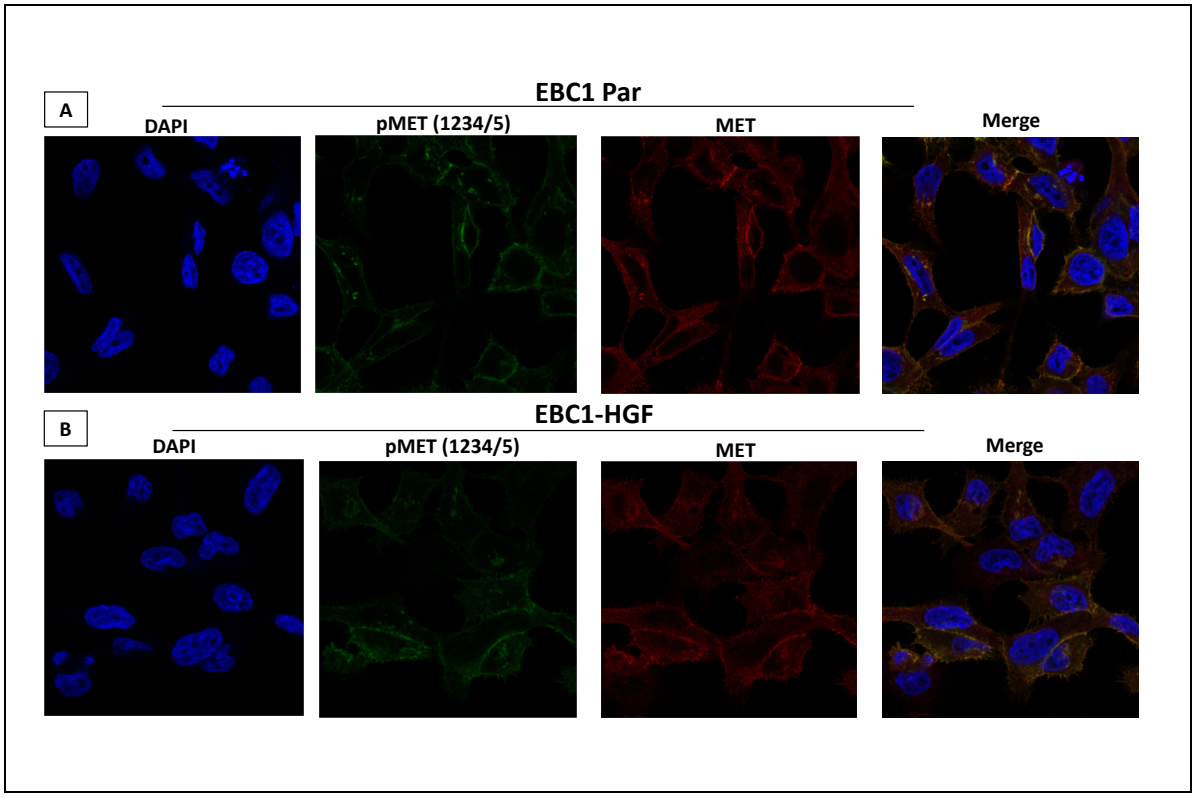

Figure 47. HGF does not alter MET and pMET localisation in EBC1 and EBC1-HGF. The localisation of pMET(1234/5) and total MET was assessed in EBC1 parental cells (A) and EBC1-HGF cells (B) by immunofluorescence. Note that the expression and localisation of total MET and pMET does not appear to differ in these cells. Note, both cytoplasmic and nuclear evidence of MET signalling.

5.2.6 Strategy 5: More potent and selective MET-TKIs.

Capmatinib (formerly, INC280), a potent and selective MET TKI, became commercially available in the final months of experimental work, as promising ASCO data from the GEOMETRY mono-1 trial[230] showed an objective response rate (ORR) of 67.9% in newly diagnosed patients with MET exon 14–altered NSCLC, which led to FDA designation of

capmatinib as a breakthrough therapy as a first-line treatment for patients with MET exon 14 skipping mutation–positive NSCLC.

Consequently, capmatinib was evaluated in our MET-addicted NSCLC models. Even at low doses, robust cell death is observed in EBC1 parental, and HGF-induced resistance is overcome in our model at lower doses than previously demonstrated (Figure 48, A). Compared with other MET TKIs, capmatinib was clearly superior in overcoming resistance in the HGF-expressed EBC1 cells and at significantly lower doses (Figure 48), as it takes higher doses of crizotinib and JNJ-38877605 (500nM and 200nM, respectively) to overcome EBC-HGF resistance. However, in Figure 48, B note that using Capmatinib, there is a still a significant ($p < 0.0114$) difference at 500nM Capmatinib.

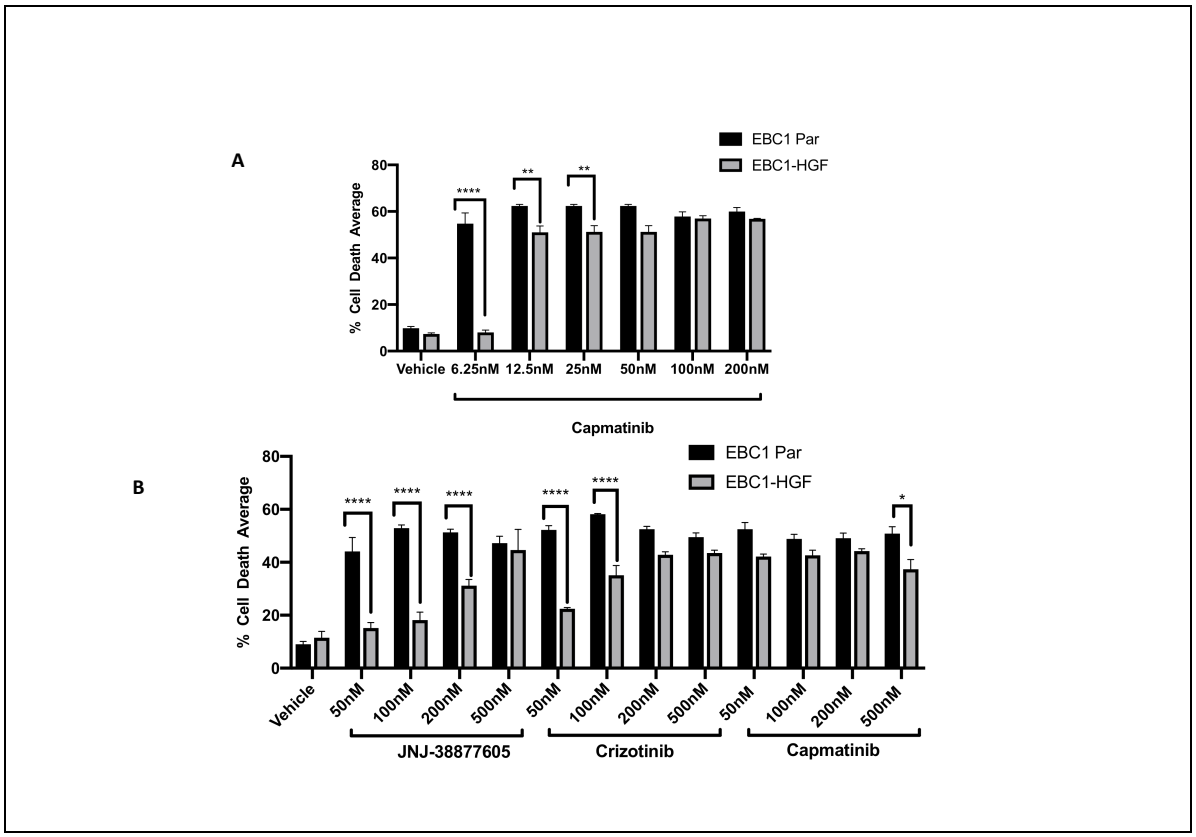

Figure 48. Capmatinib induces robust cell death in EBC1 and EBC1-HGF cells from low doses. Analysis of the responses of MET amplified cell line, EBC1 and HGF-overexpressed EBC1, to 72h treatment with MET inhibitor, capmatinib. 2-way anova performed where indicated.

Given that our previous data have suggested that duration of exposure to crizotinib and cabozantinib influences the response to these drugs (Figure 33), we wanted to know whether response to capmatinib also depended on time of exposure. Consequently, we carried out a washout experiment (Figure 49) to determine the shortest drug exposure time required for a meaningful biological response in EBC1 cells, and to assess whether resistance to capmatinib caused by excess HGF also requires prolonged drug exposure.

Intriguingly, similar to the crizotinib washout experiment described previously (Figure 33), 30mins of exposure with 200nM Capmatinib was sufficient to induce significant cell death in parental EBC1 cells. However, HGF-mediated resistance is maintained throughout, and it takes three days of continuous capmatinib treatment for resistance

to be overcome. Here, again, our data suggest that the duration of exposure to drug is a critical determinant of response, even with more potent and selective compounds.

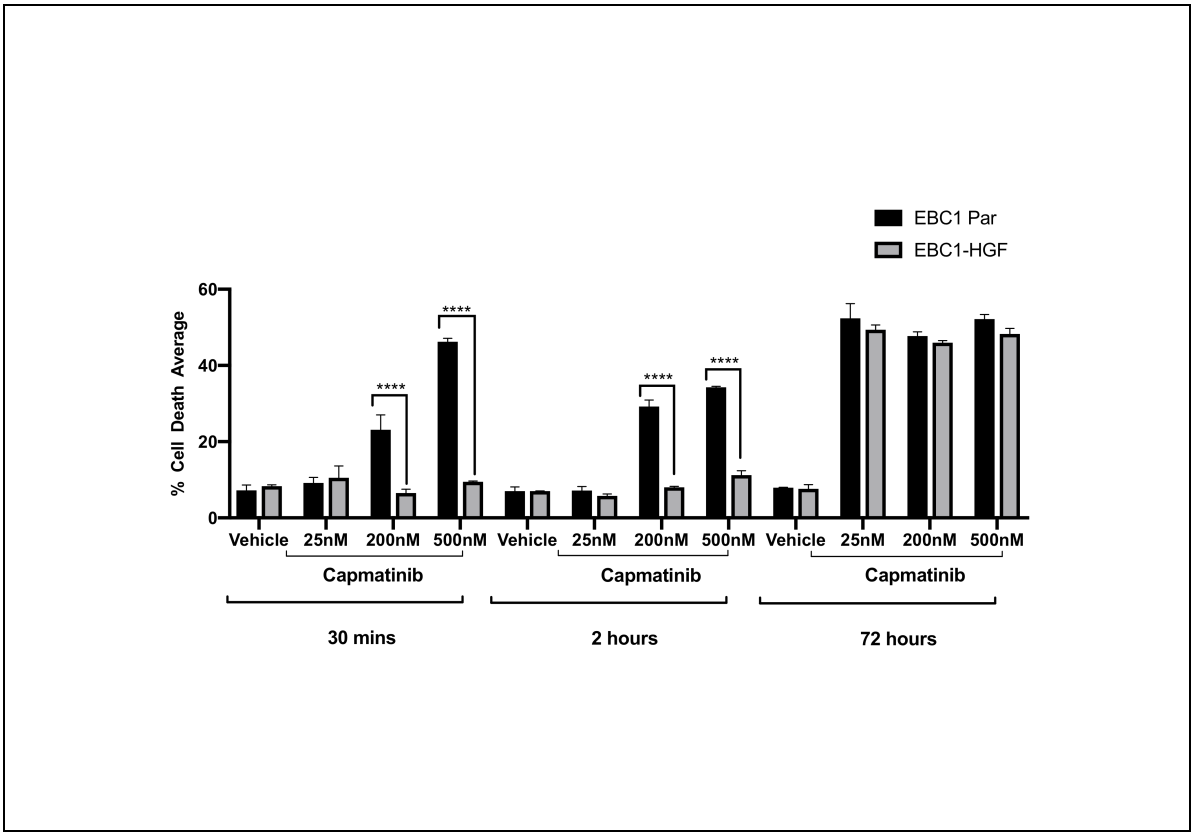

Figure 49. Capmatinib washout experiment indicating that it takes 72 hours of continuous drug exposure for HGF-driven resistance to be overcome by Capmatinib. Analysis of the responses of MET amplified cell line, EBC1 and EBC1-HGF to 30mins, 2hours and 72h treatment with MET inhibitor, Capmatinib (doses 25nM, 200nM, 500nM). Cell death percentages (mean ± SEM) were assessed via automated trypan blue method (ViCell), and expressed as the fraction of stain-positive cells.

5.3 Discussion

5.3.1 Strategy 1: Overcoming resistance with increasing dose MET TKI.

We have identified a number of rational potential strategies to overcome HGF-induced resistance to MET TKIs. First, we show that increasing the dose of MET TKI eventually overcomes primary HGF-induced resistance. However, this approach may be challenging in the clinical setting, given the likelihood of increased toxicity. In phase I oncology studies, a key aim has traditionally been to establish the maximum tolerated dose (MTD) of a new compound for further clinical investigation. This typically corresponds to the highest dose associated with an acceptable level of toxicity and is drawn from clinical data and preclinical dose-toxicity and dose-activity studies[231]. A meta-analysis of 24 phase I trials of targeted agents at MD Anderson Cancer Center found that higher doses led to substantially higher numbers of dropouts due to toxicity with no concomitant improvement in clinical response (complete response, partial response, or stable disease) over doses that were roughly half of the MTD[232]. Thus, increasing the dose of MET TKIs to overcome HGF-mediated resistance may not be clinically feasible.

Furthermore, we have shown that even with increased doses of MET TKIs, long and continuous high-dose exposure to MET TKI is necessary to overcome HGF-mediated resistance. For example, although a short amount of exposure to crizotinib (15mins) is required to induce robust cell death in MET-amplified NSCLC cell line EBC1, resistance is always maintained in the presence of excess HGF (Figure 33). Even at increasing doses of crizotinib (up to 200nM) it takes three full days of drug exposure to fully overcome HGF-induced resistance. These data were also replicated using the more MET-selective and more potent TKI, capmatinib, where even at high doses (up to 500nM) it takes three days of tumour cells exposed to drug for HGF-induced resistance to be overcome (Figure 49).

It is clear that in the era of targeted therapies, traditional trial design involving multiple dose de-escalation steps to determine a tolerable dose may not be sufficient. Molecularly targeted agents target specific aberrant pathways in cancer cells, while sparing normal cells, and as such the toxicity and efficacy of these novel agents may not be dose dependant. Alternative endpoints besides toxicity have been suggested for phase I trials to evaluate molecularly targeted agents, such as target inhibition in tumours or surrogate tissues and detection of biologically relevant pharmacokinetic (PK) levels[231,233–235]. Our data support this idea, that novel dose escalation strategies using creative scheduling to optimally hit the target are required.

Crizotinib is a potent oral small-molecule tyrosine kinase inhibitor of ALK, MET and ROS1 kinases[151], with half maximum inhibitory concentration values of 5–25 nmol/L based on preclinical mouse models[151,236]. Originally developed as a MET inhibitor, the first-in-man crizotinib study, PROFILE 1001[237], began in 2006 with an initial standard dose-escalation PK portion followed by a clinical efficacy portion that aimed to enrol a small number of molecularly enriched patients to assess the anti-tumour activity of crizotinib. The initial PK cohort used the standard dose-escalation finding schema to determine the MTD, and the recommended phase II dose (250 mg twice daily in 28-day cycles), and patients with ALK-positive or MET-positive tumours were enrolled into a series of molecularly defined expansion cohorts at the proposed recommended phase 2 dose.

The crizotinib PK studies were carried out on samples of patient plasma. However, non-invasive tumour PK and PD measurements can provide invaluable additional data[238]. Importantly, there are no data available assessing target inhibition in lung tumour tissue from the landmark PROFILE studies[5,108,237,239], and to the best of our knowledge, there are no published pharmacodynamic data regarding crizotinib available.

In reality, in clinical practice assessing target inhibition is a challenging aspect of clinical trial designs for a number of reasons. First, tumour tissue (or a valid surrogate tissue) must be readily available and easily accessible (an ongoing challenge for lung tumours).

Second, there must be a reliable assay for measuring the effect of the drug on the target. Finally, the optimal extent of target inhibition (i.e. inhibition that yields a meaningful clinical benefit) must be known[240]. While meeting all of these conditions is a challenge, ideal trial design should try to determine the dose at which there is optimal target inhibition (rather than an MTD alone).

From a practical point of view, this means that particular questions need to be answered during early clinical trial development, including: is the drug reaching the concentrations required for biological activity in the blood and tumour tissue, is the drug hitting the desired molecular target, is the drug modulating the biochemical pathway in which the molecular target functions, and is the drug achieving the desired biological effect?[238]. We would argue that for crizotinib in MET-amplified NSCLC, the answers to all of these questions have not been determined.

The washout data presented (Figure 33, Figure 49) are hypothesis-generating and suggest that duration of exposure of tumour cells to MET TKI, as well as increasing dose of drug, is important and influences response to treatment. Therefore, in addition to assessing HGF levels in the tumour, clinical trial design should incorporate alternative dosing strategies in MET amplified NSCLC patients, if excess HGF is to be appropriately addressed as a mechanism of MET TKI resistance. Simply increasing the dose of MET TKI may not be sufficient to overcome HGF-mediated resistance given how critical duration of exposure appears to be.

There are data based on mathematical models that continuous dosing is a clinically feasible strategy for slowing down tumour growth in GBMs, even when taking into consideration intratumor heterogeneity and drug resistance[241]. Regarding the use of high dose pulsatile crizotinib as an alternative treatment strategy in NSCLC, data are limited. The only published case study[242] reports a patient with ALK-positive NSCLC with intra-cranial metastases who received high-dose pulsatile crizotinib therapy (1000 mg/d) on a one-day-on/one-day-off basis with reported significant central nervous system

response, with time to neurological progression was prolonged to 6 months. These data suggest that high dose pulsatile crizotinib may indeed be a feasible treatment option, and so we suggest investigating using intermittent schedules of high dose pulsatile crizotinib as the first strategy in overcoming *de novo* HGF-mediated resistance in MET-amplified NSCLC.

5.3.2 Strategy 2: Overcoming resistance with combination MET TKI + MET targeting antibody.

Given that HGF-mediated resistance is MET-dependent, relying solely on the overexpression of MET's cognate ligand HGF, we sought further MET-based strategies to overcome this resistance. We first evaluated MET-specific monovalent antibody MetMAB (or onartuzumab). While this compound demonstrated weak single agent activity, when used in combination with type I and type II MET TKIs in MET-addicted NSCLC cell line EBC1 and the HGF-expressed cells, this combination induced robust cell death (Figure 34). This strategy of combining MET targeting antibody MetMAB with MET TKI also proved successful in overcoming HGF-induced resistance in our gastric MET-addicted model GTL16, and SBC-5, our endogenous SCLC model with elevated HGF levels (Figure 34).

We have proposed that chronic HGF exposure, perhaps through MET receptor desensitization, could shift the conformation of the receptor to a transitional state, between 'active' and 'inactive', which impairs the ability of both type I and type II MET TKIs to bind to the kinase domain (Figure 22). The observed rescue of MET TKI-induced toxicity by HGF overexpression, suggests that for patients whose tumours have co-amplification of MET and HGF, (or MET amplification with elevated HGF levels), single agent MET TKIs might not to be sufficient to elicit a measurable clinical response. However, interfering with HGF binding, and its ability to induce any conformational changes on MET, could re-sensitise the receptor to both type I and type II TKIs.

Onartuzumab is a single-armed, recombinant, humanized, monoclonal, monovalent antibody that binds to the extracellular domain of the receptor tyrosine kinase MET, interfering with HGF binding and subsequent activation of the MET receptor[66]. We show that using either a type 1 or a type 2 inhibitor combined with a MET targeted antibody, HGF-mediated resistance is overcome. Perhaps Onartuzumab binding to the ECD of the receptor is blocking HGF access to the receptor, while allowing concurrent TKI binding in the intracellular domain (Figure 50).

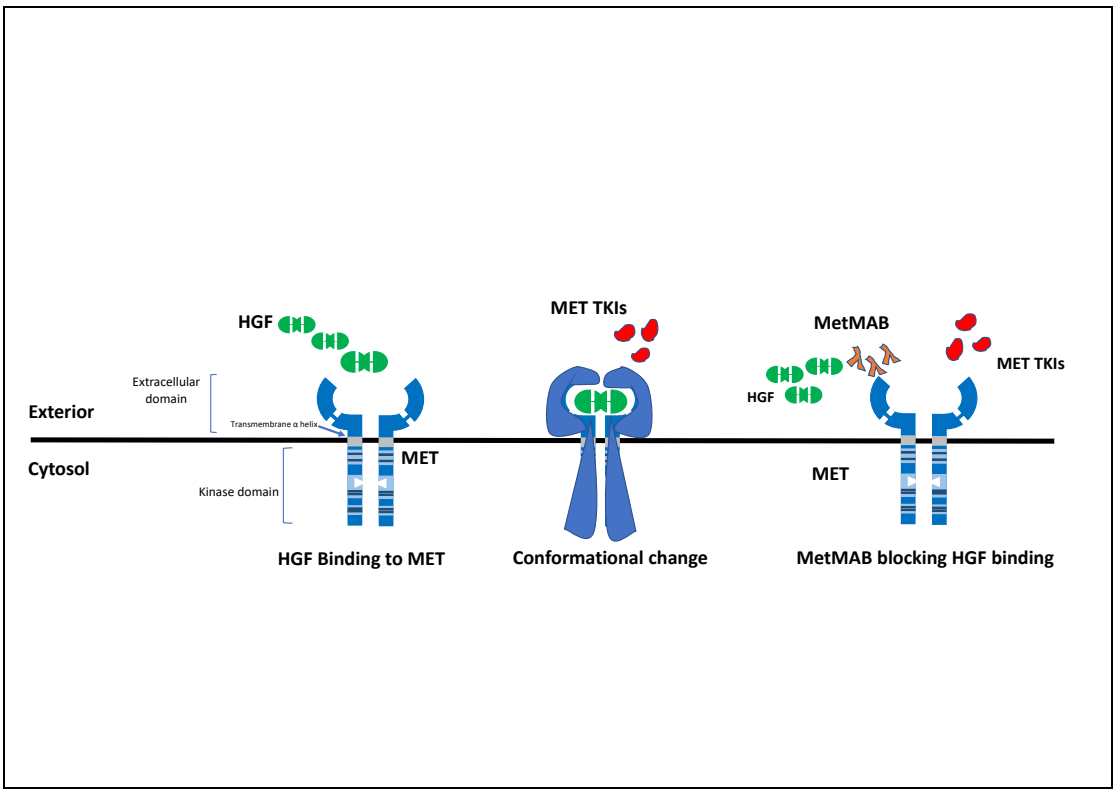

Figure 50. MetMAB, or onartuzumab, interferes with HGF binding to MET receptor. Typically, on binding of METs cognate ligand, HGF, the receptor undergoes conformational change, making receptor inaccessible to MET TKIs; binding of MetMAB however blocks HGF access to MET receptor, allowing MET TKIs to bind.

Our data provide evidence for a novel and clinically relevant approach to overcome HGF-mediated MET TKI resistance, by combining Onartuzumab with a type I or type II MET TKI (Figure 34). Whilst Onartuzumab has shown disappointing clinical activity in the pivotal MetLUNG study[109], in this phase III trial MetMAB was combined with erlotinib, an

EGFR targeting agent, and trialled in an unselected MET-positive NSCLC patient population. MetMAB was, therefore, likely deployed using an inappropriate combination strategy in a poorly selected patient population. We propose that a combination of a MET-directed TKI and a MET-antibody may fare better in cases where upfront resistance is caused by excess HGF, i.e. in patients whose tumours have co-amplification of MET and HGF, (or MET amplification with elevated HGF levels). Given the current ability to carefully select NSCLC patients with high-level MET amplification (FISH *MET*/CEP7 ratio$\geq$ 5), we propose this novel combination to form the basis of a clinical trial, with the addition of prospective HGF-level testing.

Similarly, further combination therapies which interfere with HGF-binding, such as combining MET TKIs with anti-HGF antibodies, could be trialed, to provide an alternative strategy to enhance the pharmacologic effect of MET TKIs[243], in an appropriately selected NSCLC patient population with high-level MET amplification.

5.3.2.1 Using ADCs in MET-positive NSCLC.

Our working hypothesis is that HGF excess could be inducing a conformational change in the MET receptor, shifting the conformation of the receptor to a transitional state, between 'active' and 'inactive', which makes it difficult for both type I and type II MET TKIs to bind to the kinase domain. Another targeting approach for MET currently under clinical development is the use of ADCs[226,227], and one such example of MET-targeting ADC is ABBV-399. In an effort to assess if having excess HGF could impact the response to this type of agent, and evaluate if excess HGF changes the MET receptor, we used flow cytometry to see if there was a change in availability of the receptor to bind a specific MET antibody in the presence of HGF excess.

We hypothesised that if chronic HGF exposure promotes a conformational change in MET, it could affect the availability of the epitope recognised by a MET-specific antibody and therefore change its binding efficiency. We show that in both MET-amplified cells

EBC1 and GTL16, in the presence of HGF, the availability of the binding shifts in the HGF-expressed cell line (Figure 45), suggesting that excess HGF does affect the availability of the epitope to be recognised by a MET antibody, and raising the possibility that other antibodies that target the ECD could be similarly affected. As this could also happen clinically when using an ADC (the presence of HGF might limit the response to the ADC), perhaps adding an HGF antibody – could re-expose the epitope, and help overcome this resistance.

The difference in cell surface levels of MET between parental MET-amplified and HGF-overexpressed cells seen by flow cytometry (demonstrated by the blue shift in Figure 45, images B + D) could be interpreted in two ways. 1) It could be that HGF changing the conformation of the MET receptor hides the epitope recognised by the specific MET antibody causing a loss of signal. 2) It is also possible that HGF excess enhances receptor internalisation, and there is simply less protein at the cell surface.

To address the second possibility, cell surface biotinylation experiments were performed to see if HGF excess changed the levels of MET at the cell surface. As HGF produced no change in MET protein at the cell surface, our data supports the notion that perhaps HGF excess is instead inducing a conformational change in the MET receptor that hides the epitope recognised by the MET antibody.

No MET-targeting ADCs are currently commercially available, and as such, in our models of primary HGF-induced resistance, we were unable to trial ADCs as part of a combination strategy. Regardless, our data suggest that when using MET-directed ADCs, combination strategies, as opposed to single agent treatment, may be necessary. The presence of HGF might limit the response to a MET targeting ADC, and as such perhaps adding an antibody targeting HGF, which could re-expose the epitope, may possibly help overcome HGF-induced resistance. This could certainly be another valid strategy to consider.

5.3.3 Strategy 3: Overcoming HGF-induced resistance using MET TKI + mTOR kinase inhibition.

We have demonstrated using western blotting, on numerous occasions, that ectopically over-expressing HGF in MET-amplified EBC1 cells results in increased AKT signalling (Figure 24). In addition to this, in these HGF-expressed cells we noted subtle alterations in the response of AKT phosphorylation sites to MET TKIs (Figure 24). In the HGF-overexpressed EBC1 cells, the PDK1 site, Thr308, appeared to be consistently more responsive to MET kinase inhibition, in comparison to the mTORC2 site, Ser473, which appeared to be refractory to MET TKIs (Figure 24).

Accordingly, this suggested another potential strategy to overcome primary HGF-induced resistance to MET TKIs in MET-amplified NSCLC. We suspected that mTORC2 activity was unaffected by MET TKI treatment. We, therefore, hypothesised that mTORC2 inhibition might overcome HGF-mediated MET TKI resistance.

AZD2014, or vistusertib, is an ATP-competitive dual m-TORC1/2 inhibitor, and has shown preclinical activity across a range of *in vitro* and *in vivo* preclinical models[244]. We show that combining AZD2014 together with either crizotinib or cabozantinib (type I and type II TKIs) overcomes HGF-mediated resistance to MET TKIs in MET-addicted NSCLC cells (Figure 36).

The PI3K/AKT pathway is, arguably, the most commonly disrupted signalling pathway in human cancers[208], including lung cancer. Mechanisms of deregulation include activating mutations in *PIK3CA* and *AKT* and loss of function of tumour suppressor genes such as *PTEN*[245]. m-TOR consists of two essential complexes,mTORC1 and mTORC2, and is a crucial node in the PI3K signalling network[246]. mTORC1 regulates protein synthesis through activation of S6K and EIF4e, and while regulation of mTORC2 is less well understood, it is thought to phosphorylate AKT on Ser473 contributing to its kinase activation[246]; m-TORC2 is therefore critical to AKT signaling[247].

In the first-in-human phase I study of AZD2014, crucially, robust PD and PK data are presented. Basu et al[248] confirmed target engagement by demonstrating m-TORC1 inhibition in tumour and normal tissue, as shown by reduction in the phosphorylation of 4EBP1 and S6(m-TORC1 inhibition), respectively, and importantly, m-TORC2 inhibition (as shown by reduction in p-AKT) in normal tissue and tumour tissue[248]. We have demonstrated that in the presence of HGF excess there is increased levels of total and active AKT by western blot, and phosphoproteomic profiling, in our MET-amplified lung cancer model, EBC1. Consistently, we find that targeting mTORC2, the kinase that phosphorylates a key regulatory site (Ser473), is another effective combination strategy for overcoming HGF-induced resistance to MET TKIs.

Currently, there are no published data investigating AZD2014 specifically in MET-driven NSCLC, either as a single agent or in combination with MET TKIs. The compound has been investigated in the phase I setting in combination with chemotherapy agent, paclitaxel, and shown encouraging activity in the expansion cohorts in high-grade serous ovarian cancer (HGSOC) and squamous non-small-cell lung cancer (sqNSCLC)[249]: in patients with sqNSCLC the RECIST response rate was 35% (8/23), and the mPFS was 5.8 months (95% CI: 2.76–21.25), while in the HGSOC expansion, RECIST and GCIG CA125 response rates were 52% (13/25) and 64% (16/25), respectively, with median progression-free survival (mPFS) of 5.8 months (95% CI: 3.28–18.54).

As part of the NLMT, patients with advanced NSCLC with serine/threonine kinase 11 (LKB1/ STK11), TSC1 or TSC2 tumour mutations were deemed eligible for treatment with AZD2014 as a single agent. (LKB1 is a tumour suppressor gene, and approximately half of NSCLC patients with activating KRAS lesions have also deletions or inactivating mutations in the (LKB1/STK11)[250–252]).

However, recruitment to the LKB1 single mutation arm was halted at interim due to futility[220]. As part of the NLMT, for single agents, clinically relevant outcomes are defined as either median progression-free survival for more than three months or

objective response rate and/or durable clinical benefit rate (DCBR) at 24 weeks greater than 30 percent. Data presented at the World Conference on Lung Cancer (WCLC) demonstrated that at the interim, for AZD2014 in this cohort of patients, the predicted probability of success for DCBR in those with KRAS mutation with concomitant STK11 loss was DCBR of 27% and there were no objective responses[220].

The abject failure of AZD2014 in the NLMT suggests that this compound should be evaluated differently. We have provided data (Figure 20), consistent with previous published research[140], that demonstrates detectable HGF levels are a common finding in lung tumours. The reason single agent MET TKIs have failed in the clinic could potentially be attributed to HGF overexpression in tumours. These data suggest that HGF overexpression may be a common event. Therefore, the development of rationale combination strategies to overcome this HGF-induced resistance is warranted.

We provide pre-clinical evidence that AZD2014 in combination with MET TKIs is another attractive therapeutic strategy in MET-driven NSCLC, for use in both rare cases of NSCLC patients whose tumours have co-amplification of MET and HGF, or more frequent cases of MET amplified NSCLC with elevated levels of HGF.

5.3.4 Strategy 4: Overcoming HGF-induced resistance using MET TKI + AKT inhibition.

Our data, western blot analyses and phosphoproteomic profiling data, show increased total AKT and phosphorylated AKT levels. Given the importance of AKT in cancer cell survival, this suggests that HGF-mediated resistance to MET TKIs might be driven by AKT. Consequently, we show that combing MET TKI with allosteric AKT inhibitors is an effective strategy to overcome this resistance.

Finding a clinically relevant strategy for the treatment MET-amplified NSCLC patients was an essential part of my PhD project. As a result of this, initially I evaluated potent, selective, allosteric AKT inhibitor ARQ092 (also called miransertib), which has shown promising results in early phase studies[223] and is currently undergoing phase I testing in

solid tumours. As described previously, AKT inhibitors come in two well-defined classes: 1) allosteric inhibitors (such as ARQ092) bind to AKT in the inactive state, via the PH-domain/ kinase-domain interface, and 2) ATP competitive inhibitors bind to the active conformation of AKT, when the ATP-binding pocket is exposed[224] (Figure 37).

We demonstrate that combination strategies using allosteric inhibitors, such as ARQ092, and MET TKI overcomes HGF-induced resistance to MET TKIs in two cancer models (EBC1-HGF and SBC5), yet this is not true for ATP-competitive AKT inhibitors combined with MET TKI (Figure 38). Vivanco et al have previous reported on the inability of ATP-competitive inhibitors, compared to allosteric AKT inhibitors, to suppress non-catalytic AKT functions[253], representing a liability of compounds, such as AZD5363. Perhaps, in this context, ATP-competitive inhibitors such as AZD 5363 are unable to overcome HGF-induced resistance because it is not able to suppress the non-catalytic functions of AKT[253].

As a critical component in the PI3K/AKT/mTOR pathway, AKT has been an attractive target for therapeutic intervention for many years. ARQ092 is a highly potent and selective allosteric AKT inhibitor which has been shown to inhibit AKT1, 2, and 3 activities with reported IC_{50} values of 5.0, 4.5, and 16 nM[254]. Biochemical and cellular analysis have shown that ARQ 092 (and next-generation allosteric AKT inhibitor, ARQ 751) inhibit AKT activation by dephosphorylating the membrane-associated active form, and also by preventing the inactive form from localizing into plasma membrane[254]. Currently, there are no published data evaluating ARQ092 as a single agent, or as a combination strategy, in MET-amplified NSCLC.

We have provided evidence that AKT, and more specifically AKT2, is activated by HGF overexpression. It is therefore not surprising that given the known role of AKT in promoting cancer cell survival, a pan-AKT inhibitor such as ARQ092, in combination with MET TKIs was successful in overcoming HGF-mediated resistance in MET amplified or co-amplified models. Interestingly, the gastric MET amplified model appeared to have no

increased signalling in AKT in the presence of HGF-overexpression (Figure 42), and subsequent experimental testing confirmed that ARQ092 was inactive as a single agent and in combination with MET TKIs in these cells. Perhaps the nature of MET-dependence is different based on cell lineage. In both models of MET-amplification, EBC1 and GTL16, the resistance factor (the presence of excess HGF) is the same. However, only EBC1 is associated with increased AKT signalling and the combination of an AKT inhibitor and MET TKI overcoming the HGF-mediated resistance.

Perhaps, this difference is due to cell-type-specific differences in signalling networks. Unfortunately, we did not have the resources to perform multiple phosphoproteomic profiling experiments, and it is clear that examining GTL16 in the setting of HGF-overexpression in this way would perhaps have provided further answers and potential drivers of HGF-mediated resistance in the case of gastric MET-amplification.

Another important observation when examining the effects of ARQ092, is the distinct differences in AKT phosphorylation in MET-amplified NSCLC EBC1 cells as a function of HGF overexpression. We find that in parental EBC1 cells treated with ARQ092, phosphorylation of AKT on both Thr308 and Ser473 is inhibited (Figure 38). However, in the HGF-over expressed cell line EBC1-HGF, the same dose of drug causes selective inhibition of the mTORC2 phosphorylation site (Ser473), and a subtle increase in the PDK-1 phosphorylation site (Thr308) (Figure 38). This has not been seen previously when investigating the effect of ARQ092 on AKT in cell line models[254]. Importantly, however, to the best of our knowledge the biochemical effects of ARQ092 treatment in the setting of MET-amplification or HGF excess has not been examined.

Given that HGF overexpression affects the subcellular distribution of AKT (

Figure 31), it is possible that these differences in AKT phosphorylation result from localisation-dependent phosphorylation/dephosphorylation events. Alternatively, it is also possible that HGF excess is leading to impaired Thr308 dephosphorylating activity

(i.e. a defect in PP2A, the Thr308 phosphatase). Regardless, it is clear that HGF and AKT are inextricably linked, and we are currently investigating the significance of this.

Our data provide evidence for a novel and clinically relevant approach to overcome HGF-mediated MET TKI resistance, by combining an allosteric AKT inhibitor with type I or type II MET TKI (Figure 38). We therefore, propose this novel combination to form the basis of a clinical trial, with the addition of prospective HGF-level testing, in an appropriately selected NSCLC patient population with high-level MET amplification.

Admittedly, we have presented data showing that duration of exposure of tumour cells to drugs is significant when trying to overcome HGF-induced resistance MET-amplified NSCLC (Figure 33), and that it requires at least three days of constant high-dose exposure to MET TKI, for HGF-induced resistance to be overcome, even when using potent next generation MET TKIs such as capmatinib. Whether the combination of allosteric AKT inhibitor and MET TKI also requires this duration of exposure to drug in order to be effective at inducing cell death in EBC1 parental and EBC1-HGF should also be explored.

It would also be interesting to assess if the next-generation allosteric AKT inhibitor ARQ751, which is more potent than ARQ092, demonstrates the ability to overcome HGF-mediated resistance to MET TKIs in HGF-overexpressed MET-amplified NSCLC cells. Given that this is another AKT inhibitor showing exciting promise, further work should also interrogate this compound in our model of de-novo HGF resistance.

5.3.5 Understanding the relationship between AKT, HGF excess and MET

5.3.5.1 Unsuccessful shRNA knockout experiments

As an alternative way of assessing whether AKT2 specifically drives HGF-induced resistance to MET TKIs in MET-amplified cells, we knocked down AKT2 in MET-amplified

EBC1 and EBC1-HGF cells using doxycycline-inducible short hair pins (shAKT2). While western blotting confirmed knockdown of AKT2 in these cells (Figure 43, B), the extent of knockdown was incomplete and the EBC1-HGF cells with shAKT2 knockdown remained resistant to MET TKI inhibition (Figure 43, A and C). In fact, residual levels of AKT2 following induction of the AKT2-targeting shRNA in EBC1-HGF cells were still significantly higher than those seen in untreated parental controls (Figure 45, B), which could be sufficient to drive resistance. Interestingly, there is increased cell death in the untreated parental EBC1 doxycycline-inducible AKT2 knockdown cells ((Figure 43, A and C), suggesting that AKT2 is important in these cells for survival, though the significance of this is uncertain.

It is crucial that we determine whether AKT2 activation is sufficient to confer MET TKI resistance. Current efforts in the lab are centred on this: MET TKI-sensitive cell lines ectopically expressing constitutively active alleles of AKT1 or AKT2 are being generated, as are cell line models where individual AKT isoforms are selectively depleted using CRISPR/Cas9 gene editing. The idea here is to assess if this limits the ability of HGF overexpression to confer MET TKI resistance.

We also used an HGF knockdown strategy in SBC-5, the SCLC cell line with endogenous HGF and MET co-expression to see if this could then make these cells sensitive to MET TKIs (Figure 44). However, this experiment again highlights the challenge of using such a system: HGF knockdown was incomplete, and residual protein of HGF following induction of shRNA remained higher compared with untreated parental SBC5 cells. SBC5 cells with shRNA-HGF knockdown remained resistant to MET TKI inhibition at crizotinib 25nM and crizotinib 250nM (Figure 44).

To investigate this further, HGF levels are going to be assessed in these cells using ELISA to ascertain if perhaps a certain level of HGF-expression is required to induce resistance to MET TKIs. A mixing experiment involving the MET-amplified NSCLC cell EBC1 and EBC1-HGF could also be performed to generate these data. By using serial dilutions of

EBC1-HGF mixed with EBC1 parental, the response to MET TKIs could be investigated to assess if increasing levels of HGF-expression are important in inducing resistance to MET-TKIs.

5.3.5.1.1 Does HGF excess affect localisation of AKT

To assess whether chronic exposure to excess HGF changes the localisation of the MET receptor, experimental work to measure the levels of receptor at the cell surface were performed. This question is clinically relevant for ADCs. ADCs are currently in development as a potential strategy to target MET in cancer[226], and the efficacy of these drugs is dependent on high expression levels of the target at the cell surface.

Our data show that, in two MET amplified cell lines, HGF overexpression reduces binding of a MET-specific antibody that recognises an extracellular epitope (Figure 45). Here, HGF is affecting the availability of the epitope to be recognised by the antibody.

We also show, using cell surface biotinylation experiments, that in two MET-amplified cells, in the presence of HGF, there is no loss of signal in cell surface biotinylated MET (Figure 46). This indicates, that in the presence of excess HGF, there is no significant change on cell surface MET levels. Immunofluorescence data also shows that the presence of HGF does not affect the expression and localisation of MET and phosphorylated MET (Figure 46).

Altogether, these data suggest that perhaps chronic HGF exposure is promoting a conformational change in MET, thereby affecting the accessibility of the epitope to a MET-specific antibody, and changing its binding efficiency, causing a loss of signal. The cell surface biotinylation experiments argue against the possibility of HGF overexpression increasing the basal rate of receptor internalisation, causing less protein at the cell surface.

These experiments demonstrate that binding of antibodies or ADCs directed against the extracellular domain of MET could be affected by excess HGF, and subsequent binding of a MET-targeted ADC could be affected by excess HGF, its efficacy reduced.

We therefore suggest perhaps deploying an HGF antibody, as a way to reverse the effects of HGF on MET conformation, could help to overcome this resistance.

5.3.6 Strategy 5: More potent and selective MET TKIs.

The clinical development of MET inhibitors has been challenging. In addition to the presence of HGF inducing resistance to MET TKIs, the use of non-selective MET-targeting agents has likely contributed to the large-scale failure of multiple trials to date. Capmatinib (formerly known as INC280) is a highly selective and potent ATP-competitive type I MET TKI with *in vitro* activities against preclinical cancer models with MET activation, and demonstrates single-agent anti-tumour activity in MET-driven mouse xenograft models[255,256].

Capmatinib is currently under investigation as a single agent and in combination studies. Furthermore, in September 2019, the FDA designated capmatinib as a breakthrough therapy for the first-line treatment of patients with MET exon 14 skipping mutation–positive NSCLC following the presentation of the phase II GEOMETRY mono-1 trial at the ASCO annual meeting 2019[230].

Encouraging, durable responses in patients with METex14-positive NSCLC were presented at ASCO[230]. The GEOMETRY trial is a multi-cohort, multi-centre study evaluating capmatinib in patients with METexon14-mutated or MET-amplified advanced NSCLC across 6 cohorts: cohort 4 and 5b selected for presentation at ASCO. Cohort 4 contained pre-treated patients with METex14 alterations in the second- or third-line setting (n = 69) while cohort 5b included treatment-naive patients (n = 28).

GEOMETRY mono-1 included METex14 patients who were treatment naïve as well as patients who were treated with capmatinib in the second- or third-line setting. Among the pre-treated patients, the ORR by independent review was 40.6% (95% CI, 28.9%-53.1%) and the disease control rate (DCR) was 78.3% (95% CI, 66.7%-87.3%). The median duration of response (DOR) was 9.72 months and the median progression-free survival (PFS) was 5.42 months. In the treatment-naïve cohort, the ORR by independent review was 67.9% (95% CI, 47.6%-84.1%) and the DCR was 96.4% (95% CI, 81.7%-99.9%). The median DOR was 11.14 months and the median PFS was 9.69 months. The brain penetration of capmatinib is one feature which sets it apart from crizotinib - more than 10% of newly diagnosed patients had brain metastases along with 15.9% of the pre-treated patients were included and, of these, approximately half (54%; 7 of 13) experienced an intracranial response, with 4 patients experiencing a complete resolution of their brain lesions. The intracranial DCR was 92.3% (12/13).

Consistent with published data, we show that capmatinib is highly potent and active in models of MET activation (Figure 48, Figure 49), even in the presence of HGF excess[256]. We also show however, in washout experiments (Figure 49), that in EBC1 cells with HGF excess, HGF-induced resistance is seen at both 30mins and 2hours drug exposure, and, similar to the crizotinib washout experiment (Figure 33), it still takes three days of drug treatment with capmatinib for HGF-induced resistance in EBC1 cells to be overcome.

These data emphasise the critical importance of drug exposure times in determining biological response, even when using a potent and highly selective MET TKI, such as capmatinib. These data argue for the assessment of pulsatile high dose schedules in future capmatinib studies.

Of note, the recently published initial phase I study of capmatinib[257], does not include PD data involving METex14 NSCLC patients, or any lung cancer patients, as the phase I NSCLC expansion cohort has yet to be fully published[135], though recommended phase 2 dose of capmatinib was 600 mg bid capsule/400 mg bid tablet 400mg was determined.

PD data involving one patient with advanced colorectal cancer was provided, showing near-complete immunohistochemically determined phospho-MET inhibition using 450mg capmatinib in paired biopsies[257]. Rather strikingly, similar to crizotinib, there are no published PD data regarding capmatinib in MET-driven lung tumours. Even in the phase I dose-escalation study of capmatinib in Japanese patients with advanced solid tumours, there are no published data showing convincing target inhibition as post-treatment tumour samples were collected only from one patient, therefore, no formal analysis was performed.

Thus, the questions of whether capmatinib is reaching the concentrations required for biological activity in tumour tissue, and whether capmatinib is hitting the desired molecular target remains to be adequately answered.

6 Investigation of a novel target in MET-driven cancer

6.1 Introduction

Our group has been interested, for a number of years, in understanding the functional crosstalk between RTKs (including MET and EGFR) and the lipid kinase, PI3K. During the course of these studies, phosphatidylinositol-3-phosphate 5-kinase (PIKfyve) was identified as a potential therapeutic target in GTL16 cells, the gastric MET-amplified model described earlier. I have been working together with another PhD student in the laboratory to characterise the relevance of this target in MET-driven lung cancer.

PIKfyve is an endosomal lipid kinase, that phosphorylates the D-5 position in endosomal phosphatidylinositol-3-phosphate (PI3P) to yield the 3,5-bisphosphate (PI(3,5)P2)[258], which in turn serves to control endolysosomal membrane traffic[259–262]. PIKfyve inhibition, as a cancer treatment, has only been minimally explored. Here, we report on the activity of apilimod, a first-in-class PIKfyve kinase inhibitor with exquisite specificity for PIKfyve lipid kinase[263], which has shown promise in treatment of B cell malignancies[264]. We report the findings of apilimod single-agent treatment in MET-driven cancer models, and in doing so report another strategy in overcoming HGF-induced resistance to MET TKIs in MET-amplified lung cancer.

6.2 Results

6.2.1 Apilimod has single-agent cell killing activity in MET-amplified and METex14 cancer cells.

Sensitivity to PIKfyve inhibitor, apilimod, was assessed in a panel of MET-amplified and METex14 skipping mutant cancer cell lines. Significant induction of cell death was noted in MET-amplified EBC1 (lung), GTL16 (gastric), SBC5 (lung) and VMRC_RCW (renal) and METex14 skipping cells (gastric) Hs746t (Figure 51). In contrast to this, no effect was

seen in hTERT-immortalized human non-transformed bronchial epithelial cells HBEC3-KT (Figure 51).

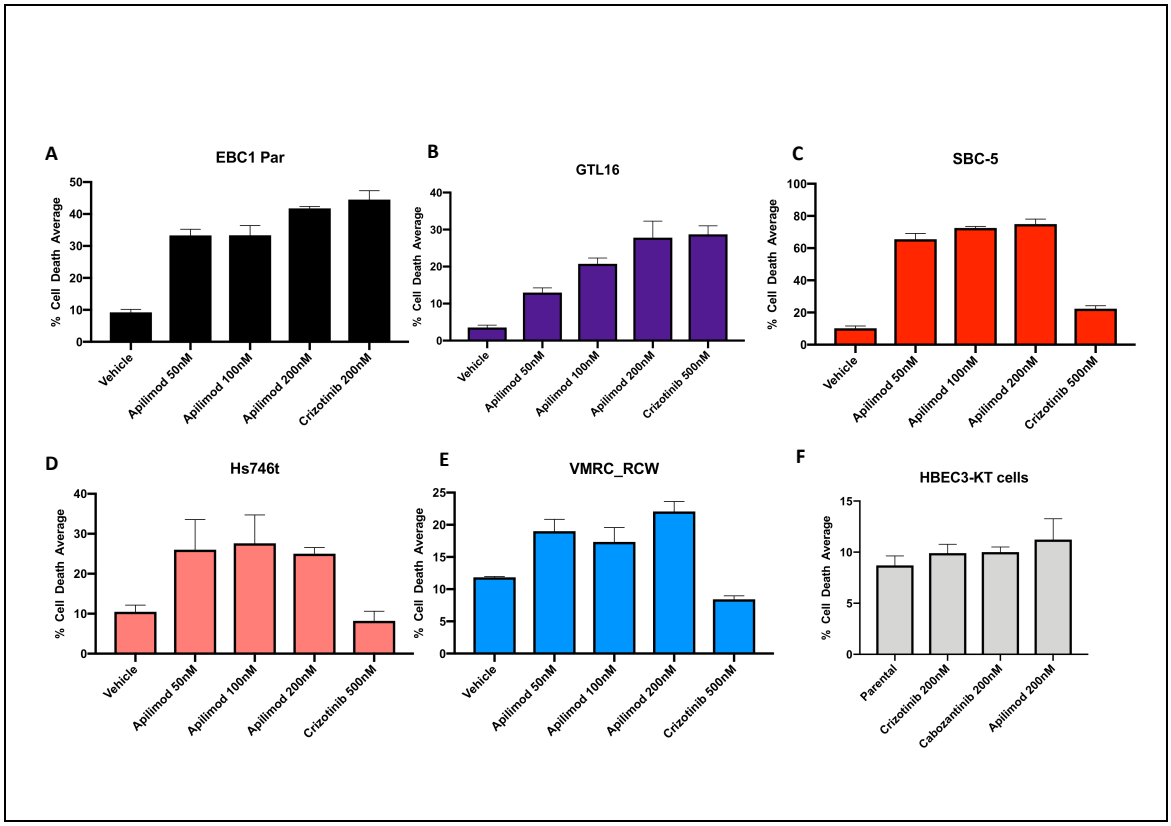

Figure 51. Apilimod induces robust cell death in MET-driven cancer cell lines. Apilimod demonstrates single-agent cell killing activity in MET-amplified EBC1 (lung), SBC5 (lung, HGF co-expression), GTL16 (gastric), VMRC RCW (kidney), and METex14 skipping (gastric) Hs746t cancer cells (A-E). hTERT immortalised human bronchial epithelial cells are insensitive to apilimod (F). (A-f) Analysis of cells to 72h treatment with MET inhibitor, crizotinib 500nM, and apilimod, 50nM – 200nM, as indicated. Cell death percentages (mean ± SEM) were assessed via automated trypan blue method (ViCell), and expressed as the fraction of stain-positive cells.

Further MET-amplified cells were evaluated for sensitivity to apilimod, H1993 (lung) and SNU-638 (gastric). In addition to impaired cell proliferation, apilimod induced significant cell death in these models of MET amplification (Figure 52).

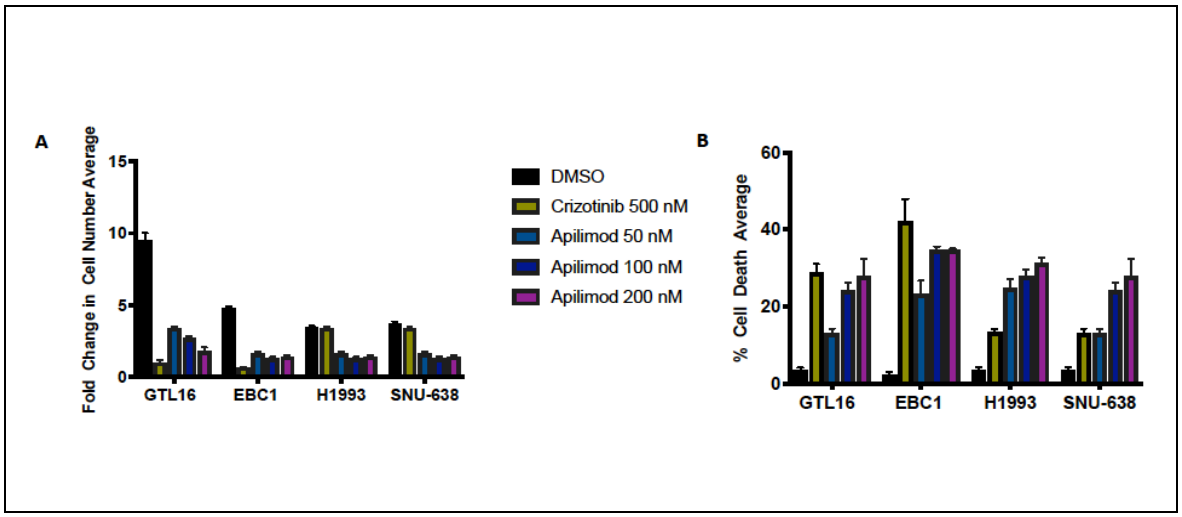

Figure 52. Apilimod induces robust cell death in MET-amplified cells. (A, C) Analysis of the responses of MET amplified cell lines, EBC1 (lung), GTL16 (gastric), H1993 (lung) and SNU-638 (gastric), to 72h treatment with MET inhibitor, type I inhibitor crizotinib and PIKfyve inhibitor, apilimod. Cell death percentages (mean ± SEM) were assessed via automated trypan blue method (ViCell), and expressed as the fraction of stain-positive cells.

6.2.2 Apilimod overcomes HGF-induced resistance to MET TKIs in lung cancer.

Sensitivity to PIKfyve inhibitor, apilimod, was then assessed in MET-amplified lung cancer in the setting of excess-HGF. In both models of HGF-excess, SBC5 cells our endogenous model of HGF expression, with MET-amplification and HGF co-expression, and in the generated resistance model EBC1-HGF, MET-amplified cell with HGF-overexpressed, HGF overexpression did not significantly impact sensitivity to apilimod (Figure 53).

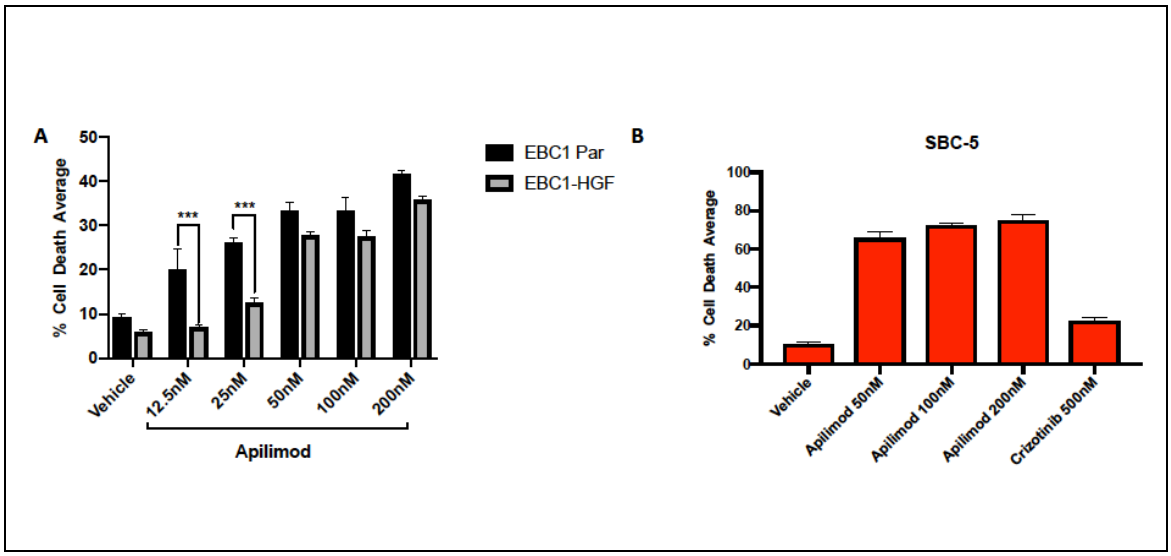

Figure 53. Single-agent apilimod is effective at overcoming HGF-mediated resistance to MET TKIs in MET-amplified NSCLC and SCLC. Analysis of the responses of MET amplified cell line, EBC, EBC1-HGF and MET-amplified HGF co-expressed SCLC cell line SBC5, to 72h treatment with MET inhibitor, crizotinib and PIKfyve inhibitor, apilimod. Cell death percentages (mean ± SEM) were assessed via automated trypan blue method (ViCell), and expressed as the fraction of stain-positive cells.

6.3 Discussion

6.3.1 Apilimod has single-agent cell killing activity in MET-amplified and METex14 cancer cells.

PIKfyve is in its infancy as a cancer therapeutics target, and consequently PIKfyve inhibitors have only recently entered development as anti-cancer drugs. Among these, apilimod is most promising. Apilimod was identified as an inhibitor of Toll-like receptor (TLR) –induced interleukin 12 (IL-12) and IL-23 cytokine production, pro-inflammatory cytokines[265]. Some of the pro-inflammatory functions of IL-23 are related to the induction of terminal differentiation and proliferation of IL-17-producing CD4+ T helper (TH17) cells[266] and TH17 cells are involved in the pathogenesis of inflammatory

autoimmune diseases, including rheumatoid arthritis, multiple sclerosis, psoriasis, and inflammatory bowel disease[267]. Due to this fact, apilimod was initially trialled as an immunomodulatory agent in inflammatory diseases, such as rheumatoid arthritis and crohn's disease. Although initial promise was shown[268,269], ultimately no efficacy was demonstrated[270,271].

It has been shown that IL-23 provides a connection between the pro-inflammatory processes that promote tumour growth and the failure of adaptive immune mediators to penetrate tumours[272,273]. As such, targeting IL-23 mediated Th17 responses may have important implications in the treatment of pro-inflammatory conditions, including cancer[274]. Thus, apilimod is now being explored as an anti-cancer agent.

PIKfyve is an endosomal lipid kinase targeted to the cytoplasmic leaflet of endosomes via protein-lipid interactions between its FYVE domain and PI3P within the endosomal membrane[275]. PIKfyve phosphorylates PI3P to generate PI(3,5)P2 at endosomes: PI(3,5)P2) then controls endolysosomal membrane traffic[259–262]. PIKfyve has been shown to lead to the selective inhibition of immune cell production of IL-12/IL-23[265]. IL-23 production, which apilimod inhibits, is thought to be positively regulated by PI3K[276] and IL-23 can mediate STAT3 and PI3K signaling pathways[277] . More specifically, IL-23 promotes inflammatory responses such as in the defence against bacterial infection, up-regulation of angiogenic factors and MMPs and drives an IL-17 producing T cell population (Th 17) in part through the activation of the STAT3 pathway[272,278]. The exact mechanism by which apilimod induces robust cell death in MET-driven cells remains to be fully elucidated.

We present the first evidence of the robust single-agent cell killing activity of apilimod in MET-driven lung cancer, in addition to gastric and kidney cancer models (Figure 51, 52) To the best of our knowledge there are no existing data that have determined whether any NSCLC driver mutational status alters or affects the IL-23/IL-23R axis.

In lung cancer, there are published data that IL-23 is pro-proliferative, and epigenetically regulated and modulated by chemotherapy in NSCLC[277]. Baird et al found that IL-23A expression was significantly elevated in NSCLC patient tumour samples[277], data that were recently replicated[279]. These data however, are from before the advent of the precision medicine era, and details are lacking regarding the presence of oncogenic drivers. The group also noted that Gemcitabine, a chemotherapy drug previously used in the first-line treatment of NSCLC also induced IL-23A expression, and that recombinant IL-23 increased cellular proliferation in two NSCLC cell line models[277]. They also provided the only pre-clinical evidence of apilimod activity in NSCLC cells[277], showing the antiproliferative activity of apilimod. These data, however, only show apilimod-induced reduced proliferation in a single adenocarcinoma NSCLC model, A549 and, in contrast to our findings, no induction of cell death was reported[277].

We provide clear evidence of a novel new target in MET-driven lung cancer, and using apilimod demonstrate clear single-agent activity in MET-driven lung cancer, both NSCLC and SCLC. To our knowledge, we provide the first evidence linking PIKfyve and MET-driven lung cancer, and these data have provided the rationale for the possible incorporation of apilimod as a new treatment arm into the MET-study arm of the phase II genomic-driven National Lung Matrix Trial[158].

6.3.2 Investigating the mechanism of Apilimod killing.

Determining the mechanism by which apilimod is inducing robust cell death in MET-driven cancer cells is an ongoing focus in our laboratory. PIKfyve is an endosomal lipid kinase, the primary target of apilimod, that regulates endosomal trafficking[259–262]. This endosomal regulation is likely having an impact on the function of MET, and current experimental work is exploring this.

Gayle et al demonstrated that that apilimod-mediated cytotoxicity is driven by PIKfyve inhibition in B-cell non-Hodgkin lymphoma[263]. Furthermore, they identified lysosome dysfunction as a major contributing factor to apilimod's cytotoxicity, and consequently

found that Apilimod-induced cell death in B-NHL correlated with autophagy dysfunction[263]. We are currently exploring if apilimod is modulating autophagy in MET-driven cancer.

Macro-autophagy (autophagy hereafter) is the process by which cells form double-membraned vesicles that sequester organelles and proteins and target them for degradation in the lysosome[280]. It is a complex multistep process, and currently it is believed that there are at least seven steps, with conserved autophagy genes (ATG genes) regulating the first five steps, and genes common to other endosomal/lysosomal pathways promoting steps 6 and 7[280]. When ATG genes have been deleted, tumour inhibition, as opposed to promotion, has been observed. For example, in RAS-driven cancers in which autophagy genes, such as Atg5 or Atg7, were conditionally deleted in tumour cells[281,282]and in a polyoma middle T–driven model of breast cancer with conditional knockout of the Fip200 autophagy gene in mammary tissue, a significant delay in tumour initiation and progression of established tumour was noted[283].

The role of autophagy in lung cancer has not been well established. Autophagy recycles intracellular components which sustain mitochondrial metabolism which may promote the growth, stress tolerance and malignancy of lung cancers[284]. Consequently, this suggests that inhibiting autophagy may have anti-tumour effect, and unsurprisingly, autophagy inhibition is currently being explored as an anti-cancer treatment strategy in many cancer subtypes.

Previous data has provided evidence suggesting that apilimod blocks autophagy[263]. To this end, we have generated essential autophagy gene autophagy-related-7 (ATG-7) CRISPR knockout GTL16 cells, and plan to see if this deletion has any effect on apilimod-induced cell killing. Phosphoproteomic profiling experiments are also underway, to determine exactly how apilimod effects the phosphoproteome. In addition to this, immunofluorescence studies will examine MET amplified cells and further characterise the location of MET when cells are treated with apilimod. Perhaps, the action of

apilimod regulating its effect on endosomal trafficking and influencing MET will be visualised using immunofluorescence imaging.

Regardless, we provide evidence of a novel target in MET-driven lung cancer. Current efforts are focused on understanding how apilimod exerts its robust killing in MET-driven cancer models.

6.3.3 Apilimod overcomes HGF-induced resistance to MET TKIs in lung cancer.

Following the impressive single-agent activity of apilimod demonstrated in MET-driven cancer models, the logical next step was to assess if apilimod treatment could be another effective treatment strategy used in overcoming HGF-mediated resistance to MET-TKIs. Excitingly, we present another strategy effective in overcoming HGF-mediated resistance to MET TKIs in MET-amplified lung cancer. We demonstrate in MET-amplified NSCLC (EBC1) and MET-amplified SCLC (SBC5), in the presence of HGF-excess single agent apilimod overcomes HGF-mediated resistance and causes robust cell death in these cells (Figure 53). All previous described strategies of overcoming HGF-induced resistance to MET TKIs, using clinically feasible drug doses, have included combination strategies. We therefore present the first single agent compound which appears successful in MET-driven models.

We have presented data that illustrates detectable HGF levels are a common finding in lung tumours (Figure 20), consistent with published reports[171]. A reason single agent MET TKIs have failed in the clinic could possibly be attributed to HGF overexpression in tumours. Therefore, the development of a single-agent strategy to overcome this HGF-induced resistance is welcome.

Our previous data strongly suggests that time of drug exposure is a critical factor in determining the biological response to targeted agents, therefore assessing whether apilimod demonstrates the ability to kill HGF-overexpressing MET-amplified cells using shorter drug exposure times is warranted. There are no published PK data assessing

target inhibition in lung tumour tissue using apilimod, and these data could certainly be important. Incorporation of apilimod into a genomic-driven NSCLC trial should involve PK data collection to confirm that apilimod is being used at an appropriate dose to induce target inhibition.

Further experimental work including the use of immunofluorescence studies, could also assess how the presence of HGF influences apilimod changes the localisation of MET. Phosphoproteomic profiling experiments will also potentially aid the pursuit of a PD biomarker for apilimod activity, which, of course, may not necessarily be linked to MET.

Nevertheless, we provide another novel strategy to overcome HGF-induced resistance in the setting of MET-amplification in lung cancer, worthy of evaluation in a molecularly selected clinical trial.

7 Conclusions

7.1 General Discussion

The era of precision medicine in lung cancer, heralded by the discovery that small molecule EGFR tyrosine kinase inhibitors are effective in the treatment of EGFR-mutant NSCLC [217,218], has led to radical changes in the management of lung cancer patients. Indeed, the recently reported unprecedented 29% overall decline in mortality from cancer in the US is thought to be largely driven by advances in lung cancer treatment strategies[285]. Nevertheless, survival rates in lung cancer remain dismal: the five-year relative survival rate for lung cancer is 15% for men and 21% for women[285]. Furthermore, not all patients will respond to current molecularly targeted treatments, or immunotherapies, and drug resistance, and resulting disease progression remains inevitable, in most if not all patients. A pressing need for novel cancer treatments, therefore, persists.

7.1.1 Excess HGF produces *de novo* resistance to MET TKIs

In this thesis, we explored potential reasons for the failure of MET TKIs in the clinic to date, and confirmed excess HGF as an over-looked innate mechanism of resistance to MET TKIs in MET-driven lung cancer. We demonstrated in our *in-vitro* models of MET-addiction sensitivity to type I and type II MET TKIs (Figure 10-12), and subsequently proved HGF-expression induces resistance to MET TKIs in these models (Figure 14, 15). These data are consistent with published reports demonstrating that overexpression of MET's ligand HGF, causes resistance to MET inhibitors in MET-addicted NSCLC cell lines[34,139]. In addition, data demonstrating that this resistance mechanism is comparable to known robust resistance mechanism (KRAS mutation) is provided.

HGF, the sole ligand of MET, can be produced by the tumour microenvironment, by cells such as fibroblasts, or by the lung tumour itself[32,33]. In this thesis, we confirmed that

HGF is produced by lung cancer associated fibroblasts (Figure 17), a significantly higher levels than parental MET amplified cancer cells. Furthermore, together with our collaborators, we also demonstrated that HGF is detectable in a significant proportion of NSCLC tumour samples, consistent with published research[171,185].

These data underscore the importance of HGF: given its frequent presence in the microenvironment and in lung tumours, and the ability of HGF to produce *de novo* resistance to MET TKIs, we argue for its inclusion in the design of MET-driven clinical trials. The presence of excess HGF should no longer be overlooked.

Currently, HGF levels are not routinely assessed in the clinic. We confirm excess HGF as a *de novo* mechanism of resistance and thus, suggest it as a potential cause for the failure of MET TKIs. Moving forward, in MET-targeted clinical trials, HGF excess levels should ideally be measured prospectively before treatment commencement involving MET TKIs.

Future work should aim to clarify a consistent standardised method of assessing HGF excess in patients, including agreement on an acceptable cut-off value of 'HGF-High'. Consideration should also be given to the retrospective investigation of completed clinical trials involving MET TKIs. Perhaps IHC evaluation of these patients' lung tumours could be performed to confirm HGF levels and assess if this could have impacted their response to treatment, thereby acting as possible retrospective validation of the significance of HGF excess.

As part of the NLMT, advanced NSCLC patients with MET-amplification, METex14 skipping and ROS1 gene fusions have been stratified to treatment with crizotinib[220]. While data for crizotinib showed greater than 90 percent predicted probability of success in ROS1 gene fusions and MET exon 14 skipping mutation, the signal was less clear for MET-amplified NSCLC as less than 1 percent objective response rate was noted[220]. We propose excess HGF levels as a potential unexplored cause of resistance in these patients.

Future MET-driven trials may continue to disregard excess HGF at their peril.

7.1.2 Strategies to overcome HGF-mediated resistance

To date, the strategies proposed to overcome HGF-induced resistance to MET TKIs have included using a small molecule inhibitor of pro-HGF activation[139] or using HGF-antibody ficlatuzumab[34], however these options are not clinically feasible solutions. Recently, studies have suggested AKT/PI3K re-activation as a possible mediator of HGF-induced drug resistance[32,34,139,198]

Our data reinforce these findings. Using multiple approaches, including western blot analysis and phosphoproteomic profiling, we have demonstrated that HGF excess in MET amplified NSCLC causes increased AKT signalling. Moreover, our data implicating AKT2 specifically as the major AKT isoform associated with HGF-mediated MET TKI-resistance, to the best of our knowledge, are entirely novel. Altogether, these data strongly suggest that the activation of pro-survival AKT signalling pathways in MET amplified NSCLC tumour cells in the presence of excess HGF plays a major role in *de novo* MET TKI resistance.

Given the likely ubiquity of HGF in lung tumours, and in the tumour microenvironment, there is an absolute need to provide rationale strategies to overcome HGF-induced resistance to MET TKIs. We have, therefore, presented a number of strategies to overcome HGF-induced resistance to MET TKIs.

These include pairing a type I or type II MET TKI with a

- MET-targeted antibody
- HGF antibody
- Allosteric AKT inhibitor, ARQ092
- m-TORC1/2 inhibitor, AZD2014

or

using single agent

- PIKfyve inhibitor, apilimod.

One challenge moving forward using these rationale drug combinations will be assessing how drug exposure times impact biological response. In this work, data which emphasise the critical importance of drug exposure times in determining biological response have been presented (Figure 33), even when using a potent and highly selective MET TKI, such as capmatinib (Figure 49). Therefore, it is possible that the development of more potent and selective MET inhibitors, such as capmatinib and tepotinib, could still be met with difficulty, in the MET amplified NSCLC population.

7.1.3 Clinical trial design for un-MET needs

Ultimately, an ongoing issue with MET-based clinical trials to date has been inefficient clinical trial design: trials to date have been designed to treat a pool of unselected patients, patients incorrectly labelled as 'MET-positive', with poorly selected compounds. A potential important mechanism of *de novo* resistance to MET inhibitors, HGF excess, thus far has been overlooked.

It is of critical importance that in MET amplified NSCLC patients, further clinical trial design is focused on including those with true MET-positive disease, i.e. NSCLC patients with high levels of MET amplification (MET/CEP7 ratio ≥5 by FISH) with no overlap of other oncogenic drivers. Appropriate molecular selection is key, and selecting patients on the basis of tumour MET overexpression alone is unlikely to represent a viable strategy for accrual. In addition to this, HGF levels should be evaluated prior to treatment. Currently, there is no universally decided method to determine a 'MET-positive' lung cancer patient.

Moving forward, we should learn from the previous efforts in biomarker-based therapy, to better identify the lung cancer patients who will benefit from treatment. We propose clinical trial design which involves selecting the appropriate NSCLC patients with high

level MET amplification, and treating them with the appropriate drugs, which could include combination strategies which I have outlined, or single-agent apilimod. Pulmonary sarcomatoid carcinomas are a subgroup of lung cancer patients with higher reported incidence rate of MET amplification[93]. Future MET-driven trial design should involve enrichment for this subgroup of patients.

The work of this research project has therapeutic implications. My ambition is that the unMET needs of MET-positive lung cancer patients can be adequately addressed by incorporating some of the changes suggested from these data.

7.2 Potential future work

As with any sizeable research project, a wealth of knowledge has been presented, and a number of questions remain to be answered. Currently, there are ongoing research efforts in the laboratory, aiming to address these.

7.2.1 Addressing AKT2 activity in the presence of HGF-excess

For instance, we have demonstrated data suggesting AKT, and specifically AKT2, is activated by HGF overexpression. It is unclear, however, why isoform AKT2, above other isoforms, is so active in the presence of excess HGF in MET-amplified NSCLC cells. We aim to determine whether AKT2 activation is sufficient to confer MET TKI resistance.

To address this, we are currently generating MET TKI-sensitive cell lines ectopically expressing constitutively active alleles of AKT1 or AKT2, and also generating cell line models where individual AKT isoforms are selectively depleted using CRISPR/Cas9 gene editing. The aim is to test whether this restricts the ability of HGF overexpression to confer MET TKI resistance. AKT2 mutants will also be expressed to assess whether AKT2 can still confer resistance to MET TKIs in this model.

Investigating whether AKT2 is sufficient for resistance as a function of cell type (e.g. GTL16 (gastric) vs EBC1 (lung) vs H1993 (lung)) may also be crucial. For example, one important consideration is whether, in gastric MET amplified GTL16 cells, HGF drives resistance through an AKT-independent mechanism, because HGF signals differently in gastric cancer cells and thus, cannot drive the expression or activation of AKT2. Future work should aim to address this.

7.2.2 *In vivo* work

The *in-vivo* experimental work relating to my project is also currently ongoing. We have demonstrated in *in-vitro* models that over-expression of HGF confers resistance to MET-inhibitors in MET-driven lung cancer, and our aim is to see if this is replicated in *in-vivo* models. To this end, we are assessing if HGF produced by CAFs induces response to MET TKI crizotinib *in-vivo.*

Briefly, cells will be subcutaneously inoculated into the flank of NSG nude mice. $1x10^5$ cells will be used per injection. For comparison of susceptibility to cancer cell engraftment, there will be 4 different tumour groups:

1. EBC1 (a MET amplified NSCLC cell line)

2. EBC1-HGF (where HGF was ectopically overexpressed in parental EBC1 cells)

3. EBC1+CAFs (hTERT-immortalised human lung cancer-associated fibroblasts)

4. EBC1+CAF-HGF (same CAFs where HGF was ectopically overexpressed)

Each tumour group will be allowed to establish tumours, and will then be randomised to two treatment arms, vehicle or crizotinib. Crizotinib (50mg/kg) or vehicle will be administered once daily by oral gavage, once tumours are established and animals will be treatment for 28 days.

Generating *in-vivo* data which replicates our in-vitro models, and evaluates the effect of HGF supplemented by the tumour microenvironment influencing MET TKIs may be crucial. All tumours will be collected and fixed in formalin, which could provide further genomic tissue worthy of evaluation.

During the process of thesis writing, the initial data of this *in-vivo* work suggests that the addition of CAFs to EBC1 cells was indeed sufficient to confer resistance to MET TKI crizotinib. The next stage will involve repeating this experiment using KO-HGF in CAFs.

7.2.3 Apilimod mechanism of killing

The identification of PIKfyve as a novel target in MET-driven cancer, coupled with the impressive single-agent activity of apilimod in MET-driven NSCLC cells (including models with HGF excess) was a revelation in the final months of experimental work. Current efforts are being directed at uncovering the mechanism by which apilimod exerts its robust cell death, including

- Phosphoproteomics profiling
- Immunofluorescence studies
- Generating CRISPR-generated ATG-7 knock out cells
- Generating apilimod-resistant cell models.

Importantly, our data has provided the rationale for the possible incorporation of apilimod as a new treatment for the phase II genomic-driven NLMT[158] for MET-driven NSCLC, which will shortly begin to recruit patients with MET-driven lung cancer in the Royal Marsden Hospital. Finding clinically relevant treatment strategies and optimising clinical trial design has been a key objective of this project. Thus, the recruitment and results of the new MET-positive arm of this genomic-driven umbrella study, the NLMT, are eagerly awaited.

7.3 Concluding statement

In our model: MET can be activated through several mechanisms, which include co-amplification/overexpression of MET and HGF. HGF overexpression can cause upfront resistance to MET TKIs possibly through changes in receptor conformation, or via upregulation of AKT signalling, or both. HGF can be produced by lung tumours and by the tumour microenvironment, thus, strategies are required to overcome resistance. We provide a number of strategies to overcome this *de novo* HGF-induced resistance, using combination treatment with MET TKIs (either different MET-targeting agents, allosteric AKT inhibitors, mTORC inhibitors) or single-agent PIKfyve inhibition.

8 Materials and Methods

8.1 Materials

8.1.1 Cell Lines

EBC-1, GTL-16, H1993, Hs746T, SBC5, H441, HEK 293T were obtained from the American Type Culture Collection (ATCC) (Manassas, VA) and were cultured and maintained in DMEM (Sigma) or RPMI (Sigma) media supplemented with 10% fetal bovine serum and antibiotics (normocin and primocin; InvivoGen). H596 were kindly provided by Dr Anne Bowcock. Beas2B cells were acquired from the ATCC and cultured in BEGM media (Lonza, Walkersville, MD). HBEC3-KT cells were obtained from ATCC and cultured in Epithelial Cell Basal Medium (ATCC PCS-300-030) supplemented with Bronchial Epithelial Cell Growth Kit (ATCC PCS-300-040). Cancer associated fibroblast cells (#CAF07A) were acquired from Neuromics (Edina, Minnesota) and grown in Neuromics vitro plus III low serum complete media. Trypsin-EDTA (0.25%) (Sigma) was used to remove cells from plates. Cells were grown in standard conditions of 5% CO2, 90% humidity and 37°C.

8.1.2 Antibodies

Antibodies against Vinculin (13901),MET (8198), pMET Y1234/5 (3077), pMET Y1003 (3135), AKT1 (2938), AKT2 (3063), AKT T308 (13038), AKT S473 (4060), pAKT1 S473 (9018), pAKT2 S474 (8599), panAKT (4685), GAPDH (5174) were purchased from Cell Signalling. A full list is provided in Appendices.

8.1.3 Plasmids

Human pBABE-puro HGF was purchased from Addgene. pLHCX-MET was kindly provided by Dr. Ingo Mellinghoff (MSKCC). TRIPZ doxycycline-inducible lentiviral HGF shRNAs were purchased from Dharmacon (clones: V3_THS373086, V3_THS373088, V2THS__179580, V2THS_179584). pbabe-hTERT were purchased from Addgene (11128).

TRIPZ tetracycline-inducible lentiviral shRNAs targeting human AKT1 and AKT2 were purchased from Thermo Scientific (Lafayette, CO) (AKT2 clones: V2THS_237948, V3THS_325553, and V3THS_325558).

8.2 Methods

8.2.1 General techniques and storage conditions.

Distilled water was used to prepare all stock solutions and reactions. All reagents were purchased from Sigma and all solutions and reactions were made up in water unless otherwise stated. All small volume centrifugation steps were carried out at room temperature using a desktop centrifuge (Eppendorf) and at 4°C in a refrigerated centrifuge (Eppendorf). A refrigerated centrifuge was used for the falcon tubes. DNA containing solutions were stored at -20°C in the short term and at -80°C in the long term. All antibodies were stored in the short term at -20°C (unless otherwise stated by the manufacturer's guidelines), if necessary in the dark.

8.2.2 Preparation of drug treatments and storage conditions

All drugs were prepared under sterile conditions under a cell culture-hood. Unless otherwise stated, drugs were dissolved in DMSO and diluted according to the manufacturer's instructions and used at the indicated concentrations. JNJ-38877605, crizotinib, cabozantinib, capmatinib, MK2206, SGX-523 were purchased from Selleck Chemicals. Onartuzumab was kindly provided by Genetech and dissolved in PBS. ADC11368 and ADC8830 were kindly provided by Almac. ARQ092 (or miransertib) was purchased form ArQule. Apilimod was purchased from MedChemExpress. Please see the main text for the final drug concentrations.

8.2.3 Assessment of cell death induction

Cell viability was determined with a Vi-CELL cell viability analyzer (Beckman Coulter, Brea, CA, USA) according to the manufacturer's instructions. Cells were seeded on 6cm

dishes and allowed to attach overnight. Cells were then treated with the indicated drugs at the indicated doses for 72hours, unless otherwise indicated. Each treatment group was seeded in triplicate. Following treatment, both attached and unattached cells were harvested and counted. The instrument uses trypan blue to assess cell death. Cell death was expressed as the fraction of trypan-blue-positive cells over the total number of cells. GraphPad was used for statistical analysis.

8.2.4 Western blot and Immunoprecipitation

Cells were harvested on ice directly on tissue culture plates. For western blotting, protein was extracted from cells using 1% triton lysis buffer (9803, Cell Signaling Technologies), supplemented with protease and phosphatase inhibitors (Millipore). When lysates were used for co-Immunoprecipitation to detect MET-AKT interaction, 50 mM HEPES (pH 7.4), 150 mM NaCl, 1mM EDTA, 1 mM EGTA, 1% Nonidet P-40, 1% glycerol lysis buffer supplemented with protease and phosphatase inhibitors (Millipore) was used. Lysates were sonicated, cleared by centrifugation and normalized to equal amounts of total protein using the DC protein assay (Biorad). Lysates for immunoprecipitation underwent a 30-minute pre-clearing step with 20 µL proteinA Agarose beads (50% slurry, Cell Signaling Technology) at 4°C, followed by MET pulldown using the Immunoprecipitation Kit Dynabeads protein A, according to manufacturer's instructions (Thermo Scientific). Dynabeads were crosslinked to MET antibody (Cell Signaling Technology) using BS3, as per manufacturer's instructions (Thermo Scientific). Lysates were sonicated, cleared by centrifugation and normalized to equal amounts of total protein using the DC protein assay (Biorad). Equal amounts of protein lysates were run on NuPAGE Novex 4-20% Tris-Acetate gels (Biorad) using SDS Tris-Acetate Running buffer (Fisher Scientific), and transferred to nitrocellulose membrane (GE Healthcare) using 1x transfer buffer (25 mM Tris-HCl (pH 7.6), 192 mM glycine, 20% methanol, 0.03% sodium dodecyl sulfate). Membranes were blocked for 1h in 5% milk at room temperature and subsequently incubated overnight at 4°C with primary antibodies (Cell Signalling if not otherwise indicated): MET (1:1000), pMET Y1234/1235, Y1003 (1:1000),

AKT (1:1000), pAkt (1:1000), Erk(1:1000), pErk (1:1000), Vinculin (1:1000), GAB (1:1000), pGAB (1:1000). The following day, membranes were incubated with a horseradish peroxidase (HRP) conjugated anti-rabbit secondary (1:5000, Jackson ImmunoResearch) for 1 hour and developed using Clarity Max ECL (Biorad).

8.2.5 Retroviral or lentiviral vectors and stable transduction

Stable transduction of lung cancer cells with retroviral or lentiviral vectors has been previously described. Briefly, cDNAs were co-transfected with packaging plasmids into 293T cells. Viral particles were collected 36 and 56 hours post-transfection and target cells were infected for 12 hours with each virus collection. Stable expressors were derived through antibiotic selection, and overexpression monitored by Western blot. Similar technique was used for the following constructs: KRAS mutant G12C/V, KRAS mutant G12V, hTERT, AKT2 shRNA, HGFshRNA

8.2.6 Quantitative detection of HGF and IL-6 by ELISA

The secretion of HGF by cell lysates was assessed using the Human HGF ELISA (cat. no. ab100534; Abcam) kit. IL-6 release was measured using the Quantikine Human IL-6 Immunoassay (Catalog Number D6050, R&D Systems, Minneapolis), used on concentrated cell medium. The assay was performed according to the manufacturer's instructions as previously published. Values were expressed as pg/mL of IL-6 from the original supernatant (non-concentrated).

Briefly, cells were seeded 3 days prior to procedure. The ELISA assay employs a quantitative sandwich enzyme immunoassay technique, where a monoclonal antibody specific for human IL-6 or HGF has been pre-coated onto a microplate. Standards and samples are pipetted into the wells and any IL-6 or HGF, respectively, present is bound by the immobilized antibody. After washing away any unbound substances, an enzyme-linked polyclonal antibody specific for human IL-6 or HGF is added to the wells. Following a wash to remove any unbound antibody-enzyme reagent, a substrate

solution is added to the wells and colour develops in proportion to the amount of IL-6 or HGF bound in the initial step. The colour development is stopped and the intensity of the colour is measured at 450 nm wavelength.

8.2.7 Immunohistochemistry (performed by collaborators)

This work was performed by our collaborators in Central Pathology Lab, St. James's Hospital, Trinity College Dublin, Ireland. In short, 3-µm thick sections cut from paraffin-embedded specimens were prepared on glass slides for the phosphorylation of HGF IHC staining. All of the specimens were stained with hematoxylin and eosin for the histopathologic diagnosis. The sections were placed in 0.01 mol/L citrate buffer (pH 6.0) and autoclaved at 121°C for 10 minutes. They were treated with 3% H2O2 for 5 minutes to block the endogenous peroxidase activity. Anti-Human HGF-alpha (H487) Rabbit IgG was purchased from TECAN. Anti-HGF Antibody (10463-T24) was purchased from Sino Biological. EBC1-HGF, the MET amplified cell line with HGF ectopically expressed, was used as a positive control (EBC1-HGF was confirmed to have cytoplasmic HGF staining). EBC1 parental served as a negative control.

The primary HGF antibodies used were a monoclonal Ab against HGF, diluted 1:100 in phosphate buffered-saline, and incubated for 18 hours at 4°C. Thereafter, IHC staining was performed by the labeled polymer method (Histofine Simple Stain MAX-PO kit, Nichirei, Tokyo, Japan) according to the manufacturer's instructions. The stained specimens were then categorized into 8 degrees according to the IHC Allred score[174] Initially, 6 degrees of the proportional score for the positive staining cells were assigned according to the frequency of positive tumour cells (0, none; 1, <1/100; 2, 1/100 to 1/10; 3, 1/10 to 1/3; 4, 1/3 to 2/3; and 5, >2/3). Thereafter, 4 degrees for the intensity score were assigned according to the intensity of the staining (0, none; 1, weak; 2, intermediate; and 3, strong). The proportional score and the intensity score were then added to each other to obtain a total score, which ranged from 0 to 8. According to the total IHC Allred score, the HGF-score of the tumour was categorized as a negative expression when the score was 0 to 1 and a positive expression when the score was 3 to

8. The slides were independently examined by two pathologists, who were blinded to the clinicopathological data.

8.2.8 Immunofluorescence staining.

For the IF procedure, 10^5 EBC1 cells (parental or HGF overexpressing) were plated onto coverslips. After 24h, cells underwent fixation with 4% paraformaldehyde in PBS for 10 min at room temperature. Subsequently, paraformaldehyde was quenched using 50nM NH4Cl in PBS for 10min, followed with three consecutive PBS washes. Next, cells were permeabilised using 0.1% Triton X-100 in PBS for 15 min at room temperature. After three washes with PBS, non-specific antibody binding sites were blocked by incubating cells in blocking solution (1% BSA, 0.1% Tween 20 in PBS) for 30 minutes at room temperature. Next, cells were incubated with 30µL of pre-diluted antibodies in blocking solution (Human MET Antibody (AF276), R&D systems; pMet (3077) and AKT (9272), Cell signaling) overnight at 4°C. Afterwards, cells were washed with PBS three times. Dye-coupled secondary antibodies in blocking solution were incubated 1h at room temperature in a dark chamber (AlexaFluor568 anti-goat to detect MET, AlexaFluor488 anti-rabbit for pMet and AlexaFluor555 anti-rabbit to detect AKT). After three washes with PBS, nuclei were stained with DAPI for 5 min in PBS. Finally, after three washes in PBS and one in water, cells were mounted in Mowiol. Cells were examined under a 63x magnification lens and pictures were acquired using a Zeiss LSM700 Confocal.

8.2.9 Flow cytometry

Cells were seeded two days prior to experimental work, $1x10^6$ cells per assay. Cells were pelleted by centrifugation and supernatant removed. PBS solution was used to wash cells. Cells were resuspended cells in 100 µl of diluted primary antibody, prepared in Antibody Dilution Buffer at a recommended dilution. Cells were then incubated for 30 minutes to 1 hr on ice, protected from light. Cells were washed by centrifugation in PBS, supernatant discarded, repeated. Cells were resuspended in 100 µl of diluted fluorochrome-conjugated secondary antibody (prepared in Antibody Dilution Buffer at

the recommended dilution), and incubated for 30minutes on ice. Cells were washed by centrifugation in PBS, supernatant discarded, and wash repeated x2. Cells were resuspended in PBS and analysed on flow cytometer. MET primary antibody used: Met (11C4) Mouse mAb (Flow Specific), Cell signalling catalogue number #5631; Anti-Mouse IgG (H+L), F(ab')2 Fragment (Alexa Fluor® 488 Conjugate) Cell signalling catalogue number #4408.

8.2.10 Cell Surface Protein Biotinylation Assay and Western Blot Analysis

Cells (EBC1, EBC1-HGF, GTL16, GTL16-HGF) were plated two days prior to procedure. Cells were maintained in Dulbecco's Modified Eagle's Medium supplemented with 10% fetal bovine serum, puromycin and normomycin. On day of procedure, cells were washed twice with PBS, 10mM stock of Sulfo-NHS-SS-Biotin (Thermofisher, 21331) was prepared. Cells were incubated in 2.5 mg/ml biotin reagent, Sulfo-NHS-SS-Biotin, for 30mins (or a time-point as specified) with gentle rocking. After incubation, cells were washed with 100 mM glycine in PBS three times and PBS once, with each washing lasting 10 min. All incubations were performed on ice. Cells were lysed with 200 µl of lysis buffer, incubated on ice, then placed in a rotating wheel at slow speed 1 hr in the cold room. Lysates were spun at 16,000 x g for 15 min at 4 °C, supernatants transferred. 15% of each supernatant in another tube and store at -80 °C (these were the INPUT/ whole cell lysate samples), and the rest of the supernatant is the PULL-DOWN/eluate samples). Lysates are subjected to a neutravidin pull down, incubated with 40 µl of NeutrAvidin beads overnight in the rotating wheel at slow speed in the cold room. The pull-down samples were washed and eluted using Laemmli buffer. DC assay was performed to quantify protein and western blotting performed on samples as described above.

8.2.11 Phosphoproteomic Profiling Experiment

8.2.11.1 Cell lysis and sample preparation for mass spectrometry

For each treatment condition, five independent biological replicates were performed. Cells were washed twice with cold phosphate-buffered saline supplemented with 1 mM

Na3VO4 and 1 mM NaF, and lysed in 1 ml of urea buffer [8 M urea in 20 mM Hepes (pH 8.0), supplemented with 1 mM Na3VO4, 1 mM NaF, 1 mM Na4P2O7 and 1 mM β-glycerophosphate]. Cell lysates were further homogenized by sonication (30 cycles of 30s on and 30s off in a Diagenode Bioruptor® Plus) and insoluble material was removed by centrifugation. Protein was quantified by the BCI assay. For each replicate, 325µg of protein was reduced, alkylated and digested with TLCK-trypsin (Thermo-Fisher Scientific) as previously described[196]. The resultant peptide solutions were desalted with C18-Oasis cartridges (Waters, Manchester, UK) as indicated by the manufacturer with slight modifications as previously described[286]. Enrichment of phosphorylated peptides was performed with TiO2 as previously described[196,286].

8.2.11.2 Phosphopeptide detection, identification and quantification

Phosphopeptides were resuspended in 12µL of reconstitution buffer (20 fmol/µL enolase in 3% ACN, 0.1% TFA) and 5.0 µL were loaded onto an LC-MS/MS system consisting of a Dionex UltiMate 3000 RSLC directly coupled to an Orbitrap Q-Exactive Plus mass spectrometer (Thermo Fisher Scientific) through an EasySpray system. LC-MS/MS was performed as previously described[196]. Mascot Daemon 2.5.0 was used to automate peptide identification from MS data as indicated before[196]. Label-free peptide quantification was performed using Pescal, an in-house developed software, that constructed of XICs for all identified peptides across all samples (±7 ppm mass and ±2 min retention time windows) and calculated the peak areas of the generated XICs1,2. Normalized peak areas of phosphopeptides were used to calculate fold change and statistical significance between conditions.

8.2.11.3 Kinase substrate enrichment analysis (KSEA).

Kinase activity was estimated from phosphoproteomics data using a kinase substrate enrichment analysis (KSEA) approach][196,286,287]. Briefly, phosphorylated peptides were grouped into substrate groups associated to particular kinases as annotated in the PhosphoSite database. Z-scores for each kinase were calculated as (mS−mP) *m1/2/d, where mS is the log2 of the mean abundances for each kinase group, mP is the log2 of

the mean abundances of the whole data set, m is the size of each substrate group and d is the SD of the mean abundances of the entire data set. Excel software was used to transform Z-scores into P-values.

9 Appendix

9.1 Supplementary Figures

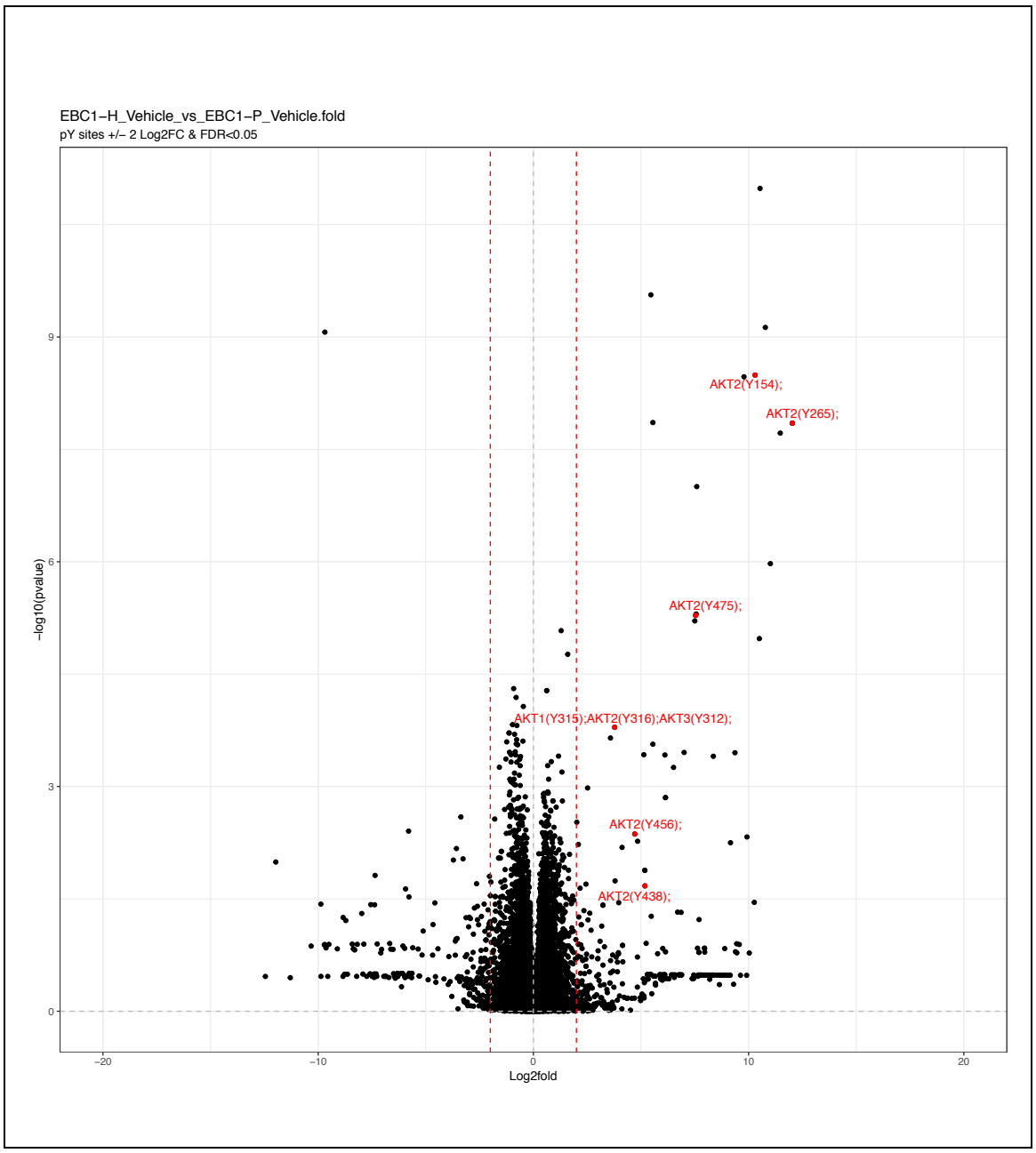

Supplementary Figure 1. AKT2 is a potential mediator of resistance in HGF-expressed MET-addicted lung cancer. Volcano plot of phosphoproteomic data, comparing vehicles in EBC1 Parental and EBC1-HGF, with regards to tyrosine-phosphorylated peptides. The colour

intensities correspond to the values of the scores of each signalling pathway indicating upregulated sites (red, upregulated; blue, downregulated). AKT2-specific tyrosine phosphosites are upregulated.

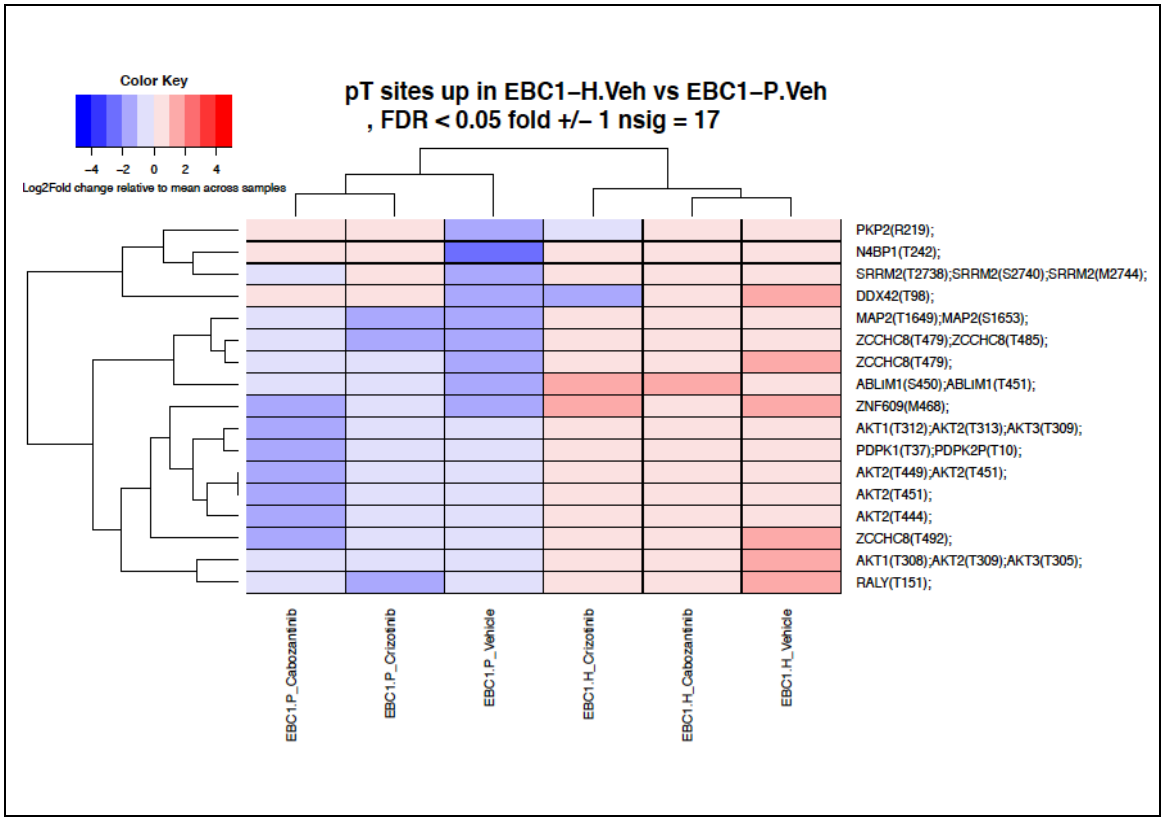

Supplementary Figure 2. AKT2 is a potential mediator of resistance in HGF-expressed MET-addicted lung cancer. Clustered heatmap of KSEA analysis showing AKT2 phosphosites with increased signal, comparing vehicles in EBC1 Parental and EBC1-HGF, with regards to threonine-phosphorylated peptides. AKT2-specific threonine phosphosites are upregulated.

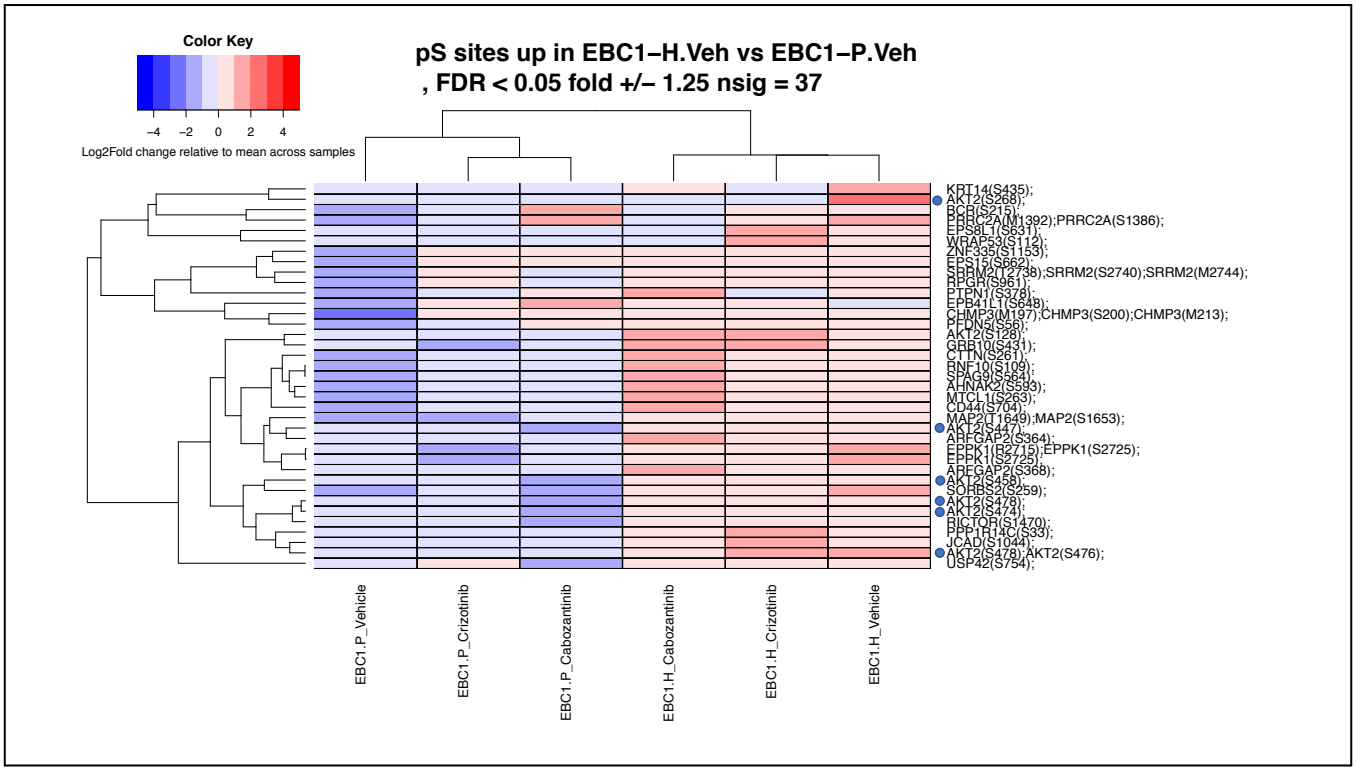

Supplementary Figure 3. AKT2 is a potential mediator of resistance in HGF-expressed MET-addicted lung cancer. Clustered heatmap of KSEA analysis of phosphoproteomic data, comparing vehicles in EBC1 Parental and EBC1-HGF, with regards to serine-phosphorylated peptides. The colour intensities correspond to the values of the scores of each signalling pathway indicating upregulated sites (red, upregulated; blue, downregulated). AKT2-specific serine phosphosites are upregulated.

9.2 Supplementary Tables

Antibody name	Species	Description/ isotype	Purpose/ comment	Company	Cat number
MET	Rabbit	IgG	Western, IP	CST	8198
pMET Y1003	Rabbit	IgG	Western	CST	3135
pMET Y1234/5	Rabbit	IgG	Western	CST	3077
pMET Y1349	Rabbit	IgG	Western	CST	3121
PAN AKT	Rabbit	IgG	Western, IP, IF	CST	4685
pAKT S473	Rabbit	IgG	Western	CST	4060
pAKT T308	Rabbit	IgG	Western	CST	13038
pAKT2 S474	Rabbit	IgG	Western	CST	8599
pAKT1 S473	Rabbit	IgG	Western	CST	9018
AKT1	Rabbit	IgG	Western	CST	2938
AKT2	Rabbit	IgG	Western	CST	3063
GAPDH	Rabbit	IgG	Western	CST	5174
Vinculin	Rabbit	IgG	Western	CST	13901
MET	Mouse	IgG1	Flow	CST	5631
Secondary to Mouse IgG	Mouse	IgG1	Flow, Alexa Fluor 488 Conjugate	CST	4408

Isotype control	Goat	IgG1	Flow, Anti-mouse IgG (PE Conjugate)	CST	59997
MET	Goat	Polyclonal Goat IgG	IF	R&D Systems	AF276
Anti-HGF	Rabbit	IgG	IHC	Tecan	H487
Anti-HGF	Rabbit	IgG	IHC	SinoBiological	10463-T24

Supplementary Table 1. Summary of antibody reagents used. Abbreviations: CST, Cell Signaling Technology.

10 References

1. Jemal A, Bray F, Center MM, Ferlay J, Ward E FD. Global cancer statistics. *Cancer J Clin*. 2011;61:69–90. doi:10.3322/caac.20107

2. R R, E C, R G, et al. Erlotinib versus standard chemotherapy as first-line treatment for European patients with advanced EGFR mutation-positive non-small-cell lung cancer (EURTAC): a multicentre, open-label, randomised phase 3 trial. *Lancet Oncol*. 2012;13(3):239-246 8p. http://search.ebscohost.com/login.aspx?direct=true&AuthType=ip,shib&db=jlh&AN=104547243&site=ehost-live&scope=site.

3. Yang JCH, Wu YL, Schuler M, et al. Afatinib versus cisplatin-based chemotherapy for EGFR mutation-positive lung adenocarcinoma (LUX-Lung 3 and LUX-Lung 6): Analysis of overall survival data from two randomised, phase 3 trials. *Lancet Oncol*. 2015;16(2):141-151. doi:10.1016/S1470-2045(14)71173-8

4. Shaw AT, Ou S-HI, Bang Y-J, et al. Crizotinib in ROS1-Rearranged Non-Small-Cell Lung Cancer. *N Engl J Med*. 2014;371(21):1963-1971. doi:10.1056/NEJMoa1406766

5. Solomon BJ, Mok T, Kim D-W, et al. First-line crizotinib versus chemotherapy in ALK-positive lung cancer. *N Engl J Med*. 2014;371(23):2167-2177. doi:10.1056/NEJMoa1408440

6. Drilon A, Siena S, Ou SHI, et al. Safety and antitumor activity of the multitargeted pan-TRK, ROS1, and ALK inhibitor entrectinib: Combined results from two phase I trials (ALKA-372-001 and STARTRK-1). *Cancer Discov*. 2017. doi:10.1158/2159-8290.CD-16-1237

7. Shaw AT, Felip E, Bauer TM, et al. Lorlatinib in non-small-cell lung cancer with ALK or ROS1 rearrangement: an international, multicentre, open-label, single-arm first-in-man phase 1 trial. *Lancet Oncol*. 2017. doi:10.1016/S1470-2045(17)30680-0

8. Reck M, Rodríguez-Abreu D, Robinson AG, et al. KEYNOTE-024: Pembrolizumab (pembro) vs platinum-based chemotherapy (chemo) as first-line therapy for advanced NSCLC with a PD-L1 tumor proportion score (TPS) ≥50%. *Ann Oncol*. 2016;27(suppl_6):LBA8_PR-LBA8_PR. doi:10.1093/ANNONC/MDW435.40

9. Herbst RS, Baas P, Kim DW, et al. Pembrolizumab versus docetaxel for previously treated, PD-L1-positive, advanced non-small-cell lung cancer (KEYNOTE-010): A randomised controlled trial. *Lancet*. 2016;387(10027):1540-1550. doi:10.1016/S0140-6736(15)01281-7

10. Rittmeyer A, Barlesi F, Waterkamp D, et al. Atezolizumab versus docetaxel in patients with previously treated non-small-cell lung cancer (OAK): a phase 3, open-label, multicentre randomised controlled trial. *Lancet*. 2017;389(10066):255-265. doi:10.1016/S0140-6736(16)32517-X

11. Antonia SJ, Villegas A, Daniel D, et al. Durvalumab after Chemoradiotherapy in Stage III Non-Small-Cell Lung Cancer. *N Engl J Med*. 2017:NEJMoa1709937. doi:10.1056/NEJMoa1709937

12. Gil-Sierra MD, Fenix-Caballero S, Alegre-del Rey EJ. Pembrolizumab plus chemotherapy in lung cancer. *N Engl J Med*. 2018. doi:10.1056/NEJMc1808567

13. Cerami E, Gao J, Dogrusoz U, et al. The cBio Cancer Genomics Portal: An open platform for exploring multidimensional cancer genomics data. *Cancer Discov*. 2012. doi:10.1158/2159-8290.CD-12-0095

14. Gao J, Aksoy BA, Dogrusoz U, et al. Integrative analysis of complex cancer genomics and clinical profiles using the cBioPortal. *Sci Signal*. 2013. doi:10.1126/scisignal.2004088

15. Network TCGAR, institution.) (Participants are arranged by area of contribution and then by, Institute G sequencing centres: B, et al. Comprehensive genomic characterization of squamous cell lung cancers. *Nature*. 2012;489(7417):519-525. doi:10.1038/nature11404

16. The Cancer Genome Atlas Research Network. Comprehensive molecular profiling of lung adenocarcinoma. *Nature*. 2014;511(7511):543-550. doi:10.1038/nature13385

17. Govindan R, Ding L, Griffith M, et al. Genomic landscape of non-small cell lung cancer in smokers and never-smokers. *Cell*. 2012;150(6):1121-1134. doi:10.1016/j.cell.2012.08.024

18. Middleton G, Crack LR, Popat S, et al. The National Lung Matrix Trial: Translating the biology of stratification in advanced non-small-cell lung cancer. *Ann Oncol*. 2015;26(12):2464-2469. doi:10.1093/annonc/mdv394

19. Mullard A. NCI-MATCH trial pushes cancer umbrella trial paradigm. *Nat Rev Drug Discov*. 2015. doi:10.1038/nrd4694

20. Sadiq AA, Salgia R. MET As a possible target for non-small-cell lung cancer. *J Clin Oncol*. 2013;31(8):1089-1096. doi:10.1200/JCO.2012.43.9422

21. Scagliotti G V., Novello S, von Pawel J. The emerging role of MET/HGF inhibitors in oncology. *Cancer Treat Rev*. 2013;39(7):793-801. doi:10.1016/j.ctrv.2013.02.001

22. Schmidt C, Bladt F, Goedecke S, et al. Scatter factor/hepatocyte growth factor is

essential for liver development. *Nature*. 1995;373(6516):699-702. doi:10.1038/373699a0

23. Smyth EC, Sclafani F, Cunningham D. Emerging molecular targets in oncology: clinical potential of MET/hepatocyte growth-factor inhibitors. *Onco Targets Ther*. 2014;7:1001-1014. doi:10.2147/OTT.S44941

24. Liu X, Newton RC, Scherle PA. Developing c-MET pathway inhibitors for cancer therapy: progress and challenges. *Trends Mol Med*. 2010;16(1):37-45. doi:10.1016/j.molmed.2009.11.005

25. Ma PC, Tretiakova MS, MacKinnon AC, et al. Expression and mutational analysis of MET in human solid cancers. *Genes Chromosom Cancer*. 2008. doi:10.1002/gcc.20604

26. Voutsina A, Tzardi M, Kalikaki A, et al. Combined analysis of KRAS and PIK3CA mutations, MET and PTEN expression in primary tumors and corresponding metastases in colorectal cancer. *Mod Pathol*. 2013. doi:10.1038/modpathol.2012.150

27. Masuya D, Huang C, Liu D, et al. The tumour-stromal interaction between intratumoral c-Met and stromal hepatocyte growth factor associated with tumour growth and prognosis in non-small-cell lung cancer patients. *Br J Cancer*. 2004. doi:10.1038/sj.bjc.6601718

28. Lee WY, Chen HHW, Chow NH, Su WC, Lin PW, Guo HR. Prognostic significance of co-expression of RON and MET receptors in node-negative breast cancer patients. *Clin Cancer Res*. 2005. doi:10.1158/1078-0432.CCR-04-1761

29. Garouniatis A, Zizi-Sermpetzoglou A, Rizos S, Kostakis A, Nikiteas N, Papavassiliou AG. FAK, CD44v6, c-Met and EGFR in colorectal cancer parameters: Tumour

progression, metastasis, patient survival and receptor crosstalk. *Int J Colorectal Dis*. 2013. doi:10.1007/s00384-012-1520-9

30. Kishiki T, Ohnishi H, Masaki T, et al. Overexpression of MET is a new predictive marker for anti-EGFR therapy in metastatic colorectal cancer with wild-type KRAS. *Cancer Chemother Pharmacol*. 2014. doi:10.1007/s00280-014-2401-4

31. Ujiie H, Tomida M, Akiyama H, et al. Serum hepatocyte growth factor and interleukin-6 are effective prognostic markers for non-small cell lung cancer. *Anticancer Res*. 2012;32(8):3251-3258.

32. Straussman R, Morikawa T, Shee K, et al. Tumour micro-environment elicits innate resistance to RAF inhibitors through HGF secretion. *Nature*. 2012;487(7408):500-504. doi:10.1038/nature11183

33. Bhowmick NA, Neilson EG, Moses HL. Stromal fibroblasts in cancer initiation and progression. *Nature*. 2004;432(7015):332-337. doi:10.1038/nature03096

34. Pennacchietti S, Cazzanti M, Bertotti A, et al. Microenvironment-derived HGF overcomes genetically determined sensitivity to anti-MET drugs. *Cancer Res*. 2014;74(22):6598-6609. doi:10.1158/0008-5472.CAN-14-0761

35. Klemm F, Joyce JA. Microenvironmental regulation of therapeutic response in cancer. *Trends Cell Biol*. 2015;25(4):198-213. doi:10.1016/j.tcb.2014.11.006

36. Scagliotti G, Von Pawel J, Novello S, et al. Phase III multinational, randomized, double-blind, placebo-controlled study of tivantinib (ARQ 197) plus erlotinib versus erlotinib alone in previously treated patients with locally advanced or metastatic nonsquamous non-small-cell lung cancer. *J Clin Oncol*. 2015. doi:10.1200/JCO.2014.60.7317

37. Onartuzumab plus erlotinib versus erlotinib in previously treated stage IIIb or IV NSCLC: Results from the pivotal phase III randomized, multicenter, placebo-controlled METLung (OAM4971g) global trial. *Clin Adv Hematol Oncol*. 2014. doi:10.1200/jco.2014.32.15_suppl.8000

38. Yoshioka H, Azuma K, Yamamoto N, et al. A randomized, double-blind, placebo-controlled, phase III trial of erlotinib with or without a c-Met inhibitor tivantinib (ARQ 197) in Asian patients with previously treated stage IIIB/IV nonsquamous nonsmall-cell lung cancer harboring wild-type epidermal. *Ann Oncol*. 2015. doi:10.1093/annonc/mdv288

39. Paik PK, Drilon A, Fan PD, et al. Response to MET inhibitors in patients with stage IV lung adenocarcinomas harboring met mutations causing exon 14 skipping. *Cancer Discov*. 2015;5(8):842-850. doi:10.1158/2159-8290.CD-14-1467

40. Frampton GM, Ali SM, Rosenzweig M, et al. Activation of MET via diverse exon 14 splicing alterations occurs in multiple tumor types and confers clinical sensitivity to MET inhibitors. *Cancer Discov*. 2015;5(8):850-860. doi:10.1158/2159-8290.CD-15-0285

41. Cooper CS, Park M, Blair DG, et al. Molecular cloning of a new transforming gene from a chemically transformed human cell line. *Nature*. 1984;311(5981):29-33. doi:10.1038/311029a0

42. Ponzetto C, Bardelli A, Zhen Z, et al. A multifunctional docking site mediates signaling and transformation by the hepatocyte growth factor/scatter factor receptor family. *Cell*. 1994;77(2):261-271. doi:10.1016/0092-8674(94)90318-2

43. Naldini L, Vigna E, Narsimhan RP, et al. Hepatocyte growth factor (HGF) stimulates the tyrosine kinase activity of the receptor encoded by the proto-oncogene c-MET. *Oncogene*. 1991.

44. Fixman ED, Fournier TM, Kamikura DM, Naujokas MA, Park M. Pathways downstream of Shc and Grb2 are required for cell transformation by the Tpr-Met oncoprotein. *J Biol Chem*. 1996. doi:10.1074/jbc.271.22.13116

45. Bottaro DP, Rubin JS, Faletto DL, et al. Identification of the hepatocyte growth factor receptor as the c-met proto-oncogene product. *Science (80-)*. 1991. doi:10.1126/science.1846706

46. Miyazawa K, Tsubouchi H, Naka D, et al. Molecular cloning and sequence analysis of cDNA for human hepatocyte growth factor. *Biochem Biophys Res Commun*. 1989. doi:10.1016/0006-291X(89)92316-4

47. Zarnegar R, Michalopoulos G. Purification and Biological Characterization of Human Hepatopoietin A, a Polypeptide Growth Factor for Hepatocytes. *Cancer Res*. 1989.

48. Nakamura T, Nawa K, Ichihara A, Kaise N, Nishino T. Purification and subunit structure of hepatocyte growth factor from rat platelets. *FEBS Lett*. 1987. doi:0014-5793(87)80475-1 [pii]

49. Stoker M, Gherardi E, Perryman M, Gray J. Scatter factor is a fibroblast-derived modulator of epithelial cell mobility. *Nature*. 1987. doi:10.1038/327239a0

50. Gherardi E, Gray J, Stoker M, Perryman M, Furlong R. Purification of scatter factor, a fibroblast-derived basic protein that modulates epithelial interactions and movement. *Proc Natl Acad Sci U S A*. 1989. doi:10.1073/pnas.86.15.5844

51. Gherardi E, Stoker M. Hepatocytes and scatter factor. *Nature*. 1990. doi:10.1038/346228b0

52. Weidner KM, Arakaki N, Hartmann G, et al. Evidence for the identity of human

scatter factor and human hepatocyte growth factor. *Proc Natl Acad Sci U S A*. 1991. doi:10.1073/pnas.88.16.7001

53. Skead GG, Govender D. Erratum: Gene of the month: MET (J Clin Pathol (2015) 68 (405-409) DOI: 10.1136/jclinpath-2015-203050). *J Clin Pathol*. 2015. doi:10.1136/jclinpath-2015-203050

54. Liu Y. The human hepatocyte growth factor receptor gene: Complete structural organization and promoter characterization. *Gene*. 1998. doi:10.1016/S0378-1119(98)00264-9

55. Lemmon MA, Schlessinger J. Cell signaling by receptor tyrosine kinases. *Cell*. 2010. doi:10.1016/j.cell.2010.06.011

56. Schaeper U, Gehring NH, Fuchs KP, Sachs M, Kempkes B, Birchmeier W. Coupling of Gab1 to c-Met, Grb2, and Shp2 mediates biological responses. *J Cell Biol*. 2000. doi:10.1083/jcb.149.7.1419

57. Paliouras GN, Naujokas MA, Park M. Pak4, a Novel Gab1 Binding Partner, Modulates Cell Migration and Invasion by the Met Receptor. *Mol Cell Biol*. 2009. doi:10.1128/mcb.01286-08

58. Maroun CR, Naujokas MA, Holgado-Madruga M, Wong AJ, Park M. The Tyrosine Phosphatase SHP-2 Is Required for Sustained Activation of Extracellular Signal-Regulated Kinase and Epithelial Morphogenesis Downstream from the Met Receptor Tyrosine Kinase. *Mol Cell Biol*. 2000. doi:10.1128/mcb.20.22.8513-8525.2000

59. Gherardi E, Birchmeier W, Birchmeier C, Woude G Vande. Targeting MET in cancer: Rationale and progress. *Nat Rev Cancer*. 2012. doi:10.1038/nrc3205

60. Lokker NA, Mark MR, Luis EA, et al. Structure-function analysis of hepatocyte growth factor: identification of variants that lack mitogenic activity yet retain high affinity receptor binding. *EMBO J*. 1992. doi:10.1002/j.1460-2075.1992.tb05315.x

61. Lee‡SL DR and LC. Activation of Hepatocyte Growth Factor and Urokinase/Plasminogen Activator by Matriptase, an Epithelial Membrane Serine Protease. *J Biol Chem*. 2000;(708).

62. Owen KA, Qiu D, Alves J, et al. Pericellular activation of hepatocyte growth factor by the transmembrane serine proteases matriptase and hepsin, but not by the membrane-associated protease uPA. *Biochem J*. 2010. doi:10.1042/BJ20091448

63. Kawaguchi T, Qin L, Shimomura T, et al. Purification and cloning of hepatocyte growth factor activator inhibitor type 2, a Kunitz-type serine protease inhibitor. *J Biol Chem*. 1997. doi:10.1074/jbc.272.44.27558

64. Shimomura T, Denda K, Kitamura A, et al. Hepatocyte growth factor activator inhibitor, a novel Kunitz-type serine protease inhibitor. *J Biol Chem*. 1997. doi:10.1074/jbc.272.10.6370

65. Morris MR, Gentle D, Abdulrahman M, et al. Tumor suppressor activity and epigenetic inactivation of hepatocyte growth factor activator inhibitor type 2/SPINT2 in papillary and clear cell renal cell carcinoma. *Cancer Res*. 2005. doi:10.1158/0008-5472.CAN-04-3371

66. Merchant M, Ma X, Maun HR, et al. Monovalent antibody design and mechanism of action of onartuzumab, a MET antagonist with anti-tumor activity as a therapeutic agent. *Proc Natl Acad Sci U S A*. 2013. doi:10.1073/pnas.1302725110

67. Lai AZ, Abella J V., Park M. Crosstalk in Met receptor oncogenesis. *Trends Cell Biol*. 2009. doi:10.1016/j.tcb.2009.07.002

68. Weidner KM, Di Cesare S, Sachs M, Brinkmann V, Behrens J, Birchmeier W. Interaction between Gab1 and the c-Met receptor tyrosine kinase is responsible for epithelial morphogenesis. *Nature*. 1996. doi:10.1038/384173a0

69. Birchmeier C, Birchmeier W, Gherardi E, Vande Woude GF. Met, metastasis, motility and more. *Nat Rev Mol Cell Biol*. 2003. doi:10.1038/nrm1261

70. Weidner KM, Di Cesare S, Sachs M, Brinkmann V, Behrens J, Birchmeier W. Interaction between Gab1 and the c-Met receptor tyrosine kinase is responsible for epithelial morphogenesis. *Nature*. 1996. doi:10.1038/384173a0

71. Sipeki S, Bander E, Buday L, et al. Phosphatidylinositol 3-kinase Contributes to Erk1/Erk2 MAP Kinase Activation Associated with Hepatocyte Growth Factor-induced Cell Scattering. *Cell Signal*. 1999;11(12):885-890. doi:https://doi.org/10.1016/S0898-6568(99)00060-1

72. Zhang YW, Wang LM, Jove R, Vande Woude GF. Requirement of Stat3 signaling for HGF/SF-Met mediated tumorigenesis. *Oncogene*. 2002. doi:10.1038/sj.onc.1205004

73. Van Der Steen N, Pauwels P, Gil-Bazo I, et al. cMET in NSCLC: Can We Cut off the Head of the Hydra? From the Pathway to the Resistance. Cho W, ed. *Cancers (Basel)*. 2015;7(2):556-573. doi:10.3390/cancers7020556

74. Ishibe S, Karihaloo A, Ma H, et al. Met and the epidermal growth factor receptor act cooperatively to regulate final nephron number and maintain collecting duct morphology. *Development*. 2009. doi:10.1242/dev.024463

75. Finocchiaro G, Toschi L, Gianoncelli L, Baretti M, Santoro A. Prognostic and predictive value of MET deregulation in non-small cell lung cancer. *Ann Transl Med*. 2015. doi:10.3978/j.issn.2305-5839.2015.03.43

76. Organ SL, Tsao MS. An overview of the c-MET signaling pathway. *Ther Adv Med Oncol*. 2011. doi:10.1177/1758834011422556

77. Eming SA, Martin P., Tomic-Canic M, et al. Wound repair and regeneration: mechanisms, signaling, and translation. *Sci Transl Med*. 2014. doi:10.1126/scitranslmed.3009337

78. Mosesson Y, Mills GB, Yarden Y. Derailed endocytosis: an emerging feature of cancer. *Nat Rev Cancer*. 2008;8:835. http://dx.doi.org/10.1038/nrc2521.

79. Peschard P, Fournier TM, Lamorte L, et al. Mutation of the c-Cbl TKB domain binding site on the Met receptor tyrosine kinase converts it into a transforming protein. *Mol Cell*. 2001. doi:10.1016/S1097-2765(01)00378-1

80. Van Der Steen N, Giovannetti E, Pauwels P, et al. CMET Exon 14 Skipping: From the structure to the clinic. *J Thorac Oncol*. 2016. doi:10.1016/j.jtho.2016.05.005

81. Hammond DE, Urbé S, Vande Woude GF, Clague MJ. Down-regulation of MET, the receptor for hepatocyte growth factor. *Oncogene*. 2001. doi:10.1038/sj.onc.1204475

82. Petrelli A, Gilestro GF, Lanzardo S, Comoglio PM, Migone N, Giordano S. The endophilin–CIN85–Cbl complex mediates ligand-dependent downregulation of c-Met. *Nature*. 2002;416:187. http://dx.doi.org/10.1038/416187a.

83. Krishnaswamy S, Kanteti R, Duke-Cohan JS, et al. Ethnic differences and functional analysis of MET mutations in lung cancer. *Clin Cancer Res*. 2009;15(18):5714-5723. doi:10.1158/1078-0432.CCR-09-0070

84. Ma PC, Jagadeeswaran R, Jagadeesh S, et al. Functional expression and mutations of c-Met and its therapeutic inhibition with SU11274 and small interfering RNA in

non-small cell lung cancer. *Cancer Res*. 2005. doi:10.1158/0008-5472.CAN-04-2650

85. Okuda K, Sasaki H, Yukiue H, Yano M, Fujii Y. Met gene copy number predicts the prognosis for completely resected non-small cell lung cancer. *Cancer Sci*. 2008. doi:10.1111/j.1349-7006.2008.00916.x

86. Onozato R, Kosaka T, Kuwano H, Sekido Y, Yatabe Y, Mitsudomi T. Activation of MET by gene amplification or by splice mutations deleting the juxtamembrane domain in primary resected lung cancers. *J Thorac Oncol*. 2009. doi:10.1097/JTO.0b013e3181913e0e

87. Seo JS, Ju YS, Lee WC, et al. The transcriptional landscape and mutational profile of lung adenocarcinoma. *Genome Res*. 2012. doi:10.1101/gr.145144.112

88. Collisson EA, Campbell JD, Brooks AN, et al. Comprehensive molecular profiling of lung adenocarcinoma: The cancer genome atlas research network. *Nature*. 2014. doi:10.1038/nature13385

89. Dhanasekaran SM, Balbin OA, Chen G, et al. Transcriptome meta-analysis of lung cancer reveals recurrent aberrations in NRG1 and Hippo pathway genes. *Nat Commun*. 2014. doi:10.1038/ncomms6893

90. Asaoka Y, Tada M, Ikenoue T, et al. Gastric cancer cell line Hs746T harbors a splice site mutation of c-Met causing juxtamembrane domain deletion. *Biochem Biophys Res Commun*. 2010. doi:10.1016/j.bbrc.2010.03.120

91. Yan B, Lim M, Zhou L, et al. Identification of MET genomic amplification, protein expression and alternative splice isoforms in neuroblastomas. *J Clin Pathol*. 2013. doi:10.1136/jclinpath-2012-201375

92. Park S, Choi Y La, Sung CO, et al. High MET copy number and MET overexpression: Poor outcome in non-small cell lung cancer patients. *Histol Histopathol*. 2012. doi:10.14670/HH-27.197

93. Solomon BJ, Besse B, Bauer TM, et al. Lorlatinib in patients with ALK-positive non-small-cell lung cancer: results from a global phase 2 study. *Lancet Oncol*. 2018. doi:10.1016/S1470-2045(18)30649-1

94. Camidge DR, Kim HR, Ahn MJ, et al. Brigatinib versus crizotinib in ALK-positive non-small-cell lung cancer. *N Engl J Med*. 2018. doi:10.1056/NEJMoa1810171

95. Ma PC, Kijima T, Maulik G, et al. c-MET mutational analysis in small cell lung cancer: Novel juxtamembrane domain mutations regulating cytoskeletal functions. *Cancer Res*. 2003.

96. Kong-Beltran M, Seshagiri S, Zha J, et al. Somatic Mutations Lead to an Oncogenic Deletion of Met in Lung Cancer. *Cancer Res*. 2006;66(1):283 LP - 289. http://cancerres.aacrjournals.org/content/66/1/283.abstract.

97. Tong JH, Yeung SF, Chan AWH, et al. MET amplification and exon 14 splice site mutation define unique molecular subgroups of non-small cell lung carcinoma with poor prognosis. *Clin Cancer Res*. 2016;22(12):3048-3056. doi:10.1158/1078-0432.CCR-15-2061

98. Awad MM, Oxnard GR, Jackman DM, et al. MET exon 14 mutations in Non-small-cell lung cancer are associated with advanced age and stage-dependent MET genomic amplification and c-Met overexpression. *J Clin Oncol*. 2016. doi:10.1200/JCO.2015.63.4600

99. Frampton GM, Ali SM, Rosenzweig M, et al. Activation of MET via diverse exon 14 splicing alterations occurs in multiple tumor types and confers clinical sensitivity

to MET inhibitors. *Cancer Discov*. 2015. doi:10.1158/2159-8290.CD-15-0285

100. Drilon A, Cappuzzo F, Ou SHI, Camidge DR. Targeting MET in Lung Cancer: Will Expectations Finally Be MET? *J Thorac Oncol*. 2017. doi:10.1016/j.jtho.2016.10.014

101. Baldacci S, Figeac M, Antoine M, et al. High MET Overexpression Does Not Predict the presence of MET exon 14 Splice Mutations in NSCLC: Results From the IFCT PREDICT.amm study. *J Thorac Oncol*. 2020;15(1):120-124. doi:10.1016/j.jtho.2019.09.196

102. Guo R, Berry LD, Aisner DL, et al. MET IHC Is a Poor Screen for MET Amplification or MET Exon 14 Mutations in Lung Adenocarcinomas: Data from a Tri-Institutional Cohort of the Lung Cancer Mutation Consortium. *J Thorac Oncol*. 2019;14(9):1666-1671. doi:10.1016/j.jtho.2019.06.009

103. Collisson EA, Campbell JD, Brooks AN, et al. Comprehensive molecular profiling of lung adenocarcinoma: The cancer genome atlas research network. *Nature*. 2014. doi:10.1038/nature13385

104. Awad MM, Oxnard GR, Jackman DM, et al. MET exon 14 mutations in Non-small-cell lung cancer are associated with advanced age and stage-dependent MET genomic amplification and c-Met overexpression. *J Clin Oncol*. 2016. doi:10.1200/JCO.2015.63.4600

105. Drilon A, Wang L, Arcila ME, et al. Broad, hybrid capture-based next-generation sequencing identifies actionable genomic alterations in lung adenocarcinomas otherwise negative for such alterations by other genomic testing approaches. *Clin Cancer Res*. 2015. doi:10.1158/1078-0432.CCR-14-2683

106. Liu X, Jia Y, Stoopler MB, et al. Next-generation sequencing of pulmonary

sarcomatoid carcinoma reveals high frequency of actionable MET gene mutations. *J Clin Oncol*. 2016. doi:10.1200/JCO.2015.62.0674

107. Puri N, Khramtsov A, Ahmed S, et al. A selective small molecule inhibitor of c-Met, PHA665752, inhibits tumorigenicity and angiogenesis in mouse lung cancer xenografts. *Cancer Res*. 2007;67(8):3529-3534. doi:10.1158/0008-5472.CAN-06-4416

108. Drilon AE, Camidge DR, Ou S-HI, et al. Efficacy and safety of crizotinib in patients (pts) with advanced MET exon 14-altered non-small cell lung cancer (NSCLC). *J Clin Oncol*. 2016;34(15_suppl):108-108. doi:10.1200/JCO.2016.34.15_SUPPL.108

109. David R. Spigel , Martin J. Edelman , Kenneth O'Byrne , Luis Paz-Ares , David S. Shames , Wei YuVirginia E. Paton TM. Onartuzumab plus erlotinib versus erlotinib in previously treated stage IIIb or IV NSCLC: Results from the pivotal phase III randomized, multicenter, placebo-controlled METLung (OAM4971g) global trial. *Clin Adv Hematol Oncol*. 2014;12(10):15-16.

110. Spigel DR, Ervin TJ, Ramlau RA, et al. Randomized phase II trial of Onartuzumab in combination with erlotinib in patients with advanced non-small-cell lung cancer. *J Clin Oncol*. 2013. doi:10.1200/JCO.2012.47.4189

111. Spigel DR, Edelman MJ, O'Byrne K, et al. Results From the Phase III Randomized Trial of Onartuzumab Plus Erlotinib Versus Erlotinib in Previously Treated Stage IIIB or IV Non-Small-Cell Lung Cancer: METLung. *J Clin Oncol*. 2017;35(4):412-420. doi:10.1200/JCO.2016.69.2160

112. Scagliotti G, Von Pawel J, Novello S, et al. Phase III multinational, randomized, double-blind, placebo-controlled study of tivantinib (ARQ 197) plus erlotinib versus erlotinib alone in previously treated patients with locally advanced or metastatic nonsquamous non-small-cell lung cancer. *J Clin Oncol*.

2015;33(24):2667-2674. doi:10.1200/JCO.2014.60.7317

113. Eathiraj S, Palma R, Volckova E, et al. Discovery of a novel mode of protein kinase inhibition characterized by the mechanism of inhibition of human mesenchymal-epithelial transition factor (c-Met) protein autophosphorylation by ARQ 197. *J Biol Chem*. 2011. doi:10.1074/jbc.M110.213801

114. Munshi N, Jeay S, Li Y, et al. ARQ 197, a novel and selective inhibitor of the human c-Met receptor tyrosine kinase with antitumor activity. *Mol Cancer Ther*. 2010. doi:10.1158/1535-7163.MCT-09-1173

115. Watermann I, Schmitt B, Stellmacher F, et al. Improved diagnostics targeting c-MET in non-small cell lung cancer: Expression, amplification and activation? *Diagn Pathol*. 2015. doi:10.1186/s13000-015-0362-5

116. D. Ross Camidge; Sai-Hong Ignatius Ou; Geoffrey Shapiro; Gregory Alan Otterson; Liza Cosca Villaruz; Miguel Angel Villalona-Calero; A. John Iafrate; Marileila Varella-Garcia; Sanja Dacic; Stephanie Cardarella; Weiqiang Zhao; Lesley Tye; Patricia Stephenso ;Mark A. Socinski. Efficacy and safety of crizotinib in patients with advanced c-MET-amplified non-small cell lung cancer (NSCLC). *J Clin Oncol*. 204AD:suppl. abstr 8001.

117. Noonan SA, Berry L, Lu X, et al. Identifying the appropriate FISH criteria for defining MET copy number-driven lung adenocarcinoma through oncogene overlap analysis. *J Thorac Oncol*. 2016. doi:10.1016/j.jtho.2016.04.033

118. Schildhaus HU, Schultheis AM, Rüuschoff J, et al. Met amplification status in therapy-naïve adeno- And squamous cell carcinomas of the lung. *Clin Cancer Res*. 2015. doi:10.1158/1078-0432.CCR-14-0450

119. Heist RS, Shim HS, Gingipally S, et al. MET Exon 14 Skipping in Non-Small Cell Lung

Cancer . *Oncologist*. 2016. doi:10.1634/theoncologist.2015-0510

120. Jenkins RW, Oxnard GR, Elkin S, Sullivan EK, Carter JL, Barbie DA. Response to Crizotinib in a Patient With Lung Adenocarcinoma Harboring a MET Splice Site Mutation. *Clin Lung Cancer*. 2015. doi:10.1016/j.cllc.2015.01.009

121. Lee C, Usenko D, Frampton GM, McMahon C, Ali SM, Weiss J. MET 14 Deletion in Sarcomatoid Non-Small-Cell Lung Cancer Detected by Next-Generation Sequencing and Successfully Treated with a MET Inhibitor. *J Thorac Oncol*. 2015. doi:10.1097/JTO.0000000000000645

122. Mendenhall MA, Goldman JW. MET-mutated NSCLC with major response to crizotinib. *J Thorac Oncol*. 2015. doi:10.1097/JTO.0000000000000491

123. Awad MM, Leonardi GC, Kravets S, et al. Impact of MET inhibitors on survival among patients with non-small cell lung cancer harboring MET exon 14 mutations: a retrospective analysis. *Lung Cancer*. 2019. doi:10.1016/j.lungcan.2019.05.011

124. Landi L, Chiari R, Tiseo M, et al. Crizotinib in MET deregulated or ROS1 rearranged pretreated non-small-cell lung cancer (METROS): a phase II, prospective, multicentre, two-arms trial . *Clin Cancer Res*. 2019. doi:10.1158/1078-0432.ccr-19-0994

125. Waqar SN, Morgensztern D, Sehn J. MET mutation associated with responsiveness to crizotinib. *J Thorac Oncol*. 2015. doi:10.1097/JTO.0000000000000478

126. Drilon A, Clark JW, Weiss J, et al. Antitumor activity of crizotinib in lung cancers harboring a MET exon 14 alteration. *Nat Med*. 2020;26(1):47-51. doi:10.1038/s41591-019-0716-8

127. Cui JJ, Tran-Dubé M, Shen H, et al. Structure based drug design of crizotinib (PF-02341066), a potent and selective dual inhibitor of mesenchymal-epithelial transition factor (c-MET) kinase and anaplastic lymphoma kinase (ALK). *J Med Chem*. 2011. doi:10.1021/jm2007613

128. Scagliotti GV, Parikh P, Von Pawel J, et al. Phase III study comparing cisplatin plus gemcitabine with cisplatin plus pemetrexed in chemotherapy-naive patients with advanced-stage non-small-cell lung cancer. *J Clin Oncol*. 2008. doi:10.1200/JCO.2007.15.0375

129. Ou SI, Camidge DR, Engelman J, et al. Non-small cell lung cancer, locally advanced. *Ann Oncol*. 2012. doi:10.1093/annonc/mds408

130. Garon EB, Ciuleanu TE, Arrieta O, et al. Ramucirumab plus docetaxel versus placebo plus docetaxel for second-line treatment of stage IV non-small-cell lung cancer after disease progression on platinum-based therapy (REVEL): A multicentre, double-blind, randomised phase 3 trial. *Lancet*. 2014. doi:10.1016/S0140-6736(14)60845-X

131. Shepherd FA, Dancey J, Ramlau R, et al. Prospective randomized trial of docetaxel versus best supportive care in patients with non-small-cell lung cancer previously treated with platinum- based chemotherapy. *J Clin Oncol*. 2000. doi:10.1200/JCO.2000.18.10.2095

132. Socinski MA, Jotte RM, Cappuzzo F, et al. Atezolizumab for first-line treatment of metastatic nonsquamous NSCLC. *N Engl J Med*. 2018. doi:10.1056/NEJMoa1716948

133. Soria JC, Ohe Y, Vansteenkiste J, et al. Osimertinib in untreated EGFR-Mutated advanced non-small-cell lung cancer. *N Engl J Med*. 2018. doi:10.1056/NEJMoa1713137

134. Camidge DR, Otterson GA, Clark JW, et al. Crizotinib in patients (pts) with MET-amplified non-small cell lung cancer (NSCLC): Updated safety and efficacy findings from a phase 1 trial. *J Clin Oncol*. 2018;36(15_suppl):9062. doi:10.1200/JCO.2018.36.15_suppl.9062

135. Schuler MH, Berardi R, Lim W-T, et al. Phase (Ph) I study of the safety and efficacy of the cMET inhibitor capmatinib (INC280) in patients (pts) with advanced cMET+ non-small cell lung cancer (NSCLC). *J Clin Oncol*. 2016. doi:10.1200/jco.2016.34.15_suppl.9067

136. Falchook GS, Kurzrock R, Amin HM, et al. First-in-Man Phase I Trial of the Selective MET Inhibitor Tepotinib in Patients with Advanced Solid Tumors. *Clin Cancer Res*. 2019. doi:10.1158/1078-0432.CCR-19-2860

137. Heist RS, Wolf J, Seto T, et al. OA01.07 Capmatinib (INC280) in METΔEX14-Mutated Advanced NSCLC: Efficacy Data from the Phase 2 Geometry MONO-1 Study. *J Thorac Oncol*. 2019. doi:10.1016/j.jtho.2019.09.021

138. Paik PK, Veillon R, Cortot AB, et al. Phase II study of tepotinib in NSCLC patients with METex14 mutations. *J Clin Oncol*. 2019. doi:10.1200/JCO.2019.37.15_suppl.9005

139. Owusu BY, Thomas S, Venukadasula P, et al. Targeting the tumor-promoting microenvironment in MET-amplified NSCLC cells with a novel inhibitor of pro-HGF activation. *Oncotarget*. 2017. doi:10.18632/oncotarget.18260

140. Tsao MS, Yang Y, Marcus a, Liu N, Mou L. Hepatocyte growth factor is predominantly expressed by the carcinoma cells in non-small-cell lung cancer. *Hum Pathol*. 2001;32(1):57-65. doi:10.1053/hupa.2001.21133

141. Kanaji N, Yokohira M, Nakano-Narusawa Y, et al. Hepatocyte growth factor

produced in lung fibroblasts enhances non-small cell lung cancer cell survival and tumor progression. *Respir Res*. 2017. doi:10.1186/s12931-017-0604-z

142. Guo R, Offin M, Brannon AR, et al. MET inhibitor resistance in patients with MET exon 14-altered lung cancers. *J Clin Oncol*. 2019;37(15_suppl):9006. doi:10.1200/JCO.2019.37.15_suppl.9006

143. Awad MM, Bahcall M, Sholl LM, et al. Mechanisms of acquired resistance to MET tyrosine kinase inhibitors (TKIs) in MET exon 14 (METex14) mutant non-small cell lung cancer (NSCLC). *J Clin Oncol*. 2018;36(15_suppl):9069. doi:10.1200/JCO.2018.36.15_suppl.9069

144. Riedel R, Heydt C, Scheel AH, et al. Acquired resistance to MET inhibition in MET driven NSCLC. *J Clin Oncol*. 2019;37(15_suppl):9030. doi:10.1200/JCO.2019.37.15_suppl.9030

145. Bahcall M, Sim T, Paweletz CP, et al. Acquired METD1228V mutation and resistance to MET inhibition in lung cancer. *Cancer Discov*. 2016. doi:10.1158/2159-8290.CD-16-0686

146. Heist RS, Sequist L V., Borger D, et al. Acquired resistance to crizotinib in NSCLC with MET exon 14 skipping. *J Thorac Oncol*. 2016. doi:10.1016/j.jtho.2016.06.013

147. Ou SHI, Young L, Schrock AB, et al. Emergence of Preexisting MET Y1230C Mutation as a Resistance Mechanism to Crizotinib in NSCLC with MET Exon 14 Skipping. *J Thorac Oncol*. 2017. doi:10.1016/j.jtho.2016.09.119

148. Suzawa K, Offin M, Lu D, et al. Activation of KRAS Mediates Resistance to Targeted Therapy in MET Exon 14–mutant Non–small Cell Lung Cancer. *Clin Cancer Res*. 2019. doi:10.1158/1078-0432.CCR-18-1640

149. Huang L, Fu L. Mechanisms of resistance to EGFR tyrosine kinase inhibitors. *Acta Pharm Sin B*. 2015. doi:10.1016/j.apsb.2015.07.001

150. Vivanco I, Ian Robins H, Rohle D, et al. Differential sensitivity of glioma- versus lung cancer-specific EGFR mutations to EGFR kinase inhibitors. *Cancer Discov*. 2012. doi:10.1158/2159-8290.CD-11-0284

151. Christensen JG, Zou HY, Arango ME, et al. Cytoreductive antitumor activity of PF-2341066, a novel inhibitor of anaplastic lymphoma kinase and c-Met, in experimental models of anaplastic large-cell lymphoma. *Mol Cancer Ther*. 2007. doi:10.1158/1535-7163.MCT-07-0365

152. Yakes FM, Chen J, Tan J, et al. Cabozantinib (XL184), a novel MET and VEGFR2 inhibitor, simultaneously suppresses metastasis, angiogenesis, and tumor growth. *Mol Cancer Ther*. 2011. doi:10.1158/1535-7163.MCT-11-0264

153. Lolkema MP, Bohets HH, Arkenau HT, et al. The c-Met tyrosine kinase inhibitor JNJ-38877605 causes renal toxicity through species-specific insoluble metabolite formation. *Clin Cancer Res*. 2015. doi:10.1158/1078-0432.CCR-14-3258

154. Buchanan SG, Hendle J, Lee PS, et al. SGX523 is an exquisitely selective, ATP-competitive inhibitor of the MET receptor tyrosine kinase with antitumor activity in vivo. *Mol Cancer Ther*. 2009. doi:10.1158/1535-7163.MCT-09-0477

155. Tanizaki J, Okamoto I, Okamoto K, et al. MET tyrosine kinase inhibitor crizotinib (PF-02341066) shows differential antitumor effects in non-small cell lung cancer according to MET alterations. *J Thorac Oncol*. 2011. doi:10.1097/JTO.0b013e31822591e9

156. Tretiakova M, Salama AKS, Karrison T, et al. MET and phosphorylated MET as potential biomarkers in lung cancer. *J Environ Pathol Toxicol Oncol*. 2011.

doi:10.1615/JEnvironPatholToxicolOncol.v30.i4.70

157. Koeppen H, Rost S, Yauch RL. Developing biomarkers to predict benefit from HGF/MET pathway inhibitors. *J Pathol*. 2014. doi:10.1002/path.4268

158. Middleton G, Crack LR, Popat S, et al. The National Lung Matrix Trial: Translating the biology of stratification in advanced non-small-cell lung cancer. *Ann Oncol*. 2015. doi:10.1093/annonc/mdv394

159. Conley BA, Gray R, Chen A, et al. Abstract CT101: NCI-molecular analysis for therapy choice (NCI-MATCH) clinical trial: interim analysis. In: ; 2016. doi:10.1158/1538-7445.am2016-ct101

160. Reungwetwattana T, Liang Y, Zhu V, Ou SHI. The race to target MET exon 14 skipping alterations in non-small cell lung cancer: The Why, the How, the Who, the Unknown, and the Inevitable. *Lung Cancer*. 2017. doi:10.1016/j.lungcan.2016.11.011

161. Tentler JJ, Tan AC, Weekes CD, et al. Patient-derived tumour xenografts as models for oncology drug development. *Nat Rev Clin Oncol*. 2012. doi:10.1038/nrclinonc.2012.61

162. Kalluri R. The biology and function of fibroblasts in cancer. *Nat Rev Cancer*. 2016. doi:10.1038/nrc.2016.73

163. Majety M, Pradel LP, Gies M, Ries CH. Fibroblasts influence survival and therapeutic response in a 3D co-culture model. *PLoS One*. 2015. doi:10.1371/journal.pone.0127948

164. Treat J, Scagliotti G V, Peng G, Monberg MJ, Obasaju CK, Socinski MA. Comparison of pemetrexed plus cisplatin with other first-line doublets in advanced non-small

cell lung cancer (NSCLC): A combined analysis of three phase 3 trials. *Lung Cancer*. 2012;76(2):222-227. doi:10.1016/j.lungcan.2011.10.021

165. Mansell A, Jenkins BJ. Dangerous liaisons between interleukin-6 cytokine and toll-like receptor families: A potent combination in inflammation and cancer. *Cytokine Growth Factor Rev*. 2013. doi:10.1016/j.cytogfr.2013.03.007

166. Schuett H, Luchtefeld M, Grothusen C, Grote K, Schieffer B. How much is too much? Interleukin-6 and its signalling in atherosclerosis. In: *Thrombosis and Haemostasis*. ; 2009. doi:10.1160/TH09-05-0297

167. Erta M, Quintana A, Hidalgo J. Interleukin-6, a major cytokine in the central nervous system. *Int J Biol Sci*. 2012. doi:10.7150/ijbs.4679

168. Garbers C, Hermanns HM, Schaper F, et al. Plasticity and cross-talk of Interleukin 6-type cytokines. *Cytokine Growth Factor Rev*. 2012. doi:10.1016/j.cytogfr.2012.04.001

169. Mihara M, Hashizume M, Yoshida H, Suzuki M, Shiina M. IL-6/IL-6 receptor system and its role in physiological and pathological conditions. *Clin Sci*. 2012. doi:10.1042/CS20110340

170. Liu Y, Michalopoulos GK, Zarnegar R. Structural and functional characterization of the mouse hepatocyte growth factor gene promoter. *J Biol Chem*. 1994.

171. Tsao MS, Yang Y, Marcus A, Liu N, Mou L. Hepatocyte growth factor is predominantly expressed by the carcinoma cells in non-small-cell lung cancer. *Hum Pathol*. 2001. doi:10.1053/hupa.2001.21133

172. Allred DC, Harvey JM, Berardo M, Clark GM. Prognostic and predictive factors in breast cancer by immunohistochemical analysis. *Mod Pathol*. 1998.

173. Allred DC. Issues and updates: Evaluating estrogen receptor-α, progesterone receptor, and HER2 in breast cancer. *Mod Pathol*. 2010. doi:10.1038/modpathol.2010.55

174. Hammond MEH, Hayes DF, Dowsett M, et al. American society of clinical oncology/college of american pathologists guideline recommendations for immunohistochemical testing of estrogen and progesterone receptors in breast cancer. *J Clin Oncol*. 2010. doi:10.1200/JCO.2009.25.6529

175. Campbell EJ, Tesson M, Doogan F, Mohammed ZMA, Mallon E, Edwards J. The combined endocrine receptor in breast cancer, a novel approach to traditional hormone receptor interpretation and a better discriminator of outcome than ER and PR alone. *Br J Cancer*. 2016. doi:10.1038/bjc.2016.206

176. Jin W, Shan B, Liu H, et al. Acquired Mechanism of Crizotinib Resistance in NSCLC with MET Exon 14 Skipping. *J Thorac Oncol*. 2019. doi:10.1016/j.jtho.2019.04.021

177. Harvey L, Arnold B, S Lawrence Z, Pau l M, David B, James D. *Molecular Cell Biology. 4th Edition*.; 2000. doi:10.1016/j.jasms.2009.08.001

178. Huse M, Kuriyan J. The conformational plasticity of protein kinases. *Cell*. 2002. doi:10.1016/S0092-8674(02)00741-9

179. Masterson LR, Cheng C, Yu T, et al. Dynamics connect substrate recognition to catalysis in protein kinase A. *Nat Chem Biol*. 2010. doi:10.1038/nchembio.452

180. Regales L, Gong Y, Shen R, et al. Dual targeting of EGFR can overcome a major drug resistance mutation in mouse models of EGFR mutant lung cancer. *J Clin Invest*. 2009;119(10):3000-3010. doi:10.1172/JCI38746

181. Janjigian YY, Smit EF, Groen HJM, et al. Dual inhibition of EGFR with afatinib and

cetuximab in kinase inhibitor-resistant EGFR-mutant lung cancer with and without T790M mutations. *Cancer Discov*. 2014;4(9):1036-1045. doi:10.1158/2159-8290.CD-14-0326

182. Egeblad M, Nakasone ES, Werb Z. Tumors as organs: Complex tissues that interface with the entire organism. *Dev Cell*. 2010. doi:10.1016/j.devcel.2010.05.012

183. Li H, Fan X, Houghton JM. Tumor microenvironment: The role of the tumor stroma in cancer. *J Cell Biochem*. 2007. doi:10.1002/jcb.21159

184. Sun Y. Tumor microenvironment and cancer therapy resistance. *Cancer Lett*. 2016. doi:10.1016/j.canlet.2015.07.044

185. Olivero M, Rizzo M, Madeddu R, et al. Overexpression and activation of hepatocyte growth factor/scatter factor in human non-small-cell lung carcinomas. *Br J Cancer*. 1996;74(12):1862-1868. doi:10.1038/bjc.1996.646

186. Klemm F, Joyce JA. Microenvironmental regulation of therapeutic response in cancer. *Trends Cell Biol*. 2015. doi:10.1016/j.tcb.2014.11.006

187. Yamada T, Matsumoto K, Wang W, et al. Hepatocyte growth factor reduces susceptibility to an irreversible epidermal growth factor receptor inhibitor in EGFR-T790M mutant lung cancer. *Clin Cancer Res*. 2010. doi:10.1158/1078-0432.CCR-09-1204

188. Yano S, Wang W, Li Q, et al. Hepatocyte growth factor induces gefitinib resistance of lung adenocarcinoma with epidermal growth factor receptor-activating mutations. *Cancer Res*. 2008. doi:10.1158/0008-5472.CAN-08-1643

189. Turke AB, Zejnullahu K, Wu YL, et al. Preexistence and Clonal Selection of MET

Amplification in EGFR Mutant NSCLC. *Cancer Cell*. 2010. doi:10.1016/j.ccr.2009.11.022

190. Yano S, Yamada T, Takeuchi S, et al. Hepatocyte growth factor expression in EGFR -mutant lung cancer with intrinsic and acquired resistance to tyrosine kinase inhibitors in a Japanese cohort. . *J Clin Oncol*. 2011. doi:10.1200/jco.2011.29.15_suppl.7531

191. Han JY, Kim JY, Lee SH, Yoo NJ, Choi BG. Association between plasma hepatocyte growth factor and gefitinib resistance in patients with advanced non-small cell lung cancer. *Lung Cancer*. 2011. doi:10.1016/j.lungcan.2011.02.021

192. Ding X, Ji J, Jiang J, et al. HGF-mediated crosstalk between cancer-associated fibroblasts and MET-unamplified gastric cancer cells activates coordinated tumorigenesis and metastasis. *Cell Death Dis*. 2018. doi:10.1038/s41419-018-0922-1

193. D H, RA W. The Hallmarks of Cancer. *Cell*. 2000.

194. Sawyers CL. Chronic myeloid leukemia. *N Engl J Med*. 1999. doi:10.1056/NEJM199904293401706

195. Sawyers CL, Hochhaus A, Feldman E, et al. Imatinib induces hematologic and cytogenetic responses in patients with chronic myelogenous leukemia in myeloid blast crisis: Results of a phase II study. *Blood*. 2002. doi:10.1182/blood.V99.10.3530

196. Casado P, Rodriguez-Prados J-C, Cosulich SC, et al. Kinase-substrate enrichment analysis provides insights into the heterogeneity of signaling pathway activation in leukemia cells. *Sci Signal*. 2013;6(268):rs6-rs6. doi:10.1126/scisignal.2003573

197. Wirbel J, Cutillas P, Saez-Rodriguez J. Phosphoproteomics-based profiling of kinase activities in cancer cells. In: *Methods in Molecular Biology*. ; 2018. doi:10.1007/978-1-4939-7493-1_6

198. Wilson TR, Fridlyand J, Yan Y, et al. Widespread potential for growth-factor-driven resistance to anticancer kinase inhibitors. *Nature*. 2012. doi:10.1038/nature11249

199. Bertotti A, Burbridge MF, Gastaldi S, et al. Only a subset of met-activated pathways are required to sustain oncogene addiction. *Sci Signal*. 2009. doi:10.1126/scisignal.2000643

200. Engelman JA, Zejnullahu K, Mitsudomi T, et al. MET amplification leads to gefitinib resistance in lung cancer by activating ERBB3 signaling. *Science (80-)*. 2007. doi:10.1126/science.1141478

201. Manning BD, Toker A. AKT/PKB Signaling: Navigating the Network. *Cell*. 2017;169(3):381-405. doi:10.1016/j.cell.2017.04.001

202. Bayer EA, Wilchek M. Protein biotinylation. *Methods Enzymol*. 1990. doi:10.1016/0076-6879(90)84268-L

203. Cull MG, Schatz PJ. Biotinylation of proteins in vivo and in vitro using small peptide tags. *Methods Enzymol*. 2000. doi:10.1016/s0076-6879(00)26068-0

204. Cronan JE, Reed KE. Biotinylation of proteins in vivo: A useful posttranslational modification for protein analysis. *Methods Enzymol*. 2000. doi:10.1016/s0076-6879(00)26069-2

205. Li Y, Sousa R. Novel system for in vivo biotinylation and its application to crab antimicrobial protein scygonadin. *Biotechnol Lett*. 2012. doi:10.1007/s10529-012-0942-3

206. Tsurutani J, Steinberg SM, Ballas M, et al. Prognostic significance of clinical factors and Akt activation in patients with bronchioloalveolar carcinoma. *Lung Cancer*. 2007. doi:10.1016/j.lungcan.2006.09.026

207. Tsurutani J, Fukuoka J, Tsurutani H, et al. Evaluation of two phosphorylation sites improves the prognostic significance of Akt activation in non-small-cell lung cancer tumors. *J Clin Oncol*. 2006. doi:10.1200/JCO.2005.02.4133

208. Millis SZ, Ikeda S, Reddy S, Gatalica Z, Kurzrock R. Landscape of phosphatidylinositol-3-kinase pathway alterations across 19 784 diverse solid tumors. *JAMA Oncol*. 2016. doi:10.1001/jamaoncol.2016.0891

209. Brown JS, Banerji U. Maximising the potential of AKT inhibitors as anti-cancer treatments. *Pharmacol Ther*. 2017. doi:10.1016/j.pharmthera.2016.12.001

210. Iacovides DC, Johnson AB, Wang N, Boddapati S, Korkola J, Gray JW. Identification and quantification of AKT isoforms and phosphoforms in breast cancer using a novel nanofluidic immunoassay. *Mol Cell Proteomics*. 2013. doi:10.1074/mcp.M112.023119

211. Coffer PJ, Jin J, Woodgett JR. Protein kinase B (c-Akt): A multifunctional mediator of phosphatidylinositol 3-kinase activation. *Biochem J*. 1998. doi:10.1042/bj3350001

212. Alessi DR, Cohen P. Mechanism of activation and function of protein kinase B. *Curr Opin Genet Dev*. 1998. doi:10.1016/S0959-437X(98)80062-2

213. Cho H, Thorvaldsen JL, Chu Q, Feng F, Birnbaum MJ. Akt1/PKBα Is Required for Normal Growth but Dispensable for Maintenance of Glucose Homeostasis in Mice. *J Biol Chem*. 2001. doi:10.1074/jbc.C100462200

214. George S, Rochford JJ, Wolfrum C, et al. A family with severe insulin resistance and diabetes due to a mutation in AKT2. *Science (80-)*. 2004. doi:10.1126/science.1096706

215. Easton RM, Cho H, Roovers K, et al. Role for Akt3/Protein Kinase B in Attainment of Normal Brain Size. *Mol Cell Biol*. 2005. doi:10.1128/mcb.25.5.1869-1878.2005

216. Sanidas I, Polytarchou C, Hatziapostolou M, et al. Phosphoproteomics Screen Reveals Akt Isoform-Specific Signals Linking RNA Processing to Lung Cancer. *Mol Cell*. 2014. doi:10.1016/j.molcel.2013.12.018

217. Paez JG, Jänne PA, Lee JC, et al. EGFR mutations in lung cancer: correlation with clinical response to gefitinib therapy. *Science*. 2004;304(5676):1497-1500. doi:10.1126/science.1099314

218. Wass RE, Lang D, Lamprecht B, Studnicka M. Targeted therapy in lung cancer—ASCO 2019 update. *Memo - Mag Eur Med Oncol*. 2019. doi:10.1007/s12254-019-00538-3

219. Yap TA, Omlin A, De Bono JS. Development of therapeutic combinations targeting major cancer signaling pathways. *J Clin Oncol*. 2013. doi:10.1200/JCO.2011.37.6418

220. Middleton G, Popat S, Fletcher P, et al. PL02.09 National Lung Matrix Trial (NLMT): First Results from an Umbrella Phase II Trial in Advanced Non-Small Cell Lung Cancer (NSCLC). *J Thorac Oncol*. 2019;14(10):S7. doi:10.1016/j.jtho.2019.08.060

221. Hyman DM, Smyth LM, Donoghue MTA, et al. AKT inhibition in solid tumors with AKT1 mutations. *J Clin Oncol*. 2017. doi:10.1200/JCO.2017.73.0143

222. Capivasertib Active against AKT1-Mutated Cancers. *Cancer Discov*. 2019.

doi:10.1158/2159-8290.CD-NB2018-153

223. Harb W, Saleh MN, Papadopoulos KP, et al. Clinical Trial Results from the Subgroup of Lymphoma/CLL in a Phase 1 Study of ARQ 092, a Novel Pan AKT-Inhibitor. *Blood*. 2015;126(23):5116. doi:10.1182/blood.V126.23.5116.5116

224. Wu WI, Voegtli WC, Sturgis HL, Dizon FP, Vigers GPA, Brandhuber BJ. Crystal structure of human AKT1 with an allosteric inhibitor reveals a new mode of kinase inhibition. *PLoS One*. 2010. doi:10.1371/journal.pone.0012913

225. Ericson K, Gan C, Cheong I, et al. Genetic inactivation of AKT1, AKT2, and PDPK1 in human colorectal cancer cells clarifies their roles in tumor growth regulation. *Proc Natl Acad Sci U S A*. 2010. doi:10.1073/pnas.0914018107

226. Wang J, Anderson MG, Oleksijew A, et al. ABBV-399, a c-Met antibody-drug conjugate that targets both MET-amplified and c-Met-overexpressing tumors, irrespective of MET pathway dependence. *Clin Cancer Res*. 2017. doi:10.1158/1078-0432.CCR-16-1568

227. Tong M, Gao M, Xu Y, et al. SHR-A1403, a novel c-mesenchymal-epithelial transition factor (c-Met) antibody-drug conjugate, overcomes AZD9291 resistance in non-small cell lung cancer cells overexpressing c-Met. *Cancer Sci*. 2019. doi:10.1111/cas.14180

228. Doronina SO, Toki BE, Torgov MY, et al. Development of potent monoclonal antibody auristatin conjugates for cancer therapy. *Nat Biotechnol*. 2003. doi:10.1038/nbt832

229. Okeley NM, Alley SC, Senter PD. Advancing antibody drug conjugation: From the laboratory to a clinically approved anticancer drug. *Hematol Oncol Clin North Am*. 2014. doi:10.1016/j.hoc.2013.10.009

230. Wolf J, Seto T, Han J-Y, et al. Capmatinib (INC280) in METΔex14-mutated advanced non-small cell lung cancer (NSCLC): Efficacy data from the phase II GEOMETRY mono-1 study. *J Clin Oncol*. 2019;37(15_suppl):9004. doi:10.1200/JCO.2019.37.15_suppl.9004

231. Korn EL, Arbuck SG, Pluda JM, Simon R, Kaplan RS, Christian MC. Clinical trial designs for cytostatic agents: Are new approaches needed? *J Clin Oncol*. 2001. doi:10.1200/JCO.2001.19.1.265

232. Jain RK, Lee JJ, Hong D, et al. Phase I oncology studies: Evidence that in the era of targeted therapies patients on lower doses do not fare worse. *Clin Cancer Res*. 2010. doi:10.1158/1078-0432.CCR-09-2684

233. Parulekar WR, Eisenhauer EA. Phase I trial design for solid tumor studies of targeted, non-cytotoxic agents: Theory and practice. *J Natl Cancer Inst*. 2004. doi:10.1093/jnci/djh182

234. Sleijfer S, Wiemer E. Dose selection in phase I studies: Why we should always go for the top. *J Clin Oncol*. 2008. doi:10.1200/JCO.2007.15.5192

235. Cannistra SA. Challenges and pitfalls of combining targeted agents in phase I studies. *J Clin Oncol*. 2008. doi:10.1200/JCO.2008.17.2676

236. Zou HY, Li Q, Lee JH, et al. An orally available small-molecule inhibitor of c-Met, PF-2341066, exhibits cytoreductive antitumor efficacy through antiproliferative and antiangiogenic mechanisms. *Cancer Res*. 2007. doi:10.1158/0008-5472.CAN-06-4443

237. Camidge DR, Bang YJ, Kwak EL, et al. Activity and safety of crizotinib in patients with ALK-positive non-small-cell lung cancer: Updated results from a phase 1 study. *Lancet Oncol*. 2012. doi:10.1016/S1470-2045(12)70344-3

238. Workman P. Challenges of PK/PD measurements in modern drug development. *Eur J Cancer*. 2002. doi:10.1016/S0959-8049(02)00395-7

239. Shaw AT, Ou SHI, Bang YJ, et al. Crizotinib in ROS1-rearranged non-small-cell lung cancer. *N Engl J Med*. 2014. doi:10.1056/NEJMoa1406766

240. Le Tourneau C, Lee JJ, Siu LL. Dose escalation methods in phase i cancer clinical trials. *J Natl Cancer Inst*. 2009. doi:10.1093/jnci/djp079

241. Stein S, Zhao R, Haeno H, Vivanco I, Michor F. Mathematical modeling identifies optimum lapatinib dosing schedules for the treatment of glioblastoma patients. *PLoS Comput Biol*. 2018. doi:10.1371/journal.pcbi.1005924

242. Wang S, Chen J, Xie Z, et al. Pulsatile crizotinib treatment for brain metastasis in a patient with non-small-cell lung cancer. *J Clin Pharm Ther*. 2017. doi:10.1111/jcpt.12550

243. Gordon MS, Sweeney CS, Mendelson DS, et al. Safety, pharmacokinetics, and pharmacodynamics of AMG 102, a fully human hepatocyte growth factor-neutralizing monoclonal antibody, in a first-in-human study of patients with advanced solid tumors. *Clin Cancer Res*. 2010. doi:10.1158/1078-0432.CCR-09-1365

244. Pike KG, Malagu K, Hummersone MG, et al. Optimization of potent and selective dual mTORC1 and mTORC2 inhibitors: The discovery of AZD8055 and AZD2014. *Bioorganic Med Chem Lett*. 2013. doi:10.1016/j.bmcl.2013.01.019

245. Liu P, Cheng H, Roberts TM, Zhao JJ. Targeting the phosphoinositide 3-kinase pathway in cancer. *Nat Rev Drug Discov*. 2009. doi:10.1038/nrd2926

246. Guertin DA, Sabatini DM. Defining the Role of mTOR in Cancer. *Cancer Cell*. 2007.

doi:10.1016/j.ccr.2007.05.008

247. Liu P, Gan W, Inuzuka H, et al. Sin1 phosphorylation impairs mTORC2 complex integrity and inhibits downstream Akt signalling to suppress tumorigenesis. *Nat Cell Biol*. 2013. doi:10.1038/ncb2860

248. Basu B, Dean E, Puglisi M, et al. First-in-human pharmacokinetic and pharmacodynamic study of the dual m-TORC 1/2 inhibitor AZD2014. *Clin Cancer Res*. 2015. doi:10.1158/1078-0432.CCR-14-2422

249. Basu B, Krebs MG, Sundar R, et al. Vistusertib (dual m-TORC1/2 inhibitor) in combination with paclitaxel in patients with high-grade serous ovarian and squamous non-small-cell lung cancer. *Ann Oncol*. 2018. doi:10.1093/annonc/mdy245

250. Sanchez-Cespedes M, Parrella P, Esteller M, et al. Inactivation of LKB1/STK11 is a common event in adenocarcinomas of the lung. *Cancer Res*. 2002.

251. Shah U, Sharpless NE, Hayes DN. LKB1 and lung cancer: More than the usual suspects. *Cancer Res*. 2008. doi:10.1158/0008-5472.CAN-07-6620

252. Gao Y, Ge G, Ji H. LKB1 in lung cancerigenesis: A serine/threonine kinase as tumor suppressor. *Protein Cell*. 2011. doi:10.1007/s13238-011-1021-6

253. Vivanco I, Chen ZC, Tanos B, et al. A kinase-independent function of AKT promotes cancer cell survival. *Elife*. 2014;3. doi:10.7554/eLife.03751

254. Yu Y, Savage RE, Eathiraj S, et al. Targeting AKT1-E17K and the PI3K/AKT pathway with an allosteric AKT inhibitor, ARQ 092. *PLoS One*. 2015. doi:10.1371/journal.pone.0140479

255. Liu X, Wang Q, Yang G, et al. A novel kinase inhibitor, INCB28060, blocks c-MET-dependent signaling, neoplastic activities, and cross-talk with EGFR and HER-3. *Clin Cancer Res*. 2011. doi:10.1158/1078-0432.CCR-11-1157

256. Baltschukat S, Engstler BS, Huang A, et al. Capmatinib (INC280) is active against models of non–small cell lung cancer and other cancer types with defined mechanisms of MET activation. *Clin Cancer Res*. 2019. doi:10.1158/1078-0432.CCR-18-2814

257. Su YBW, Schuler M, Teck W, et al. Phase 1 study of capmatinib in MET-positive solid tumor patients : Dose escalation and expansion of selected cohorts. 2019;(September):1-12. doi:10.1111/cas.14254

258. Shisheva A. PIKfyve: Partners, significance, debates and paradoxes. *Cell Biol Int*. 2008. doi:10.1016/j.cellbi.2008.01.006

259. Ikonomov OC, Sbrissa D, Shisheva A. Mammalian Cell Morphology and Endocytic Membrane Homeostasis Require Enzymatically Active Phosphoinositide 5-Kinase PIKfyve. *J Biol Chem*. 2001. doi:10.1074/jbc.M101722200

260. Ikonomov OC, Sbrissa D, Mlak K, Kanzaki M, Pessin J, Shisheva A. Functional dissection of lipid and protein kinase signals of PIKfyve reveals the role of PtdIns 3,5-P2 production for endomembrane integrity. *J Biol Chem*. 2002. doi:10.1074/jbc.M108750200

261. Zolov SN, Bridges D, Zhang Y, et al. In vivo, Pikfyve generates PI(3,5)P2, which serves as both a signaling lipid and the major precursor for PI5P. *Proc Natl Acad Sci U S A*. 2012. doi:10.1073/pnas.1203106109

262. de Lartigue J, Polson H, Feldman M, et al. PIKfyve regulation of endosome-linked pathways. *Traffic*. 2009. doi:10.1111/j.1600-0854.2009.00915.x

263. Gayle S, Landrette S, Beeharry N, et al. Identification of apilimod as a first-in-class PIKfyve kinase inhibitor for treatment of B-cell non-Hodgkin lymphoma. *Blood*. 2017. doi:10.1182/blood-2016-09-736892

264. Harb, W.A., Diefenbach, C.S. et al. Phase 1 clinical safety, pharmacokinetics (PK), and activity of apilimod mesylate (LAM-002A), a first-in-class inhibitor of phosphatidylinositol-3 phosphate 5-kinase (PIKfyve), in patients with relapsed B-cell malignancies. ASH Ann. Meeting 4119. In: *ASH Ann. Meeting 4119.*

265. Cai X, Xu Y, Cheung AK, et al. PIKfyve, a class III PI kinase, is the target of the small molecular IL-12/IL-23 inhibitor apilimod and a player in Toll-like receptor signaling. *Chem Biol*. 2013;20(7):912-921. doi:10.1016/j.chembiol.2013.05.010

266. McGeachy MJ, Chen Y, Tato CM, et al. The interleukin 23 receptor is essential for the terminal differentiation of interleukin 17-producing effector T helper cells in vivo. *Nat Immunol*. 2009. doi:10.1038/ni.1698

267. Bettelli E, Oukka M, Kuchroo VK. TH-17 cells in the circle of immunity and autoimmunity. *Nat Immunol*. 2007. doi:10.1038/ni0407-345

268. Wada Y, Cardinale I, Khatcherian A, et al. Apilimod inhibits the production of IL-12 and IL-23 and reduces dendritic cell infiltration in psoriasis. *PLoS One*. 2012. doi:10.1371/journal.pone.0035069

269. Burakoff R, Barish CF, Riff D, et al. A phase 1/2A trial of STA 5326, an oral interleukin-12/23 inhibitor, in patients with active moderate to severe Crohn's disease. *Inflamm Bowel Dis*. 2006. doi:10.1097/01.ibd.0000225337.14356.31

270. Krausz S, Boumans MJH, Gerlag DM, et al. A phase IIa, randomized, double-blind, placebo-controlled trial of apilimod mesylate, an interleukin-12/interleukin-23 inhibitor, in patients with rheumatoid arthritis. *Arthritis Rheum*. 2012;64(6):1750-

1755. doi:10.1002/art.34339

271. Sands BE, Jacobson EW, Sylwestrowicz T, et al. Randomized, double-blind, placebo-controlled trial of the oral interleukin-12/23 inhibitor apilimod mesylate for treatment of active Crohn's disease. *Inflamm Bowel Dis*. 2009;16(7):1209-1218. doi:10.1002/ibd.21159

272. Langowski JL, Zhang X, Wu L, et al. IL-23 promotes tumour incidence and growth. *Nature*. 2006. doi:10.1038/nature04808

273. Langowski JL, Kastelein RA, Oft M. Swords into plowshares: IL-23 repurposes tumor immune surveillance. *Trends Immunol*. 2007. doi:10.1016/j.it.2007.03.006

274. Miossec P, Kolls JK. Targeting IL-17 and T H 17 cells in chronic inflammation. *Nat Rev Drug Discov*. 2012. doi:10.1038/nrd3794

275. Sbrissa D, Ikonomov OC, Shisheva A. Phosphatidylinositol 3-phosphate-interacting domains in PIKfyve. Binding specificity and role in PIKfyve endomembrane localization. *J Biol Chem*. 2002. doi:10.1074/jbc.M110194200

276. Quan JH, Chu JQ, Kwon J, et al. Intracellular networks of the PI3K/AKT and MAPK pathways for regulating Toxoplasma gondii-induced IL-23 and IL-12 production in human THP-1 cells. *PLoS One*. 2015;10(11):1-22. doi:10.1371/journal.pone.0141550

277. Baird AM, Dockry É, Daly A, et al. IL-23R is epigenetically regulated and modulated by chemotherapy in Non-Small Cell Lung Cancer. *Front Oncol*. 2013. doi:10.3389/fonc.2013.00162

278. Harris TJ, Grosso JF, Yen H, et al. An in vivo requirement for STAT3 Signaling in TH17 development and TH17-Dependent Autoimmunity 1. *J Immunol*. 2007.

279. Cam C, Karagoz B, Muftuoglu T, et al. The inflammatory cytokine interleukin-23 is elevated in lung cancer, particularly small cell type. *Wspolczesna Onkol*. 2016. doi:10.5114/wo.2016.61562

280. Amaravadi RK, Kimmelman AC, Debnath J. Targeting autophagy in cancer: Recent advances and future directions. *Cancer Discov*. 2019. doi:10.1158/2159-8290.CD-19-0292

281. Guo JY, Chen HY, Mathew R, et al. Activated Ras requires autophagy to maintain oxidative metabolism and tumorigenesis. *Genes Dev*. 2011. doi:10.1101/gad.2016311

282. Yang S, Wang X, Contino G, et al. Pancreatic cancers require autophagy for tumor growth. *Genes Dev*. 2011. doi:10.1101/gad.2016111

283. Wei H, Wei S, Gan B, Peng X, Zou W, Guan JL. Suppression of autophagy by FIP200 deletion inhibits mammary tumorigenesis. *Genes Dev*. 2011. doi:10.1101/gad.2051011

284. Karsli-Uzunbas G, Guo JY, Price S, et al. Autophagy is required for glucose homeostasis and lung tumor maintenance. *Cancer Discov*. 2014. doi:10.1158/2159-8290.CD-14-0363

285. American Cancer Society. Cancer Facts and Figures 2017. *Genes Dev*. 2017;21(20):2525-2538. doi:10.1101/gad.1593107

286. Casado P, Wilkes EH, Miraki-Moud F, et al. Proteomic and genomic integration identifies kinase and differentiation determinants of kinase inhibitor sensitivity in leukemia cells. *Leukemia*. 2018. doi:10.1038/s41375-018-0032-1

287. Montoya A, Beltran L, Casado P, Rodríguez-Prados JC, Cutillas PR. Characterization

of a TiO2 enrichment method for label-free quantitative phosphoproteomics. *Methods*. 2011. doi:10.1016/j.ymeth.2011.02.004